

การสกัดและนำกลับไอออนเงินออกจากน้ำทิ้งในกระบวนการเกษตรกรรม  
โดยใช้เยื่อแผ่นเหลวที่พองด้วยเส้นใยกลวง

นางสาวธิดารัตน์ วงศ์สวา



บทคัดย่อและแฟ้มข้อมูลฉบับเต็มของวิทยานิพนธ์ตั้งแต่ปีการศึกษา 2554 ที่ให้บริการในคลังปัญญาจุฬาฯ (CUIR)  
เป็นแฟ้มข้อมูลของนิสิตเจ้าของวิทยานิพนธ์ ที่ส่งผ่านทางบัณฑิตวิทยาลัย

The abstract and full text of theses from the academic year 2011 in Chulalongkorn University Intellectual Repository (CUIR)  
are the thesis authors' files submitted through the University Graduate School.

วิทยานิพนธ์นี้เป็นส่วนหนึ่งของการศึกษาตามหลักสูตรปริญญาวิศวกรรมศาสตรดุษฎีบัณฑิต  
สาขาวิชาวิศวกรรมเคมี ภาควิชาวิศวกรรมเคมี  
คณะวิศวกรรมศาสตร์ จุฬาลงกรณ์มหาวิทยาลัย  
ปีการศึกษา 2557  
ลิขสิทธิ์ของจุฬาลงกรณ์มหาวิทยาลัย

EXTRACTION AND RECOVERY OF SILVER IONS  
FROM PHARMACEUTICAL PROCESSES VIA HOLLOW FIBER  
SUPPORTED LIQUID MEMBRANE

Miss Thidarat Wongsawa



A Dissertation Submitted in Partial Fulfillment of the Requirements  
for the Degree of Doctor of Engineering Program in Chemical Engineering  
Department of Chemical Engineering  
Faculty of Engineering  
Chulalongkorn University  
Academic Year 2014  
Copyright of Chulalongkorn University



ธิดารัตน์ วงศ์สวา : การสกัดและนำกลับไอออนเงินออกจากน้ำทิ้งในกระบวนการเภสัชกรรมโดยใช้เยื่อแผ่นเหลวที่พองด้วยเส้นใยกลวง (EXTRACTION AND RECOVERY OF SILVER IONS FROM PHARMACEUTICAL PROCESSES VIA HOLLOW FIBER SUPPORTED LIQUID MEMBRANE) อ.ที่ปรึกษาวิทยานิพนธ์หลัก: ศาสตราจารย์ ดร.อุรา ปานเจริญ, อ.ที่ปรึกษาวิทยานิพนธ์ร่วม: รศ. ดร.อัญชลีพร วาริตสวัสดิ์ หล่อทองคำ, 257 หน้า.

งานวิจัยนี้ศึกษาการสกัดและนำกลับไอออนเงินโดยใช้เยื่อแผ่นเหลวที่พองด้วยเส้นใยกลวง สารละลายป้อนที่ใช้คือน้ำทิ้งจากกระบวนการเภสัชกรรมที่มีค่าความเข้มข้นของไอออนเงินเริ่มต้นเท่ากับ 30 มิลลิกรัมต่อลิตร การเลือกชนิดของสารตัวทำละลายพิจารณาจากสภาพละลายได้ (solubility) พบว่าโครซินเป็นสารตัวทำละลายที่เหมาะสม ส่วนชนิดของสารสกัด คือ LIX 84-I และสารละลายนำกลับคือโซเดียมไทโอซัลเฟตเพื่อใช้ในระบบเยื่อแผ่นเหลวที่พองด้วยเส้นใยกลวงเลือกโดยวิธีการสกัดของเหลวด้วยของเหลว

ผลการสกัดและนำกลับไอออนเงินโดยใช้เยื่อแผ่นเหลวที่พองด้วยเส้นใยกลวง พบว่าการสกัดและนำกลับสูงสุด 98 และ 85 เปอร์เซ็นต์ เมื่อความเป็นกรด-เบสของสารละลายป้อนและสารละลายนำกลับเท่ากับ 3.5 และ 2 ตามลำดับ และความเข้มข้นของสารสกัดและสารละลายนำกลับเท่ากับ 0.1 และ 0.5 โมลต่อลิตร โดยที่อัตราการไหลของสารละลายป้อนและสารละลายนำกลับเท่ากับ 200 มิลลิลิตรต่อนาที เวลาในการสกัดและนำกลับเท่ากับ 26 นาที ใช้ปฏิบัติการแบบสารละลายป้อนและสารละลายนำกลับไหลวนและสวนทางกัน ความเข้มข้นของไอออนเงินที่เหลืออยู่ในสารละลายป้อนต่ำกว่า 1 มิลลิกรัมต่อลิตร นอกจากนี้ศึกษาผลของไอออนเหล็ก พบว่าไอออนเหล็กไม่มีผลต่อการสกัดและนำกลับไอออนเงิน จากนั้นสร้างแบบจำลองทางคณิตศาสตร์โดยพิจารณาการพา การแพร่ ปฏิกิริยาเคมี และการสะสมสารประกอบเชิงซ้อนของไอออนเงินในวัฏภาคเยื่อแผ่นเหลวเพื่ออธิบายการถ่ายเทมวลของไอออนเงินในระบบเยื่อแผ่นเหลวที่พองด้วยเส้นใยกลวง และทำนายประสิทธิภาพและเวลาในการสกัดและนำกลับไอออนเงินแบบจำลองที่ได้มีความแม่นยำสูง เปรียบเทียบผลการคำนวณจากแบบจำลองกับผลการทดลอง พบว่าความแตกต่างน้อยกว่า 2 เปอร์เซ็นต์

ภาควิชา วิศวกรรมเคมี

สาขาวิชา วิศวกรรมเคมี

ปีการศึกษา 2557

ลายมือชื่อนิสิต .....

ลายมือชื่อ อ.ที่ปรึกษาหลัก .....

ลายมือชื่อ อ.ที่ปรึกษาร่วม .....

# # 5171845121 : MAJOR CHEMICAL ENGINEERING

KEYWORDS: SILVER IONS / EXTRACTION / RECOVERY / HFSLM / MATHEMATICAL MODELS

THIDARAT WONGSAWA: EXTRACTION AND RECOVERY OF SILVER IONS FROM PHARMACEUTICAL PROCESSES VIA HOLLOW FIBER SUPPORTED LIQUID MEMBRANE. ADVISOR: DISTINGUISHED PROF. DR.URA PANCHAROEN, CO-ADVISOR: ASSOC. PROF. DR.ANCHALEEPORN WARITSAWAT LOTHONGKUM, 257 pp.

This work studied the extraction and recovery of silver ions via hollow fiber supported liquid membrane (HFSLM). Pharmaceutical wastewater containing silver ions of 30 mg/L was used as a feed solution. Type of organic solvents was selected by considering its solubility. Kerosene was found to be the suitable organic solvent. For an extractant and a stripping solution, respectively, LIX 84-I and sodium thiosulfate solution were selected by liquid-liquid extraction.

The maximum percentages of extraction and recovery of silver ions via the HFSLM were 98% and 85%, respectively by following conditions: pH of feed and stripping solutions at 3.5 and 2 respectively, the concentration of extractant and stripping solutions 0.1 and 0.5 mol/L, equal flow rate of feed and stripping solutions 200 mL/min, and separation time of 26 min. The operating mode in HFSLM was applied by countercurrent-circulating of feed and stripping solutions. The residual concentration of silver ions in the feed solution less than 1 mg/L was observed. The effect of ferric ions was additionally studied and found no influence on silver ion extraction. In addition, the mathematical models considering the convection, diffusion, chemical reaction and the accumulation of silver ion complexes in the liquid membrane phase were developed in order to understand mass transfer of silver ions throughout the HFSLM as well as to predict the extraction and recovery of silver ions and the separation time. The models showed high accuracy as the calculated results from the models were deviated from the experimental data less than 2%.

Department: Chemical Engineering

Field of Study: Chemical Engineering

Academic Year: 2014

Student's Signature .....

Advisor's Signature .....

Co-Advisor's Signature .....

## ACKNOWLEDGEMENTS

I would like to extend my grateful thanks to my advisor, Distinguished Professor Dr.Ura Pancharoen, my co-advisor, Associate Professor Dr.Anchaleeporn Waritswat Lothongkum, for their kindness and consistent support. My unforgettable oversea experience cannot be achieved deep without Professor Dr.Milan Hronec for allowing me to pursue my research at his laboratory in Bratislava, Slovakia. My appreciation also goes to the thesis committee, Assistant Professor Dr.Apinan Soottitantawat, Assistant Professor Dr.Suphot Phatanasri, Associate Professor Dr.Soorathep Kheawhom and Assistant Professor Dr.Weerawat Patthaveekongka for their comments and suggestions.

I deeply acknowledge the Royal Golden Jubilee Ph.D. Program (Grant no. PHD/0272/2549) from the Thailand Research Fund and Chulalongkorn University. Sincere thanks also extend to the Government Pharmaceutical Organization of Thailand for supplying wastewater.

Eternally, I am grateful to my family for their support, my friends in the research group of the Separation Laboratory at the Department of Chemical Engineering, Chulalongkorn University, Bangkok, Thailand, and Mr. Alan Wilcox, M.Ed. for his thorough reading of the publication articles and my dissertation.

CHULALONGKORN UNIVERSITY

## CONTENTS

	Page
THAI ABSTRACT .....	iv
ENGLISH ABSTRACT .....	v
ACKNOWLEDGEMENTS .....	vi
CONTENTS .....	vii
LIST OF TABLES .....	xvi
LIST OF FIGURES .....	xx
Chapter I Introduction .....	1
1.1 Rationale of research problem.....	1
1.2 Extraction and recovery of metal ions via HFSLM .....	3
1.2.1 Extractants .....	6
1.2.1.1 Organic acid extractants.....	7
1.2.1.2 Chelating extractants.....	8
1.2.1.3 Neutral or solvating extractants.....	8
1.2.1.4 Ligand substitution extractants .....	9
1.2.1.5 Basic or ion-pair extractants.....	9
1.2.2 Organic solvents .....	11
1.2.3 Stripping solutions.....	12
1.2.4 pH of feed and stripping solutions .....	13
1.2.5 Concentration of the extractants.....	14
1.2.6 Concentration of the stripping solutions.....	14
1.2.7 Flow rates of feed and stripping solutions .....	14
1.2.8 Flow directions of feed and stripping solutions.....	15

	Page
1.2.9 Flow patterns of feed and stripping solutions .....	15
1.2.10 Separation time of metal ion extraction and recovery .....	16
1.2.11 Mathematical models in separation of metal ions via HFSLM .....	17
1.3 Objectives of the dissertation .....	17
1.4 Scope of the dissertation .....	18
1.5 Expected results .....	19
1.6 Description of dissertation .....	19
Chapter II Ternary (liquid-liquid) equilibrium data of furfuryl alcohol with organic solvents at $T = 298.2$ K: experimental results and thermodynamic models .....	24
2.1 Abstract .....	25
2.2 Introduction .....	25
2.3 Experimental .....	27
2.3.1 Chemicals .....	27
2.3.2 Apparatus and procedure .....	27
2.3.3 Analysis .....	29
2.3.4 Reliability of LLE results .....	29
2.4 Results and discussion .....	30
2.4.1 Experimental solubility and tie-line data .....	30
2.4.2 Distribution coefficients and separation factors .....	35
2.4.3 Thermodynamic model correlation .....	37
2.5 Conclusion .....	40
2.6 Acknowledgements .....	41
2.7 Appendix A .....	41

	Page
2.8 References.....	44
Chapter III Experiments and thermodynamic models for ternary (liquid-liquid) equilibrium systems of water + cyclopentanone + organic solvents at $T = 298.2$ K..	
3.1 Abstract .....	49
3.2 Introduction.....	49
3.3 Experimental.....	51
3.3.1 Chemicals .....	51
3.3.2 Apparatus and procedure .....	51
3.3.3 Analysis and uncertainty measurement .....	52
3.4 Results and discussion.....	53
3.4.1 Experimental data.....	53
3.4.2 Reliability of tie-line data.....	59
3.4.3 Distribution coefficients and separation factors.....	61
3.4.4 Thermodynamic model correlation .....	63
3.5 Conclusion .....	69
3.6 Nomenclature and units.....	69
3.7 Acknowledgements.....	70
3.8 References .....	71
Chapter IV Solubility and tie-line data for ternary aqueous mixtures of cyclopentanol with organic solvents at $T = 298.2$ K: experiments and NRTL model.....	
4.1 Abstract .....	75
4.2 Introduction.....	75
4.3 Experimental.....	77

	Page
4.3.1 Chemicals .....	77
4.3.2 Apparatus and procedure.....	77
4.3.3 Analysis.....	79
4.3.4 Reliability of LLE results .....	79
4.4 Results and discussion.....	80
4.4.1 Experimental solubility and tie-line data .....	80
4.4.2 The capability of the selected organic solvents.....	85
4.4.3 NRTL model correlation.....	89
4.5 Conclusion .....	93
4.6 Nomenclature and units.....	93
4.7 Acknowledgements.....	94
4.8 References .....	95
Chapter V The role of organic solvents in the aspects of equilibrium, kinetics and thermodynamic model for silver ion extraction using an extractant D2EHPA .....	98
5.1 Abstract .....	99
5.2 Introduction.....	99
5.3 Theory.....	101
5.3.1 Competitive complexation/solvation theory for liquid-liquid extraction process .....	101
5.4 Experimental.....	102
5.4.1 Chemicals.....	102
5.4.2 Apparatus .....	103
5.4.3 Procedure.....	104
5.4.3.1 Solubility and tie-lines .....	104

	Page
5.4.3.2 Liquid-liquid extraction .....	104
5.4.4 Analysis .....	106
5.4.5 Reliability of LLE data .....	106
5.5 Results and discussion .....	107
5.5.1 Experimental LLE data at equilibrium .....	107
5.5.2 Extraction efficiency for different organic solvents .....	113
5.5.3 Extraction behaviors in different organic solvents .....	114
5.5.4 Spectroscopic analysis for silver ion extraction .....	116
5.5.5 Correlation of thermodynamic models .....	117
5.6 Conclusion .....	122
5.6 Nomenclature and units .....	122
5.8 Acknowledgements .....	124
5.9 References .....	124
Chapter VI A reaction flux model for extraction of Cu(II) with LIX 84-I in HFSLM .....	130
6.1 Abstract .....	131
6.2 Introduction .....	131
6.3 Theory .....	133
6.3.1 Transport mechanisms of copper ion extraction .....	133
6.3.2 Analysis of copper ion concentration in the feed phase .....	135
6.3.2.1 At the initial condition ( $t = 0$ ) .....	137
6.3.2.2 At time $t$ ( $t \neq 0$ ) .....	138
6.4 Experimental .....	139
6.4.1 Apparatus, feed and chemicals .....	139

	Page
6.4.2 Procedure.....	140
6.5 Results and discussion.....	141
6.5.1 Validation of the model with the experimental results and other literature.....	141
6.5.2 Estimation of separation time and separation cycle .....	145
6.6 Conclusion .....	146
6.7 Nomenclature and units.....	147
6.8 Acknowledgements.....	149
6.9 References.....	149
Chapter VII High-efficiency HFSLM for silver-ion pertraction from pharmaceutical wastewater and mass-transport models .....	153
7.1 Abstract .....	154
7.2 Introduction.....	154
7.3 Theory .....	158
7.3.1 Pertraction of silver ions in the HFSLM system .....	158
7.3.2 Reliability of the HFSLM system.....	159
7.3.3 Facilitated coupled counter-transport of silver ions across the HFSLM.	160
7.3.4 Reaction flux model for silver ion concentration in feed solution.....	167
7.4 Experimental.....	168
7.4.1 Pharmaceutical wastewater pretreatment .....	168
7.4.2 Chemicals.....	168
7.4.3 Apparatus .....	169
7.4.4 Procedure.....	170
7.5 Results and discussion.....	172

	Page
7.5.1 Effects of extractant types for silver ion extraction .....	172
7.5.2 Effects of stripping types for silver ion recovery.....	173
7.5.3 Effect of pH feed solution .....	174
7.5.4 Effect of pH stripping solution .....	175
7.5.5 Effect of extractant concentration.....	176
7.5.6 Effect of stripping concentration.....	177
7.5.7 Effects of flow rates of feed and stripping solutions.....	178
7.5.8 Effects of flow directions between feed and stripping solutions.....	179
7.5.9 Effects of flow patterns of feed and stripping solutions.....	180
7.5.10 Effect of ferric ion presence on silver ion pertraction.....	181
7.5.11 Memory effect and repeatability .....	182
7.5.12 Controlling transport regime for silver ion pertraction across the HFSLM.....	183
7.5.12 Optimization of separation time .....	185
7.6 Conclusion .....	185
7.7 Nomenclature and units.....	185
7.8 Acknowledgements.....	188
7.9 References .....	188
Chapter VIII Fluid-flow models operating on linear algebra for extraction and recovery of silver ions from pharmaceutical wastewater by HFSLM .....	195
8.1 Abstract .....	196
8.2 Introduction.....	196
8.3 Theory.....	200
8.3.1 Transport of silver ions across the liquid membrane phase .....	200

8.3.2 Fluid-flow models of silver ion transport in feed and stripping phases .	202
8.3.3 Mass transfer coefficient of silver-extractant complexes across the liquid membrane phase.....	206
8.4 Experimental.....	209
8.4.1 Chemicals .....	209
8.4.2 Apparatus.....	210
8.4.3 Procedure.....	211
8.5 Results and discussion.....	213
8.5.1 Experimental operation conditions for HFSLM stability .....	213
8.5.2 Influences of pH of feed and stripping solutions .....	213
8.5.3 Influence of extractant concentration .....	215
8.5.4 Influence of stripping concentration .....	216
8.5.5 Influences of flow rates of feed and stripping solutions .....	217
8.5.6 Mass transfer parameters in the HFSLM.....	218
8.5.6.1 Extraction equilibrium constant and distribution ratio.....	218
8.5.6.2 Permeability coefficient .....	219
8.5.6.3 Mass transfer coefficients of the complex species.....	220
8.5.7 Analysis of fluid-flow models in feed and stripping phases.....	221
8.5.7.1 Parameters in the models.....	221
8.5.7.2 Stability of HFSLM operation and validation of the fluid-flow models .....	223

8.5.7.3 Silver ion extraction: experimental and model results by fluid-flow model and other models and adaptability of fluid-flow model.....	224
8.6 Conclusion .....	226
8.7 Appendix A .....	227
8.8 Nomenclature and units.....	233
8.9 Acknowledgements.....	236
8.10 References .....	237
Chapter IX Conclusion and recommendations .....	244
9.1 Conclusion .....	244
9.2 Problems and constraints.....	246
9.3 Recommendations for future research.....	246
REFERENCES .....	248
VITA.....	257

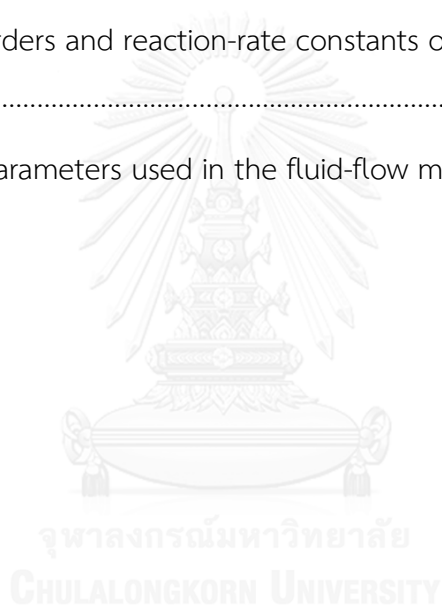
## LIST OF TABLES

	Page
<b>Table 1.1</b> The important properties of organic solvents used <sup>[43-45]</sup> .....	12
<b>Table 2.1</b> Sources and mass fraction purity of chemicals. ....	27
<b>Table 2.2</b> Experimental solubility data in mass fractions ( $w_i$ ) for [water (1) + furfuryl alcohol (2) + organic solvents (3)] at $T = 298.2$ K and atmospheric pressure. <sup>a</sup> .....	30
<b>Table 2.3</b> Experimental tie-line data in mass fractions for the ternary systems of [water (1) + furfuryl alcohol (2) + organic solvents (3)] at $T = 298.2$ K and atmospheric pressure. <sup>a</sup> .....	32
<b>Table 2.4</b> Distribution coefficients ( $D$ ) and separation factors ( $S$ ) for the ternary systems of [water (1) + furfuryl alcohol (2) + organic solvents (3)] at $T = 298.2$ K and atmospheric pressure. ....	36
<b>Table 2.5</b> UNIQUAC and UNIFAC structural parameters ( $r$ and $q$ ) for pure components.....	38
<b>Table 2.6</b> NRTL and UNIQUAC binary interaction parameters for the ternary systems (water + furfuryl alcohol + organic solvents) at $T = 298.2$ K.....	39
<b>Table 2.7</b> <i>rmsd</i> values for the NRTL, UNIQUAC and UNIFAC models for the ternary systems of (water + furfuryl alcohol + organic solvents). ....	40
<b>Table 3.1</b> Equilibrium solubility data in mass fractions ( $w_i$ ) for the ternary systems of water (1) + cyclopentanone (2) + organic solvents (3) at $T = 298.2$ K and atmospheric pressure. <sup>a</sup> .....	54
<b>Table 3.2</b> Experimental tie-line data in mass fractions for the ternary systems of water (1) + cyclopentanone (2) + organic solvents (3) at $T = 298.2$ K and atmospheric pressure. <sup>a</sup> .....	56

<b>Table 3.3</b> Othmer-Tobias and Hand correlation parameters and their correlation factors ( $R^2$ ) for the ternary systems of water (1) + cyclopentanone (2) + organic solvents (3) at $T = 298.2$ K and atmospheric pressure. ....	61
<b>Table 3.4</b> Distribution coefficients ( $D$ ) and separation factors ( $S$ ) for the ternary systems of water (1) + cyclopentanone (2) + organic solvents (3) at $T = 298.2$ K and atmospheric pressure. ....	62
<b>Table 3.5</b> UNIQUAC structural parameters ( $r$ and $q$ ) for pure components.....	66
<b>Table 3.6</b> NRTL and UNIQUAC binary interaction parameters for the ternary systems of water + cyclopentanone + organic solvents at $T = 298.2$ K. ....	67
<b>Table 3.7</b> Modeling NRTL and UNIQUAC tie-line values in mass fractions for the ternary systems of water + cyclopentanone + organic solvents at $T = 298.2$ K. ....	68
<b>Table 4.1</b> Source and important physical properties of chemicals. ....	77
<b>Table 4.2</b> Solubility data in mass fractions ( $w_i$ ) for the ternary systems of (water (1) + cyclopentanol (2) + organic solvents (3)) at $T = 298.2$ K and atmospheric pressure. <sup>a</sup> .....	81
<b>Table 4.3</b> Tie-line data in mass fractions for the ternary systems of (water (1) + cyclopentanol (2) + organic solvents (3)) at $T = 298.2$ K and atmospheric pressure. <sup>a</sup> .....	82
<b>Table 4.4</b> Distribution coefficients ( $D$ ) and separation factors ( $S$ ) for the ternary systems of (water (1) + cyclopentanol (2) + organic solvents (3)) at $T = 298.2$ K. ....	86
<b>Table 4.5</b> Total mass ( $m_{\text{total}}$ ) and percentage separation ( $E$ ) of cyclopentanol for the ternary systems of (water (1) + cyclopentanol (2) + organic solvents (3)) at $T = 298.2$ K. ....	88
<b>Table 4.6</b> NRTL binary interaction parameters for the ternary systems of (water (1) + cyclopentanol (2) + organic solvents (3)) at $T = 298.2$ K. ....	90

<b>Table 4.7</b> Modeling of the NRTL tie-line values in mass fractions for the ternary systems of (water (1) + cyclopentanol (2) + organic solvents (3)) at $T = 298.2$ K. ....	92
<b>Table 5.1</b> Sources and important physical properties of chemicals. ....	103
<b>Table 5.2</b> Characteristics of operating parameters for silver ion extraction using D2EHPA [21]. ....	105
<b>Table 5.3</b> Equilibrium data of solubility for binary systems in this work together with the literature at the temperature of 298.2 K along with pressure of 0.1 MPa. <sup>a</sup> ....	108
<b>Table 5.4</b> Equilibrium data of solubility for water (1) + D2EHPA (2) + organic solvents (3) at the temperature of 298.2 K along with pressure of 0.1 MPa. <sup>a</sup> ....	108
<b>Table 5.5</b> Equilibrium data of tie-lines for water (1) + D2EHPA (2) + organic solvents (3) at the temperature of 298.2 K along with pressure of 0.1 MPa. <sup>a</sup> ....	110
<b>Table 5.6</b> Slopes of log-log plot between $K_{d, Ag^+}$ and D2EHPA concentration in various organic solvents at aqueous pH of 1. ....	115
<b>Table 5.7</b> Binary interaction parameters for water (1) + D2EHPA (2) + organic solvents (3) at the temperature of 298.2 K. ....	119
<b>Table 5.8</b> Modeling results of tie-lines for water (1) + D2EHPA (2) + organic solvents (3) at the temperature of 298.2 K. ....	121
<b>Table 6.1</b> Properties of the hollow fiber module. ....	139
<b>Table 6.2</b> Values of R-squared and percentage of deviation for 1 and 2 orders. ....	143
<b>Table 6.3</b> The relevant parameters used in the model. ....	146
<b>Table 7.1</b> Application of HFSLM to low-level metal extraction. ....	156
<b>Table 7.2</b> Sources and mass fraction purity of chemicals. ....	169

<b>Table 7.3</b> Properties of the hollow fiber module.....	170
<b>Table 7.4</b> The relevant parameters used in the models. ....	184
<b>Table 8.1</b> Examples of the methods for the separation of silver ions.....	198
<b>Table 8.2</b> Properties of pharmaceutical wastewater. ....	209
<b>Table 8.3</b> Key features of the hollow fiber module. ....	210
<b>Table 8.4</b> Reaction orders and reaction-rate constants of extraction and recovery of silver ions.....	222
<b>Table 8.5</b> Relevant parameters used in the fluid-flow models.....	222



## LIST OF FIGURES

	Page
<b>Figure 1.1</b> Wastewater generated from quantitative analysis of NaCl and $C_{12}H_{22}O_{11}$ in the pharmaceutical processes. ....	2
<b>Figure 1.2</b> Simple facilitated transport of neutral metal complex in the HFSLM: A – neutral metal complex, B – neutral extractant, AB – metal-extractant complex.....	4
<b>Figure 1.3</b> Coupled facilitated co-transport of metal anion complex in the HFSLM: $A^-$ – metal anion complex, $H^+$ – hydrogen ion, B – basic extractant, AHB – metal-hydrogen ion-extractant complex.....	5
<b>Figure 1.4</b> Coupled facilitated counter-transport of metal cation in the HFSLM: $A^+$ – metal cation, $H^+$ – hydrogen ion, HB – acidic extractant, AB – metal-extractant complex. ....	6
<b>Figure 2.1</b> Binodal curve diagram for (water + furfuryl alcohol + organic solvents) at $T = 298.2$ K and atmospheric pressure; (-O-) MIBK, (-□-) ethyl acetate, (-Δ-) furfural and (-◇-) <i>n</i> -butanol. ....	31
<b>Figure 2.2</b> Ternary diagram for LLE of [water (1) + furfuryl alcohol (2) + MIBK (3)] at $T = 298.2$ K and atmospheric pressure; (—●—) experimental tie-line data, (—■—) calculated NRTL data, (●▲●) calculated UNIQUAC data and (—◆—) calculated UNIFAC data. ....	33
<b>Figure 2.3</b> Ternary diagram for LLE of [water (1) + furfuryl alcohol (2) + ethyl acetate (3)] at $T = 298.2$ K and atmospheric pressure; (—●—) experimental tie-line data, (—■—) calculated NRTL data, (●▲●) calculated UNIQUAC data and (—◆—) calculated UNIFAC data. ....	33

- Figure 2.4** Ternary diagram for LLE of [water (1) + furfuryl alcohol (2) + furfural (3)] at  $T = 298.2$  K and atmospheric pressure; (—●—) experimental tie-line data, (—■—) calculated NRTL data, (●▲●) calculated UNIQUAC data and (—◆—) calculated UNIFAC data. .... 34
- Figure 2.5** Ternary diagram for LLE of [water (1) + furfuryl alcohol (2) + *n*-butanol (3)] at  $T = 298.2$  K and atmospheric pressure; (—●—) experimental tie-line data, (—■—) calculated NRTL data, (●▲●) calculated UNIQUAC data and (—◆—) calculated UNIFAC data. .... 34
- Figure 2.6** Separation factor ( $S$ ) plotted against the mass fraction of furfuryl alcohol in aqueous-rich phase ( $w_{21}$ ) at  $T = 298.2$  K and atmospheric pressure; (○) MIBK, (□) ethyl acetate, (Δ) furfural and (◇) *n*-butanol. .... 37
- Figure 3.1** Chemical structure of cyclopentanone. .... 51
- Figure 3.2** Binodal curves for ternary systems of water + cyclopentanone + organic solvents at  $T = 298.2$  K and atmospheric pressure; (-○-) MIBK, (-□-) ethyl acetate, (-Δ-) furfural and (-◇-) *n*-butanol. .... 55
- Figure 3.3** Ternary diagram for LLE of the system of water (1) + cyclopentanone (2) + MIBK (3) at  $T = 298.2$  K and atmospheric pressure; (—●—) experimental tie-line data, (—■—) calculated NRTL data and (●▲●) calculated UNIQUAC data. .... 57
- Figure 3.4** Ternary diagram for LLE of the system of water (1) + cyclopentanone (2) + ethyl acetate (3) at  $T = 298.2$  K and atmospheric pressure; (—●—) experimental tie-line data, (—■—) calculated NRTL data and (●▲●) calculated UNIQUAC data. .... 57
- Figure 3.5** Ternary diagram for LLE of the system of water (1) + cyclopentanone (2) + furfural (3) at  $T = 298.2$  K and atmospheric pressure; (—●—) experimental tie-line data, (—■—) calculated NRTL data and (●▲●) calculated UNIQUAC data. .... 58

- Figure 3.6** Ternary diagram for LLE of the system of water (1) + cyclopentanone (2) + *n*-butanol (3) at  $T = 298.2$  K and atmospheric pressure; (—●—) experimental tie-line data, (—■—) calculated NRTL data and (●▲●) calculated UNIQUAC data. .... 58
- Figure 3.7** Othmer-Tobias plot for the ternary systems of water (1) + cyclopentanone (2) + organic solvents (3) at  $T = 298.2$  K and atmospheric pressure; (○) MIBK, (□) ethyl acetate, (Δ) furfural and (◇) *n*-butanol..... 60
- Figure 3.8** Hand plot for the ternary systems of water (1) + cyclopentanone (2) + organic solvents (3) at  $T = 298.2$  K and atmospheric pressure; (○) MIBK, (□) ethyl acetate, (Δ) furfural and (◇) *n*-butanol..... 60
- Figure 3.9** Separation factors ( $S$ ) plotted against the mass fraction of cyclopentanone in aqueous-rich phase ( $w_{21}$ ) at  $T = 298.2$  K and atmospheric pressure; (○) MIBK, (□) ethyl acetate, (Δ) furfural and (◇) *n*-butanol..... 63
- Figure 4.1** Solubility curves for ternary systems of (water + cyclopentanol + organic solvents) at  $T = 298.2$  K and atmospheric pressure; (-○-) MIBK, (-□-) ethyl acetate, (-Δ-) furfural and (-◇-) *n*-butanol. .... 81
- Figure 4.2** Ternary diagram for the LLE system of (water (1) + cyclopentanol (2) + MIBK (3)) at  $T = 298.2$  K and atmospheric pressure; (—●—) experimental tie-line data and (—■—) calculated NRTL data. .... 83
- Figure 4.3** Ternary diagram for the LLE system of (water (1) + cyclopentanol (2) + ethyl acetate (3)) at  $T = 298.2$  K and atmospheric pressure; (—●—) experimental tie-line data and (—■—) calculated NRTL data..... 83
- Figure 4.4** Ternary diagram for the LLE system of (water (1) + cyclopentanol (2) + furfural (3)) at  $T = 298.2$  K and atmospheric pressure; (—●—) experimental tie-line data and (—■—) calculated NRTL data. .... 84

- Figure 4.5** Ternary diagram for the LLE system of (water (1) + cyclopentanol (2) + *n*-butanol (3)) at  $T = 298.2$  K and atmospheric pressure; (—●—) experimental tie-line data and (—■—) calculated NRTL data..... 84
- Figure 4.6** Separation factors plotted against the mass fraction of cyclopentanol in aqueous-rich phase ( $w_{21}$ ) at  $T = 298.2$  K and atmospheric pressure; (○) MIBK, (□) ethyl acetate, (Δ) furfural and (◇) *n*-butanol..... 87
- Figure 5.1** Solubility curves for water + D2EHPA + organic solvents at the temperature of 298.2 K and atmospheric pressure; (—●—) kerosene, (—■—) cyclohexane, (—▲—) chloroform and (—◆—) 1-octanol. .... 109
- Figure 5.2** LLE ternary diagram of water (1) + D2EHPA (2) + kerosene (3) at the temperature of 298.2 K along with atmospheric pressure; (—) solubility line for kerosene, (—●—) experimental tie-lines and (—■—) modeling NRTL results. .... 111
- Figure 5.3** LLE ternary diagram of water (1) + D2EHPA (2) + cyclohexane (3) at the temperature of 298.2 K along with atmospheric pressure; (—) solubility line for cyclohexane, (—●—) experimental tie-lines and (—■—) modeling NRTL results. 111
- Figure 5.4** LLE ternary diagram of water (1) + D2EHPA (2) + chloroform (3) at the temperature of 298.2 K along with atmospheric pressure; (—) solubility line for chloroform, (—●—) experimental tie-lines and (—■—) modeling NRTL results. .... 112
- Figure 5.5** LLE ternary diagram of water (1) + D2EHPA (2) + 1-octanol (3) at the temperature of 298.2 K along with atmospheric pressure; (—) solubility line for 1-octanol, (—●—) experimental tie-lines and (—■—) modeling NRTL results. .... 112
- Figure 5.6** Percentage extractions of silver ions by liquid-liquid extraction for different organic solvents: aqueous pH of 1, 0.01 mol/L of silver ions, 0.001 mol/L of D2EHPA and volume per phase of 0.045 L..... 113

<b>Figure 5.7</b> Plot of $K_{d, Ag^+}$ versus log [D2EHPA]: aqueous pH of 1, 0.01 mol/L of silver ions and volume per phase of 0.045 L. ....	115
<b>Figure 5.8</b> IR spectra of silver-D2EHPA complex in the different organic solvents and pure D2EHPA: (a) 1-octanol, (b) chloroform, (c) cyclohexane, (d) kerosene and (e) pure D2EHPA. ....	117
<b>Figure 6.1</b> Schematic transport mechanism of copper ion in the liquid membrane phase. ....	134
<b>Figure 6.2</b> Transport of copper ions in the hollow fiber. ....	136
<b>Figure 6.3</b> Chemical structure of LIX 84-I. ....	140
<b>Figure 6.4</b> Schematic counter-current flow diagram for a single-module operation in the HFSLM: 1) feed reservoir, 2) gear pumps, 3) inlet pressure gauges, 4) outlet pressure gauges, 5) hollow fiber module, 6) flow meters and 7) stripping reservoir. ....	141
<b>Figure 6.5</b> The integral concentrations of Cu(II) and separation time. ....	142
<b>Figure 6.6</b> Comparison of Cu(II) extraction by HFSLM with different extractants at different Cu(II) concentrations in feed solution. ....	144
<b>Figure 6.7</b> Comparison of Cu(II) extraction by HFSLM with different extractants at different feed flow rates. ....	145
<b>Figure 6.8</b> The relationship between Cu(II) concentration and separation time. ....	146
<b>Figure 7.1</b> Facilitated coupled counter-transport of silver ions across HFSLM. ....	161
<b>Figure 7.2</b> Schematic diagram of a single hollow-fiber module with counter-current circulating flow patterns of feed and stripping solutions: 1) feed reservoir 2) gear pumps 3) gate valves 4) flow meters 5) inlet pressure gauges 6) hollow-fiber module 7) outlet pressure gauges and 8) stripping reservoir. ....	172

- Figure 7.3** Silver ion extraction ( $E$ ) by liquid-liquid extraction: Cyanex 923, D2EHPA and LIX 84-I dissolving in kerosene at the concentration of each 0.1 M..... 173
- Figure 7.4** Silver ion pertraction ( $P$ ) by liquid-liquid extraction:  $\text{CH}_4\text{N}_2\text{S}$  and  $\text{Na}_2\text{S}_2\text{O}_3$  solutions with each concentration 0.1 M. .... 174
- Figure 7.5** Extraction ( $E$ ) and pertraction ( $P$ ) of silver ions by HFSLM in counter-current circulating flow patterns against pH of feed solution: pH sodium thiosulphate solution of 2; 0.1 M of LIX 84-I concentration; 0.5 M of sodium thiosulphate concentration; equal flow rates of feed and sodium thiosulphate solutions at  $0.2 \text{ dm}^3/\text{min}$ . .... 175
- Figure 7.6** Extraction ( $E$ ) and pertraction ( $P$ ) of silver ions by HFSLM in counter-current circulating flow patterns against pH of sodium thiosulphate solution: pH feed solution of 3.5; 0.1 M of LIX 84-I concentration; 0.5 M of sodium thiosulphate concentration; equal flow rates of feed and sodium thiosulphate solutions at  $0.2 \text{ dm}^3/\text{min}$ . .... 176
- Figure 7.7** Extraction ( $E$ ) and pertraction ( $P$ ) of silver ions by HFSLM in counter-current circulating flow patterns against the concentration of LIX 84-I: pH feed and pH sodium thiosulphate solutions of 3.5 and 2, respectively; 0.5 M of sodium thiosulphate concentration; equal flow rates of feed and sodium thiosulphate solutions at  $0.2 \text{ dm}^3/\text{min}$ . .... 177
- Figure 7.8** Extraction ( $E$ ) and pertraction ( $P$ ) of silver ions by HFSLM in counter-current circulating flow patterns against the concentration of sodium thiosulphate solution: pH feed and pH sodium thiosulphate solutions of 3.5 and 2, respectively; 0.1 M of LIX 84-I concentration; equal flow rates of feed and sodium thiosulphate solutions at  $0.2 \text{ dm}^3/\text{min}$ . .... 178

- Figure 7.9** Extraction ( $E$ ) and pertraction ( $P$ ) of silver ions by HFSLM in counter-current circulating flow patterns against the flow rates of feed and sodium thiosulphate solutions: pH feed and pH sodium thiosulphate solutions of 3.5 and 2, respectively; 0.1 M of LIX 84-I concentration; 0.5 M of sodium thiosulphate concentration. .... 179
- Figure 7.10** Extraction ( $E$ ) and pertraction ( $P$ ) of silver ions by HFSLM in circulating flow patterns against the flow direction: pH feed and pH sodium thiosulphate solutions of 3.5 and 2, respectively; 0.1 M of LIX 84-I concentration; 0.5 M of sodium thiosulphate concentration; equal flow rates of feed and sodium thiosulphate solution at  $0.2 \text{ dm}^3/\text{min}$ . .... 180
- Figure 7.11** Extraction ( $E$ ) and pertraction ( $P$ ) of silver ions by HFSLM in counter-current flow directions against the flow pattern: pH feed and pH sodium thiosulphate solutions of 3.5 and 2, respectively; 0.1 M of LIX 84-I concentration; 0.5 M of sodium thiosulphate concentration; equal flow rates of feed and sodium thiosulphate solutions at  $0.2 \text{ dm}^3/\text{min}$ . .... 181
- Figure 7.12** Effect of ferric ions in wastewater on silver ion pertraction by HFSLM: pH of wastewater in ferric ion presence and ferric ion precipitation of 6 and 3.5; pH sodium thiosulphate solution of 2; 0.1 M of LIX 84-I concentration; 0.5 M of sodium thiosulphate concentration; equal flow rates of feed and sodium thiosulphate solutions at  $0.2 \text{ dm}^3/\text{min}$ . .... 182
- Figure 7.13** Concentration of silver ions in HFSLM system with respect to diffusion flux and reaction flux models at different separation times: counter-current flow directions, pH feed and pH sodium thiosulphate solutions of 3.5 and 2, respectively; 0.1 M of LIX 84-I concentration; 0.5 M of sodium thiosulphate concentration; equal flow rates of feed and sodium thiosulphate solutions at  $0.2 \text{ dm}^3/\text{min}$ . .... 184

<b>Figure 8.1</b> Transport of silver ion in the HFSLM system.....	201
<b>Figure 8.2</b> Transport of silver ions through small segments (a) in feed phase (inside the hollow fibers) (b) in stripping phase (outside the hollow fibers). .....	204
<b>Figure 8.3</b> Chemical structure of LIX 84-I.....	210
<b>Figure 8.4</b> Schematic diagram of a single hollow fiber module with counter-current circulating flow patterns of feed and stripping solutions: (1) feed reservoir, (2) gear pumps, (3) gate valves, (4) flow meters, (5) inlet pressure gauges, (6) hollow fiber module, (7) outlet pressure gauges, and (8) stripping reservoir. ....	212
<b>Figure 8.5</b> Extraction and recovery of silver ions via the HFSLM by counter-current flow against (a) pH of feed solution and (b) pH of stripping solution ( 0.1 M LIX 84-I, 0.5 M Na <sub>2</sub> S <sub>2</sub> O <sub>3</sub> , and equal flow rates of feed and stripping solutions at 0.2 dm <sup>3</sup> /min). .....	214
<b>Figure 8.6</b> Extraction and recovery of silver ions via the HFSLM by counter-current flow against concentration of the extractant (pH of feed and stripping solutions at 3.5 and 2, 0.5 M Na <sub>2</sub> S <sub>2</sub> O <sub>3</sub> , and equal flow rates of feed and stripping solutions at 0.2 dm <sup>3</sup> /min).....	215
<b>Figure 8.7</b> Extraction and recovery of silver ions via the HFSLM by counter-current flow against concentration of the stripping solution (pH of feed and stripping solutions at 3.5 and 2, 0.1 M LIX 84-I, and equal flow rates of feed and stripping solutions at 0.2 dm <sup>3</sup> /min). .....	216
<b>Figure 8.8</b> Extraction and recovery of silver ions via the HFSLM by counter-current flow against flow rates of feed and stripping solutions (pH of feed and stripping solutions at 3.5 and 2, 0.1 M of LIX 84-I, and 0.5 M Na <sub>2</sub> S <sub>2</sub> O <sub>3</sub> ).....	218

- Figure 8.9** Plot of  $\overline{[AgR]}_m [H^+]_f$  against  $[Ag^+]_f \overline{[HR]}_m^2$  for the extraction equilibrium constant of silver ion extraction via the HFSLM at the optimum conditions (pH of feed and stripping solutions at 3.5 and 2, 0.1 M LIX 84-I, 0.5 M Na<sub>2</sub>S<sub>2</sub>O<sub>3</sub>, and equal flow rates of feed and stripping solutions at 0.2 dm<sup>3</sup>/min). ..... 219
- Figure 8.10** Plot of  $-V_f \ln(C_{z,f}^j / C_{0,f}^j)$  against  $t$  for the permeability coefficient of silver ions in the feed phase at the optimum conditions (pH of feed and stripping solutions at 3.5 and 2, 0.1 M LIX 84-I, 0.5 M Na<sub>2</sub>S<sub>2</sub>O<sub>3</sub>, and equal flow rates of feed and stripping solutions at 0.2 dm<sup>3</sup>/min). ..... 220
- Figure 8.11** Plot of  $1/P$  against  $[H^+]_f / \overline{[HR]}_m^2$  for mass transfer coefficient of silver ions in feed solution and in liquid membrane at the optimum experimental conditions (pH of feed and stripping solutions at 3.5 and 2, 0.5 M Na<sub>2</sub>S<sub>2</sub>O<sub>3</sub>, and equal flow rates of feed and stripping solutions at 0.2 dm<sup>3</sup>/min). ..... 221
- Figure 8.12** Stability of HFSLM for extraction and recovery of silver ions and the validation of fluid-flow models at the optimum conditions (pH of feed and stripping solutions at 3.5 and 2, 0.1 M LIX 84-I, 0.5 M Na<sub>2</sub>S<sub>2</sub>O<sub>3</sub>, and equal flow rates of feed and stripping solutions at 0.2 dm<sup>3</sup>/min). ..... 224
- Figure 8.13** Experimental and model results by fluid flow model compared with other models and adaptability of fluid-flow model (FFM = fluid-flow model; RFM = reaction flux model; MTM = mass transfer model). ..... 226

# Chapter I

## Introduction

### 1.1 Rationale of research problem

In the pharmaceutical processes of the Government Pharmaceutical Organization of Thailand, silver nitrate solution is used to determine the quantity of sodium chloride. Thus, in the end of the process, the wastewater contains silver ions. It is normally mixed with wastewater containing ferric ions from quantitative analysis of sucrose by ferric chloride solution. Figure 1.1 summarizes flowchart of the wastewater generated from quantitative analysis of NaCl and C<sub>12</sub>H<sub>22</sub>O<sub>11</sub> in the pharmaceutical processes. Wastewater that contains 30 mg/L silver ions and 120 mg/L ferric ions, totally 100 L/month, was generated. The wastewater is then transferred to the Safety and Environment Division for treatment. Based on Industrial Wastewater Regulation, for less environmental impact, the concentration of silver and ferric ions must be lower than 1 and 10 mg/L, respectively<sup>1</sup>. It is reported that silver ions at 1-5 mg/L can kill aquatic micro-organisms, insects, trout and flounder<sup>2</sup>. Moreover, the accumulation of silver ions in the human body of 3.8 g can lead to argyria disease that gives the appearance of blue skin<sup>3</sup>. In the case of ferric ions, its accumulation of 100-200 mg/weight of body mass can kill all animals<sup>4</sup>. Ferric ions are generally treated by chemical precipitation using phosphoric acid solution. In fact, chemical precipitation is of most effective in separating metal ions at high concentration<sup>5</sup>. By using this method, the concentration of ferric ions reaches 0.35 mg/L, which is lower than the mandatory discharge limit. However, in regard to treat and separate silver ions, particularly at a low concentration, as silver is valuable, it is difficult to seek an appropriate method.

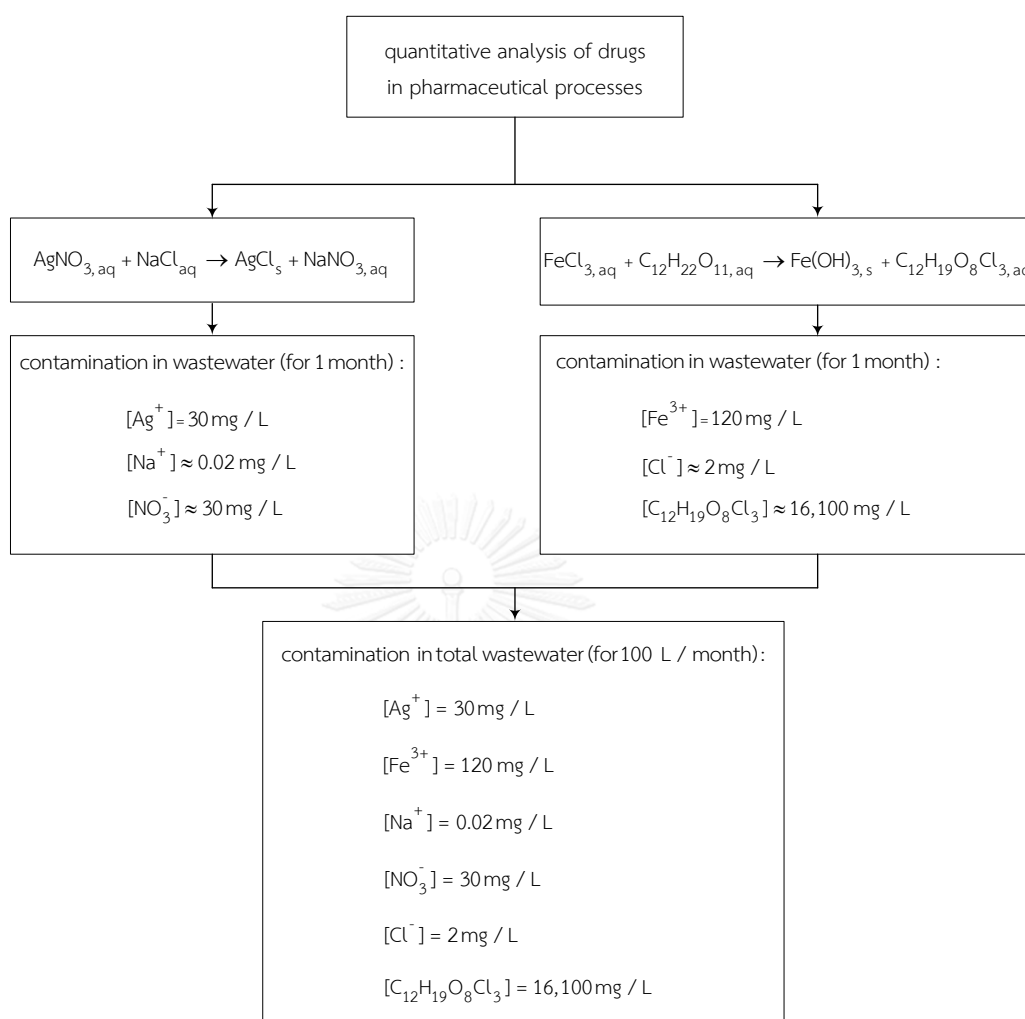


**Figure 1.1** Wastewater generated from quantitative analysis of NaCl and  $\text{C}_{12}\text{H}_{22}\text{O}_{11}$  in the pharmaceutical processes.

Concerning the point mentioned above, a high-efficiency separation method is required to extract and recover silver ions from pharmaceutical wastewater. It is known that hollow fiber supported liquid membrane (HFSLM) has been successful in separating metal ions at a very low concentration in ppm- or ppb-level<sup>6-9</sup>. Other advantages of HFSLM are simultaneous extraction and recovery in one single stage, high mass transfer flux of metal-extractant complexes through liquid membrane phase, low energy and operating costs<sup>10</sup>. In the HFSLM, the mixture of extractant and organic solvent is used as the liquid membrane which is embedded into the micro-

pores of the hollow fibers. Wastewater or feed solution and stripping solution are pumped into the tube and shell sides of the hollow fibers, respectively. The feed and stripping solutions contact with liquid membrane phase at the interfaces of tube and shell sides. This characteristic results in a highly effective surface area for metal ion separation. The suitable extractant, organic solvent and stripping solution can then be selected for use in the HFSLM. Since the physical and chemical properties of the extractants and stripping solutions, and the organic solvents are different, and therefore the metal-ion separation efficiencies are different<sup>11-13</sup>. It is reported that types of the organic solvents affect the stability of liquid membrane<sup>14</sup>. According to the merits of the HFSLM, it was used in this work to separate silver ions from the pharmaceutical wastewater.

## 1.2 Extraction and recovery of metal ions via HFSLM

HFSLM is composed of 3 phases as follows:

- a) Feed phase – wastewater or aqueous solution containing metal ions or target species
- b) Liquid membrane phase – a mixture of extractant and organic solvent (or a mixture of extractants and organic solvent in case of synergistic extraction) for the extraction of metal ions or target species from feed phase
- c) Stripping phase – distilled water or stripping solution for the recovery of metal ions or target species from liquid membrane phase

The transport mechanisms of metal ions in the HFSLM can be divided into 3 cases based on types of the extractants and metal ion forms (cation, neutral complex or anion complex). Details of each transport mechanism are shown below<sup>15</sup>:

- a) Simple facilitated transport – this transport mechanism is presented in Figure 1.2 to describe the extraction and recovery of neutral metal complex using a neutral extractant. The neutral extractant reacts with the neutral

metal complex at the feed-liquid membrane interface to form metal-extractant complex, which diffuses through the liquid membrane phase to the liquid membrane-stripping interface. Thereafter, the neutral metal complex is released into the stripping phase. At the same time, the neutral extractant diffuses backwards to the feed-liquid membrane interface, and reacts again with the neutral metal complex in the feed phase.

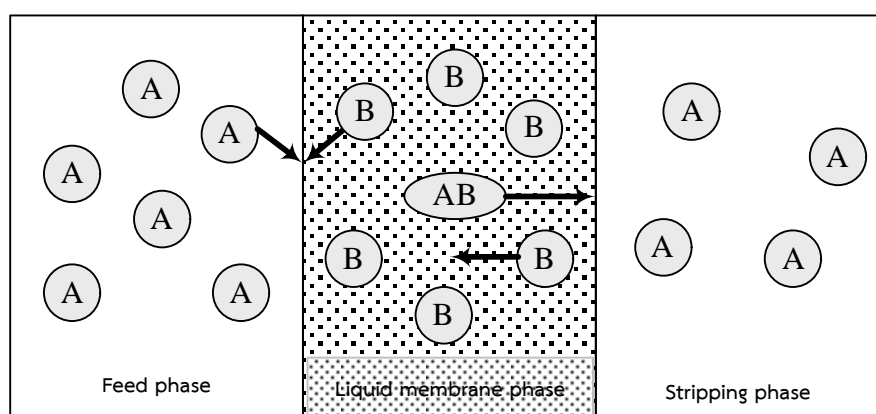


**Figure 1.2** Simple facilitated transport of neutral metal complex in the HFSLM: A – neutral metal complex, B – neutral extractant, AB – metal-extractant complex.

- b) Coupled facilitated co-transport – this transport mechanism is presented in Figure 1.3 to describe the extraction and recovery of metal anion complex using a basic extractant. The metal anion complex and hydrogen ion in the feed phase react with the basic extractant at the feed-liquid membrane interface to form complex of metal anion complex, hydrogen ion and extractant (or metal-hydrogen ion-extractant complex). Thereafter, the metal-hydrogen ion-extractant complex diffuses through the liquid membrane phase, reacts with the basic stripping solution at the liquid membrane-stripping interface, and releases the metal anion complex and hydrogen ion into the stripping phase. The basic extractant diffuses backwards to the feed-liquid membrane interface, and reacts again with the metal anion complex and hydrogen ion in the feed phase.

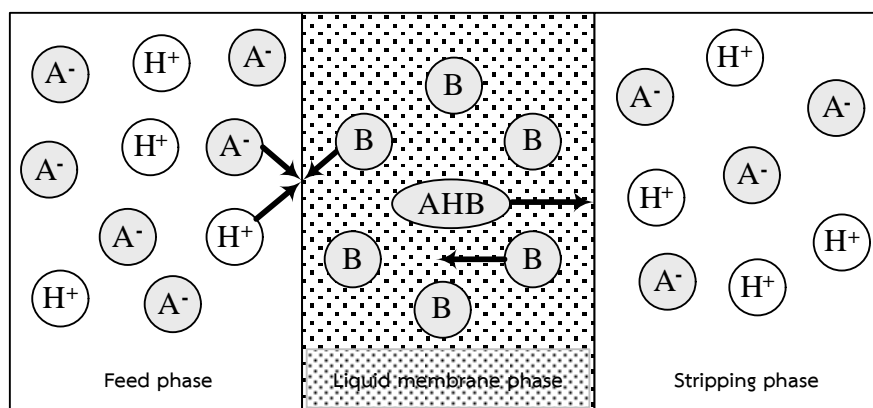


**Figure 1.3** Coupled facilitated co-transport of metal anion complex in the HFSLM:  $A^-$  – metal anion complex,  $H^+$  – hydrogen ion, B – basic extractant, AHB – metal-hydrogen ion-extractant complex.

- c) Coupled facilitated counter-transport – this transport mechanism is presented in Figure 1.4 to describe the extraction and recovery of metal cation using an acidic extractant. The acidic extractant reacts with metal cation at the feed-liquid membrane interface to form metal-extractant complex in the liquid membrane phase, and releases hydrogen ion into the feed phase. Thereafter, the metal-extractant complex diffuses through the liquid membrane phase, reacts with the acidic stripping solution at the liquid membrane-stripping interface, and releases metal cation into the stripping phase. The acidic extractant interacts with the hydrogen ion in the stripping phase and then diffuses backwards to the feed-liquid membrane interface, and reacts again with the metal cation in the feed phase.

In this work, the extraction and recovery of silver ions can be described by the coupled facilitated counter-transport.

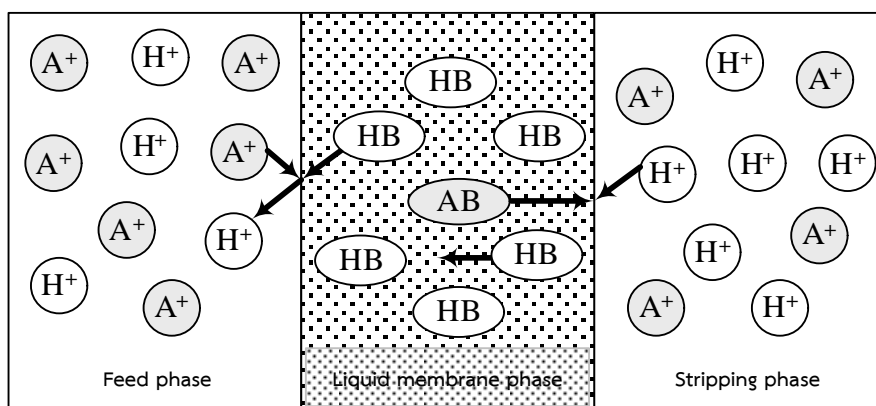


**Figure 1.4** Coupled facilitated counter-transport of metal cation in the HFSLM:  $A^+$  – metal cation,  $H^+$  – hydrogen ion, HB – acidic extractant, AB – metal-extractant complex.

Based on the transport mechanisms, the following parameters, e.g., physical and chemical properties of the extractants, organic solvents and stripping solutions, play important roles to the extraction and recovery of metal ions via the HFSLM. The mathematical models likewise are used as a tool to describe the transport of metal ions through the HFSLM and to predict the extraction and recovery efficiency as well as the separation time<sup>16</sup>. A brief summary of the parameters and mathematical models is given below:

### 1.2.1 Extractants

The chemical structure of extractants for metal ion extraction is ligand-liked<sup>17</sup>, consisting of a functional group with one donor atom such as nitrogen, phosphorus, oxygen, or sulfuric. Generally, functional groups are classified as acidic functional groups, e.g., carboxylic ( $-CO_2H$ ), sulfonic ( $-SO_3H$ ), phosphoric ( $-PO(OH)_2$ ), and basic functional groups, e.g., ether ( $-O-$ ), alcohol ( $-OH$ ), oxime ( $=N-OH$ ). During the last decade, an increase of functional groups into the extractant molecule has been adopted to improve the stability of chemical bonding of the metal-extractant

complexes. Chelating agent is very well-known extractant using for metal ion extraction. It contains two functional groups that are acid-acid, base-base or acid-base. The extraction behaviors of chelating agents include:

- a) Functional groups of acid-acid – the donor atoms in the acidic functional groups give hydrogen ions to dissociate electrons to interact with metal ion.
- b) Functional groups of base-base – the donor atoms in the basic functional groups carry the lone pairs of electrons to interact with metal ion.
- c) Functional groups of acid-base – their extraction behavior is similar to that of the acidic-acidic functional groups<sup>17</sup>.

According to chemical structure of the extractant, transport mechanism and metal ion forms<sup>18</sup>, the extractants can be classified into:

- a) Organic acid extractants – for extraction of metal cations
- b) Chelating extractants – for extraction of metal cations
- c) Neutral or solvating extractants – for extraction of neutral metal complexes
- d) Ligand substitution extractants – for extraction of metal anion complexes
- e) Basic or ion-pair extractants – for extraction of metal anion complexes

Details of each class are shown below:

#### 1.2.1.1 Organic acid extractants

Organic acid extractant reacts with metal cations at the feed-liquid membrane interface by releasing hydrogen ions into the feed phase. Thus, the extraction efficiency depends on the pH of feed solution that corresponds to the concentration of hydrogen ions in the feed phase. Examples of organic acid extractants are di(2-ethylhexyl) phosphoric acid (D2EHPA), bis(2,2,4-trimethyl-pentyl) phosphinic acid

(Cyanex 272)<sup>18</sup>. In addition, the chemical reaction of metal cation and D2EHPA ((C<sub>8</sub>H<sub>17</sub>O)<sub>2</sub>PO<sub>2</sub>H) is shown in Eq. (1.1)<sup>19</sup>:



where the subscripts of <sub>aq</sub> and <sub>org</sub> are the aqueous (feed) and organic (liquid membrane) phases, respectively.

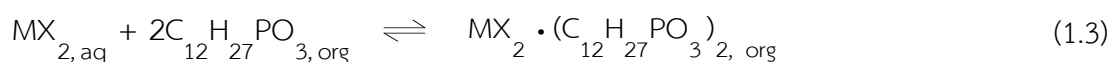
### 1.2.1.2 Chelating extractants

Chelating extractants with the functional groups of acid-acid and acid-base show similar extraction behavior to the organic acid extractants. Chelating extractant with base-base functional groups has similar extraction behavior to that of the basic or ion-pair extractants that is described in section 1.2.1.5. An example of chelating extractant is 2-hydroxy-5-nonylacetophenone oxime (LIX 84-I)<sup>18</sup>. The chemical reaction of metal cation and LIX 84-I (C<sub>17</sub>H<sub>27</sub>NO<sub>2</sub>) is shown in Eq. (1.2)<sup>20</sup>:



### 1.2.1.3 Neutral or solvating extractants

Neutral or solvating extractant reacts with neutral metal complexes at the feed-liquid membrane interface by replacing the molecules of water that hydrated around the neutral metal complexes. The examples of the neutral or solvating extractants are tri-*n*-octylphosphine oxide (TOPO), tributyl phosphate (TBP) and dibutyl butylphosphonate (DBBP)<sup>18</sup>. An example of the chemical reaction between the neutral metal complex (MX<sub>2</sub>) and DBBP (C<sub>12</sub>H<sub>27</sub>PO<sub>3</sub>) is expressed as follows<sup>21</sup>:

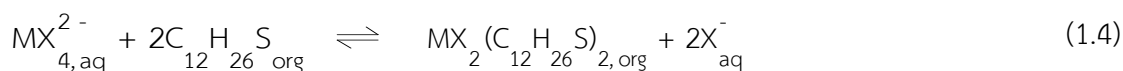


However, the extraction efficiency of neutral or solvating extractants is limited by the following factors:

- a) Stability of the chemical bonding of neutral metal complexes – the neutral metal complexes with low stability of chemical bonding dissociate to metal cations together with anions ( $X^-$ ) in the feed phase where the metal cations do not react with the neutral or solvating extractant.
- b) Solubility of metal-extractant complexes in the liquid membrane phase – the metal-extractant complexes with high solubility can diffuse rapidly through the liquid membrane phase.

#### 1.2.1.4 Ligand substitution extractants

Ligand substitution extractant reacts with metal anion complexes by giving the electron pairs to the inner shell of metal atoms and releasing anions into the feed phase. An example of a ligand substitution extractant is di-*n*-hexyl sulfide ( $C_{12}H_{26}S$ )<sup>18</sup>, and its chemical reaction with metal anion complex ( $MX_4^{2-}$ ) is presented in Eq. (1.4)<sup>22</sup>:

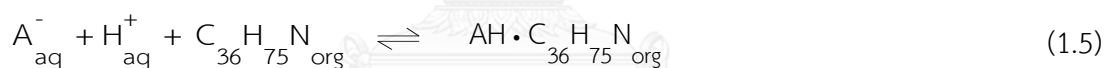


#### 1.2.1.5 Basic or ion-pair extractants

Basic or ion-pair extractant reacts with metal anion complexes in two steps as follows:

- a) Acidic molecules in the feed phase dissociate to hydrogen ions and anions to interact with the basic or ion-pair extractant at the feed-liquid membrane interface.
- b) Metal anion complexes interact with the new molecules of basic or ion-pair extractant by replacing anions to metal-co-ion-extractant complexes in the liquid membrane phase. The anions are then released in the feed phase.

Thus, the extraction efficiency of basic or ion-pair extractant is closely related to the capability of anions to attach to metal anion complexes in the feed phase. The common basic or ion-pair extractants are Alamine and Aliquat groups such as tri-lauryl ammine (Alamine 304-I), tri-*n*-octylamine (Alamine 336) and *n*-methyl-*n,n,n*-trioctyloctan-1-ammonium chloride (Aliquat 336)<sup>18</sup>. Examples of the chemical reaction between the acid (HA) and Alamine 304-I (C<sub>36</sub>H<sub>75</sub>N), and the chemical reaction between the metal anion complex and acid-Alamine 304-I are presented in Eqs. (1.5) and (1.6), respectively<sup>23</sup>:



Other concerned properties of extractants are<sup>24</sup>:

- a) High selective separation capacity of the extracted metal ions
- b) Rapid chemical reaction with metal ions
- c) No side reactions generated
- d) Low solubility in the feed and stripping phases
- e) Suitable density, viscosity and surface tension

For silver ion extraction, the efficient extractants mostly used are di(2-ethylhexyl) phosphoric acid (D2EHPA)<sup>5, 25-27</sup>, dicyclohexano18crown6 (DC18C6)<sup>28, 29</sup>, hexathia-18-crown-6 (HT18C6)<sup>30, 31</sup> and bis(2,4,4 trimethylpentyl) monothio phosphinic acid (Cyanex 302)<sup>32, 33</sup>.

### 1.2.2 Organic solvents

Organic solvents can be divided into 2 groups: polar and non-polar. The polarity of organic solvents is indicated by the dielectric constant that represents the strength of the electric field surrounding the molecules of organic solvents. Organic solvents which have dielectric constants lower than 15 are non-polar solvents<sup>34, 35</sup>. For extraction and recovery of metal ions, the organic solvent is a media for the diffusion of metal-extractant complexes and extractant. The metal-extractant complexes and the extractant form solvation molecules in the organic solvent by hydrogen bonding<sup>36</sup>. The stability of solvation molecules depends on the polarity of organic solvents<sup>37</sup>. Thus, the metal-extractant complexes and extractant interact well with polar solvents than non-polar solvents<sup>13</sup>. However, the polar solvents also interact well with water leading to the loss of liquid membrane phase to the feed and stripping phases<sup>38</sup>. Moreover, a high polar solvent like nitrobenzene strongly interacts with the extractant and results in lower extraction efficiency<sup>39</sup>. Other significant properties of organic solvents are viscosity and volatility. The organic solvents having low viscosity help the diffusion of metal-extractant complexes and extractant through the liquid membrane phase<sup>40</sup>. Organic solvents of high volatility can easily volatile from the liquid membrane phase, and consequently reduces the extraction efficiency. The typical organic solvents used are aliphatic and aromatic hydrocarbons, hydrophobic ethers and esters, long chain alcohols and mixtures of technical solvents like kerosene. Other important properties of the organic solvents are presented in Table 1.1. For silver ion extraction, kerosene and chloroform are frequently used<sup>25, 26, 41, 42</sup>.

**Table 1.1** The important properties of organic solvents used<sup>43-45</sup>.

Organic solvents	Solubility in water $\times 10^{-3}$ (kg/m <sup>3</sup> )	Viscosity $\times 10^3$ (Pa·sec)
Chloroform	0.01 <sup>a</sup>	0.56 <sup>b</sup>
Dihexyl ether	-	1.87
Diphenyl methane	6.51	2.96
Di- <i>n</i> -butyl phthalate	8.91	15.4
Dodecane	0.07	1.50
Heptane	-	0.38
Kerosene	-	1.24
<i>n</i> -Amyl benzoate	8.06	3.42
<i>o</i> -Nitrophenyloctylether	0.16	12.5
1-Octanol	-	7.47

<sup>a, b</sup> are the references of <sup>43</sup> and <sup>44</sup>, respectively.

### 1.2.3 Stripping solutions

Stripping solution recovers metal ions at the liquid membrane-stripping interface. Recovery reactions are the reverse reactions of their extraction. In order to select a suitable stripping solution, the following principles are taken into account<sup>46</sup>:

- a) Acidic stripping solutions for metal cation recovery – these stripping solutions give the hydrogen ions for replacing the metal cations in the molecules of metal-extractant complexes. The examples of acidic stripping solutions are nitric acid solution (HNO<sub>3</sub>)<sup>47</sup>, sulfuric acid solution (H<sub>2</sub>SO<sub>4</sub>)<sup>48</sup> and hydrochloric acid solution (HCl)<sup>49</sup>.
- b) Distilled water for the recovery of neutral metal complexes – molecules of distilled water replace the molecules of the extractant in the metal-extractant complexes to build new complexes with the neutral metal complexes, and release them into the stripping phase.
- c) Basic stripping solutions for the recovery of metal anion complexes – these stripping solutions give anions to replace the metal anion complexes in

the molecules of metal-hydrogen ion-extractant complexes, and release the metal anion complexes into the stripping phase. In this step, the hydrogen ions were also released into the stripping phase. The examples of basic stripping solutions are sodium hydroxide (NaOH)<sup>50</sup> and thiourea (SC(NH<sub>2</sub>)<sub>2</sub>)<sup>51</sup>.

Moreover, the stripping solutions having the donor atoms are favorable to high recovery efficiency. For silver ion recovery, sodium thiosulfate (Na<sub>2</sub>S<sub>2</sub>O<sub>3</sub>) is frequently used as the stripping solution<sup>28, 52, 53</sup>.

#### 1.2.4 pH of feed and stripping solutions

The pH of feed and stripping solutions influences the transport mechanisms of metal ions through the HFSLM. In order to determine the suitable pH of feed and stripping solutions, the transport mechanisms of metal ions are considered as follows<sup>54</sup>:

- a) Coupled facilitated counter-transport of metal cations corresponds to the transport of hydrogen ions from the stripping phase to the feed phase. In order to provide the driving force of hydrogen ion transport, the pH of feed and stripping solutions is considered together with the dissociation equilibrium constant (pKa) of the extractant. These values decrease in the following order  $\text{pH}_{\text{feed}} > \text{pKa} > \text{pH}_{\text{stripping}}$ .
- b) Coupled facilitated co-transport of metal anion complexes corresponds to the decomposition of acidic molecules in the feed phase and the reaction of metal anion complexes with anions in the stripping phase. Thus, feed pH must be low, but stripping pH must be high<sup>55</sup>.

The pH of feed and stripping solutions has no effect on simple facilitated transport of neutral metal complexes. This is because the extraction and recovery of neutral metal complexes correspond to the solvating interactions at the feed-liquid

membrane and liquid membrane-stripping interfaces<sup>56</sup>. For silver ion extraction and recovery involving coupled facilitated counter-transport, the pH of feed solution must be higher than the pH of stripping solution.

### 1.2.5 Concentration of the extractants

The concentration of the extractant has an influence on extraction and recovery efficiency as well as the diffusion of metal-extractant complexes through the liquid membrane phase. The extraction and recovery efficiency increase with the concentration of extractant<sup>57</sup>. Low concentration extractant results in low extraction and recovery of metal ions<sup>58</sup>. However, too high concentration of extractant leads to a decrease in extraction and recovery efficiency. For most extractant, high concentration relates to high viscosity which obstructs the diffusion of metal-extractant complexes<sup>59</sup>.

### 1.2.6 Concentration of the stripping solutions

The concentration of stripping solution also has an influence on the extraction and recovery of metal ions. An increase in stripping concentration results in higher extraction and recovery efficiency. However, too high a concentration of stripping solution leads to a decrease in efficiency. This is because the stripping solution reaches equilibrium which cannot recover the metal ions<sup>56</sup>. The concentration of the stripping solution must be based on the concentration of the extractant. For the recovery of silver ions, the concentration of anions is careful due to the precipitation of silver-anion complexes in the stripping phase<sup>28</sup>.

### 1.2.7 Flow rates of feed and stripping solutions

Flow rates of feed and stripping solutions in the feed and stripping phases have an influence on the contacting time of metal ions with the liquid membrane phase.

Moreover, the flow rates of both solutions have an influence on the stability of the liquid membrane phase. An increase in flow rates results in an increase in extraction and recovery efficiency. However, higher flow rates cause a decrease in contacting time and results in turbulent force which disturbs the stability of the liquid membrane phase. In addition, flow rates of feed and stripping solutions must be equal for prevention of different pressures which can disturb the liquid membrane stability<sup>60, 61</sup>. For the extraction and recovery of silver ions, low flow rates of both solutions are required to increase contacting time since silver ions have a slow reaction<sup>62</sup>.

### 1.2.8 Flow directions of feed and stripping solutions

Feed and stripping solutions flow through the HFSLM by means of two directions: co-current and counter-current. The counter-current direction results in different concentrations of metal ions and hydrogen ions in the feed and stripping phases. The different concentrations are the driving force which improves extraction and recovery efficiency<sup>63</sup>. Thus, flow direction of the most metal ions including silver ions is operated by counter-current direction.

### 1.2.9 Flow patterns of feed and stripping solutions

Flow patterns of feed and stripping solutions through the HFSLM are circulating, single-pass and semi-circulating. Characteristics of flow patterns are shown below:

- a) Circulating flow pattern – feed and stripping solutions flow through the HFSLM and then return back to the original reservoirs.
- b) Single-pass flow pattern – feed and stripping solutions flow from the original reservoirs into the new reservoirs.

- c) Semi-circulating flow pattern – feed solution flows through the HFSLM to the new reservoir while the stripping solution flows back to its original reservoir.

In order to select the flow pattern used, it can be considered case by case as follows:

- a) Circulating flow pattern is operated when feed and stripping solutions have a small volume and reactions of metal ions occur slowly.
- b) Single-pass flow pattern is operated in the cases of a large volume of feed and stripping solutions and rapid reactions of metal ions. However, when reactions occur slowly, the single-pass flow pattern is operated using the series modules of hollow fibers to increase the contacting time of metal ions with the liquid membrane phase.
- c) Semi-circulating flow pattern is operated when feed solution has a large volume and reactions of metal ions occur rapidly. However, in the case of slow reactions the semi-circulating flow pattern is operated using the series modules of hollow fibers.

In general, for the extraction and recovery of silver ions, the circulating flow pattern is used due to their slow reactions. However, if the feed solution has a large volume, the semi-circulating flow pattern is employed using the series modules of hollow fibers.

#### **1.2.10 Separation time of metal ion extraction and recovery**

The extraction and recovery of metal ions are operated using different times. The separation time for extraction and recovery of metal ions including silver ions is determined by the time that results in the highest amount of extraction and recovery.

### 1.2.11 Mathematical models in separation of metal ions via HFSLM

Mathematical models for metal ion extraction and recovery via HFSLM have been developed to describe the transport mechanism of metal ions in the HFSLM. The first model is based on the diffusion of metal ions through the liquid membrane phase. In this case, the mass transfer coefficients ( $k$ ) are calculated in order to obtain the phase controlling step. Then, the permeability coefficient ( $P$ ) of metal-extractant complexes in the liquid membrane phase is determined<sup>64-66</sup>. Lin and Juang<sup>67</sup> used this model to predict the concentration of copper ions in the feed phase. Kandwal et al.<sup>68</sup> also developed the model by considering convection and diffusion for the cesium ion extraction. However, Yang and Kocherginsky<sup>69</sup> discovered that the model cannot completely describe the extraction and recovery of copper ions in the HFSLM.

In this study, a mathematical model for copper ion extraction was developed. The model corresponds to the convection, reaction and accumulation of copper ions in the HFSLM. The extraction and recovery of palladium ions was also studied<sup>70</sup>. Thereafter, the model investigated silver ion extraction and recovery. The validity of the model was enhanced by including diffusion of silver ions. This model also examined the extraction of copper and tantalum ions.

### 1.3 Objectives of the dissertation

1. To extract and recover silver ions from the pharmaceutical wastewater via HFSLM.
2. To obtain final concentration of silver ions in the pharmaceutical wastewater lower than 1 mg/L.
3. To develop appropriate mathematical models for silver ion extraction and recovery.

#### 1.4 Scope of the dissertation

This work investigates the extraction and recovery of silver ions from pharmaceutical wastewater via HFSLM. The mathematical model is also examined to describe transport of silver ions in the HFSLM. The scope of this work is as follows:

1. First experiments focused on the selection of a suitable organic solvent by studying its solubility with the extractant and distilled water. Kerosene, cyclohexane, chloroform and 1-octanol were used as organic solvents in this work. Thereafter, a suitable extractant and stripping solution was determined by liquid-liquid extraction. LIX 84-I, D2EHPA and Cyanex 923 were employed as extractants while thiourea and sodium thiosulfate solutions were used as stripping solutions.
2. Second experiments focused on the extraction and recovery of silver ions via HFSLM. The selected extractant, organic solvent and stripping solution were used in the HFSLM. Feed and stripping solutions were operated by counter-circulating mode. Optimum conditions for the studied parameters were investigated as follows:
  - a) pH of feed and stripping solutions:
    - feed pH of 2-4
    - stripping pH of 1-3
  - b) Concentration of the selected extractant: 0.01-0.2 mol/L
  - c) Concentration of the selected stripping solution: 0.1-2 mol/L
  - d) Flow rates of feed and stripping solutions: 200-1,000 mL/min
  - e) Flow directions of feed and stripping solutions:
    - co-current flow direction
    - counter-current flow direction
  - f) Flow patterns of feed and stripping solutions:
    - circulating flow pattern

- single-pass flow pattern
  - semi-circulating flow pattern
  - g) Separation time: 0-30 min
  - h) Influence of ferric ion presence on silver ion extraction
3. Mathematical model involving convection, reaction and accumulation was developed for copper ion extraction via HFSLM. The model was also applied for silver ion extraction. Subsequently, the model was developed by including diffusion of silver ions and again applied for silver ion extraction and recovery.
  4. From the models, the concentration of copper ions in the feed solution and the concentration of silver ions in the feed and stripping phases were predicted by varying the time interval. Modeling results were validated by comparison with the experimental results and confirmed by the percentage deviation. Thereafter, the model was applied for extracting other metal ions such as copper and tantalum ions.

### 1.5 Expected results

1. High extraction and recovery of silver ions
2. Low concentration of silver ions in the pharmaceutical wastewater less than 1 mg/L
3. Practical mathematical models for silver ion extraction and recovery

### 1.6 Description of dissertation

This dissertation is divided into 9 chapters. Chapter I is the introduction that reports the rationale of the extraction and recovery of silver ions from pharmaceutical wastewater and the merits of the HFSLM for metal ions separation. The transport mechanisms of metal ions in the HFSLM, the important parameters

such as extractants, organic solvents, stripping solutions, pH of feed and stripping solutions, concentration of extractants, and so on, as well as the mathematical models are also presented in this chapter. Chapters II-VIII shows the published articles that included in the dissertation. For Chapters II-IV, various organic solvents were studied regarding their solubility in order to select the most suitable organic solvent for extraction of organic compounds. In Chapter V, experiments carried out in Chapters II-IV were used to determine the most suitable organic solvent for silver ion extraction. Chapter VI presents the mathematical model involving convection, reaction and accumulation of \*copper ions in the HFSLM in order to promote this mathematical model and its reliability.

*Note: \* The published article in chapter VI was presented before taking the proposal exam. For the study, the feed solution of copper ions from the previous student was firstly applied to this model before it was used with the feed solution of silver ions.*

Thus, the model was applied for silver ion extraction via the HFSLM as shown in Chapter VII and its results were compared with the diffusion model to describe the transport of silver ions. Optimum conditions were also determined to achieve the highest extraction and recovery of silver ions. Chapter VIII presents the development of this model by including diffusion of silver ions. Thereafter, the model was applied again for silver ion extraction and recovery. In addition, the model was applied for extractions of copper and tantalum ions. Chapter IX is the conclusion of the dissertation. Its limitations and recommendations are also presented in this chapter. Further details of this research are outlined below:

## Chapter II

This chapter presents the liquid-liquid equilibrium (LLE) solubility for the ternary systems of distilled water, furfuryl alcohol and organic solvents. Methyl isobutyl ketone (MIBK), ethyl acetate, furfural and *n*-butanol were used as the organic solvents. The solubility of furfuryl alcohol in the organic and aqueous phases was

also investigated and expressed by the tie-line data. A suitable organic solvent having high solubility with furfuryl alcohol but low solubility with distilled water was determined for furfuryl alcohol extraction. In addition, distribution coefficients and separation factors were determined for confirming the extraction capability of each organic solvent. Correlations of experimental tie-line data and modeling NRTL, UNIQUAC and UNIFAC results were also studied. Details are available in the published article of Fluid Phase Equilibria (page: 88-96, volume: 365 and year: 2014)<sup>71</sup>.

### Chapter III

This chapter focuses on the LLE solubility for the ternary systems of distilled water, cyclopentanone and organic solvents that were used in chapter II. Their solubility exhibited different behaviors when compared to the case of furfuryl alcohol. The tie-line data of cyclopentanone were determined and correlated with the modeling results of NRTL and UNIQUAC models. A suitable organic solvent was selected. Distribution coefficients and separation factors were also obtained. Details are described in the published article of Journal of Molecular Liquids (page: 98-106, volume: 196 and year: 2014)<sup>72</sup>.

### Chapter IV

This chapter highlights the LLE solubility for the ternary systems of distilled water, cyclopentanol and organic solvents using the same manner as in chapters II and III. Their solubility exhibited similar behavior as in the case of cyclopentanone. The tie-line data of cyclopentanol were determined and correlated with the modeling NRTL results. A suitable organic solvent was selected. Distribution coefficients and separation factors were also determined. Details are available in the published article of Fluid Phase Equilibria (page: 10-18, volume: 379 and year: 2014)<sup>73</sup>.

## Chapter V

This chapter applied the experimental method from the above chapters to study the LLE solubility of D2EHPA extractant with various organic solvents and distilled water for silver ion extraction. Kerosene, cyclohexane, chloroform and 1-octanol were used in this work. Influence of organic solvents on silver ion extraction was also investigated using D2EHPA. The extraction behavior of silver ion and D2EHPA was also studied by varying the organic solvents and the results were analyzed using the fourier transform infrared spectrometer (FT-IR). In addition, the tie-line data of D2EHPA were determined and correlated with the modeling NRTL results. Details are available in the published article of Fluid Phase Equilibria (page: 22-30, volume: 388 and year: 2015)<sup>74</sup>.

## Chapter VI

This chapter presents the mathematical model for copper ion extraction via HFSLM. The model was considered involving convection, reaction and accumulation of copper ions in the HFSLM. Concentration of copper ions in the feed phase was determined varying the time interval in order to predict the separation time and number of separation cycles. In addition, the reliability of the model was considered and then used to describe the transport mechanism of copper ions. Details are available in the published article of Separation Science and Technology (page: 2183-2190, volume: 46 and year: 2011)<sup>75</sup>.

## Chapter VII

This chapter focuses on the application of the mathematical model in chapter VI for silver ion extraction via HFSLM. The model of diffusion was also studied and its reliability was compared with the first model to describe the transport mechanism of silver ions. Moreover, the influence of important parameters on silver ion extraction and recovery was investigated such as types of extractant and stripping solution, pH

of feed and stripping solutions, concentrations of extractant and stripping solution, flow rates/flow directions/flow patterns of feed and stripping solutions as well as separation time. The influence of ferric ion presence on silver ion extraction was also studied. Details are available in the published article of Chemical Engineering Research and Design (page: 2681-2693, volume: 92 and year: 2014)<sup>76</sup>.

### Chapter VIII

This chapter highlights the development of reaction model as shown in chapter VII by including diffusion of silver ions and using the matrix formation. Concentration of silver ions in the feed phase was determined varying the time interval and the results were validated by comparison with the experimental results. Thereafter, the model was applied to obtain concentration of silver ions in the stripping phase. For this application, concentration of metal-extractant complexes at the liquid membrane-stripping interface was used and obtained by the mass balance and flux equations. In addition, the developed model was applied for the extractions of copper and tantalum ions. Details are available in the published article of Chemical Engineering Journal (page: 361-373, volume: 222 and year: 2013)<sup>77</sup>.

## Chapter II

Ternary (liquid-liquid) equilibrium data of furfuryl alcohol with organic solvents  
at  $T = 298.2$  K: experimental results and thermodynamic models

Thidarat Wongsawa<sup>a</sup>, Milan Hronec<sup>b</sup>, Tomáš Soták<sup>b</sup>,  
Natchanun Leepipatpiboon<sup>c</sup>, Ura Pancharoen<sup>a</sup>, Suphot Phatanasri<sup>a</sup>

<sup>a</sup> *Department of Chemical Engineering, Faculty of Engineering, Chulalongkorn University, Phyathai Rd., Bangkok 10330, Thailand*

<sup>b</sup> *Department of Organic Technology, Slovak University of Technology, Radlinského 9, 812 37 Bratislava, Slovakia*

<sup>c</sup> *Chromatography and Separation Research Unit, Department of Chemistry, Faculty of Science, Chulalongkorn University, Patumwan, Bangkok 10330, Thailand*

CHULALONGKORN UNIVERSITY

---

This article has been published in journal: Fluid Phase Equilibria.

Page: 88-96. Volume: 365. Year: 2014.

---

## 2.1 Abstract

Basing on the importance of liquid-liquid equilibrium (LLE) data for the chemical industry, ternary LLE systems of water + furfuryl alcohol + (MIBK, ethyl acetate, furfural or *n*-butanol) were investigated at  $T = 298.2$  K and atmospheric pressure. Solubility and tie-line data of these ternary LLE systems were determined by a direct measurement method. An uncertainty propagation calculation was used to validate the reliability of LLE results. Distribution coefficients ( $D$ ) and separation factors ( $S$ ) were calculated to evaluate the capability of selective organic solvents for separation of furfuryl alcohol from water. The correlations of experimental results with results obtained by using NRTL, UNIQUAC and UNIFAC models were presented and confirmed by *rmsd* values which were less than 5%.

**Keywords:** Furfuryl alcohol; Solubility; Ternary LLE; Thermodynamic models; Tie-line data.

## 2.2 Introduction

Furfuryl alcohol is a toxic component which may cause adverse health effects by the following exposures: inhalation, ingestion or eyes/dermal contact. The National Institute for Occupational Safety and Health (NIOSH) listed furfuryl alcohol as a carcinogen [1, 2]. However, furfuryl alcohol has been widely applied in the chemical and polymer industries. Nowadays, the major applications of furfuryl alcohol are production of resins, acid proof bricks as well as corrosion resistant fiber glass and polymer concrete. In addition, furfuryl alcohol is also an intermediate chemical for the synthesis of dispersing agents, lubricants, lysine, plasticizers, tetrahydrofurfuryl alcohol and vitamin C [3, 4]. In these productions, furfuryl alcohol may contaminate industrial wastewaters. Due to the toxicity of furfuryl alcohol and considering also its adverse environmental impact, separation of furfuryl alcohol from wastewaters before their discharge should be highly important.

Liquid-liquid extraction has long been used in chemical engineering processes and wastewater treatment due to its industrially applicable and economical method. In the development and design of separation processes liquid-liquid equilibrium (LLE) data are mainly required. In particular, the LLE data of ternary systems have a fundamental and important role in the industrial units [5, 6]. The ternary LLE data are usually determined by direct measurement or by cloud-point titration methods. For the method of direct measurement, a ternary mixture is separated into two liquid phases. The compositions of these phases in equilibrium state are obtained by analysis. The method of cloud-point titration has been used in many measurements to obtain the concentration of components in liquid phases. The type of measurement was selected based on the property of the ternary mixture e.g. density, pH, viscosity, sound velocity and refractive index. Again, refractive index measurements have been used extensively [7].

In addition, in the design of separation processes for the industries, thermodynamic models are also required. Many authors have reported in the literature the activity coefficient models for prediction of different ternary liquid-liquid systems, e.g. the non-random two liquid (NRTL) model [8-11], the universal quasi chemical (UNIQUAC) model [12-14] and the universal functional activity coefficient (UNIFAC) model [15-17]. These models involve the binary interaction parameters which can be obtained by a software program and regression with experimental data. However, no attempt has been made for correlating LLE data of furfuryl alcohol with the above mentioned NRTL, UNIQUAC and UNIFAC models.

The main purpose of this work was to provide a new series of LLE data. The ternary systems of furfuryl alcohol with efficient organic solvents were investigated at a temperature of 298.2 K and atmospheric pressure. Methyl isobutyl ketone (MIBK), ethyl acetate, furfural and *n*-butanol were selected as organic solvents. MIBK is highly selective, non-toxic and relatively less miscible in aqueous solutions [18]. Ethyl acetate is a good solvent and safe for the environment [19]. In addition, furfural and *n*-butanol are the preferable solvents for use in industry [20, 21]. For each ternary system, the solubility and tie-line data were determined by a direct measurement method. The reliability of experimental results was validated with the uncertainty

propagation calculation. Distribution coefficients ( $D$ ) and separation factors ( $S$ ) were obtained from the tie-line data to present the separation capability of the selective organic solvents. The LLE data were correlated using NRTL, UNIQUAC and UNIFAC models. The values of binary interaction parameters for these equilibrium models were obtained by the Aspen Plus v. 2006.5 simulation program (AspenTech, Burlington, MA, USA) and regressed with the experimental data.

## 2.3 Experimental

### 2.3.1 Chemicals

Chemicals consisting of furfuryl alcohol ( $C_5H_6O_2$ , MW 98.10 g/mol), furfural ( $C_5H_4O_2$ , MW 96.08 g/mol), *n*-butanol ( $C_4H_9OH$ , MW 74.12 g/mol), methyl isobutyl ketone ( $C_6H_{12}O$ , MW 100.16 g/mol) and ethyl acetate ( $C_4H_8O_2$ , MW 88.11 g/mol) were used in this work. The source and mass fraction purity of chemicals are listed in Table 2.1. All chemicals were used without further purification. Distilled water was used in all experiments.

**Table 2.1** Sources and mass fraction purity of chemicals.

Chemical name	Source	Purity/% mass	Analytical method
Furfuryl alcohol	Sigma-Aldrich	99.0	GC
Furfural	Sigma-Aldrich	99.0	GC
<i>n</i> -Butanol	Erba Lachema	99.5	GC
Methyl isobutyl ketone	MicroChem	99.5	GC
Ethyl acetate	MicroChem	99.8	HPLC

### 2.3.2 Apparatus and procedure

The solubility data for the ternary systems were determined by the direct measurement method in organic-rich and aqueous-rich phases at equilibrium.

A digital analytical balance-Mettler Toledo AE200 (with an accuracy of  $\pm 0.0001$  g) was used to obtain the weights of all components. The temperature of the systems was controlled by a water jacket that was checked using a digital thermometer (with an accuracy of  $\pm 0.1$  K). The binary mixtures of known compositions of furfuryl alcohol and organic solvents were prepared in closed glass vessels. The binary mixtures were continually titrated with water until they became turbid. The end point of titration was achieved when the mixtures remained turbid for 15 minutes. During this time the glass vessels were agitated periodically to observe the turbidity. These procedures were used to determine the solubility curve of the organic-rich phase. To repeat all measurements at least three times, the known quantity of furfuryl alcohol was then added into the mixtures for back transparent. The mixtures were again titrated with water until they became turbid, and the same end point of titration was taken. The solubility curve of aqueous-rich phase was determined using the binary mixtures of furfuryl alcohol and water in the same manner. The organic solvents were added to titration.

The tie-line data were obtained from the ternary mixtures after reaching equilibrium compositions. More water was successively added until transition from homogeneous to heterogeneous state appeared in the mixtures. Thereafter, the mixtures were agitated vigorously at 200 rpm for 2 hours, then centrifugated and left to complete separation for 14 hours. These periods were long enough for samples reaching two equilibrium liquid layers. The organic-rich phase was carefully withdrawn from the top layer of the glass vessel by syringe and then weighed. The remaining aqueous-rich sample was also weighed and analyzed by gas chromatography. The compositions of all components were calculated directly basing on the analytical results and the mass balance equation. The ProSim program was used to plot triangular phase diagrams for all ternary LLE data.

### 2.3.3 Analysis

The separated phases were analyzed by gas chromatography (Hewlett Packard 5890 Series II, with FID detector) using a 1.4 m × 3 mm glass column packed with 5% C20M + 5% SE. The quantitative determination of the reaction samples was done by the external standard method using an aqueous solution of each sample with known concentration and response factor.

### 2.3.4 Reliability of LLE results

The reliability of LLE results was validated by the uncertainty propagation calculation as according to the GUM and NIST [22, 23]. In this work, the standard uncertainty ( $u(x_i)$ ), as shown in the respective footnote tables, were calculated based on Eqs. (2.1) and (2.2):

$$u(x_i) = \sqrt{\frac{1}{n(n-1)} \sum_{k=1}^n (X_{i,k} - \bar{X}_i)^2} \quad (2.1)$$

$$\bar{X}_i = \frac{1}{n} \sum_{k=1}^n X_{i,k} \quad (2.2)$$

where  $n$  is the number of independent observations,  $X_{i,k}$  is the input quantity as obtained under the same conditions of measurement and  $k = 1, 2, \dots, n$ .

## 2.4 Results and discussion

### 2.4.1 Experimental solubility and tie-line data

Experimental solubility data from the binodal curve diagrams (Figure 2.1) of four ternary systems (water + furfuryl alcohol + organic solvents) at  $T = 298.2$  K and atmospheric pressure are shown in Table 2.2 and Figure 2.1. As can be seen in Figure 2.1, only one liquid pair (water + organic solvents) is partially miscible and two liquid pairs (furfuryl alcohol + water or organic solvents) are completely miscible. It indicates that all four ternary systems exhibit the type-1 behavior of LLE [24]. The area of the two-phase region decreased in the following order of organic solvents: MIBK > ethyl acetate > furfural > *n*-butanol. This area depends on the mutual solubility of water and the organic solvents. Thus, the type of organic solvent is an important factor for the two-phase region of the investigated systems.

**Table 2.2** Experimental solubility data in mass fractions ( $w_i$ ) for [water (1) + furfuryl alcohol (2) + organic solvents (3)] at  $T = 298.2$  K and atmospheric pressure.<sup>a</sup>

MIBK		Ethyl acetate		Furfural		<i>n</i> -Butanol	
$w_1$ (Water)	$w_2$ (FA)	$w_1$ (Water)	$w_2$ (FA)	$w_1$ (Water)	$w_2$ (FA)	$w_1$ (Water)	$w_2$ (FA)
0.0190	0.0000	0.0407	0.0000	0.0457	0.0000	0.1637	0.0000
0.0198	0.0997	0.0528	0.1557	0.0580	0.0758	0.1690	0.0846
0.0253	0.1742	0.0624	0.2181	0.0717	0.1458	0.1819	0.1484
0.0285	0.2442	0.0734	0.2881	0.0872	0.2155	0.1960	0.2045
0.0374	0.3150	0.0823	0.3486	0.1017	0.2904	0.2113	0.2624
0.0447	0.3810	0.0956	0.4099	0.1187	0.3700	0.2333	0.3327
0.0512	0.4393	0.1177	0.4759	0.1438	0.4250	0.2487	0.3701
0.0582	0.4997	0.1330	0.5145	0.1918	0.4932	0.2658	0.4068
0.0805	0.5680	0.1725	0.5667	0.2607	0.5211	0.3074	0.4463
0.1138	0.6233	0.2427	0.5838	0.3233	0.5233	0.3620	0.4529
0.9810	0.0000	0.9198	0.0000	0.9135	0.0000	0.9372	0.0000
0.8307	0.1582	0.8554	0.0845	0.8480	0.0801	0.8606	0.0855
0.6317	0.3540	0.7175	0.2489	0.7900	0.1511	0.7721	0.1688
0.4345	0.5377	0.6321	0.3343	0.6519	0.2975	0.6770	0.2515
0.2903	0.6296	0.5398	0.4199	0.5522	0.3850	0.5906	0.3212
0.2113	0.6583	0.3875	0.5378	0.4636	0.4546	0.5029	0.3841
0.1415	0.6523	0.3110	0.5785	0.3776	0.5046	0.4285	0.4271

<sup>a</sup> Standard uncertainties  $u$  are  $u(T) = 0.1$  K and  $u(w) = 0.0007$ , FA is furfuryl alcohol.

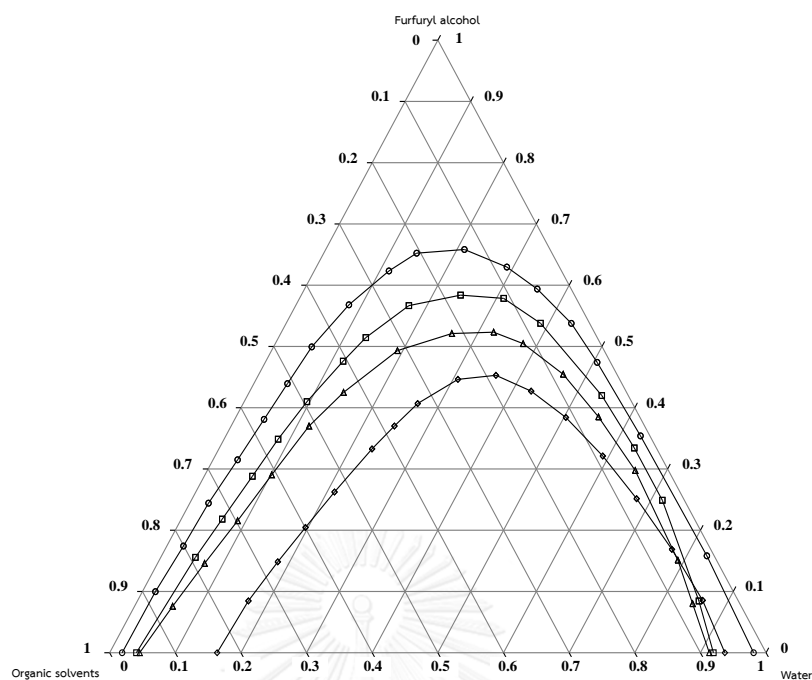


**Figure 2.1** Binodal curve diagram for (water + furfuryl alcohol + organic solvents) at  $T = 298.2$  K and atmospheric pressure; (-○-) MIBK, (-□-) ethyl acetate, (-△-) furfural and (-◇-) *n*-butanol.

Tie-line data of these ternary systems were obtained experimentally at the same temperature as shown in Table 2.3. The corresponding triangular phase diagrams for these tie-line data are plotted in Figures 2.2 to 2.5. In these figures, the slopes of tie-lines express that furfuryl alcohol is more soluble in organic solvents than in water. This may be due to the intermolecular interaction of furfuryl alcohol with organic solvent and water. In water, weak hydrogen bonds with molecules of water can be formed [25]. Probably the amount of component soluble in water depends on the intermolecular interaction.

**Table 2.3** Experimental tie-line data in mass fractions for the ternary systems of [water (1) + furfuryl alcohol (2) + organic solvents (3)] at  $T = 298.2$  K and atmospheric pressure.<sup>a</sup>

Aqueous-rich phase			Organic-rich phase		
$w_1$	$w_2$	$w_3$	$w_1$	$w_2$	$w_3$
[Water (1) + Furfuryl alcohol (2) + MIBK (3)]					
0.9645	0.0164	0.0191	0.0220	0.0731	0.9049
0.9622	0.0192	0.0186	0.0239	0.1069	0.8692
0.9413	0.0389	0.0198	0.0232	0.1737	0.8031
0.9386	0.0454	0.0160	0.0313	0.2047	0.7640
0.9190	0.0665	0.0145	0.0345	0.2670	0.6985
0.9145	0.0730	0.0125	0.0378	0.2921	0.6701
0.9008	0.0899	0.0093	0.0409	0.3316	0.6275
0.8600	0.1294	0.0106	0.0504	0.4035	0.5461
0.8000	0.1890	0.0110	0.0595	0.4900	0.4505
0.7821	0.2070	0.0109	0.1103	0.6144	0.2753
[Water (1) + Furfuryl alcohol (2) + Ethyl acetate (3)]					
0.9073	0.0159	0.0768	0.0444	0.0782	0.8774
0.9014	0.0240	0.0746	0.0521	0.1415	0.8064
0.8862	0.0434	0.0704	0.0523	0.1624	0.7853
0.8819	0.0493	0.0688	0.0848	0.3511	0.5641
0.8705	0.0660	0.0635	0.0975	0.4021	0.5004
0.8409	0.1040	0.0551	0.1338	0.5034	0.3628
0.8137	0.1395	0.0468	0.1429	0.5267	0.3304
0.7688	0.1912	0.0400	0.1900	0.5700	0.2400
[Water (1) + Furfuryl alcohol (2) + Furfural (3)]					
0.8885	0.0307	0.0808	0.0665	0.1254	0.8081
0.8817	0.0400	0.0783	0.0843	0.1963	0.7194
0.8653	0.0595	0.0752	0.0976	0.2651	0.6373
0.8517	0.0774	0.0709	0.1127	0.3324	0.5549
0.8400	0.0897	0.0703	0.1403	0.4145	0.4452
0.8039	0.1353	0.0608	0.1635	0.4476	0.3889
0.7655	0.1791	0.0554	0.1897	0.4852	0.3251
0.7170	0.2299	0.0531	0.2157	0.5044	0.2799
0.7200	0.2155	0.0645	0.2573	0.3908	0.3519
[Water (1) + Furfuryl alcohol (2) + <i>n</i> -Butanol (3)]					
0.9230	0.0165	0.0605	0.1684	0.0776	0.7540
0.9120	0.0295	0.0585	0.1795	0.1376	0.6829
0.9005	0.0413	0.0582	0.1835	0.1610	0.6555
0.8855	0.0572	0.0573	0.1991	0.2084	0.5925
0.8665	0.0788	0.0547	0.2158	0.2691	0.5151
0.8539	0.0916	0.0545	0.2220	0.2914	0.4866
0.8405	0.1056	0.0539	0.2230	0.3056	0.4714
0.7842	0.1571	0.0587	0.2345	0.3300	0.4355
0.7200	0.2155	0.0645	0.2573	0.3908	0.3519

<sup>a</sup> Standard uncertainties  $u$  are  $u(T) = 0.1$  K and  $u(w) = 0.0007$ .

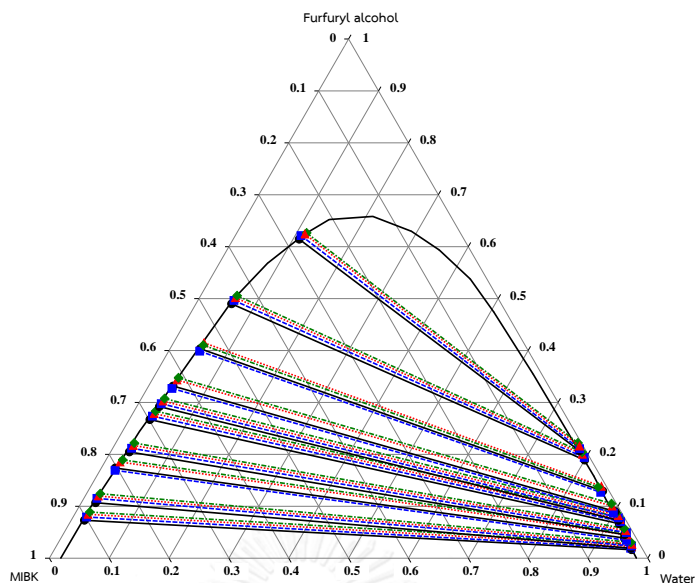


**Figure 2.2** Ternary diagram for LLE of [water (1) + furfuryl alcohol (2) + MIBK (3)] at  $T = 298.2$  K and atmospheric pressure; (—●—) experimental tie-line data, (---■---) calculated NRTL data, (··▲··) calculated UNIQUAC data and (-·◆-·) calculated UNIFAC data.

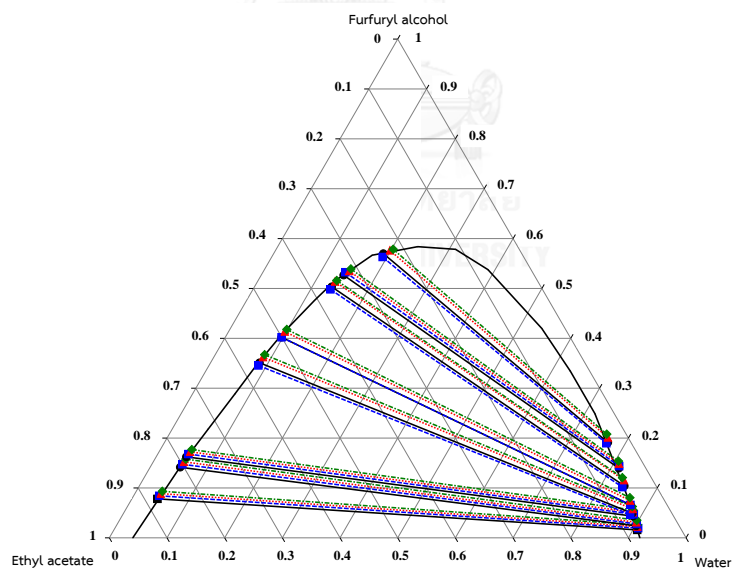


**Figure 2.3** Ternary diagram for LLE of [water (1) + furfuryl alcohol (2) + ethyl acetate (3)] at  $T = 298.2$  K and atmospheric pressure; (—●—) experimental tie-line data, (---■---) calculated NRTL data, (··▲··) calculated UNIQUAC data and (-·◆-·) calculated UNIFAC data.

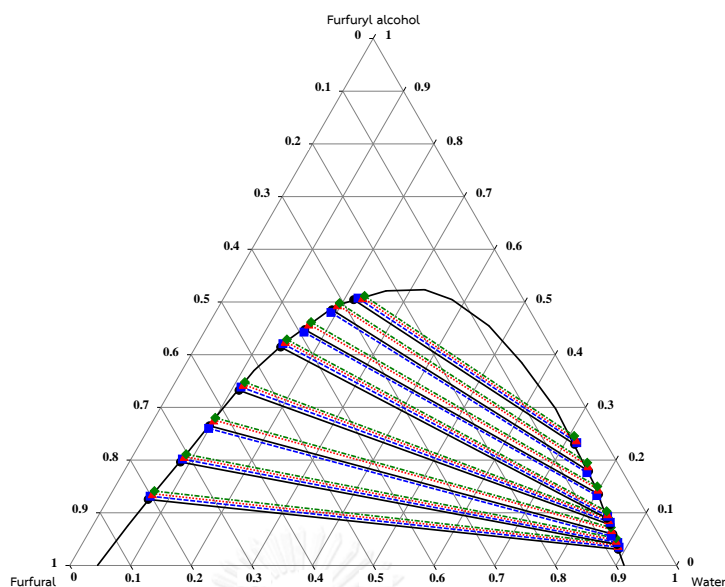


**Figure 2.4** Ternary diagram for LLE of [water (1) + furfuryl alcohol (2) + furfural (3)] at  $T = 298.2$  K and atmospheric pressure; (—●—) experimental tie-line data, (---■---) calculated NRTL data, (··▲··) calculated UNIQUAC data and (-·◆-·) calculated UNIFAC data.

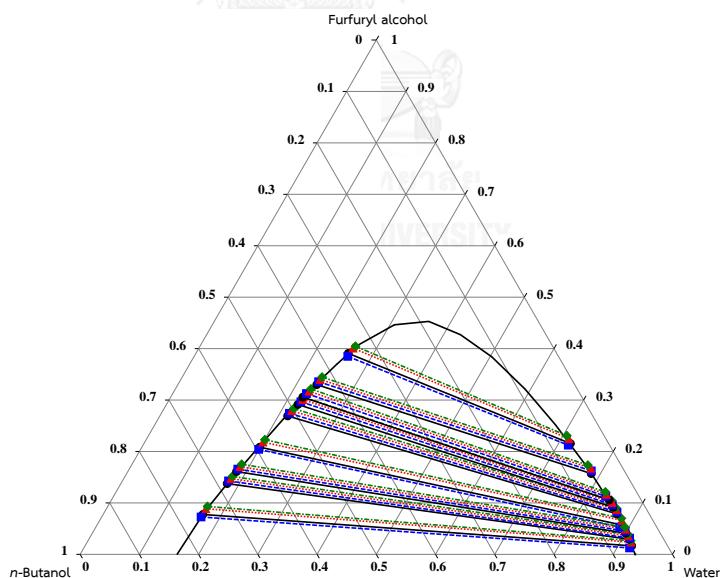


**Figure 2.5** Ternary diagram for LLE of [water (1) + furfuryl alcohol (2) + *n*-butanol (3)] at  $T = 298.2$  K and atmospheric pressure; (—●—) experimental tie-line data, (---■---) calculated NRTL data, (··▲··) calculated UNIQUAC data and (-·◆-·) calculated UNIFAC data.

#### 2.4.2 Distribution coefficients and separation factors

To determine the selectivity of organic solvents for furfuryl alcohol separation, the distribution coefficients ( $D$ ) and the separation factor ( $S$ ) were calculated using Eq. (2.3).

$$S = \frac{D_2}{D_1} = \frac{w_{23} / w_{21}}{w_{13} / w_{11}} \quad (2.3)$$

where  $D_1$  and  $D_2$  are the distribution coefficients of water and furfuryl alcohol,  $w_{13}$  and  $w_{23}$  are the mass fractions of water and furfuryl alcohol in organic-rich phase, respectively and  $w_{11}$  and  $w_{21}$  are the mass fractions of water and furfuryl alcohol in aqueous-rich phase, respectively.

The values of experimental distribution coefficients and separation factors of each ternary system are listed in Table 2.4. The variation of the separation factor as a function of the mass fraction of furfuryl alcohol in aqueous-rich phase is shown in Figure 2.6. For the investigated ternary systems, the selective organic solvents have high  $D$  and  $S$  values, indicating the capability of these solvents to separate furfuryl alcohol from water. Since MIBK has the highest separation factor at  $T = 298.2$  K (separation factors are varying between 21 and 195), this solvent is superior among the studied organic solvents for furfuryl alcohol separation.

**Table 2.4** Distribution coefficients ( $D$ ) and separation factors ( $S$ ) for the ternary systems of [water (1) + furfuryl alcohol (2) + organic solvents (3)] at  $T = 298.2$  K and atmospheric pressure.

Ternary system	$w_{21}$	$D_2$	$D_1$	$S$
(Water + Furfuryl alcohol + MIBK)	0.0164	4.4573	0.0228	195.4128
	0.0665	4.0150	0.0394	101.9513
	0.1294	3.1182	0.0586	53.2080
	0.2070	2.9681	0.1410	21.0459
(Water + Furfuryl alcohol + Ethyl acetate)	0.0159	4.9182	0.0449	109.5027
	0.0493	7.1217	0.1206	59.0640
	0.1040	4.8404	0.1591	30.4206
	0.1912	2.9812	0.2471	12.0628
(Water + Furfuryl alcohol + Furfural)	0.0307	4.0847	0.0722	56.5752
	0.0774	4.2946	0.1323	32.4551
	0.1353	3.3082	0.2034	16.2658
	0.2299	2.1940	0.3008	7.2930
(Water + Furfuryl alcohol + <i>n</i> -Butanol)	0.0165	4.7030	0.0841	55.9394
	0.0788	3.4150	0.3106	10.9962
	0.1571	2.1006	0.4208	4.9917
	0.2155	1.8135	0.5428	3.3411

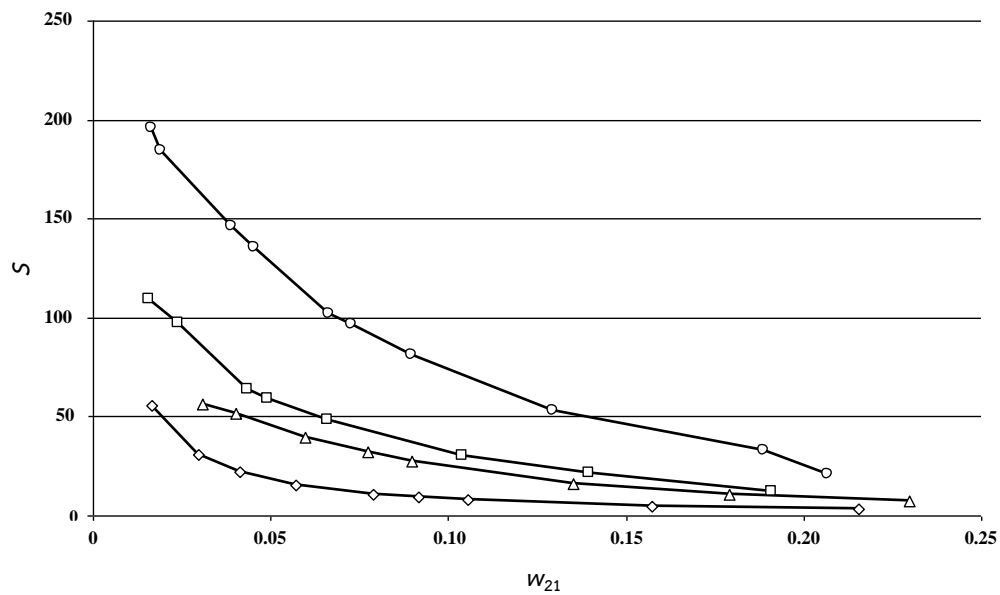


**Figure 2.6** Separation factor ( $S$ ) plotted against the mass fraction of furfuryl alcohol in aqueous-rich phase ( $w_{21}$ ) at  $T = 298.2$  K and atmospheric pressure; ( $\circ$ ) MIBK, ( $\square$ ) ethyl acetate, ( $\Delta$ ) furfural and ( $\diamond$ ) *n*-butanol.

### 2.4.3 Thermodynamic model correlation

In order to present LLE data by thermodynamic models, the experimental tie-line data for each investigated ternary system were correlated using NRTL [26], UNIQUAC [27] and UNIFAC [28] models at  $T = 298.2$  K. The detailed descriptions of these models are given in Appendix A. At LLE conditions, the modeling results in terms of activity coefficients ( $\gamma_i$ ) for any component  $i$  in aqueous-rich and organic-rich phases are equal, and mole fractions ( $x_i$ ) in both phases can be calculated by the following equations:

$$x_i^I \gamma_i^I = x_i^{II} \gamma_i^{II} \quad (2.4)$$

$$\sum x_i^I = \sum x_i^{II} = 1 \quad (2.5)$$

where  $x_i^I$ ,  $x_i^{II}$ ,  $\gamma_i^I$  and  $\gamma_i^{II}$  are the mole fractions and activity coefficients of component  $i$  in aqueous-rich (I) and organic-rich (II) phases, respectively.

In this work, the value of non-randomness parameter ( $\alpha$ ) of the NRTL model was determined and then the appropriate value was taken to be 0.2. The values of structural parameters  $r$  and  $q$  (Table 2.5) used for UNIQUAC and UNIFAC models were taken from the literature [21, 29, 30]. The binary interaction parameters of NRTL ( $b_{ij}$ ) and UNIQUAC ( $a_{ij}$ ) models were obtained by the Aspen Plus software program and regression with experimental LLE data. Both values for each ternary system are listed in Table 2.6.

**Table 2.5** UNIQUAC and UNIFAC structural parameters ( $r$  and  $q$ ) for pure components.

Component	$r$	$q$
MIBK	4.60	4.03
Ethyl acetate	3.48	3.12
Furfural	3.17	2.48
<i>n</i> -Butanol	3.45	3.05
Furfuryl alcohol	3.84	3.27
Water	0.92	1.40

**Table 2.6** NRTL and UNIQUAC binary interaction parameters for the ternary systems (water + furfuryl alcohol + organic solvents) at  $T = 298.2$  K.

$i-j$	NRTL		UNIQUAC	
	$b_{ij}$ (K)	$b_{ji}$ (K)	$a_{ij}$ (K)	$a_{ji}$ (K)
(Water + Furfuryl alcohol + MIBK)				
1-2	919.0915	146.8671	68.9100	2,683.0490
1-3	-761.6760	-12,671.4629	1,068.2748	569.1948
2-3	-196.9682	927.1125	-896.1102	1,876.1429
(Water + Furfuryl alcohol + Ethyl acetate)				
1-2	923.1648	156.3642	342.5162	3,748.2119
1-3	-1,705.6830	1,286.1383	531.0333	-1,212.8892
2-3	-894.0158	74.2105	-192.8614	849.0211
(Water + Furfuryl alcohol + Furfural)				
1-2	930.5618	159.4362	-0.0768	13,052.5630
1-3	-2,808.5376	-4,131.4375	-0.1050	-7,657.2258
2-3	989.9048	55.7108	0.3806	-81.8089
(Water + Furfuryl alcohol + <i>n</i> -Butanol)				
1-2	917.5642	149.0183	232.4316	8,598.5914
1-3	-4,983.1548	-9,291.7021	252.7914	-1,132.8296
2-3	-637.1569	746.5924	-432.4582	3,946.2147

The experimental and modeling results of the tie-line data for the ternary systems are plotted in Figures 2.2 to 2.5. The correlation of both results in terms of the root-mean square deviation (*rmsd*) is presented in Table 2.7. The *rmsd* values were calculated as follows:

$$rmsd = 100 \left( \frac{\sum_{k=1}^n \sum_{j=1}^2 \sum_{i=1}^3 (w_{ijk}^{expt.} - w_{ijk}^{cal.})}{6n} \right)^{1/2} \quad (2.6)$$

where  $n$  is the number of tie-lines,  $w^{expt.}$  and  $w^{cal.}$  are the experimental mass fraction and the modeling mass fraction, respectively. Subscript  $i$  is the component,  $j$  is the phase and  $k = 1, 2, \dots, n$  (number of tie-lines).

As can be seen in Table 2.7, the correlation of experimental results with modeling results exhibits a good agreement, especially for the NRTL model which was found to be the most consistent for all ternary systems. In addition, the low  $rmsd$  values for NRTL, UNIQUAC and UNIFAC models confirm the capability of these models to provide the LLE data in this work.

**Table 2.7**  $rmsd$  values for the NRTL, UNIQUAC and UNIFAC models for the ternary systems of (water + furfuryl alcohol + organic solvents).

Ternary system	$rmsd$ (%)		
	NRTL	UNIQUAC	UNIFAC
(Water + Furfuryl alcohol + MIBK)	1.93	2.14	3.12
(Water + Furfuryl alcohol + Ethyl acetate)	2.02	2.68	3.18
(Water + Furfuryl alcohol + Furfural)	1.23	2.42	2.94
(Water + Furfuryl alcohol + <i>n</i> -Butanol)	1.27	3.06	3.92

## 2.5 Conclusion

The ternary LLE systems of water + furfuryl alcohol + (MIBK, ethyl acetate, furfural or *n*-butanol) were investigated at  $T = 298.2$  K and atmospheric pressure. These four ternary systems exhibit the type-1 behavior of LLE. The reliability of experimental tie-line data was validated by the uncertainty propagation calculation. The selected organic solvents have a high capability for separation of furfuryl alcohol from water, especially MIBK, as shown by its highest value of the separation factor.

NRTL, UNIQUAC and UNIFAC models were used to provide the LLE data. All of the modeling results have a good agreement with the experimental results as shown by the *rmsd* values which are less than 5%.

## 2.6 Acknowledgements

The authors gratefully acknowledge the financial support by the Thailand Research Fund and Chulalongkorn University under the Royal Golden Jubilee Ph.D. program (Grant No. PHD/0272/2549). Sincere thanks also go to the Department of Organic Technology, Slovak University of Technology, Bratislava, Slovakia, Ing. Fulajtárová Katarína and Dr. Michal Ilčín for their kind supports.

## 2.7 Appendix A

### Thermodynamic models

#### A.1 The NRTL model

The NRTL activity coefficient ( $\gamma_i$ ) is given by:

$$\ln \gamma_i = \frac{\sum_{j=1}^3 \tau_{ji} G_{ji} x_j}{\sum_{k=1}^3 G_{ki} x_k} + \sum_{j=1}^3 \frac{x_j G_{ij}}{\sum_{k=1}^3 G_{kj} x_k} \left( \tau_{ij} - \frac{\sum_{k=1}^3 x_k \tau_{kj} G_{kj}}{\sum_{k=1}^3 G_{kj} x_k} \right) \quad (\text{A-2.1})$$

where  $x_i$  is the mole fraction of component  $i$ , the parameters  $\tau_{ij}$ ,  $\tau_{ji}$ ,  $\tau_{kj}$ ,  $G_{ij}$ ,  $G_{ji}$ ,  $G_{ki}$  and  $G_{kj}$  are the adjustable parameters for each binary pair in the NRTL model and  $i, j, k$  are the indices for all components.

The adjustable parameters can be calculated as follows:

$$\tau_{ij} = a_{ij} + \frac{b_{ij}}{T} + e_{ij} \ln T \quad (\text{A-2.2})$$

$$\alpha_{ij} = \alpha_{ji} = c_{ij} \quad (\text{A-2.3})$$

$$G_{ij} = \exp(-\alpha_{ij} \tau_{ij}) \quad (\text{A-2.4})$$

where  $a_{ij}$ ,  $b_{ij}$ ,  $c_{ij}$  and  $e_{ij}$  are the NRTL coefficients for the binary interaction parameters and  $\alpha_{ij}$  and  $\alpha_{ji}$  are the non-random parameters.

## A.2 The UNIQUAC model

The logarithm of activity coefficient ( $\ln \gamma_i$ ) in this model is assumed to be the sum of logarithms between combinational ( $\ln \gamma_i^C$ ) and residual ( $\ln \gamma_i^R$ ) activity coefficients as given by:

$$\ln \gamma_i = \ln \gamma_i^C + \ln \gamma_i^R \quad (\text{A-2.5})$$

$$\ln \gamma_i^C = \ln \left( \frac{\Phi_i}{x_i} \right) + \frac{z}{2} q_i \ln \left( \frac{\theta_i}{\Phi_i} \right) + \zeta_i - \frac{\Phi_i}{x_i} \sum_{j=1}^3 x_j \zeta_j \quad (\text{A-2.6})$$

$$\ln \gamma_i^R = q_i \left[ 1 - \ln \left( \sum_{j=1}^3 \theta_j \tau_{ji} \right) - \sum_{j=1}^3 \left( \frac{\theta_j \tau_{ij}}{\sum_{k=1}^3 \theta_k \tau_{kj}} \right) \right] \quad (\text{A-2.7})$$

where  $\tau_{ij}$ ,  $\tau_{ji}$ ,  $\tau_{kj}$ ,  $l_i$  and  $l_j$  are the adjustable parameters,  $i$ ,  $j$  and  $k$  are the indices for all components,  $z$  is the integral number equal to 10 and  $\theta_i$ ,  $\theta_j$ ,  $\theta_k$  and  $\Phi_i$  are the surface areas and volume fractions in the UNIQUAC model, respectively.

The adjustable parameters can be calculated by the following equations:

$$l_i = \frac{z}{2} (r_i - q_i) - (r_i - 1) \quad (\text{A-2.8})$$

$$\tau_{ij} = a_{ij} + \frac{b_{ij}}{T} + c_{ij} \ln T + d_{ij} T \quad (\text{A-2.9})$$

$$\Phi_i = \frac{x_i r_i}{\sum_{j=1}^3 x_j r_j} \quad (\text{A-2.10})$$

$$\theta_i = \frac{x_i q_i}{\sum_{j=1}^3 x_j q_j} \quad (\text{A-2.11})$$

where  $a_{ij}$ ,  $b_{ij}$ ,  $c_{ij}$  and  $d_{ij}$  are the UNIQUAC coefficients for the binary interaction parameters. The UNIQUAC structural parameters  $r_i$  and  $q_i$  are the number of segments per molecule and the relative surface area per molecule, respectively, which can be calculated from the number of molecular groups and the individual values of the van der Waals volume together with the area of molecule by the Bondi Method [7].

### A.3 The UNIFAC model

Firstly, the concept of UNIFAC model follows the Derr and Deal's (1969) ASOG model in which the activity coefficient is separated into two parts: part I is the contribution from the differences in molecular size and part II is the contribution from the molecular interactions. The first part can be obtained by the Flory-Huggins equation, and the Wilson equation is applied to obtain the second part. Thereafter, the concept of combining groups with UNIQUAC model is chosen to remove the arbitraries. Thus, the concept of UNIFAC model is based on the concept of UNIQUAC model, and the UNIFAC equation follows Eq. (A-2.6) [28].

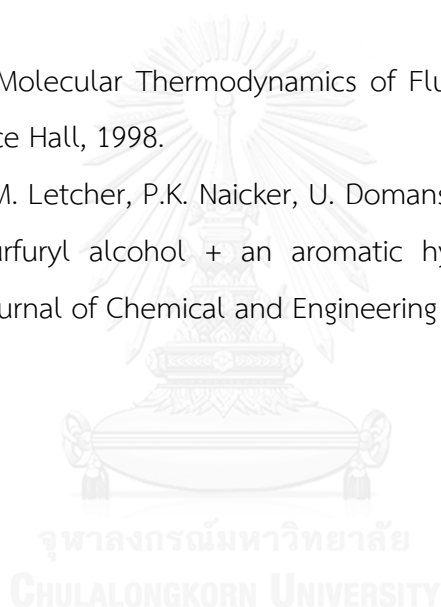
### 2.8 References

- [1] M.T. Oliva-Teles, C. Delerue-Matos, M.C.M. Alvim-Ferraz, Determination of free furfuryl alcohol in foundry resins by chromatographic techniques, *Analytica Chimica Acta* 537 (2005) 47-51.
- [2] U.S. Department of Health and Human Services, Occupational Safety and Health Guideline for Furfuryl Alcohol, Rockville, 1988.
- [3] R.V. Sharma, U. Das, R. Sammynaiken, A.K. Dalai, Liquid phase chemo-selective catalytic hydrogenation of furfural to furfuryl alcohol, *Applied Catalysis A: General* 454 (2013) 127-136.
- [4] B.M. Nagaraja, V.S. Kumar, V. Shasikala, A.H. Padmasri, B. Sreedhar, B. David Raju, K.S. Rama Rao, A highly efficient Cu/MgO catalyst for vapour phase hydrogenation of furfural to furfuryl alcohol, *Catalysis Communications* 4 (2003) 287-293.
- [5] H. Ghanadzadeh, M. Ganji, S. Fallahi, Mathematical model of liquid-liquid equilibrium for a ternary system using the GMDH-type neural network and genetic algorithm, *Applied Mathematical Modelling* 36 (2012) 4096-4105.

- [6] H.G. Gilani, A.G. Gilani, M. Sangashekan, Tie-line data for the aqueous solutions of phenol with organic solvents at  $T = 298.2$  K, *Journal of Chemical Thermodynamics* 58 (2013) 142-148.
- [7] J. Saien, M. Norouzi, H. Dehghani, The choice of solvent and liquid-liquid equilibrium for ternary water + 2-methylaziridine + chloroform system: Experimental data and modeling, *Fluid Phase Equilibria* 338 (2013) 224-231.
- [8] B. Mokhtarani, J. Musavi, M. Parvini, M. Mafi, A. Sharifi, M. Mirzaei, Ternary (liquid-liquid) equilibria of nitrate based ionic liquid + alkane + benzene at 298.15 K: Experiments and correlation, *Fluid Phase Equilibria* 341 (2013) 35-41.
- [9] U. Domanska, E.V. Lukoshko, M. Królikowski, Separation of thiophene from heptane with ionic liquids, *Journal of Chemical Thermodynamics* 61 (2013) 126-131.
- [10] T.P. Kumar, P.K. Das, Solubility and tie-line data for water + formic acid + methyl isobutyl ketone ternary system at different temperatures, *Chemical Engineering Communications* 197 (2010) 1163-1171.
- [11] P. Steltenpohl, E. Gracsová, Application of extended NRTL equation for ternary liquid-liquid and vapor-liquid-liquid equilibria description, *Chemical Papers* 64(3) (2010) 310-317.
- [12] B.E. García-Flores, J. Águila-Hernández, F. García-Sánchez, M.A. Aquino-Olivos, (Liquid-liquid) equilibria for ternary and quaternary systems of representative compounds of gasoline + methanol at 293.15 K: experimental data and correlation, *Fluid Phase Equilibria* 348 (2013) 60-69.
- [13] J. Yang, Y. Liu, Y. Ma, Q. Meng, Y. Wang, Liquid-liquid equilibrium data for ternary aqueous mixtures containing 1-pentanol and 2-methyl-1-propanol at (298.15, 323.15, and 348.15) K, *Fluid Phase Equilibria* 349 (2013) 31-36.
- [14] Kh. Bahrpaima, S. Frydooni, M. Behzadi, Phase diagrams for (water + 1,2-butanediol or propanediol + 2-ethyl-1-hexanol) systems, *Journal of Chemical Thermodynamics* 58 (2013) 385-388.

- [15] R.S. Santiago, M. Aznar, Liquid-liquid equilibrium in ternary ionic liquid systems by UNIFAC: new volume, surface area and interaction parameters, Part II, *Fluid Phase Equilibria* 303 (2011) 111-114.
- [16] J.J. Espada, B. Coto, J.L. Peña, Liquid-liquid equilibrium in the systems furfural + light lubricating oils using UNIFAC, *Fluid Phase Equilibria* 259 (2007) 201-209.
- [17] S. Çehreli, B. Tatlı, P. Bağman, (Liquid + liquid) equilibria of (water + propionic acid + cyclohexanone) at several temperatures, *Journal of Chemical Thermodynamics* 37 (2005) 1288-1293.
- [18] H. Ahmed, H. Diamonta, C. Chaker, R. Abdelhamid, Purification of wet process phosphoric acid by solvent extraction with TBP and MIBK mixtures, *Separation and Purification Technology* 55 (2007) 212-216.
- [19] H. Sah, Microencapsulation techniques using ethyl acetate as a dispersed solvent: effects of its extraction rate on the characteristics of PLGA microspheres, *Journal of Controlled Release* 47 (1997) 233-245.
- [20] S. Kamila, J.K. Dash, Studies on molecular interactions in different solvent extractants with n-butanol at temperature 303.15 K: a thermoacoustic investigation *Journal of Molecular Liquids* 172 (2012) 71-75.
- [21] B.F. de Almeida, T.M. Waldrigui, T. de Castro Alves, L.H. de Oliveira, M. Aznar, Experimental and calculated liquid-liquid equilibrium data for water + furfural + solvents, *Fluid Phase Equilibria* 334 (2012) 97-105.
- [22] JCGM 100:2008; GUM 1995 with minor corrections, Evaluation of Measurement Data-Guide to the Expression of Uncertainty in Measurement, JCGM, 2008, pp. 1-120.
- [23] B.N. Taylor, C.E. Kuyatt, National Institute of Standards and Technology (NIST)-Guidelines for Evaluating and Expressing the Uncertainty of NIST Measurement Results, NIST Technical Note 1297, 1994, pp. 1-20.
- [24] R.E. Treybal, *Liquid Extraction*, McGraw-Hill, New York, 1963.
- [25] Introducing alcohols < <http://www.chemguide.co.uk/organicprops/alcohols/background.html> > (accessed 03.12.13).
- [26] J. Saien, M. Mozafarvandi, S. Daliri, M. Norouzi, (Liquid + liquid) equilibria for the ternary (water + acetic acid + toluene) system at different temperatures:

- experimental data and correlation, *Journal of Chemical Thermodynamics* 57 (2013) 76-81.
- [27] H. Haghazarloo, M.N. Lotfollahi, J. Mahmoudi, A.H. Asl, Liquid-liquid equilibria for ternary systems of (ethylene glycol + toluene + heptane) at temperatures (303.15, 308.15, and 313.15) K and atmospheric pressure: Experimental results and correlation with UNIQUAC and NRTL models, *Journal of Chemical Thermodynamics* 60 (2013) 126-131.
- [28] A. Fredenslund, R.L. Jones, J.M. Prausnitz, Group-contribution estimation of activity coefficients in nonideal liquid mixtures, *AIChE Journal* 21 (1975) 1086-1099.
- [29] J.M. Prausnitz, *Molecular Thermodynamics of Fluid-Phase Equilibria*, third ed., 258-291, Prentice Hall, 1998.
- [30] P. Morawski, T.M. Letcher, P.K. Naicker, U. Domanska, Liquid-liquid equilibria for mixtures of (furfuryl alcohol + an aromatic hydrocarbon + an alkane) at  $T = 298.15$  K *Journal of Chemical and Engineering Data* 47 (2002) 1453-1456.



## Chapter III

Experiments and thermodynamic models for ternary (liquid-liquid) equilibrium systems of water + cyclopentanone + organic solvents at  $T = 298.2$  K

Thidarat Wongsawa<sup>a</sup>, Milan Hronec<sup>b</sup>,  
Anchaleeporn Waritswat Lothongkum<sup>c</sup>, Ura Pancharoen<sup>a</sup>, Suphot Phatanasri<sup>a</sup>

<sup>a</sup> *Department of Chemical Engineering, Faculty of Engineering, Chulalongkorn University, Phyathai Rd., Bangkok 10330, Thailand*

<sup>b</sup> *Department of Organic Technology, Slovak University of Technology, Radlinského 9, 812 37 Bratislava, Slovakia*

<sup>c</sup> *Department of Chemical Engineering, Faculty of Engineering, King Mongkut's Institute of Technology Ladkrabang, Chalongkrung Rd., Bangkok 10520, Thailand*

### 3.1 Abstract

The aim of this paper is to obtain liquid-liquid equilibrium (LLE) data for cyclopentanone extraction. Ternary LLE systems of water + cyclopentanone + organic solvents (MIBK, ethyl acetate, furfural or *n*-butanol) were investigated at  $T = 298.2$  K and atmospheric pressure. The solubility and tie-line data of these ternary LLE systems were determined by direct analysis. The reliability of the LLE experimental results was validated by the Othmer-Tobias and Hand correlation equations. Distribution coefficients ( $D$ ) and separation factors ( $S$ ) were calculated in order to evaluate the capability of selective organic solvents for cyclopentanone extraction. NRTL and UNIQUAC models were employed to correlate the results obtained by the modeling with the experimental data. Good correlation results were confirmed by the *rmsd* values of less than 6%.

**Keywords:** Cyclopentanone; Solubility; Ternary systems; Tie-line data; Liquid-liquid equilibrium; Thermodynamic models.

### 3.2 Introduction

In recent years, cyclopentanone has received increased attention due to its versatility in the chemical industry. Cyclopentanone is used in the preparation of fungicides and fragrance ingredients as well as in the manufacture of other productions [1-3]. In the prevention of environmental contamination, extraction of cyclopentanone from wastewater is of significant importance.

Solvent extraction is a wide-spread technique because of its low energy consumption and high efficiency over traditional techniques [4]. The efficiency of this technique depends on the physical and chemical properties of the organic solvent used for extracting the component contained in water. The selection of an organic solvent must be considered from the view point of thermal stability, favorable density, viscosity, boiling point and interfacial tension [5]. In order to design and

perform solvent extraction processes, liquid-liquid equilibrium (LLE) data of ternary systems are mainly required. Ternary diagrams involving the binodal curve of solubility and tie-lines have an important role in ascertaining ternary LLE data. They can normally be obtained by direct analysis or by cloud-point titration [6].

Thermodynamic models, especially the non-random two liquid (NRTL) model and the universal quasi chemical (UNIQUAC) model [7-11], are also necessary to estimate the thermodynamic properties of the ternary systems. These models involve binary interaction parameters. To the best of our knowledge, LLE data of the ternary system for cyclopentanone extraction, within the above mentioned models, has not been reported in the literature.

This work focuses on studying the liquid phase behavior for cyclopentanone extraction from water. The ternary LLE systems consisting of water, cyclopentanone and organic solvents were investigated at a temperature of 298.2 K and atmospheric pressure. Various organic solvents such as methyl isobutyl ketone (MIBK), ethyl acetate, furfural and *n*-butanol were selected as organic solvents because they are non-toxic and are very efficient to use in industry [12-15]. For each ternary system, both solubility and tie-line data were obtained by direct analysis. The reliability of the experimental results was validated by the Othmer-Tobias and Hand correlation equations. Distribution coefficients (*D*) and separation factors (*S*) were calculated from the tie-line data in order to express the extraction capability of selected organic solvents. The LLE data of the investigated systems was correlated with the modeling results as calculated by the NRTL and UNIQUAC models. The values of the binary interaction parameters used in these models were determined by the Aspen Plus software program (AspenTech, Burlington, MA, USA) and regressed with the experimental equilibrium results.

### 3.3 Experimental

#### 3.3.1 Chemicals

Cyclopentanone ( $C_5H_8O$ , MW 84.12 g/mol) and furfural ( $C_5H_4O_2$ , MW 96.08 g/mol) were purchased from Sigma-Aldrich. The chemical structure of cyclopentanone is presented in Figure 3.1. *n*-Butanol ( $C_4H_9OH$ , MW 74.12 g/mol) was purchased from Erba Lachema s.r.o. Methyl isobutyl ketone ( $C_6H_{12}O$ , MW 100.16 g/mol) and ethyl acetate ( $C_4H_8O_2$ , MW 88.11 g/mol) were purchased from MicroChem Corp. All chemicals with purity higher than 99% were used without further purification. Distilled water was used in all experiments.



**Figure 3.1** Chemical structure of cyclopentanone.

#### 3.3.2 Apparatus and procedure

The solubility data for the ternary systems consisting of water, cyclopentanone and organic solvents was obtained by direct analysis. The experimental measurements were made in organic-rich and aqueous-rich phases at equilibrium. A digital analytical balance-Mettler Toledo AE200 (with an accuracy of  $\pm 0.0001$  g) was used to determine the weight of all components. The temperature of the systems was controlled by a water jacket that was checked using a digital thermometer (with an accuracy of  $\pm 0.1$  K). The procedure for obtaining the solubility curves of the organic-rich and aqueous-rich phases was carried out the same manner as reported by Wongsawa et al. [16]. All measurements were repeated at least three times.

After reaching equilibrium, tie-line data was obtained from the ternary mixtures. Extra water was added to the mixtures until transition from a homogeneous state to heterogeneous state appeared. Thereafter, the mixtures were agitated vigorously at 200 rpm for 2 hours. Then, they were centrifugated and left for 14 hours to complete separation. Thereafter, the organic-rich phase was carefully withdrawn from the top layer of the glass vessel by syringe and then weighed. The remaining aqueous-rich sample was also weighed and analyzed by gas chromatography. All compositions of the components were calculated on the basis of analytical results and the mass balance equation. Ternary diagrams were plotted by the ProSim program for all ternary LLE data.

### 3.3.3 Analysis and uncertainty measurement

The aqueous phases were analyzed by gas chromatography (Hewlett Packard 5890 Series II, with FID detector) using a 1.4 m × 3 mm glass column packed with 5% C20M + 5% SE. The quantitative determination of component concentrations in the separated phases was made by the external standard method.

The uncertainties of each experimental variable are shown in the footnote of the corresponding table and were calculated according to the GUM and Eurachem, as shown in Eq. (3.1)

$$u_c(v) = \sqrt{\sum \left( \frac{\partial v}{\partial v_i} \right)^2 \cdot u_{v_i}^2} \quad (3.1)$$

where  $u_c(v)$  is the combined uncertainty of variable  $v$  which is considered to be dependent on another variable  $v_i$  and its uncertainty ( $u_{v_i}$ ) [17].

### 3.4 Results and discussion

#### 3.4.1 Experimental data

The equilibrium solubility data on the binodal curves for the ternary systems of (water + cyclopentanone + organic solvents) at  $T = 298.2$  K and atmospheric pressure is given in Table 3.1. All compositions are expressed in terms of mass fraction. The same solubility data was plotted in Figure 3.2. In the case of *n*-butanol, the binodal curves have different characteristics in comparison with the other mixtures. However, this characteristic is similar to the basic type of LLE behavior as reported by Novák et al. [18]. Since only a liquid pair (cyclopentanone + organic solvent) is completely miscible and two liquid pairs (water + cyclopentanone and water + organic solvent) are partially miscible, each ternary system exhibited type-2 behavior of LLE [19]. The area of biphasic region decreased in the following order of organic solvents: MIBK > ethyl acetate > furfural > *n*-butanol. This was because the area of biphasic region depended on the mutual solubility of water and the organic solvents. Thus, the type of organic solvent is an important factor for the biphasic region of the investigated systems.

**Table 3.1** Equilibrium solubility data in mass fractions ( $w_i$ ) for the ternary systems of water (1) + cyclopentanone (2) + organic solvents (3) at  $T = 298.2$  K and atmospheric pressure.<sup>a</sup>

MIBK		Ethyl acetate		Furfural		<i>n</i> -Butanol	
$w_1$	$w_2$	$w_1$	$w_2$	$w_1$	$w_2$	$w_1$	$w_2$
0.0190	0.0000	0.0407	0.0000	0.0457	0.0000	0.1637	0.0000
0.0134	0.0840	0.0323	0.0843	0.0530	0.1428	0.1695	0.0762
0.0141	0.1947	0.0346	0.1735	0.0641	0.2184	0.1775	0.1462
0.0192	0.3251	0.0437	0.3103	0.0732	0.3212	0.1823	0.2518
0.0198	0.4351	0.0532	0.4667	0.0791	0.4301	0.1816	0.3364
0.0207	0.5581	0.0618	0.5336	0.0820	0.4937	0.1775	0.4322
0.0242	0.6612	0.0685	0.6131	0.0853	0.5954	0.1675	0.5422
0.0242	0.7612	0.0814	0.6796	0.0916	0.7355	0.1559	0.6337
0.0390	0.8435	0.0938	0.7765	0.1005	0.8407	0.1359	0.7487
0.0973	0.9027	0.1116	0.8884	0.1116	0.8884	0.1116	0.8884
0.9810	0.0000	0.9332	0.0000	0.9135	0.0000	0.9372	0.0000
0.9433	0.0425	0.8976	0.0391	0.8724	0.0568	0.8598	0.0775
0.9055	0.0862	0.8616	0.0869	0.8274	0.1170	0.8118	0.1330
0.8222	0.1750	0.8264	0.1366	0.8008	0.1563	0.7886	0.1797
0.7674	0.2326	0.7616	0.2384	0.7616	0.2384	0.7616	0.2384

<sup>a</sup> Standard uncertainties are  $u(T) = 0.1$  K and  $u(w) = 0.0008$ .

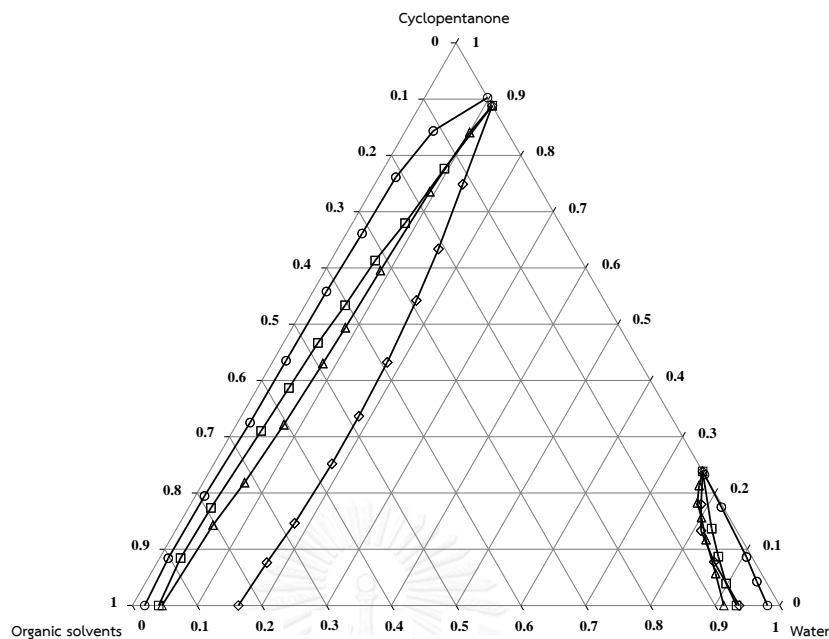


**Figure 3.2** Binodal curves for ternary systems of water + cyclopentanone + organic solvents at  $T = 298.2$  K and atmospheric pressure; (-○-) MIBK, (-□-) ethyl acetate, (-△-) furfural and (-◇-) *n*-butanol.

The experimental tie-line data of these ternary systems was achieved at the same temperature as shown in Table 3.2. Corresponding triangular phase diagrams for these tie-line data are plotted in Figures 3.3 to 3.6. As regards these figures, the slopes of the tie-lines highlight the fact that cyclopentanone is more soluble in the organic solvent than in water. Probably, this is due to the presence of a carbonyl group in the molecule of cyclopentanone which can interact with the organic solvent and water. However, cyclopentanone can form only weak bonds with hydrogen atoms of water [20]. Usually, the quantity of a soluble component in water is directly based on its intermolecular force.

**Table 3.2** Experimental tie-line data in mass fractions for the ternary systems of water (1) + cyclopentanone (2) + organic solvents (3) at  $T = 298.2$  K and atmospheric pressure.<sup>a</sup>

Aqueous-rich phase			Organic-rich phase		
$w_1$	$w_2$	$w_3$	$w_1$	$w_2$	$w_3$
Water (1) + Cyclopentanone (2) + MIBK (3)					
0.9554	0.0106	0.0327	0.0191	0.0812	0.8896
0.9542	0.0280	0.0177	0.0165	0.1277	0.8478
0.9454	0.0344	0.0202	0.0178	0.1895	0.7888
0.9283	0.0594	0.0123	0.0242	0.2181	0.7577
0.9225	0.0680	0.0195	0.0202	0.2832	0.7117
0.9119	0.0788	0.0103	0.0174	0.3662	0.6164
0.9090	0.0807	0.0073	0.0282	0.4749	0.4970
0.9101	0.0839	0.0060	0.0236	0.6301	0.3394
0.9031	0.0895	0.0060	0.0286	0.7701	0.2013
Water (1) + Cyclopentanone (2) + Ethyl acetate (3)					
0.9007	0.0131	0.0922	0.0330	0.1148	0.8182
0.8904	0.0211	0.0885	0.0351	0.1375	0.8287
0.8705	0.0580	0.0800	0.0437	0.2821	0.6692
0.8600	0.0700	0.0796	0.0445	0.3529	0.5983
0.8517	0.0811	0.0719	0.0488	0.3991	0.5479
0.8407	0.0910	0.0703	0.0539	0.4530	0.4871
0.8395	0.1011	0.0594	0.0699	0.6033	0.3270
0.8214	0.1307	0.0489	0.0803	0.6852	0.2314
0.8029	0.1595	0.0339	0.1032	0.8127	0.0837
Water (1) + Cyclopentanone (2) + Furfural (3)					
0.8973	0.0238	0.0819	0.0539	0.1370	0.7991
0.8825	0.0404	0.0786	0.0613	0.1989	0.7308
0.8675	0.0631	0.0744	0.0694	0.2884	0.6422
0.8543	0.0801	0.0700	0.0742	0.3684	0.5584
0.8291	0.1110	0.0620	0.0800	0.4237	0.4963
0.8115	0.1408	0.0468	0.0822	0.5499	0.3603
0.7760	0.1935	0.0350	0.0876	0.6662	0.2462
0.7735	0.2014	0.0304	0.0929	0.7738	0.1332
Water (1) + Cyclopentanone (2) + <i>n</i> -Butanol (3)					
0.9215	0.0131	0.0764	0.1685	0.0665	0.7650
0.9062	0.0267	0.0771	0.1739	0.1250	0.7011
0.8973	0.0335	0.0692	0.1797	0.2159	0.6044
0.8901	0.0443	0.0686	0.1828	0.2553	0.5619
0.8613	0.0726	0.0661	0.1844	0.3085	0.5071
0.8338	0.1064	0.0598	0.1751	0.4554	0.3695
0.8212	0.1198	0.0590	0.1709	0.5156	0.3135
0.8112	0.1327	0.0561	0.1686	0.5474	0.2840
0.7900	0.1769	0.0331	0.1608	0.6174	0.2218

<sup>a</sup> Standard uncertainties are  $u(T) = 0.1$  K and  $u(w) = 0.0009$ .

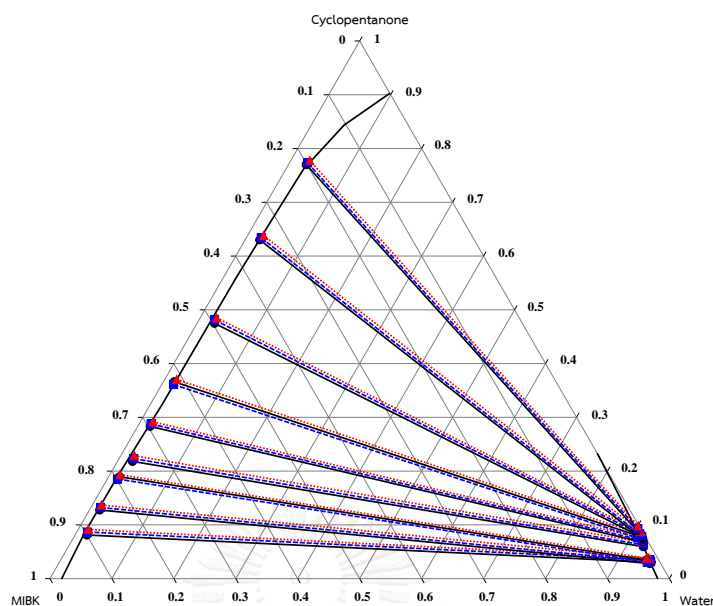


**Figure 3.3** Ternary diagram for LLE of the system of water (1) + cyclopentanone (2) + MIBK (3) at  $T = 298.2$  K and atmospheric pressure; (—●—) experimental tie-line data, (---■---) calculated NRTL data and (··▲··) calculated UNIQUAC data.

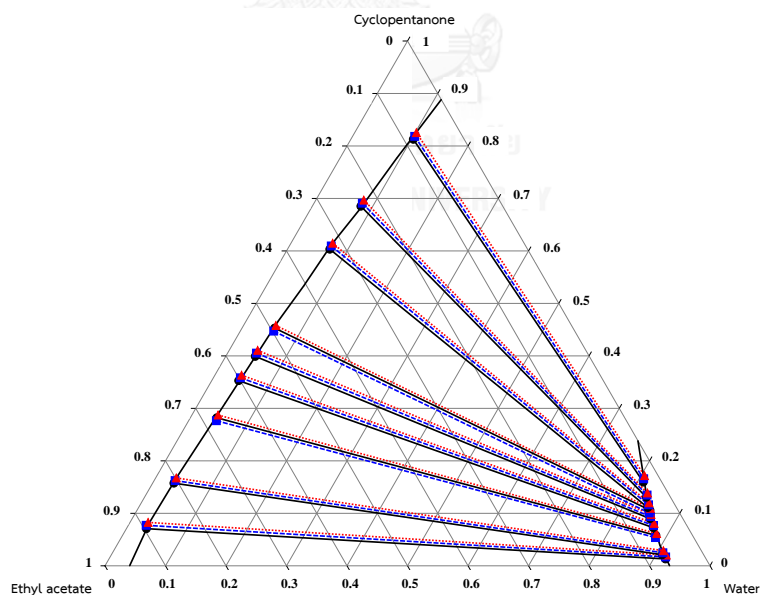


**Figure 3.4** Ternary diagram for LLE of the system of water (1) + cyclopentanone (2) + ethyl acetate (3) at  $T = 298.2$  K and atmospheric pressure; (—●—) experimental tie-line data, (---■---) calculated NRTL data and (··▲··) calculated UNIQUAC data.

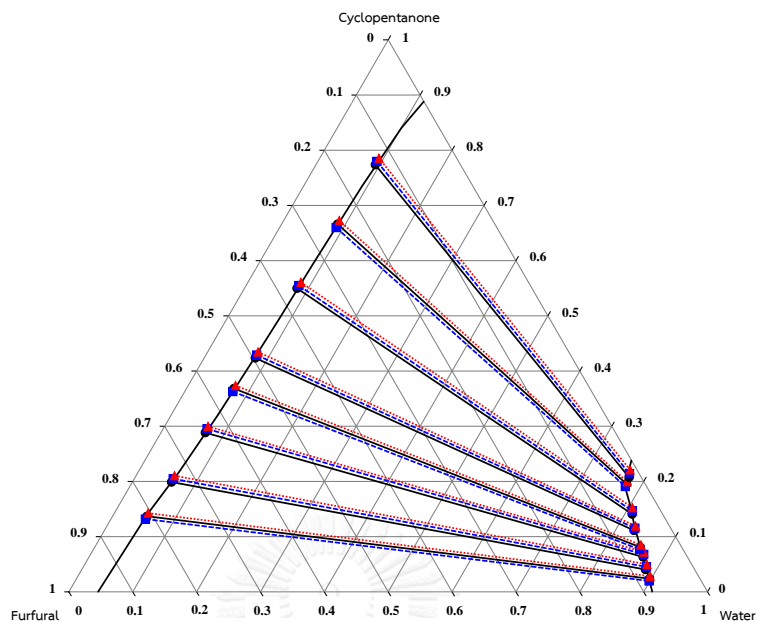


**Figure 3.5** Ternary diagram for LLE of the system of water (1) + cyclopentanone (2) + furfural (3) at  $T = 298.2$  K and atmospheric pressure; (—●—) experimental tie-line data, (---■---) calculated NRTL data and (··▲··) calculated UNIQUAC data.

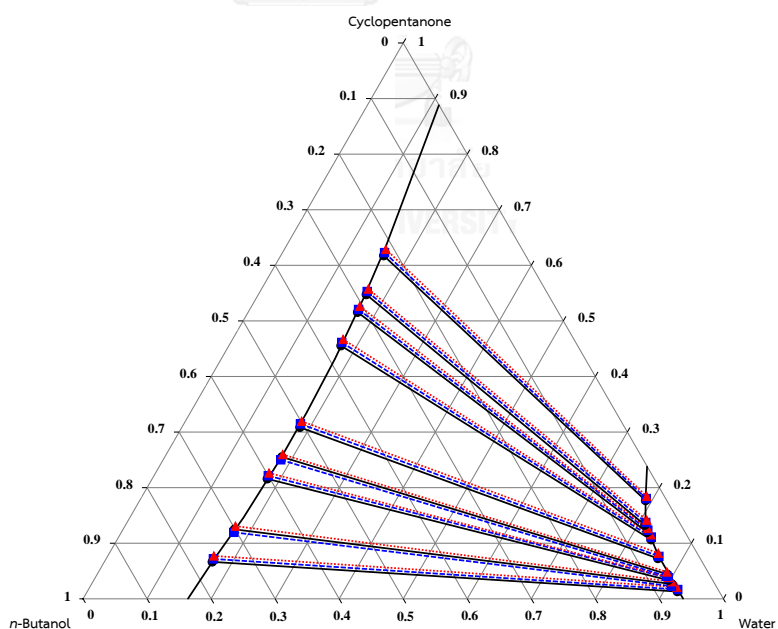


**Figure 3.6** Ternary diagram for LLE of the system of water (1) + cyclopentanone (2) + *n*-butanol (3) at  $T = 298.2$  K and atmospheric pressure; (—●—) experimental tie-line data, (---■---) calculated NRTL data and (··▲··) calculated UNIQUAC data.

### 3.4.2 Reliability of tie-line data

The reliability of experimental tie-line data was validated by the Othmer-Tobias and Hand correlation equations [21] as follows:

$$\ln\left(\frac{1-w_{33}}{w_{33}}\right) = A + B\ln\left(\frac{1-w_{11}}{w_{11}}\right) \quad (3.2)$$

$$\ln\left(\frac{w_{21}}{w_{11}}\right) = A' + B'\ln\left(\frac{w_{23}}{w_{33}}\right) \quad (3.3)$$

where  $w_{11}$  is the mass fraction of water in aqueous-rich phase,  $w_{21}$  and  $w_{23}$  are the mass fractions of cyclopentanone in aqueous-rich and organic-rich phases, respectively,  $w_{33}$  is the mass fraction of organic solvent in organic-rich phase.  $A, B, A'$  and  $B'$  are the Othmer-Tobias and Hand correlation parameters, respectively. These numerical constants depend on the type of ternary system and equilibrium component.

The parameters of the Othmer-Tobias and Hand correlations were obtained at the intercepts of the slopes of the plots, as shown in Figures 3.7 and 3.8, respectively. The values of these parameters are listed in Table 3.3. The results showed that the plots were linear with a high acceptable correlation factor ( $R^2$ ). This indicates the reliability of the experimental tie-line data obtained in this work.

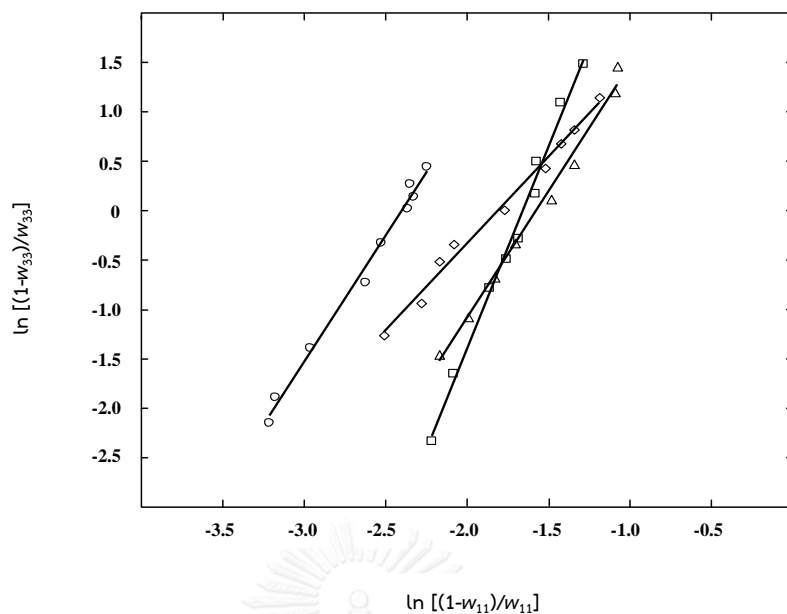


**Figure 3.7** Othmer-Tobias plot for the ternary systems of water (1) + cyclopentanone (2) + organic solvents (3) at  $T = 298.2$  K and atmospheric pressure; (○) MIBK, (□) ethyl acetate, (△) furfural and (◇) *n*-butanol.

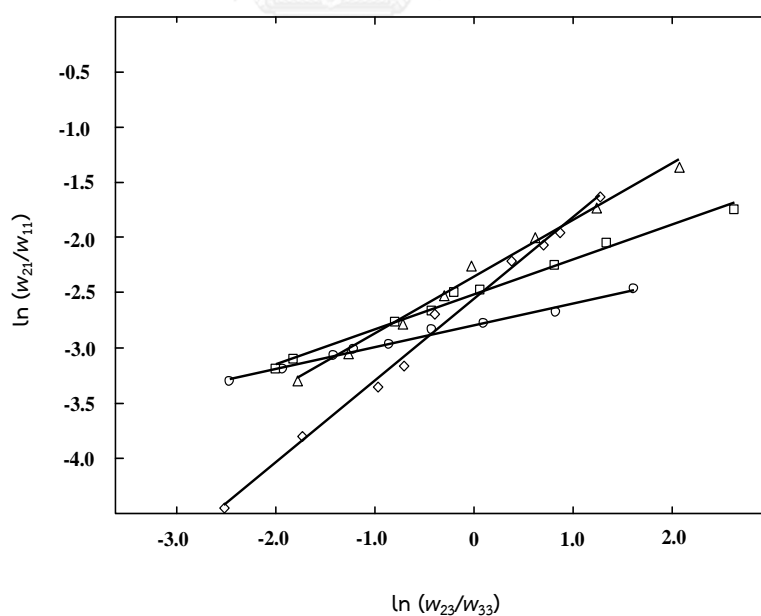


**Figure 3.8** Hand plot for the ternary systems of water (1) + cyclopentanone (2) + organic solvents (3) at  $T = 298.2$  K and atmospheric pressure; (○) MIBK, (□) ethyl acetate, (△) furfural and (◇) *n*-butanol.

**Table 3.3** Othmer-Tobias and Hand correlation parameters and their correlation factors ( $R^2$ ) for the ternary systems of water (1) + cyclopentanone (2) + organic solvents (3) at  $T = 298.2$  K and atmospheric pressure.

Ternary system	Othmer-Tobias correlation			Hand correlation		
	A	B	$R^2$	A'	B'	$R^2$
Water + Cyclopentanone + MIBK	7.1849	2.9988	0.9909	-2.6093	0.2143	0.9903
Water + Cyclopentanone + Ethyl acetate	8.4124	4.8206	0.9904	-2.3183	0.3383	0.9912
Water + Cyclopentanone + Furfural	5.1003	3.0227	0.9916	-2.1351	0.5525	0.9926
Water + Cyclopentanone + <i>n</i> -Butanol	3.9420	2.0666	0.9900	-2.2926	0.7951	0.9934

### 3.4.3 Distribution coefficients and separation factors

The efficient extraction of cyclopentanone from water is an important element in this process. To indicate the capability of the organic solvents for cyclopentanone extraction, the distribution coefficients ( $D$ ) and the separation factors ( $S$ ) were calculated by the following equation:

$$S = \frac{D_2}{D_1} = \frac{w_{23} / w_{21}}{w_{13} / w_{11}} \quad (3.4)$$

where  $D_1$  and  $D_2$  are the distribution coefficients of water and cyclopentanone,  $w_{13}$  and  $w_{23}$  are the mass fractions of water and cyclopentanone in organic-rich phase, and  $w_{11}$  and  $w_{21}$  are the mass fractions of water and cyclopentanone in aqueous-rich phase, respectively.

The values of the experimental distribution coefficients and separation factors for each ternary system are listed in Table 3.4. The variation of the separation factor as a function of the mass fraction of cyclopentanone in the aqueous-rich phase is shown in Figure 3.9. As regards the investigated ternary systems, all selected organic solvents have high distribution coefficients and separation factor values i.e.  $> 1$ . This indicates the capability of these solvents to extract cyclopentanone from water. MIBK has the

highest separation factor at  $T = 298.2$  K where separation factors varied between 134 and 383. Thus, this solvent proved to be superior for cyclopentanone extraction among the studied organic solvents. As can be seen in Figure 3.9, separation factors decreased when there was an increase in mass fraction of cyclopentanone in the aqueous-rich phase due to more water present in the organic-rich phase [6].

**Table 3.4** Distribution coefficients ( $D$ ) and separation factors ( $S$ ) for the ternary systems of water (1) + cyclopentanone (2) + organic solvents (3) at  $T = 298.2$  K and atmospheric pressure.

Ternary system	$w_{21}$	$D_1$	$D_2$	$S$
Water + Cyclopentanone + MIBK	0.0106	0.0200	7.6604	383.1793
	0.0280	0.0153	4.5607	297.7475
	0.0344	0.0201	5.5087	273.5812
	0.0594	0.0187	3.6717	195.8453
	0.0680	0.0236	4.1647	176.1951
	0.0788	0.0305	4.6472	152.5511
	0.0807	0.0398	5.8848	147.6896
	0.0839	0.0535	7.5101	140.4207
	0.0895	0.0644	8.6045	133.7027
Water + Cyclopentanone + Ethyl acetate	0.0131	0.0366	8.7634	239.1866
	0.0211	0.0325	6.5166	200.3097
	0.0420	0.0468	4.8638	135.8863
	0.0700	0.0557	5.0414	90.4299
	0.0811	0.0624	4.9211	78.8871
	0.0910	0.0695	4.9780	71.6442
	0.1011	0.0923	5.9674	64.6681
	0.1307	0.0978	5.2425	53.6267
	0.1595	0.1285	5.0953	39.6416
Water + Cyclopentanone + Furfural	0.0238	0.0601	5.7563	95.8280
	0.0404	0.0695	4.9233	70.8774
	0.0631	0.0800	4.5705	57.1315
	0.0801	0.0940	4.5993	48.9534
	0.1110	0.0965	3.8171	39.5596
	0.1408	0.1068	3.9055	36.5565
	0.1935	0.1129	3.4429	30.4987
	0.2014	0.1281	3.8421	29.9900
Water + Cyclopentanone + <i>n</i> -Butanol	0.0131	0.1549	5.0763	32.7617
	0.0267	0.1540	4.6816	30.3963
	0.0335	0.1595	4.6537	29.1808
	0.0443	0.1651	4.6343	28.0614
	0.0726	0.1857	4.8003	25.8478
	0.1064	0.1991	4.6560	23.3811
	0.1198	0.2081	4.3038	20.6806
	0.1327	0.2192	4.3512	19.8474
	0.1769	0.2299	3.9423	17.1467

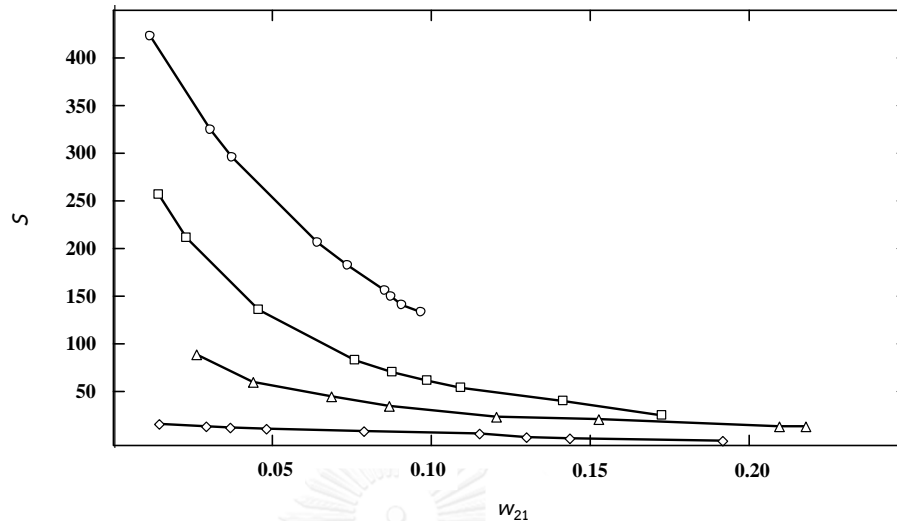


**Figure 3.9** Separation factors ( $S$ ) plotted against the mass fraction of cyclopentanone in aqueous-rich phase ( $w_{21}$ ) at  $T = 298.2$  K and atmospheric pressure; ( $\circ$ ) MIBK, ( $\square$ ) ethyl acetate, ( $\Delta$ ) furfural and ( $\diamond$ )  $n$ -butanol.

#### 3.4.4 Thermodynamic model correlation

The experimental tie-line data can be represented by the thermodynamic models of activity coefficients. The experimental tie-line data at  $T = 298.2$  K, for each ternary system, was used to correlate with the NRTL and UNIQUAC models. Thus, the basic relationship for any component  $i$  in the aqueous-rich and organic-rich phases at equilibrium is as follows:

$$x_i^I \gamma_i^I = x_i^{II} \gamma_i^{II} \quad (3.5)$$

$$\sum x_i^I = \sum x_i^{II} = 1 \quad (3.6)$$

where  $x_i^I$ ,  $x_i^{II}$ ,  $\gamma_i^I$  and  $\gamma_i^{II}$  are the mole fractions and activity coefficients of the component  $i$  in aqueous-rich (I) and organic-rich (II) phases, respectively.

The activity coefficient ( $\gamma_i$ ) in the NRTL model is expressed as [22]:

$$\ln \gamma_i = \frac{\sum_{j=1}^3 \tau_{ji} G_{ji} x_j}{\sum_{k=1}^3 G_{ki} x_k} + \sum_{j=1}^3 \frac{x_j G_{ij}}{\sum_{k=1}^3 G_{kj} x_k} \left( \tau_{ij} - \frac{\sum_{k=1}^3 x_k \tau_{kj} G_{kj}}{\sum_{k=1}^3 G_{kj} x_k} \right) \quad (3.7)$$

where  $x_i$  is the mole fraction of component  $i$ , the parameters  $\tau_{ij}$ ,  $\tau_{ji}$ ,  $\tau_{kj}$ ,  $G_{ij}$ ,  $G_{ji}$ ,  $G_{ki}$  and  $G_{kj}$  are the adjustable parameters for each binary pair in the NRTL model and  $i, j, k$  are the indices for all components.

These adjustable parameters can be calculated as follows:

$$\tau_{ij} = a_{ij} + \frac{b_{ij}}{T} + e_{ij} \ln T \quad (3.8)$$

$$\alpha_{ij} = \alpha_{ji} = c_{ij} \quad (3.9)$$

$$G_{ij} = \exp(-\alpha_{ij} \tau_{ij}) \quad (3.10)$$

where  $a_{ij}$ ,  $b_{ij}$ ,  $c_{ij}$  and  $e_{ij}$  are the NRTL coefficients for the binary interaction parameters and  $\alpha_{ij}$  and  $\alpha_{ji}$  are the non-randomness parameters.

The activity coefficient ( $\gamma_i$ ) in the UNIQUAC model is determined using the assumption of the sum between the combinational ( $\gamma_i^C$ ) and residual ( $\gamma_i^R$ ) activity coefficients as given by [23]:

$$\ln \gamma_i = \ln \gamma_i^C + \ln \gamma_i^R \quad (3.11)$$

$$\ln \gamma_i^C = \ln \left( \frac{\Phi_i}{x_i} \right) + \frac{z}{2} q_i \ln \left( \frac{\theta_i}{\Phi_i} \right) + l_i - \frac{\Phi_i}{x_i} \sum_{j=1}^3 x_j l_j \quad (3.12)$$

$$\ln \gamma_i^R = q_i \left[ 1 - \ln \left( \sum_{j=1}^3 \theta_j \tau_{ji} \right) - \sum_{j=1}^3 \left( \frac{\theta_j \tau_{ij}}{\sum_{k=1}^3 \theta_k \tau_{kj}} \right) \right] \quad (3.13)$$

where  $\tau_{ij}$ ,  $\tau_{ji}$ ,  $\tau_{kj}$ ,  $l_i$  and  $l_j$  are the adjustable parameters,  $i$ ,  $j$  and  $k$  are the indices for all components,  $z$  is the integral number equal to 10 and  $\theta_i$ ,  $\theta_j$ ,  $\theta_k$  and  $\Phi_i$  are the surface areas and volume fractions in the UNIQUAC model, respectively.

These adjustable parameters can be calculated from the following equations:

$$l_i = \frac{z}{2} (r_i - q_i) - (r_i - 1) \quad (3.14)$$

$$\tau_{ij} = a_{ij} + \frac{b_{ij}}{T} + c_{ij} \ln T + d_{ij} T \quad (3.15)$$

$$\Phi_i = \frac{x_i r_i}{\sum_{j=1}^3 x_j r_j} \quad (3.16)$$

$$\theta_i = \frac{x_i q_i}{\sum_{j=1}^3 x_j q_j} \quad (3.17)$$

where  $a_{ij}$ ,  $b_{ij}$ ,  $c_{ij}$  and  $d_{ij}$  are the UNIQUAC coefficients for the binary interaction parameters. The UNIQUAC structural parameters  $r_i$  and  $q_i$  are the number of segments per molecule and the relative surface area per molecule, respectively.

They can be calculated from the number of molecular groups and the individual values of the van der Waals volume together with the area of molecule by the Bondi Method [6].

In this work, the value of the non-randomness parameter ( $\alpha$ ) of the NRTL model was determined. Thus, the appropriate value was taken to be 0.2. The values of the structural parameters  $r$  and  $q$  used for the UNIQUAC model were taken from the literature as shown in Table 3.5 [15, 24, 25]. The binary interaction parameters of NRTL ( $b_{ij}$ ) and UNIQUAC ( $a_{ij}$ ) models were obtained by the Aspen Plus software program and regression with the experimental LLE data. Both values for each ternary system are listed in Table 3.6.

**Table 3.5** UNIQUAC structural parameters ( $r$  and  $q$ ) for pure components.

Component	$r$	$q$
MIBK	4.60	4.03
Ethyl acetate	3.48	3.12
Furfural	3.17	2.48
<i>n</i> -Butanol	3.45	3.05
Cyclopentanone	3.03	2.44
Water	0.92	1.40

**Table 3.6** NRTL and UNIQUAC binary interaction parameters for the ternary systems of water + cyclopentanone + organic solvents at  $T = 298.2$  K.

$i-j$	NRTL		UNIQUAC		$rmsd$ (%)	
	$b_{ij}$ (K)	$b_{ji}$ (K)	$a_{ij}$ (K)	$a_{ji}$ (K)	NRTL	UNIQUAC
Water + Cyclopentanone + MIBK						
1-2	1,302.2816	97.0446	-911.6002	-57.9696	2.74	5.31
1-3	61.6760	2,671.4629	-5,117.8520	968.3500		
2-3	18.1436	652.1729	957.9842	1,798.2365		
Water + Cyclopentanone + Ethyl acetate						
1-2	1,073.1837	98.1663	-136.1218	564.3772	2.90	4.83
1-3	1,165.6357	470.8551	107.0128	2,116.4193		
2-3	-138.0162	164.9172	-74.1523	1,867.0376		
Water + Cyclopentanone + Furfural						
1-2	5.4362	902.9418	-0.1695	5,819.4117	3.16	5.48
1-3	-1,957.9372	-6,282.9915	-237.4438	-286.1295		
2-3	586.1674	37.7013	168.9230	-92.6174		
Water + Cyclopentanone + <i>n</i> -Butanol						
1-2	578.8451	81.1264	-127.3297	1,572.1743	2.90	5.24
1-3	-3,983.1548	-9,293.6148	-4.1000	-93.1794		
2-3	-48.1683	572.9837	116.4516	127.9993		

The modeling results were correlated with the experimental tie-line data of each ternary system as shown in Table 3.7 and Figures 3.3 to 3.6. The correlation of both results in terms of the root-mean square deviation ( $rmsd$ ) is again shown in Table 3.6. As can be seen in Table 3.7, the modeling results correlated well with the experimental results. The NRTL model, especially, provided the best correlation for all studied ternary systems. In addition, the low  $rmsd$  values for NRTL and UNIQUAC models confirmed their ability to predict the LLE data obtained in this work.

**Table 3.7** Modeling NRTL and UNIQUAC tie-line values in mass fractions for the ternary systems of water + cyclopentanone + organic solvents at  $T = 298.2$  K.

Aqueous-rich phase						Organic-rich phase					
$W_{11}$			$W_{21}$			$W_{13}$			$W_{23}$		
Expt.	NRTL	UNIQUAC	Expt.	NRTL	UNIQUAC	Expt.	NRTL	UNIQUAC	Expt.	NRTL	UNIQUAC
Water + Cyclopentanone + MIBK											
0.9554	0.9512	0.9471	0.0106	0.0348	0.0384	0.0191	0.0173	0.0162	0.0812	0.0867	0.0914
0.9542	0.9538	0.9501	0.0280	0.0316	0.0369	0.0165	0.0154	0.0148	0.1277	0.1324	0.1369
0.9454	0.9487	0.9441	0.0344	0.0308	0.0379	0.0178	0.0164	0.0164	0.1895	0.1853	0.1933
0.9283	0.9267	0.9212	0.0594	0.0628	0.0682	0.0242	0.0235	0.0221	0.2181	0.2232	0.2286
0.9225	0.9209	0.9172	0.0680	0.0711	0.0753	0.0202	0.0195	0.0206	0.2832	0.2877	0.2917
0.9119	0.9105	0.9112	0.0788	0.0758	0.0826	0.0174	0.0189	0.0194	0.3662	0.3611	0.3704
0.9090	0.9105	0.9087	0.0807	0.0832	0.0873	0.0282	0.0253	0.0267	0.4749	0.4811	0.4850
0.9101	0.9156	0.9101	0.0839	0.0797	0.0872	0.0236	0.0242	0.0259	0.6301	0.6339	0.6382
0.9031	0.9027	0.9005	0.0895	0.0928	0.0979	0.0286	0.0294	0.0306	0.7701	0.7732	0.7776
Water + Cyclopentanone + Ethyl acetate											
0.9007	0.9182	0.9174	0.0131	0.0169	0.0205	0.0330	0.0294	0.0299	0.1148	0.0772	0.0827
0.8904	0.9096	0.9085	0.0211	0.0249	0.0288	0.0351	0.0347	0.0341	0.1375	0.1624	0.1674
0.8705	0.8829	0.8809	0.0580	0.0538	0.0615	0.0437	0.0458	0.0432	0.2821	0.2765	0.2873
0.8600	0.8682	0.8671	0.0700	0.0769	0.0809	0.0445	0.0446	0.0441	0.3529	0.3583	0.3632
0.8517	0.8546	0.8535	0.0811	0.0938	0.0979	0.0488	0.0476	0.0470	0.3991	0.4053	0.4106
0.8407	0.8489	0.8465	0.0910	0.1009	0.1096	0.0539	0.0552	0.0534	0.4530	0.4472	0.4579
0.8395	0.8402	0.8391	0.1011	0.1163	0.1201	0.0699	0.0692	0.0689	0.6033	0.6095	0.6147
0.8214	0.8285	0.8272	0.1307	0.1349	0.1388	0.0803	0.0798	0.0793	0.6852	0.6910	0.6968
0.8029	0.8074	0.8058	0.1595	0.1659	0.1718	0.1032	0.1027	0.1019	0.8127	0.8183	0.8254
Water + Cyclopentanone + Furfural											
0.8973	0.8986	0.8958	0.0238	0.0197	0.0283	0.0539	0.0539	0.0527	0.1370	0.1319	0.1426
0.8825	0.8817	0.8802	0.0404	0.0452	0.0497	0.0613	0.0609	0.0602	0.1989	0.2049	0.2104
0.8675	0.8661	0.8640	0.0631	0.0678	0.0721	0.0694	0.0687	0.0680	0.2884	0.2952	0.2997
0.8543	0.8555	0.8532	0.0801	0.0767	0.0850	0.0742	0.0751	0.0740	0.3684	0.3629	0.3738
0.8291	0.8285	0.8276	0.1110	0.1154	0.1192	0.0800	0.0796	0.0789	0.4237	0.4290	0.4346
0.8115	0.8091	0.8061	0.1408	0.1465	0.1525	0.0822	0.0827	0.0829	0.5499	0.5549	0.5607
0.7760	0.7758	0.7742	0.1935	0.1909	0.1996	0.0876	0.0884	0.0871	0.6662	0.6600	0.6726
0.7735	0.7706	0.7681	0.2014	0.2141	0.2211	0.0929	0.0925	0.0927	0.7738	0.7798	0.7856
Water + Cyclopentanone + <i>n</i> -Butanol											
0.9215	0.9203	0.9164	0.0131	0.0168	0.0211	0.1685	0.1676	0.1657	0.0665	0.0718	0.0772
0.9062	0.9074	0.9042	0.0267	0.0229	0.0308	0.1739	0.1758	0.1726	0.1250	0.1196	0.1308
0.8973	0.8952	0.8944	0.0335	0.0376	0.0389	0.1797	0.1785	0.1772	0.2159	0.2214	0.2264
0.8901	0.8914	0.8876	0.0443	0.0406	0.0483	0.1828	0.1837	0.1819	0.2553	0.2501	0.2597
0.8613	0.8611	0.8572	0.0726	0.0764	0.0821	0.1844	0.1821	0.1817	0.3085	0.3147	0.3194
0.8338	0.8316	0.8291	0.1064	0.1112	0.1153	0.1751	0.1734	0.1727	0.4554	0.4613	0.4667
0.8212	0.8201	0.8185	0.1198	0.1237	0.1267	0.1709	0.1699	0.1689	0.5156	0.5206	0.5263
0.8112	0.8101	0.8095	0.1327	0.1374	0.1416	0.1686	0.1672	0.1668	0.5474	0.5529	0.5574
0.7900	0.7892	0.7880	0.1769	0.1804	0.1844	0.1608	0.1594	0.1585	0.6174	0.6229	0.6287

### 3.5 Conclusion

The ternary LLE systems of water + cyclopentanone + organic solvents (MIBK, ethyl acetate, furfural or *n*-butanol) were investigated at  $T = 298.2$  K and atmospheric pressure. All ternary systems exhibited type-2 behavior of LLE with large biphasic regions. The reliability of the experimental tie-line data was validated by the Othmer-Tobias and Hand correlation equations. High separation factors for the selected organic solvents, especially MIBK, confirmed their capability to extract cyclopentanone from water. The NRTL ( $\alpha = 0.2$ ) and UNIQUAC models provide relatively good correlations with the experimental results as shown by the *rmsd* values which are less than 6%.

### 3.6 Nomenclature and units

$A, B$	Othmer-Tobias correlation parameters in Eq. (3.2)
$A', B'$	Hand correlation parameters in Eq. (3.3)
$a, b, c, d, e$	NRTL and UNIQUAC coefficients for the binary interaction parameters
$D$	distribution coefficient
$G$	NRTL parameter in Eqs. (3.7) and (3.10)
$l$	UNIQUAC parameter in Eqs. (3.12) and (3.14)
$q$	relative surface area per molecule of relative component
$R^2$	acceptable correlation factor
$r$	number of segments per molecule of relative component
<i>rmsd</i>	root-mean square deviation (%)
$S$	separation factor
$T$	temperature (K)
$u$	uncertainty
$u_c$	combined uncertainty
$v$	experimental variable
$w$	mass fraction

$x$	mole fraction
$z$	integral number in Eqs. (3.12) and (3.14)

#### *Greek letters*

$\alpha$	non-random parameter
$\gamma$	activity coefficient
$\gamma^c$	combinational activity coefficient
$\gamma^R$	residual activity coefficient
$\theta$	UNIQUAC parameter in Eqs. (3.12-3.13) and (3.17)
$\tau$	NRTL and UNIQUAC parameters in Eqs. (3.7-3.8), (3.10), (3.13) and (3.15)

#### *Symbol*

$\Phi$	UNIQUAC parameter in Eqs. (3.12) and (3.16)
--------	---

#### *Subscripts*

$i, j, k$	indices for all components
I	water-rich phase
II	organic-rich phase
1	water
2	cyclopentanone
3	organic solvents

### **3.7 Acknowledgements**

The authors gratefully acknowledge the financial support given by the Thailand Research Fund and Chulalongkorn University under the Royal Golden Jubilee Ph.D. program (Grant No. PHD/0272/2549). Sincere thanks are also given to the Department

of Organic Technology, Slovak University of Technology, Bratislava, Slovakia, Ing. Fulajtárová Katarína and Dr. Tomáš Soták for their kind support.

### 3.8 References

- [1] P. Sudarsanam, L. Katta, G. Thrimurthulu, B.M. Reddy, Vapor phase synthesis of cyclopentanone over nanostructured ceria-zirconia solid solution catalysts, *Journal of Industrial and Engineering Chemistry* 19 (2013) 1517-1524.
- [2] J. Scognamiglio, L. Jones, C.S. Letizia, A.M. Api, Review: fragrance material review on cyclopentanone, *Food and Chemical Toxicology* 50 (2012) S608-S612.
- [3] M. Hronec, K. Fulajtarová, T. Liptaj, Effect of catalyst and solvent on the furan ring rearrangement to cyclopentanone, *Applied Catalysis A: General* 437-438 (2012) 104-111.
- [4] P. Reddy, T.M. Letcher, Chapter 5: phase equilibrium studies on ionic liquid systems for industrial separation processes of complex organic mixtures, in: T.M. Letcher (Ed.), *Thermodynamics, Solubility and Environmental Issues*, 85-111, Elsevier B.V., 2007.
- [5] T.P. Kumar, P.K. Das, Solubility and tie-line data for water + formic acid + methyl isobutyl ketone ternary system at different temperatures, *Chemical Engineering Communications* 197 (2010) 1163-1171.
- [6] J. Saien, M. Norouzi, H. Dehghani, The choice of solvent and liquid-liquid equilibrium for ternary water + 2-methylaziridine + chloroform system: experimental data and modeling, *Fluid Phase Equilibria* 338 (2013) 224-231.
- [7] H. Hagnazarloo, M.N. Lotfollahi, J. Mahmoudi, A.H. Asl, Liquid-liquid equilibria for ternary systems of (ethylene glycol + toluene + heptane) at temperatures (303.15, 308.15 and 313.15 K) and atmospheric pressure: experimental results and correlation with UNIQUAC and NRTL models, *The Journal of Chemical Thermodynamics* 60 (2013) 126-131.
- [8] S.H. Shin, In-C. Hwang, So-J. Park, Liquid-liquid equilibria at 298.15 K for ternary mixtures of methyl *tert*-butyl ether + methanol (or ethanol) + imidazolium-

- based ionic liquids at atmospheric pressure, *Fluid Phase Equilibria* 342 (2013) 82-87.
- [9] J. Saien, M. Mozafarvandi, S. Daliri, M. Norouzi, (Liquid + liquid) equilibria for the ternary (water + acetic acid + toluene) system at different temperatures: experimental data and correlation, *The Journal of Chemical Thermodynamics* 57 (2013) 76-81.
- [10] H.G. Gilani, A.G. Gilani, S. Shekarsaraee, Solubility and tie line data of the water-phosphoric acid-solvents at  $T = 303.2, 313.2$  and  $323.2$  K: an experimental and correlational study, *Thermochimica Acta* 558 (2013) 36-45.
- [11] T. Qiu, X. da Wang, H. Tian, Z.X. Huang, Liquid-liquid equilibrium for the system water + 1,4-dioxane + cyclohexanol over the temperature range of 313.2-343.2 K, *Fluid Phase Equilibria* 324 (2012) 28-32.
- [12] H. Ahmed, H. Diamonta, C. Chaker, R. Abdelhamid, Purification of wet process phosphoric acid by solvent extraction with TBP and MIBK mixtures, *Separation and Purification Technology* 55 (2007) 212-216.
- [13] H. Sah, Microencapsulation techniques using ethyl acetate as a dispersed solvent: effects of its extraction rate on the characteristics of PLGA microspheres, *Journal of Controlled Release* 47 (1997) 233-245.
- [14] B.F. de Almeida, T.M. Waldrigui, T. de Castro Alves, L.H. de Oliveira, M. Aznar, Experimental and calculated liquid-liquid equilibrium data for water + furfural + solvents, *Fluid Phase Equilibria* 334 (2012) 97-105.
- [15] S. Kamila, J.K. Dash, Studies on molecular interactions in different solvent extractants with *n*-butanol at temperature 303.15 K: a thermoacoustic investigation, *Journal of Molecular Liquids* 172 (2012) 71-75.
- [16] T. Wongsawa, M. Hronec, T. Soták, N. Leepipatpiboon, U. Pancharoen, S. Phatanasri, Ternary (liquid-liquid) equilibrium data of furfuryl alcohol with organic solvents at  $T = 298.2$  K: Experimental results and thermodynamic models, *Fluid Phase Equilibria* 365 (2014) 88-96.
- [17] L. Domingues, P.A. Cussolin, J.L. da Silva Jr., L.H. de Oliveira, M. Aznar, Liquid-liquid equilibrium data for ternary systems of water + lactic acid + C4-C7

- alcohols at 298.2 K and atmospheric pressure, *Fluid Phase Equilibria* 354 (2013) 12-18.
- [18] J.P. Novák, K. Reháč, P. Vonka, J. Matouš, Critical curves of liquid-liquid equilibria in ternary systems description by a regular-solution model, *Fluid Phase Equilibria* 208 (2003) 199-221.
- [19] H.G. Gilani, A.G. Gilani, M. Sangashekan, Tie-line data for the aqueous solutions of phenol with organic solvents at  $T = 298.2$  K, *The Journal of Chemical Thermodynamics* 58 (2013) 142-148.
- [20] K.A. Boudreaux, *Chem 2353: fundamentals of organic chemistry, aldehydes and ketones*, <[www.angelo.edu/faculty/kboudrea/index\\_2353/Notes\\_Chapter\\_04.pdf](http://www.angelo.edu/faculty/kboudrea/index_2353/Notes_Chapter_04.pdf)> (accessed 11.11.2013).
- [21] H. Ghanadzadeh, A. Ghanadzadeh, S. Asgharzadeh, M. Moghadam, Measurement and correlation of phase equilibrium data of the mixtures consisting of butyric acid, water, cyclohexanone at different temperatures, *The Journal of Chemical Thermodynamics* 47 (2012) 288-294.
- [22] B. Mokhtarani, J. Musavi, M. Parvini, M. Mafi, A. Sharifi, M. Mirzaei, Ternary (liquid-liquid) equilibria of nitrate based ionic liquid + alkane + benzene at 298.15 K: Experiments and correlation, *Fluid Phase Equilibria* 341 (2013) 35-41.
- [23] A. Fredenslund, R.L. Jones, J.M. Prausnitz, Group-contribution estimation of activity coefficients in nonideal liquid mixtures, *AIChE Journal* 21(6) (1975) 1086-1099.
- [24] J.M. Prausnitz, *Molecular Thermodynamics of Fluid-Phase Equilibria*, third ed., 258-291, Prentice Hall, 1998.
- [25] A. Barhala, D. Dragoescu, M. Teodorescu, Vapor-liquid equilibria and excess thermodynamic properties in binary systems of cyclopentanone + chloroalkanes in view of the disquac and unifac group contribution models extension, *Revista de Chimie* 59 (2008) 531-539.

## Chapter IV

Solubility and tie-line data for ternary aqueous mixtures of cyclopentanol  
with organic solvents at  $T = 298.2$  K: experiments and NRTL model

Thidarat Wongsawa<sup>a</sup>, Milan Hronec<sup>b</sup>, Ura Pancharoen<sup>a</sup>, Suphot Phatanasri<sup>a</sup>

<sup>a</sup> *Department of Chemical Engineering, Faculty of Engineering, Chulalongkorn University, Phyathai Rd., Bangkok 10330, Thailand*

<sup>b</sup> *Department of Organic Technology, Slovak University of Technology, Radlinského 9, 812 37 Bratislava, Slovakia*



---

This article has been published in journal: Fluid Phase Equilibria.

Page: 10-18. Volume: 379. Year: 2014.

---

## 4.1 Abstract

Liquid-liquid equilibrium (LLE) data are of great importance for the separation processes that are applied in the chemical industry. Cyclopentanol is a product used by many industries that may contaminate in wastewater. The purpose of this work is to obtain LLE data for cyclopentanol separation. Ternary LLE systems of water + cyclopentanol + organic solvents (MIBK, ethyl acetate, furfural or *n*-butanol) were investigated at  $T = 298.2$  K as well as atmospheric pressure. The solubility and tie-line data of these ternary LLE systems were obtained by direct analysis method. The reliability of the LLE experimental results was validated by the uncertainty propagation calculation. Distribution coefficients ( $D$ ) and separation factors ( $S$ ) were calculated in order to evaluate the capability of organic solvents for the selective separation of cyclopentanol. Percentage separations ( $E$ ) of cyclopentanol were also studied. Good correlations of the experimental LLE data with modeling results calculated by the non-random two liquid (NRTL) model were presented and confirmed by the *rmsd* values. The latter values were found to be less than 4%.

**Keywords:** Solubility; Tie-line data; Ternary mixtures; Cyclopentanol; NRTL model.

## 4.2 Introduction

Cyclopentanol is a cyclic alcohol which is prepared by hydrogenation of cyclopentanone [1, 2]. It is mainly used in the perfume industry and in the manufacture of nylon [3]. During the operation of these processes, cyclopentanol may contaminate in wastewater. In the purification of wastewater and prevention of environmental contamination, the separation of cyclopentanol from wastewater is highly important.

Liquid-liquid extraction is a major separation process in the chemical and petrochemical industries due to its less energy consumption and high efficiency over distillation processes [4]. The efficiency of this process is based on the physical and

chemical properties of selective organic solvents used for separation of the target component present in water. There are practical concerns in selecting the organic solvent like viscosity, density, boiling point, interfacial tension and thermal stability [5]. In order to design and enhance the liquid-liquid extraction process, precise liquid-liquid equilibrium (LLE) data of ternary systems are required. Ternary diagrams involving a solubility curve and tie-lines are of great importance for the ternary LLE systems [6-8]. These are obtained by direct analysis method or by cloud-point titration [9].

Thermodynamic models are also important for predicting thermodynamic properties of the ternary LLE systems, particularly the activity coefficient models. The non-random two liquid (NRTL) model is one of the activity coefficient models which is cited in numerous literature [10-14]. This model was first reported by Renon and Prausnitz (1968) who showed its application to a wide variety of mixtures for vapor-liquid and liquid-liquid phase equilibria [15]. The model is based on a semi-empirical physical model combined with a molecular local composition concept as described by Bart [16]. Moreover, the model involves binary interaction parameters which can be obtained by experimental equilibrium results.

The main purpose of this work is to provide a new series of LLE data. The liquid phase behavior for the ternary LLE systems consisting of water, cyclopentanol and efficient organic solvents was studied at a temperature of 298.2 K together with atmospheric pressure. The organic solvents such as, methyl isobutyl ketone (MIBK), ethyl acetate, furfural and *n*-butanol were selected for such study. MIBK is non-toxic, highly selective and relatively less miscible in aqueous solutions [17]. Ethyl acetate is a good solvent and benign for the environment [18]. Furfural and *n*-butanol are the preferable solvents which are used in the industry [19, 20]. The solubility and tie-line data for each ternary system were obtained by the direct analysis method and their reliability was validated by the uncertainty propagation calculation. The separation capability of the selected organic solvents was expressed in terms of distribution coefficients ( $D$ ) and separation factors ( $S$ ) calculated by the tie-line data. The amount of cyclopentanol that was separated in the ternary systems was also studied and expressed by the percentage separation ( $E$ ). Finally, the LLE data of

the investigated systems were correlated with the modeling results obtained by the NRTL model. These correlations were evaluated by the *rmsd* values.

### 4.3 Experimental

#### 4.3.1 Chemicals

Chemicals consisting of cyclopentanol (C<sub>5</sub>H<sub>10</sub>O, MW 86.13 g/mol), furfural (C<sub>5</sub>H<sub>4</sub>O<sub>2</sub>, MW 96.08 g/mol), *n*-butanol (C<sub>4</sub>H<sub>9</sub>OH, MW 74.12 g/mol), methyl isobutyl ketone (C<sub>6</sub>H<sub>12</sub>O, MW 100.16 g/mol) and ethyl acetate (C<sub>4</sub>H<sub>8</sub>O<sub>2</sub>, MW 88.11 g/mol) were used without further purification. The source of all chemicals and their important physical properties as publicized by the wikipedia website [21] are listed in Table 4.1. Distilled water was used in all experiments.

**Table 4.1** Source and important physical properties of chemicals.

Chemical name	Source	Purity/% mass	Analytical method	Solubility in water [21] (g/100 mL H <sub>2</sub> O; 298 K)	Normal boiling point [21] (K)
Cyclopentanol	Sigma-Aldrich	99.0	GC	Soluble	412-413
Furfural	Sigma-Aldrich	99.0	GC	8.3	435.0
<i>n</i> -Butanol	Erba Lachema	99.5	GC	10.0	390.8
Methyl isobutyl ketone	MicroChem	99.5	GC	1.9	390-391
Ethyl acetate	MicroChem	99.8	HPLC	8.3	350.2

#### 4.3.2 Apparatus and procedure

The equilibrium solubility data in the organic-rich and aqueous-rich phases of the ternary systems were obtained by direct analysis method. The weights of all components were obtained by a digital analytical balance-Mettler Toledo AE200 (with an accuracy of  $\pm 0.0001$  g). A water jacket, that was checked using a digital thermometer (with an accuracy of  $\pm 0.1$  K), was used to control the temperature of the systems. The binary mixtures of the known compositions of cyclopentanol and

organic solvents were prepared in closed glass vessels. The binary mixtures were continually titrated with water until they became turbid. The end point of titration was achieved when the mixtures remained turbid for 15 minutes. During this time, the glass vessels were agitated periodically to observe the turbidity. These procedures were used to obtain the solubility curve of the organic-rich phase. In order to repeat all measurements at least three times, a known quantity of cyclopentanol was added into the mixtures for back transparency. The mixtures were again titrated with water until they became turbid, and the same end point of titration was taken. To obtain the solubility curve of the aqueous-rich phase, the binary mixtures with the predetermined compositions of cyclopentanol and water were prepared in the closed glass vessels. The organic solvents were continually added into the binary mixtures till turbidity. Thereafter, the glass vessels were agitated periodically to observe the turbidity for 15 minutes. The end point of titration was achieved when the mixtures remained turbid.

The tie-line data of the ternary systems were obtained from the ternary mixtures after reaching equilibrium composition. More water was successively added until the transition from homogeneous to heterogeneous state appeared in the mixtures. Thereafter, the mixtures were weighed and agitated vigorously at 200 rpm for 2 hours. Then they were centrifugated and left for 14 hours to complete separation. These periods were long enough for samples reaching two equilibrium liquid layers. The organic-rich phase was carefully withdrawn from the top layer of the glass vessel by syringe and then weighed. The remaining aqueous-rich sample was also weighed and analyzed by gas chromatography to determine the compositions of cyclopentanol and organic solvents. The composition of water was calculated by the mass balance equation. These results were used to be the tie-line data in the aqueous-rich phase. To obtain the tie-line data in the organic-rich phase, the composition of each component was calculated based on its composition difference in the mixtures and the aqueous-rich phase. Triangular phase diagrams for all ternary LLE data were plotted by the ProSim program.

### 4.3.3 Analysis

The aqueous-rich phases were analyzed by gas chromatography (Hewlett Packard 5890 Series II, with FID detector) using a 1.4 m × 3 mm glass column packed with 5% C20M + 5% SE. The quantitative determination of the reaction samples was done by an external standard method using an aqueous solution of each sample with known concentration and response factor.

### 4.3.4 Reliability of LLE results

The reliability of the experimental solubility data and tie-line results were validated by the uncertainty propagation calculation according to the GUM and NIST [22, 23]. In this work, the standard uncertainties ( $u(x_i)$ ), as shown in the respective footnote of the tables, were calculated as follows:

$$u(x_i) = \left( \frac{1}{n(n-1)} \sum_{k=1}^n (X_{i,k} - \bar{X}_i)^2 \right)^{1/2} \quad (4.1)$$

$$\bar{X}_i = \frac{1}{n} \sum_{k=1}^n X_{i,k} \quad (4.2)$$

where  $n$  is the number of independent observations,  $X_{i,k}$  is the input quantity as obtained under the same conditions of measurement and  $k = 1, 2, \dots, n$ .

## 4.4 Results and discussion

### 4.4.1 Experimental solubility and tie-line data

The experimental solubility curves for the ternary systems of (water + cyclopentanol + organic solvents) at  $T = 298.2$  K and atmospheric pressure are plotted in Figure 4.1. The same solubility data, as shown in terms of mass fraction, are given in Table 4.2. In the case of furfural, the solubility curve has a different characteristic compared with the other mixtures (Figure 4.1). However, this characteristic is similar to the basic type of LLE behavior as reported by Novák et al. [24]. As seen in Figure 4.1, only a liquid pair of cyclopentanol + organic solvents was completely miscible and two liquid pairs of water + cyclopentanol and water + organic solvents were partially miscible i.e. each ternary system exhibited type-2 behavior of LLE [25]. The biphasic regions for the used organic solvents have different areas due to the mutual solubility of water and the organic solvents. Thus, the type of organic solvent is an important factor influencing the biphasic region of the investigated systems.

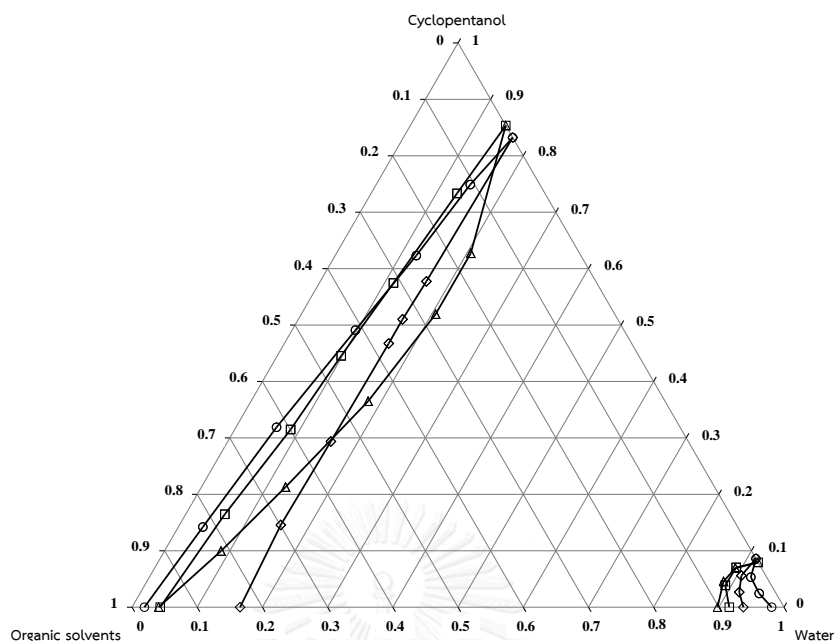


**Figure 4.1** Solubility curves for ternary systems of (water + cyclopentanol + organic solvents) at  $T = 298.2$  K and atmospheric pressure; (-○-) MIBK, (-□-) ethyl acetate, (-△-) furfural and (-◇-) *n*-butanol.

**Table 4.2** Solubility data in mass fractions ( $w_i$ ) for the ternary systems of (water (1) + cyclopentanol (2) + organic solvents (3)) at  $T = 298.2$  K and atmospheric pressure.<sup>a</sup>

MIBK		Ethyl acetate		Furfural		<i>n</i> -Butanol	
$w_1$	$w_2$	$w_1$	$w_2$	$w_1$	$w_2$	$w_1$	$w_2$
0.0190	0.0000	0.0432	0.0000	0.0408	0.0000	0.1657	0.0000
0.0376	0.1421	0.0600	0.1647	0.0867	0.0995	0.1553	0.1457
0.0622	0.3189	0.0858	0.3149	0.1290	0.2128	0.1581	0.2937
0.0972	0.4910	0.0981	0.4455	0.1796	0.3650	0.1600	0.4674
0.1244	0.6231	0.1137	0.5745	0.2060	0.5193	0.1598	0.5102
0.1443	0.7489	0.1318	0.7333	0.2001	0.6272	0.1628	0.5774
0.1677	0.8323	0.1464	0.8536	0.1464	0.8536	0.1677	0.8323
0.9810	0.0000	0.9160	0.0000	0.8979	0.0000	0.9376	0.0000
0.9502	0.0243	0.8906	0.0387	0.8844	0.0455	0.9179	0.0267
0.9253	0.0532	0.8914	0.0705	0.8906	0.0692	0.9078	0.0560
0.9139	0.0861	0.9206	0.0794	0.9206	0.0794	0.9139	0.0861

<sup>a</sup> Standard uncertainties are  $u(T) = 0.1$  K and  $u(w) = 0.0011$ .

The experimental tie-line data for these ternary systems were obtained at the same temperature as shown in Table 4.3 and as plotted in Figures 4.2 to 4.5. In these figures, the slopes of the tie-lines indicated that cyclopentanol was more soluble in the organic solvents than in water. This was probably due to lower polarity of cyclopentanol which prefers higher solubility in organic solvents than in water.

**Table 4.3** Tie-line data in mass fractions for the ternary systems of (water (1) + cyclopentanol (2) + organic solvents (3)) at  $T = 298.2$  K and atmospheric pressure.<sup>a</sup>

Aqueous-rich phase			Organic-rich phase		
$w_1$	$w_2$	$w_3$	$w_1$	$w_2$	$w_3$
Water + Cyclopentanol + MIBK					
0.9447	0.0300	0.0253	0.0379	0.1508	0.8113
0.9359	0.0359	0.0282	0.0418	0.1818	0.7764
0.9194	0.0639	0.0167	0.0667	0.3355	0.5978
0.9167	0.0686	0.0147	0.0736	0.3750	0.5514
0.9163	0.0765	0.0072	0.0949	0.4677	0.4374
0.9098	0.0806	0.0096	0.1010	0.5046	0.3944
0.9083	0.0836	0.0081	0.1094	0.5324	0.3582
0.9044	0.0932	0.0024	0.1285	0.6405	0.2310
Water + Cyclopentanol + Ethyl acetate					
0.9054	0.0149	0.0797	0.0489	0.0817	0.8694
0.9009	0.0279	0.0712	0.0590	0.1520	0.7890
0.8970	0.0358	0.0672	0.0715	0.2386	0.6899
0.8951	0.0463	0.0586	0.0883	0.3176	0.5941
0.8935	0.0559	0.0506	0.0995	0.4512	0.4493
0.8930	0.0593	0.0477	0.1116	0.5313	0.3571
0.8913	0.0710	0.0377	0.1190	0.6199	0.2611
0.8987	0.0783	0.0230	0.1285	0.6654	0.2061
0.9037	0.0756	0.0207	0.1369	0.7563	0.1068
Water + Cyclopentanol + Furfural					
0.8903	0.0210	0.0887	0.0796	0.0883	0.8321
0.8846	0.0371	0.0783	0.1229	0.1996	0.6775
0.8851	0.0463	0.0686	0.1559	0.2942	0.5499
0.8836	0.0545	0.0619	0.1787	0.3575	0.4638
0.8871	0.0603	0.0526	0.1985	0.4596	0.3419
0.8889	0.0700	0.0411	0.2053	0.5365	0.2582
0.8999	0.0726	0.0275	0.1959	0.6535	0.1506
0.9077	0.0762	0.0161	0.1708	0.7624	0.0668
Water + Cyclopentanol + <i>n</i> -Butanol					
0.9300	0.0095	0.0605	0.1631	0.0775	0.7594
0.9286	0.0170	0.0544	0.1553	0.1436	0.7011
0.9232	0.0279	0.0489	0.1579	0.2398	0.6023
0.9224	0.0359	0.0417	0.1592	0.3202	0.5206
0.9188	0.0417	0.0395	0.1600	0.3888	0.4512
0.9162	0.0559	0.0279	0.1605	0.5312	0.3083
0.9087	0.0620	0.0293	0.1632	0.6216	0.2152
0.9089	0.0710	0.0201	0.1646	0.7134	0.1220

<sup>a</sup> Standard uncertainties are  $u(T) = 0.1$  K and  $u(w) = 0.0008$ .

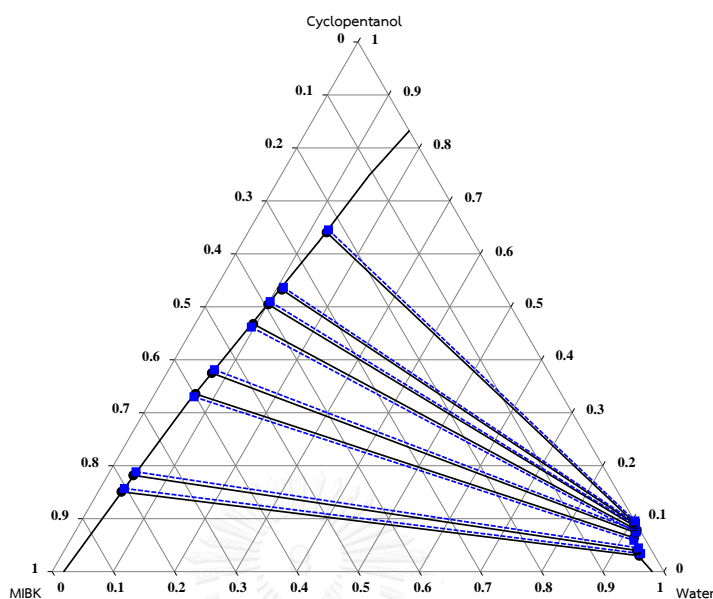


**Figure 4.2** Ternary diagram for the LLE system of (water (1) + cyclopentanol (2) + MIBK (3)) at  $T = 298.2$  K and atmospheric pressure; (—●—) experimental tie-line data and (---■---) calculated NRTL data.

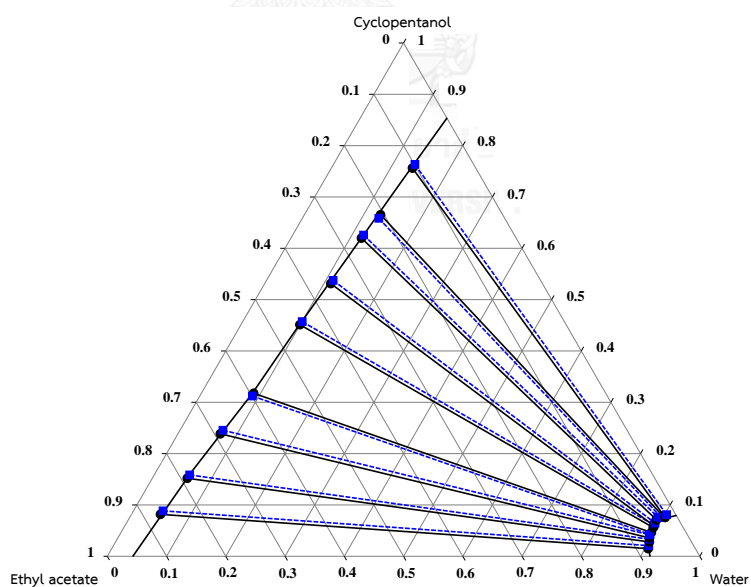


**Figure 4.3** Ternary diagram for the LLE system of (water (1) + cyclopentanol (2) + ethyl acetate (3)) at  $T = 298.2$  K and atmospheric pressure; (—●—) experimental tie-line data and (---■---) calculated NRTL data.

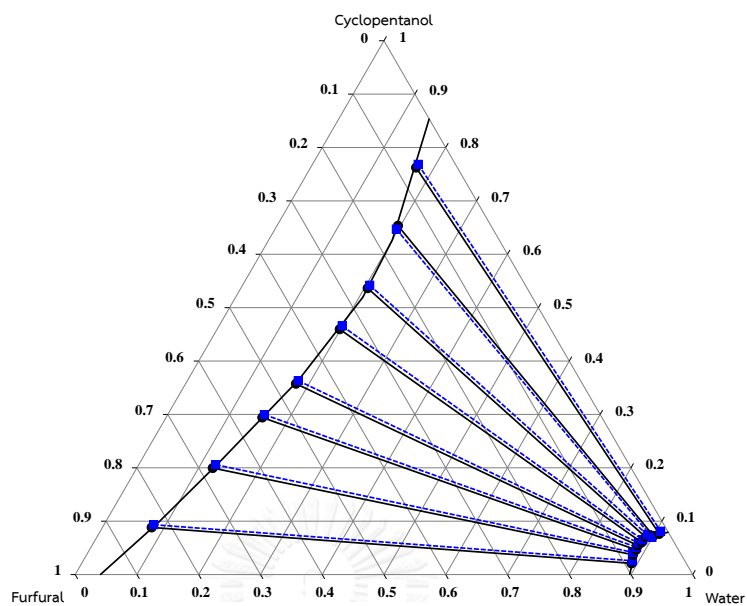


**Figure 4.4** Ternary diagram for the LLE system of (water (1) + cyclopentanol (2) + furfural (3)) at  $T = 298.2$  K and atmospheric pressure; (—●—) experimental tie-line data and (---■---) calculated NRTL data.

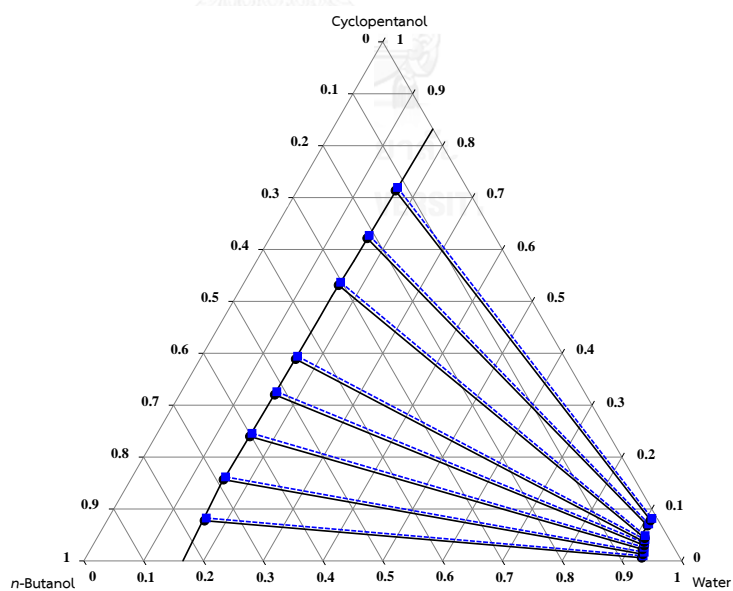


**Figure 4.5** Ternary diagram for the LLE system of (water (1) + cyclopentanol (2) + *n*-butanol (3)) at  $T = 298.2$  K and atmospheric pressure; (—●—) experimental tie-line data and (---■---) calculated NRTL data.

#### 4.4.2 The capability of the selected organic solvents

The distribution coefficients ( $D$ ) and the separation factors ( $S$ ) were calculated in order to obtain the capability of the selected organic solvents for cyclopentanol separation. The separation factor ( $S$ ) is defined as the ratio of the distribution coefficients of cyclopentanol ( $D_2$ ) to water ( $D_1$ ) as follows:

$$S = \frac{D_2}{D_1} = \frac{w_{23} / w_{21}}{w_{13} / w_{11}} \quad (4.3)$$

where  $w_{13}$  and  $w_{23}$  are the mass fractions of water and cyclopentanol in the organic-rich phase, respectively and  $w_{11}$  and  $w_{21}$  are the mass fractions of water and cyclopentanol in the aqueous-rich phase, respectively.

The values of distribution coefficients and separation factors for each ternary system are listed in Table 4.4. The variation of the separation factors as a function of the mass fraction of cyclopentanol in the aqueous-rich phase is shown in Figure 4.6. For the investigated ternary systems, all selected organic solvents have high  $D$  and  $S$  values (i.e.  $> 1$ ), indicating the capability of these solvents to separate cyclopentanol from water. As can be seen in Figure 4.6, the separation factors decreased when there was an increase in the mass fraction of cyclopentanol in the aqueous-rich phase except in the case of  $n$ -butanol. This was because more water was present in the organic-rich phase [9]. The small increase in the separation factor with regard to  $n$ -butanol is similar to that reported by Gilani et al. [25] who studied the LLE system for phenol separation using cyclohexanone as the organic solvent.

**Table 4.4** Distribution coefficients ( $D$ ) and separation factors ( $S$ ) for the ternary systems of (water (1) + cyclopentanol (2) + organic solvents (3)) at  $T = 298.2$  K.

Ternary system	$w_{21}$	$D_1$	$D_2$	$S$
Water + Cyclopentanol + MIBK	0.0300	0.0401	5.0267	125.2953
	0.0359	0.0447	5.0641	113.3842
	0.0639	0.0725	5.2504	72.3720
	0.0686	0.0803	5.4665	68.0858
	0.0765	0.1036	6.1137	59.0306
	0.0806	0.1110	6.2605	56.3945
	0.0836	0.1204	6.3684	52.8742
	0.0932	0.1421	6.8723	48.3683
Water + Cyclopentanol + Ethyl acetate	0.0149	0.0540	5.4832	101.5237
	0.0279	0.0655	5.4480	83.1886
	0.0358	0.0797	6.6648	83.6130
	0.0463	0.0986	6.8596	69.5361
	0.0559	0.1114	8.0716	72.4818
	0.0593	0.1250	8.9595	71.6923
	0.0710	0.1335	8.7310	65.3944
	0.0783	0.1430	8.4981	59.4337
	0.0756	0.1515	10.0040	66.0379
Water + Cyclopentanol + Furfural	0.0210	0.0894	4.2048	47.0289
	0.0371	0.1389	5.3801	38.7241
	0.0463	0.1761	6.3542	36.0751
	0.0545	0.2022	6.5596	32.4348
	0.0603	0.2238	7.6219	34.0624
	0.0700	0.2310	7.6643	33.1845
	0.0726	0.2177	9.0014	41.3494
Water + Cyclopentanol + <i>n</i> -Butanol	0.0095	0.1754	8.1579	46.5165
	0.0170	0.1672	8.4471	50.5083
	0.0279	0.1710	8.5950	50.2526
	0.0359	0.1726	8.9192	51.6777
	0.0417	0.1741	9.3237	53.5416
	0.0559	0.1752	9.5027	54.2452
	0.0620	0.1796	10.0258	55.8238
	0.0710	0.1811	10.0479	55.4831

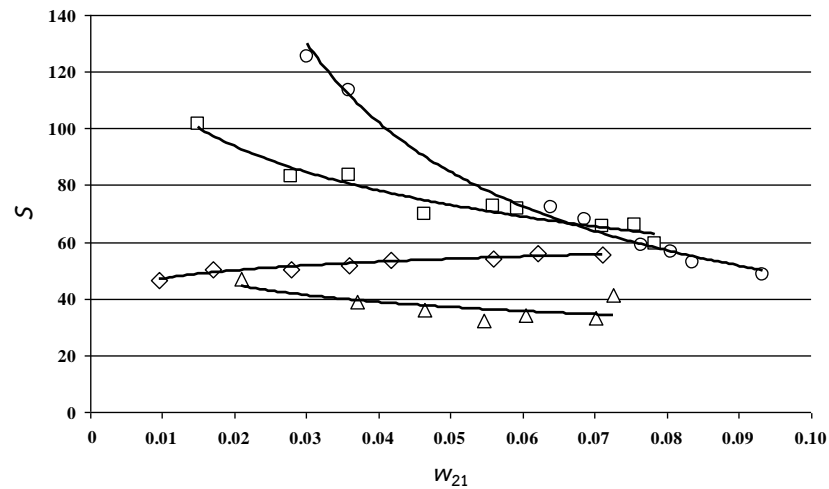


**Figure 4.6** Separation factors plotted against the mass fraction of cyclopentanol in aqueous-rich phase ( $w_{21}$ ) at  $T = 298.2$  K and atmospheric pressure; (○) MIBK, (□) ethyl acetate, (△) furfural and (◇) *n*-butanol.

The percentage separation ( $E$ ) of cyclopentanol highlights the capability of the selected organic solvents. This indicates the amount of cyclopentanol that can dissolve in the organic-rich phase when compared with its total quantity in a ternary system. For all investigated systems, the percentage separations of cyclopentanol are calculated from Eq. (4.4) and reported together with the total mass values of water ( $m_{1,\text{total}}$ ) and organic solvents ( $m_{3,\text{total}}$ ) as shown in Table 4.5.

$$E = \left( \frac{w_{23}}{w_{2,\text{total}}} \right) \times 100 \quad (4.4)$$

Where  $w_{23}$  is the mass fraction of cyclopentanol in the organic-rich phase and  $w_{2,\text{total}}$  is the total mass fraction of cyclopentanol in the ternary system which is obtained by the combination of mass fractions of cyclopentanol in aqueous-rich and organic-rich phases.

From Table 4.5, the percentage separations of cyclopentanol for selected organic solvents have analogous values which vary between 81% and 91%. In order to determine the suitable solvent for cyclopentanol separation, both the separation factor and the percentage separation of each organic solvent were considered. The percentage separations of MIBK are similar to those of the three solvents, but its separation factors have higher values. Thus, MIBK was selected as a suitable solvent.

**Table 4.5** Total mass ( $m_{\text{total}}$ ) and percentage separation ( $E$ ) of cyclopentanol for the ternary systems of (water (1) + cyclopentanol (2) + organic solvents (3)) at  $T = 298.2$  K.

Ternary system	$m_{1,\text{total}}$ (g)	$m_{3,\text{total}}$ (g)	$w_{23}$	$w_{2,\text{total}}$	$E$ (%)
Water + Cyclopentanol + MIBK	1.3033	1.5819	0.1508	0.1808	83.41
	1.8333	1.5269	0.1818	0.2177	83.51
	2.1545	1.1750	0.3355	0.3994	84.00
	2.8751	1.0907	0.3750	0.4436	84.54
	1.4612	1.3586	0.4677	0.5442	85.94
	3.9605	0.7977	0.5046	0.5852	86.23
	4.7659	0.7177	0.5324	0.6160	86.43
	5.6985	0.4749	0.6405	0.7337	87.30
Water + Cyclopentanol + Ethyl acetate	2.3875	1.7953	0.0817	0.0966	84.58
	2.8843	1.6090	0.1520	0.1799	84.49
	3.5401	1.4682	0.2386	0.2744	86.95
	4.0925	1.3024	0.3176	0.3639	87.28
	4.6675	1.0616	0.4512	0.5071	88.98
	4.5250	0.9087	0.5313	0.5906	89.96
	4.6803	0.7329	0.6199	0.6909	89.72
	5.0242	0.5598	0.6654	0.7437	89.47
5.2826	0.3185	0.7563	0.8319	90.91	
Water + Cyclopentanol + Furfural	2.3115	2.1746	0.0883	0.1093	80.79
	3.1196	1.9192	0.1996	0.2367	84.33
	3.7696	1.5911	0.2942	0.3405	86.40
	4.2578	1.3200	0.3575	0.4120	86.77
	4.9133	1.0177	0.4596	0.5199	88.40
	5.0499	0.8037	0.5365	0.6065	88.46
	5.0010	0.4731	0.6535	0.7261	90.00
	4.9736	0.2418	0.7624	0.8386	90.91
Water + Cyclopentanol + <i>n</i> -Butanol	2.4264	1.6015	0.0775	0.0870	89.08
	3.3934	1.4612	0.1436	0.1606	89.42
	3.8184	1.2978	0.2398	0.2677	89.58
	4.5061	1.1487	0.3202	0.3561	89.92
	4.8589	1.0387	0.3888	0.4305	90.31
	5.6461	0.8776	0.5312	0.5871	90.48
	6.3651	0.6468	0.6216	0.6836	90.93
	6.3066	0.4367	0.7134	0.7844	90.95

#### 4.4.3 NRTL model correlation

The relationship of the experimental tie-line data obtained at  $T = 298.2$  K for each investigated ternary system can be represented by the NRTL model. In this model, the basic relationship for any component  $i$  in the aqueous-rich and organic-rich phases at equilibrium is as follows:

$$x_i^I \gamma_i^I = x_i^{II} \gamma_i^{II} \quad (4.5)$$

$$\sum x_i^I = \sum x_i^{II} = 1 \quad (4.6)$$

where  $x_i^I$ ,  $x_i^{II}$ ,  $\gamma_i^I$  and  $\gamma_i^{II}$  are the mole fractions and activity coefficients of component  $i$  in the aqueous-rich (I) and organic-rich (II) phases, respectively.

The activity coefficient ( $\gamma_i$ ) in the NRTL model is expressed as [26]:

$$\ln \gamma_i = \frac{\sum_{j=1}^3 \tau_{ji} G_{ji} x_j}{\sum_{k=1}^3 G_{ki} x_k} + \sum_{j=1}^3 \frac{x_j G_{ij}}{\sum_{k=1}^3 G_{kj} x_k} \left( \tau_{ij} - \frac{\sum_{k=1}^3 x_k \tau_{kj} G_{kj}}{\sum_{k=1}^3 G_{kj} x_k} \right) \quad (4.7)$$

where  $x_i$  is the mole fraction of component  $i$ , the parameters  $\tau_{ij}$ ,  $\tau_{ji}$ ,  $\tau_{kj}$ ,  $G_{ij}$ ,  $G_{ji}$ ,  $G_{ki}$  and  $G_{kj}$  are the adjustable parameters for each binary pair in the NRTL model and  $i, j, k$  are the indices for all components.

These adjustable parameters can be calculated as follows:

$$\tau_{ij} = a_{ij} + \frac{b_{ij}}{T} + e_{ij} \ln T \quad (4.8)$$

$$\alpha_{ij} = \alpha_{ji} = c_{ij} \quad (4.9)$$

$$G_{ij} = \exp(-\alpha_{ij}\tau_{ij}) \quad (4.10)$$

where  $a_{ij}$ ,  $b_{ij}$ ,  $c_{ij}$  and  $e_{ij}$  are the NRTL coefficients for the binary interaction parameters and  $\alpha_{ij}$  and  $\alpha_{ji}$  are the non-randomness parameters.

In this work, the value of the non-randomness parameter ( $\alpha$ ) of the NRTL model was determined and the appropriate value was taken to be 0.2. The binary interaction parameters ( $b_{ij}$  and  $b_{ji}$ ) of the NRTL model for each ternary system were obtained by the experimental LLE data and are listed in Table 4.6.

**Table 4.6** NRTL binary interaction parameters for the ternary systems of (water (1) + cyclopentanol (2) + organic solvents (3)) at  $T = 298.2$  K.

Ternary system	$i-j$	NRTL ( $\alpha = 0.2$ )	
		$b_{ij}$ (K)	$b_{ji}$ (K)
Water + Cyclopentanol + MIBK	1-2	1,597.6421	106.5873
	1-3	995.7328	2,082.3649
	2-3	208.1647	764.3885
Water + Cyclopentanol + Ethyl acetate	1-2	1,253.7319	103.5937
	1-3	1,076.3541	582.9651
	2-3	-105.9862	176.2452
Water + Cyclopentanol + Furfural	1-2	720.8762	876.1347
	1-3	-1,538.1642	-5,721.9643
	2-3	693.6751	42.1937
Water + Cyclopentanol + <i>n</i> -Butanol	1-2	826.3927	103.6429
	1-3	-1,280.1368	-5,782.9226
	2-3	-62.9875	584.9872

The modeling results were correlated with the experimental tie-line data of each ternary system as shown in Table 4.7 and Figures 4.2 to 4.5. The correlation of both results in terms of root-mean square deviation (*rmsd*) is also listed in Table 4.7.

The *rmsd* value was calculated by the difference between the experimental and modeling mass fractions as follows:

$$rmsd = 100 \left( \frac{\sum_{k=1}^n \sum_{j=1}^2 \sum_{i=1}^3 (w_{ijk}^{expt.} - w_{ijk}^{cal.})}{6n} \right)^{1/2} \quad (4.11)$$

where  $n$  is the number of tie-lines,  $w^{expt.}$  and  $w^{cal.}$  are the experimental and modeling mass fractions, respectively. Subscript  $i$  is the component,  $j$  is the phase and  $k = 1, 2, \dots, n$  is the number of tie-lines.

As can be seen in Table 4.7, the modeling results of the NRTL model provide a good correlation with the experimental results of all investigated ternary systems. Low *rmsd* values for the NRTL model confirm its ability to predict the LLE data obtained in this work.

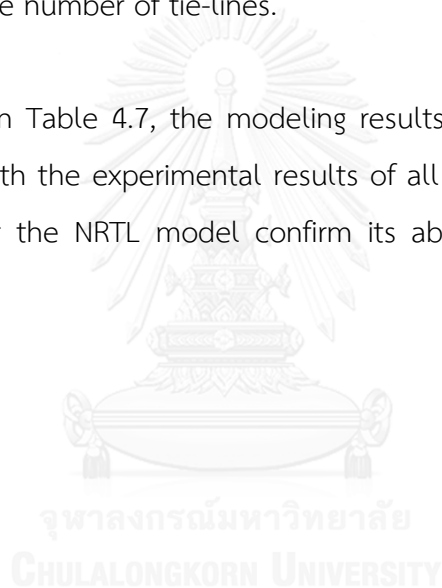


**Table 4.7** Modeling of the NRTL tie-line values in mass fractions for the ternary systems of (water (1) + cyclopentanol (2) + organic solvents (3)) at  $T = 298.2$  K.

Aqueous-rich phase				Organic-rich phase				<i>rmsd</i> (%)
$w_{11}$		$w_{21}$		$w_{13}$		$w_{23}$		
Expt.	NRTL	Expt.	NRTL	Expt.	NRTL	Expt.	NRTL	
Water + Cyclopentanol + MIBK								
0.9447	0.9449	0.0300	0.0342	0.0379	0.0397	0.1508	0.1571	2.50
0.9359	0.9360	0.0359	0.0448	0.0418	0.0429	0.1818	0.1885	
0.9194	0.9213	0.0639	0.0591	0.0667	0.0668	0.3355	0.3301	
0.9167	0.9170	0.0686	0.0771	0.0736	0.0747	0.3750	0.3813	
0.9163	0.9168	0.0765	0.0747	0.0949	0.0948	0.4677	0.4617	
0.9098	0.9100	0.0806	0.0872	0.1010	0.1015	0.5046	0.5099	
0.9083	0.9088	0.0836	0.0916	0.1094	0.1097	0.5324	0.5368	
0.9044	0.9049	0.0932	0.0957	0.1285	0.1292	0.6405	0.6453	
Water + Cyclopentanol + Ethyl acetate								
0.9054	0.9036	0.0149	0.0207	0.0489	0.0498	0.0817	0.0885	3.44
0.9009	0.8985	0.0279	0.0332	0.0590	0.0597	0.1520	0.1585	
0.8970	0.8941	0.0358	0.0418	0.0715	0.0724	0.2386	0.2456	
0.8951	0.8946	0.0463	0.0427	0.0883	0.0887	0.3176	0.3122	
0.8935	0.8921	0.0559	0.0610	0.0995	0.1004	0.4512	0.4572	
0.8930	0.8921	0.0593	0.0648	0.1116	0.1124	0.5313	0.5375	
0.8913	0.8907	0.0710	0.0766	0.1190	0.1196	0.6199	0.6258	
0.8987	0.8979	0.0783	0.0752	0.1285	0.1291	0.6654	0.6584	
0.9037	0.9034	0.0756	0.0811	0.1369	0.1375	0.7563	0.7634	
Water + Cyclopentanol + Furfural								
0.8903	0.8893	0.0210	0.0258	0.0796	0.0804	0.0883	0.0934	3.08
0.8846	0.8821	0.0371	0.0417	0.1229	0.1245	0.1996	0.2058	
0.8851	0.8838	0.0463	0.0511	0.1559	0.1564	0.2942	0.2997	
0.8836	0.8828	0.0545	0.0592	0.1787	0.1795	0.3575	0.3632	
0.8871	0.8868	0.0603	0.0648	0.1985	0.1993	0.4596	0.4657	
0.8889	0.8887	0.0700	0.0749	0.2053	0.2059	0.5365	0.5421	
0.8999	0.8991	0.0726	0.0698	0.1959	0.1963	0.6535	0.6473	
0.9077	0.9074	0.0762	0.0813	0.1708	0.1710	0.7624	0.7686	
Water + Cyclopentanol + <i>n</i> -Butanol								
0.9300	0.9306	0.0095	0.0098	0.1631	0.1635	0.0775	0.0826	2.80
0.9286	0.9289	0.0170	0.0168	0.1553	0.1561	0.1436	0.1619	
0.9232	0.9237	0.0279	0.0262	0.1579	0.1584	0.2398	0.2458	
0.9224	0.9201	0.0359	0.0349	0.1592	0.1598	0.3202	0.3260	
0.9188	0.9181	0.0417	0.0412	0.1600	0.1604	0.3888	0.3943	
0.9162	0.9145	0.0559	0.0487	0.1605	0.1611	0.5312	0.5369	
0.9087	0.9092	0.0620	0.0713	0.1632	0.1637	0.6216	0.6272	
0.9089	0.9092	0.0710	0.0819	0.1646	0.1649	0.7134	0.7195	

#### 4.5 Conclusion

The solubility and tie-line data for the ternary LLE systems of water + cyclopentanol + organic solvents (MIBK, ethyl acetate, furfural or *n*-butanol) were investigated at  $T = 298.2$  K together with atmospheric pressure. All ternary systems exhibited type-2 behavior of LLE. The reliability of the experimental data was validated by the uncertainty propagation calculation. High separation factors for the studied organic solvents, especially MIBK, confirmed their capability to separate cyclopentanol from water. The percentage separation of cyclopentanol for the investigated systems ranged from 81% to 91%. The modeling results of the NRTL model ( $\alpha = 0.2$ ) provided relatively good correlations with the experimental results as shown by the *rmsd* values which were less than 4%.

#### 4.6 Nomenclature and units

$a, b, c, e$	NRTL coefficients for the binary interaction parameters
$D$	distribution coefficient
$E$	percentage separation (%)
$G$	NRTL parameter in Eqs. (4.7) and (4.10)
$k$	integer number
$m$	mass of components (g)
$n$	number of independent observations in Eqs. (4.1) and (4.2) or number of tie-lines in Eq. (4.11)
<i>rmsd</i>	root-mean square deviation (%)
$S$	separation factor
$T$	temperature (K)
$u(X_i)$	standard uncertainty
$w$	mass fraction
$x$	mole fraction
$X$	input quantity from the measurement in Eqs. (4.1) and (4.2)

*Greek letters*

$\alpha$	non-random parameter
$\gamma$	activity coefficient
$\tau$	NRTL parameters in Eqs. (4.7 to 4.8) and (4.10)

*Superscripts*

cal.	modeling results
expt.	experimental results
I	aqueous-rich phase
II	organic-rich phase

*Subscripts*

i, j, k	indices for all components
1	water
2	cyclopentanol
3	organic solvents

**4.7 Acknowledgements**

The authors gratefully acknowledge the financial support given by the Thailand Research Fund and Chulalongkorn University under the Royal Golden Jubilee Ph.D. program (Grant No. PHD/0272/2549) as well as the Ratchadaphiseksomphot Endowment Fund 2013 of Chulalongkorn University (CU-56-387-CC). Sincere thanks are also given to the Department of Organic Technology, Slovak University of Technology, Bratislava, Slovakia, Ing. Fulajtárová Katarína and Dr. Tomáš Soták for their kind support.

#### 4.8 References

- [1] G.J. Kabo, V.V. Diky, A.A. Kozyro, A.P. Krasulin, V.M. Sevruk, Thermodynamic properties, conformational composition, and phase transitions of cyclopentanol, *The Journal of Chemical Thermodynamics* 27 (1995) 953-967.
- [2] M. Hronec, K. Fulajtarová, Selective transformation of furfural to cyclopentanone, *Catalysis Communications* 24 (2012) 100-104.
- [3] D. Nuntasri, P. Wu, T. Tatsumi, High selectivity of MCM-22 for cyclopentanol formation in liquid-phase cyclopentene hydration, *Journal of Catalysis* 213 (2003) 272-280.
- [4] P. Reddy, T.M. Letcher, in: T.M. Letcher (Ed.), *Thermodynamics, Solubility and Environmental Issues*, 85-111, Elsevier B.V., 2007.
- [5] T.P. Kumar, P.K. Das, Solubility and tie-line data for water + formic acid + methyl isobutyl ketone ternary system at different temperatures, *Chemical Engineering Communications* 197 (2010) 1163-1171.
- [6] S. Suren, N. Sunsandee, M. Štolcová, M. Hronec, N. Leepipatpiboon, U. Pancharoen, S. Kheawhom, Measurement on the solubility of adipic acid in various solvents at high temperature and its thermodynamics parameters, *Fluid Phase Equilibria* 360 (2013) 332-337.
- [7] N. Sunsandee, M. Hronec, M. Štolcová, N. Leepipatpiboon, U. Pancharoen, Thermodynamics of the solubility of 4-acetylbenzoic acid in different solvents from 303.15 to 473.15 K, *Journal of Molecular Liquids* 180 (2013) 252-259.
- [8] N. Sunsandee, S. Suren, N. Leepipatpiboon, M. Hronec, U. Pancharoen, Determination and modeling of aqueous solubility of 4-position substituted benzoic acid compounds in a high-temperature solution, *Fluid Phase Equilibria* 338 (2013) 217-223.
- [9] J. Saien, M. Norouzi, H. Dehghani, The choice of solvent and liquid-liquid equilibrium for ternary water + 2-methylaziridine + chloroform system: experimental data and modeling, *Fluid Phase Equilibria* 338 (2013) 224-231.

- [10] A.G. Gilani, H.G. Gilani, S.L.S. Saadat, M. Janbaz, Ternary liquid-liquid equilibrium data for the (water + butyric acid + n-hexane or n-hexanol) systems at  $T = (298.2, 308.2, \text{ and } 318.2) \text{ K}$ , *The Journal of Chemical Thermodynamics* 60 (2013) 63-70.
- [11] H. Hagnazarloo, M.N. Lotfollahi, J. Mahmoudi, A.H. Asl, Liquid-liquid equilibria for ternary systems of (ethylene glycol + toluene + heptane) at temperatures (303.15, 308.15, and 313.15) K and atmospheric pressure: experimental results and correlation with UNIQUAC and NRTL models, *The Journal of Chemical Thermodynamics* 60 (2013) 126-131.
- [12] J. Yang, Y. Liu, Y. Ma, Q. Meng, Y. Wang, Liquid-liquid equilibrium data for ternary aqueous mixtures containing 1-pentanol and 2-methyl-1-propanol at (298.15, 323.15 and 348.15) K, *Fluid Phase Equilibria* 349 (2013) 31-36.
- [13] H. Ghanadzadeh, A. Ghanadzadeh, M. Janbaz, S. Shekarsaraee, Experimental determination and correlation of tie line data for the system (water + butyric acid + methylcyclohexane) at four temperatures, *Fluid Phase Equilibria* 332 (2012) 151-158.
- [14] T. Wongsawa, M. Hronec, T. Soták, N. Leepipatpiboon, U. Pancharoen, S. Phatanasri, Ternary (liquid-liquid) equilibrium data of furfuryl alcohol with organic solvents at  $T = 298.2 \text{ K}$ : experimental results and thermodynamic models, *Fluid Phase Equilibria* 365 (2014) 88-96.
- [15] N. Bouneb, A.H. Meniai, W. Louaer, Introduction of the group contribution concept into the NRTL model in: S. Pierucci, G.B. Ferraris (Eds.), 20<sup>th</sup> European Symposium on Computer Aided Process Engineering-ESCAPE20, Elsevier, 2010.
- [16] H.J. Bart, in: D. Mewes, F. Mayinger (Eds.), *Heat and Mass Transfer: Reactive Attraction*, Springer, 27-28, New York, 2001.
- [17] H. Ahmed, H. Diamonta, C. Chaker, R. Abdelhamid, Purification of wet process phosphoric acid by solvent extraction with TBP and MIBK mixtures, *Separation and Purification Technology* 55 (2007) 212-216.
- [18] H. Sah, Microencapsulation techniques using ethyl acetate as a dispersed solvent: effects of its extraction rate on the characteristics of PLGA microspheres, *Journal of Controlled Release* 47 (1997) 233-245.

- [19] B.F. de Almeida, T.M. Waldrigui, T. de Castro Alves, L.H. de Oliveira, M. Aznar, Experimental and calculated liquid-liquid equilibrium data for water + furfural + solvents, *Fluid Phase Equilibria* 334 (2012) 97-105.
- [20] S. Kamila, J.K. Dash, Studies on molecular interactions in different solvent extractants with n-butanol at temperature 303.15 K: a thermoacoustic investigation, *Journal of Molecular Liquids* 172 (2012) 71-75.
- [21] Wikipedia, the free encyclopedia <<http://en.wikipedia.org/>> (revised 17.12.13; accessed 24.03.14).
- [22] JCGM 100:2008; GUM 1995 with minor corrections, Evaluation of Measurement Data-Guide to the Expression of Uncertainty in Measurement, 1-120, JCGM, 2008.
- [23] B.N. Taylor, C.E. Kuyatt, National Institute of Standards and Technology (NIST)-Guidelines for Evaluating and Expressing the Uncertainty of NIST Measurement Results, 1-20, NIST Technical Note 1297, 1994.
- [24] J.P. Novák, K. Reháč, P. Vonka, J. Matouš, Critical curves of liquid-liquid equilibria in ternary systems description by a regular-solution model, *Fluid Phase Equilibria* 208 (2003) 199-221.
- [25] H.G. Gilani, A.G. Gilani, M. Sangashekan, Tie-line data for the aqueous solutions of phenol with organic solvents at  $T = 298.2$  K, *The Journal of Chemical Thermodynamics* 58 (2013) 142-148.
- [26] B. Mokhtarani, J. Musavi, M. Parvini, M. Mafi, A. Sharifi, M. Mirzaei, Ternary (liquid-liquid) equilibria of nitrate based ionic liquid + alkane + benzene at 298.15 K: experiments and correlation, *Fluid Phase Equilibria* 341 (2013) 35-41.

## Chapter V

The role of organic solvents in the aspects of equilibrium, kinetics and thermodynamic model for silver ion extraction using an extractant D2EHPA

Thidarat Wongsawa<sup>a</sup>, Niti Sunsandee<sup>b</sup>, Anchaleeporn Waritswat Lothongkum<sup>c</sup>,  
Ura Pancharoen<sup>a</sup>, Suphot Phatanasri<sup>a</sup>

<sup>a</sup> *Department of Chemical Engineering, Faculty of Engineering, Chulalongkorn University, Phyathai Rd., Bangkok 10330, Thailand*

<sup>b</sup> *Government Pharmaceutical Organization, Ratchathewi, Bangkok 10400, Thailand*

<sup>c</sup> *Department of Chemical Engineering, Faculty of Engineering, King Mongkut's Institute of Technology Ladkrabang, Chalongkrung Rd., Bangkok 10520, Thailand*

จุฬาลงกรณ์มหาวิทยาลัย  
CHULALONGKORN UNIVERSITY

---

This article has been published in journal: Fluid Phase Equilibria.

Page: 22-30. Volume: 388. Year: 2015.

---

## 5.1 Abstract

The effects of organic solvents regarding the aspects of equilibrium data, kinetics of extraction behavior and thermodynamic model are of great importance in the extraction processes. Therefore, these effects were investigated for silver ion extraction by a liquid-liquid extraction process using D2EHPA as an extractant. Various organic solvents that have different dielectric constants like kerosene, cyclohexane, chloroform and 1-octanol were selected for use in this work. The equilibrium data of solubility and tie-lines for the ternary systems of water + D2EHPA + organic solvents exhibited type-2 LLE behavior at a temperature of 298.2 K and atmospheric pressure. Moreover, the uncertainty propagation calculation was determined to validate the reliability of the data. The extraction efficiency of silver ions for each organic solvent was also investigated; maximum extraction of 94% was obtained for 1-octanol. The extraction behaviors of silver ion with D2EHPA in the different organic solvents were reported as regards their reaction stoichiometry. They were also analyzed by spectroscopic analysis. Results of the thermodynamic NRTL model were obtained and a very good correlation with the experimental LLE data was confirmed by the root-mean square deviation (*rmsd*) values of 1%.

**Keywords:** Solvents; Equilibrium; Kinetics; Thermodynamic; Silver ions.

## 5.2 Introduction

Based on the extraction processes in the chemical industry, various organic solvents such as aliphatic/aromatic hydrocarbons, ketones and high alcohols are used as a medium for dissolving the extractant [1]. These organic solvents can be widely divided into two categories as polar and non-polar [2]. Moreover, they have a significant effect on extraction efficiency by providing solvation through hydrogen bonding and specific interaction with the extractable complexes [3]. Their interactions increase the hydrophobicity of the extractable complexes and become

more stable in the organic phase which results ultimately in the enhancement of extraction [4]. The interaction efficiency of organic solvents is mainly based on their polarity and hydrogen bonding affinity [5, 6].

Due to the important role of organic solvents in the extraction processes, studies on the aspects of their equilibrium data, kinetics of extraction behavior and thermodynamic model are fundamentally required in order to develop and design extraction systems [7-9]. Liquid-liquid equilibrium (LLE) data focusing on solubility and tie-lines for the mixture of organic solvents and extractant are also required because the limitation of its solubility has an effect on the chemical reaction of extraction [10]. In order to determine the equilibrium data of solubility and tie-lines, direct measurement or cloud-point titration is normally used [11]. In the aspect of kinetics of extraction behavior, organic solvents have a remarkable effect on the stoichiometry of extraction reaction [12]. In addition, a thermodynamic model is key for quantitative analysis and preliminary estimation for the extraction process under an individual temperature system [13]. The activity coefficient model of non-random two liquid (NRTL) is one thermodynamic model that has been reported in the literature [14-17]. This model involves the parameter of binary interactions which can be obtained by regression with the experimental LLE results.

Recently, the extraction of silver ions from industrial wastewater has been of great concern due to its toxicity [18]. Silver ion concentration of 1-5 mg/L can kill aquatic microorganisms, insects, flounder and trout [19]. The major sources of silver ions in the environment are found in wastewater from the manufacturing of silverware, electronics and jewelry as well as from pharmaceutical and photographic-imaging processes [20]. For the extraction of silver ions, organic solvents like kerosene and chloroform are frequently used along with the extractant di(2-ethyl-hexyl)phosphoric acid (D2EHPA) [21-23]. The advantages of this extractant are its good stability of chemical properties, good reaction of extraction, high loading for the extractable ions and availability in commercial quantities [24].

This work investigated the effect of organic solvents on silver ion extraction regarding the aspects of equilibrium data, kinetics of extraction behavior and thermodynamic model using the extractant D2EHPA. Further, organic solvents having

the dielectric constants such as kerosene (n/a), cyclohexane (2.02), chloroform (4.81) and 1-octanol (10.30) were selected [12, 25]. A liquid-liquid extraction process was used in this work because it was easy to operate and process for hydrometallurgical extraction [26]. In order to provide the LLE data, the solubility and tie-lines for the ternary mixtures of water + D2EHPA + organic solvents were studied at a temperature of 298.2 K and atmospheric pressure. Results were determined by direct measurement and their reliability was validated using the uncertainty propagation calculation. The extraction efficiency for each organic solvent in the case of silver ion extraction was also carried out and represented by the percentage extraction ( $E$ ). The extraction behaviors between the silver ion and D2EHPA in the different organic solvents were reported and analyzed by spectroscopic analysis. Moreover, the NRTL model was studied and its results correlated with the experimental LLE data. The correlations were confirmed by the root-mean square deviation ( $rmsd$ ) values.

### 5.3 Theory

#### 5.3.1 Competitive complexation/solvation theory for liquid-liquid extraction process

Competitive complexation/solvation (CCS) theory is applied in this work to summarize the corresponding characteristics of silver ions for loading in the organic phase. This theory is novel and explains clearly about the solvation and complexation in the extraction system [27]. The summarizations of CCS theory for silver ion extraction are listed as follows [28]:

1. Silver ions are considered to be a solute that is surrounded by other molecules of solvents such as extractant, organic solvents and water. First, the solute interacts with the solvents by hydrogen bonding that is termed solvation. Then, it exchanges their ions through the proton/electron transfer. Both interactions are constant at the individual temperature and pressure.

The strong interactions are based on the physical properties of solvents, for example, polarity,  $\pi$ - or  $n$ -donor capacity and hydrogen bonding affinity, etc.

2. The solvation between the solute and solvents is a process involving acid-base action. The solute and solvents can be the electron donor or electron acceptor depending on their acid/base property. In general, the solute in the form of ion is considered to be acid and the solvents are acid or base following on their functional groups and structure of the solute.
3. Based on summarization 1, free silver ions, free extractant and free silver-extractant complexes cannot exist in the organic phase.
4. At a low concentration of solute in the organic phase, the silver-extractant complexes interact with molecules of organic solvent by a single nucleus aggregation. When its concentration increases, their interaction changes to form linear or cyclic aggregation that is a stronger interaction than a single one.
5. In the case of high solute concentration in the organic phase, the nuclei aggregation grows in size following on its linear or cyclic form. This changes the stoichiometry of extraction reaction.

## 5.4 Experimental

### 5.4.1 Chemicals

D2EHPA ( $C_{16}H_{35}O_4P$ , MW 322.43 g/mol), kerosene ( $C_9$ - $C_{16}$ , MW  $\approx$  170 g/mol), cyclohexane ( $C_6H_{12}$ , MW 84.15 g/mol), chloroform ( $CHCl_3$ , MW 119.38 g/mol), 1-octanol ( $C_8H_{18}O$ , MW 130.23 g/mol), silver nitrate solution ( $AgNO_3$ , MW 169.87 g/mol) and nitric acid solution ( $HNO_3$ , MW 63.01 g/mol) were used in this work. The source and important physical properties of chemicals are listed in Table 5.1. The solubility of chemicals in water except silver nitrate and nitric acid solutions was determined by direct measurement whereby water was continually titrated with chemicals until it became turbid. The end point of titration was achieved when

the mixtures remained turbid for 15 min. Thereafter, the mixtures were weighted to determine the composition of chemicals. The normal boiling point of chemicals was studied by the distillation method whereby the chemicals were distilled and their condensate vapor temperatures were measured. The temperatures at constant value were recorded to be the boiling point. All chemicals were used without further purification and distilled water was used in all experiments.

**Table 5.1** Sources and important physical properties of chemicals.

Chemical name	Source	Purity/% mass	Analytical method	Solubility in water (g/0.1 L H <sub>2</sub> O, 298.2 K)	Normal boiling point (K), Literature
D2EHPA	Merck	95.0	IR	0.0844 <sup>a</sup>	533 <sup>b</sup> , n/a
Kerosene	Shell	99.0	n/a	0.0496 <sup>a</sup>	453 <sup>b</sup> , > 433 <sup>[29]</sup>
Cyclohexane	Orec	99.7	GC	0.0062 <sup>a</sup>	355 <sup>b</sup> , 353.7 <sup>[30]</sup>
1-Octanol	Panreac	99.0	IR	0.0541 <sup>a</sup>	466 <sup>b</sup> , 467 <sup>[31]</sup>
Chloroform	Analar Normapur	99.2	GC	0.7433 <sup>a</sup>	335 <sup>b</sup> , 334 <sup>[31]</sup>
Nitric acid solution	Merck	65.0	n/a	Miscible <sup>[32]</sup>	359 <sup>[32]</sup>
Silver nitrate solution	Ajex Finechem	n/a	n/a	219 <sup>[33]</sup>	717(Decomp.) <sup>[33]</sup>

<sup>a,b</sup> are data from measurement at pressure of 0.1 MPa and their standard uncertainties are  $u(m) = 0.0008$  g and  $u(T) = 0.1$  K, respectively.

## 5.4.2 Apparatus

A digital analytical balance (Mettler Toledo AG285, accuracy of  $\pm 0.0001$  g) was used to obtain the weight of all components. The temperature of the systems was controlled by a water jacket that was checked using a Gherardt Thermoshake (with an accuracy of  $\pm 0.1$  K). The pH of the aqueous phase was measured by a BP3001 TransInstruments pH meter (with an accuracy of  $\pm 0.2$ ). The aqueous and organic phases were mixed using a Gherardt Laboshake. In addition, the fourier transform

infrared spectrometer (FT-IR, Perkin Elmer, Spectrum One) and the atomic absorption spectrometer (AAS, Varian, AA 280 FS) were used to analyze the experimental results.

### 5.4.3 Procedure

#### 5.4.3.1 Solubility and tie-lines

The equilibrium solubility of organic and aqueous phases was determined in the same manner according to Wongsawa et al. [11]. The temperature of the systems was controlled at 298.2 K. Each experiment was measured three times.

To determine the data of tie-lines, more water was added to the homogeneous ternary solutions until they formed a heterogeneous state. Subsequently, the solutions were weighed and centrifuged at 200 rpm for 2 h and then left for 14 h to complete the separation of the solutions into two layers. Thereafter, the organic phase was cautiously withdrawn from the glass vessel using a syringe, and analyzed by FT-IR to obtain the compositions of D2EHPA and organic solvents. The analytical values of both organic components were calibrated via the graphs plotted between the peak areas of FT-IR analysis and their given compositions in the standard samples. Only the composition of water was obtained by the mass balance that followed on the compositions of D2EHPA and organic solvents. The remaining aqueous phase was also weighted, and the compositions of water, D2EHPA and organic solvents in this phase were determined by the mass balance equation which was calculated based on their compositions in the organic phase. The triangular diagrams for all LLE ternary systems were plotted via ProSim program.

#### 5.4.3.2 Liquid-liquid extraction

Liquid-liquid extraction of silver ions with D2EHPA in each organic solvent was carried out in a flask containing equal volumes of organic and aqueous phases. The organic phase was prepared by using a mixture of the extractant and organic

solvent while the aqueous phase was synthesized using silver nitrate solution dissolved in distilled water. Then, the operating parameters for both phases proceeded and moved towards their optimum conditions as in the work of Gherrou et al. [21] and as shown in Table 5.2. The pH of the aqueous phase was adjusted by nitric acid solution. Thereafter, both phases were mixed to a homogeneous state under the temperature of 298.2 K. Finally, the sample was centrifuged and left for 8 h to complete the separation of both phases. The aqueous solution was carefully withdrawn from the flask and then analyzed by AAS to determine the concentration of silver ions. Results were presented in the form of percentage extraction ( $E$ ) as calculated by Eq. (5.1). The remaining organic solution was also analyzed via FT-IR in order to consider the extraction behaviors of silver ion and D2EHPA.

$$\% E = \frac{[Ag_{int.}^+]_{aq} - [Ag_{fin.}^+]_{aq}}{[Ag_{int.}^+]_{aq}} \times 100 \quad (5.1)$$

where  $[Ag_{int.}^+]_{aq}$  and  $[Ag_{fin.}^+]_{aq}$  are the initial and final concentrations of silver ions in the aqueous phase (mol/L), respectively.

**Table 5.2** Characteristics of operating parameters for silver ion extraction using D2EHPA [21].

Characteristic	Optimum value
Volume per phase (L)	0.045
pH of aqueous phase	1.0
Initial concentration of silver ions in aqueous phase (mol/L)	0.01
Concentration of extractant in organic phase (mol/L)	0.001
Shaking frequency ( $\text{min}^{-1}$ )	120
Centrifuged revolution (rpm)	800
Extraction time (min)	60

#### 5.4.4 Analysis

Regarding the studies of tie-lines and liquid-liquid extraction, their organic phases were analyzed by FT-IR. Infrared spectra were recorded with KBr liquid cell at the resolution of  $4.0 \text{ cm}^{-1}$ , scan range of  $400\text{-}4,000 \text{ cm}^{-1}$  and scan number of 16. In the tie-line study, the quantitative determination of samples was integrated by the Omnic<sup>TM</sup> Spectra software and calibrated with the standard solution for each sample giving the compositions and response factor. For the aqueous phases, in the case of the liquid-liquid extraction, they were analyzed by AAS at a wave length of 328.1 nm and 5-sec delay time.

#### 5.4.5 Reliability of LLE data

The reliability of LLE data was validated in the form of the standard uncertainties ( $u(x_i)$ ) as obtained by the uncertainty propagation calculation according to GUM and NIST [34, 35]. Their values were calculated using Eqs. (5.2) and (5.3) and expressed in the footnotes of the respective tables:

$$u(x_i) = \sqrt{\frac{1}{n(n-1)} \sum_{k=1}^n (X_{i,k} - \bar{X}_i)^2} \quad (5.2)$$

$$\bar{X}_i = \frac{1}{n} \sum_{k=1}^n X_{i,k} \quad (5.3)$$

where  $n$  is the number of independent observations,  $X_{i,k}$  is the input quantity as determined under the same conditions of measurement and  $k = 1, 2, \dots, n$ .

## 5.5 Results and discussion

### 5.5.1 Experimental LLE data at equilibrium

The equilibrium solubility data in both aqueous and organic phases for the binary systems of water + D2EHPA, water + organic solvents as well as D2EHPA + organic solvents are reported in Table 5.3. Some solubility data from the literature [31, 36-38] are also reported in this table. The equilibrium solubility curves for the four ternary systems of water + D2EHPA + organic solvents at the temperature of 298.2 K and atmospheric pressure are listed in Table 5.4. Mass fractions ( $w_i$ ) were used to present all compositions in this table and the same data were also plotted in Figure 5.1. In this figure, there is only one complete soluble liquid pair (D2EHPA + organic solvents) and two partial soluble liquid pairs (water + D2EHPA and water + organic solvents). These exhibit type-2 LLE behavior of all ternary systems [39]. The two-phase region areas decreased in the order of organic solvents: kerosene > cyclohexane > chloroform > 1-octanol. Results indicated that the two-phase region area was based on the mutual solubility of organic solvents and water. Thus, type of organic solvents is a significant factor for the two-phase region of the studied systems. In the extraction processes, the organic solvent as resulted in the large area of the two-phase region is required because it is less soluble in water. Organic solvents with high solubility in water cause the loss of the organic phase into the aqueous phase [40].

**Table 5.3** Equilibrium data of solubility for binary systems in this work together with the literature at the temperature of 298.2 K along with pressure of 0.1 MPa.<sup>a</sup>

Binary system	Aqueous phase		Organic phase	
	$w_1$	$w_2$ , Literature	$w_1$ , Literature	$w_2$
Water (1) + D2EHPA (2)	0.9992	0.0008, N/A	0.0005, N/A	0.9995
Water (1) + Kerosene (2)	0.9995	0.0005, N/A	0.0006, N/A	0.9994
Water (1) + Cyclohexane (2)	0.9999	0.0001, 0.0001 <sup>[31]</sup>	0.0006, 0.0003 <sup>[36]</sup>	0.9994
Water (1) + Chloroform (2)	0.9926	0.0074, 0.0080 <sup>[31]</sup>	0.0002, 0.0008 <sup>[37]</sup>	0.9998
Water (1) + 1-Octanol (2)	0.9995	0.0005, 0.0005 <sup>[31]</sup>	0.0401, 0.0442 <sup>[38]</sup>	0.9599

<sup>a</sup> Standard uncertainties are  $u(T) = 0.1$  K,  $u(p) = 10$  kPa and  $u(w) = 0.0008$ .

**Table 5.4** Equilibrium data of solubility for water (1) + D2EHPA (2) + organic solvents (3) at the temperature of 298.2 K along with pressure of 0.1 MPa.<sup>a</sup>

Kerosene		Cyclohexane		Chloroform		1-Octanol	
$w_1$	$w_2$	$w_1$	$w_2$	$w_1$	$w_2$	$w_1$	$w_2$
0.0006	0.0000	0.0006	0.0000	0.0002	0.0000	0.0401	0.0000
0.0004	0.0732	0.0005	0.0846	0.0012	0.0571	0.0385	0.0714
0.0008	0.1523	0.0012	0.1587	0.0027	0.1356	0.0400	0.1371
0.0005	0.2451	0.0019	0.2507	0.0063	0.2372	0.0409	0.2258
0.0005	0.3483	0.0067	0.3472	0.0110	0.3509	0.0372	0.3289
0.0007	0.4619	0.0082	0.4647	0.0146	0.4807	0.0341	0.4513
0.0012	0.5969	0.0100	0.5791	0.0151	0.5849	0.0308	0.5565
0.0028	0.6943	0.0122	0.6788	0.0161	0.6601	0.0293	0.6588
0.0043	0.7814	0.0128	0.7729	0.0174	0.7540	0.0271	0.7542
0.0052	0.8835	0.0122	0.8558	0.0152	0.8603	0.0244	0.8448
0.0005	0.9995	0.0005	0.9995	0.0005	0.9995	0.0005	0.9995
0.9995	0.0000	0.9999	0.0000	0.9926	0.0000	0.9995	0.0000
0.9992	0.0008	0.9992	0.0008	0.9992	0.0008	0.9992	0.0008

<sup>a</sup> Standard uncertainties are  $u(T) = 0.1$  K,  $u(p) = 10$  kPa and  $u(w) = 0.0008$ .

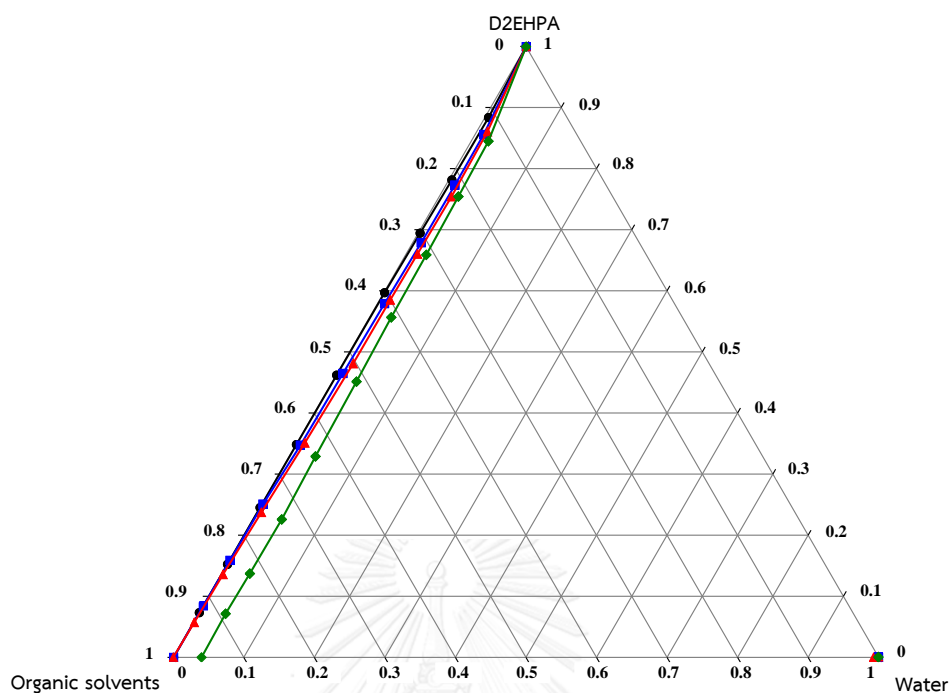


**Figure 5.1** Solubility curves for water + D2EHPA + organic solvents at the temperature of 298.2 K and atmospheric pressure; (—●—) kerosene, (—■—) cyclohexane, (—▲—) chloroform and (—◆—) 1-octanol.

The equilibrium tie-lines of the ternary systems are determined as shown in Table 5.5 and also plotted in Figures 5.2 to 5.5. From the figures, the slopes of the tie-lines emphasize that D2EHPA is more soluble in organic solvents than in water. This is because of the physical property of the functional groups in the molecule of D2EHPA. Phosphoric acid can be soluble in both organic solvents and water but 2-ethylhexanol favors solubility only in organic solvents. The low solubility of D2EHPA in water is a characteristic of a suitable extractant for use in extraction processes. Moreover, other characteristics of extractant should be considered i.e. high selectivity and rapid reaction to the target species, easy regeneration, low toxicity, etc. [41].

**Table 5.5** Equilibrium data of tie-lines for water (1) + D2EHPA (2) + organic solvents (3) at the temperature of 298.2 K along with pressure of 0.1 MPa.<sup>a</sup>

Aqueous phase			Organic phase		
$w_1$	$w_2$	$w_3$	$w_1$	$w_2$	$w_3$
Water + D2EHPA + Kerosene					
0.9979	0.0013	0.0008	0.0021	0.0871	0.9108
0.9978	0.0011	0.0011	0.0019	0.1739	0.8242
0.9981	0.0009	0.0010	0.0017	0.2473	0.7510
0.9980	0.0011	0.0009	0.0032	0.3651	0.6317
0.9978	0.0009	0.0013	0.0038	0.4480	0.5482
0.9981	0.0010	0.0009	0.0039	0.5259	0.4702
0.9980	0.0011	0.0009	0.0041	0.6285	0.3674
0.9979	0.0011	0.0010	0.0037	0.6785	0.3178
0.9981	0.0010	0.0009	0.0072	0.8233	0.1695
0.9982	0.0009	0.0009	0.0068	0.8895	0.1037
Water + D2EHPA + Cyclohexane					
0.9948	0.0011	0.0041	0.0017	0.0283	0.9700
0.9949	0.0012	0.0039	0.0019	0.0896	0.9085
0.9948	0.0013	0.0039	0.0019	0.2063	0.7918
0.9950	0.0020	0.0030	0.0020	0.3078	0.6902
0.9947	0.0017	0.0036	0.0030	0.4054	0.5916
0.9948	0.0019	0.0033	0.0062	0.5458	0.4480
0.9949	0.0021	0.0030	0.0085	0.6107	0.3808
0.9951	0.0022	0.0027	0.0112	0.7227	0.2661
0.9948	0.0023	0.0029	0.0121	0.8039	0.1840
0.9952	0.0018	0.0030	0.0132	0.8847	0.1021
Water + D2EHPA + Chloroform					
0.9947	0.0011	0.0042	0.0018	0.0274	0.9708
0.9948	0.0013	0.0039	0.0019	0.0542	0.9439
0.9950	0.0021	0.0029	0.0020	0.1169	0.8811
0.9951	0.0028	0.0021	0.0026	0.1754	0.8220
0.9949	0.0034	0.0017	0.0082	0.3151	0.6767
0.9938	0.0051	0.0011	0.0114	0.3704	0.6182
0.9935	0.0059	0.0006	0.0142	0.4893	0.4965
0.9924	0.0075	0.0001	0.0161	0.5611	0.4228
0.9906	0.0092	0.0002	0.0178	0.6516	0.3306
0.9884	0.0114	0.0002	0.0192	0.7578	0.2230
Water + D2EHPA + 1-Octanol					
0.9932	0.0012	0.0056	0.0414	0.0412	0.9174
0.9940	0.0049	0.0021	0.0411	0.0708	0.8881
0.9935	0.0053	0.0012	0.0431	0.1742	0.7827
0.9928	0.0064	0.0008	0.0421	0.3051	0.6528
0.9919	0.0078	0.0003	0.0387	0.3879	0.5734
0.9902	0.0085	0.0013	0.0327	0.4906	0.4767
0.9900	0.0093	0.0007	0.0317	0.5596	0.4087
0.9898	0.0096	0.0006	0.0310	0.6829	0.2861
0.9945	0.0051	0.0004	0.0296	0.7721	0.1983
0.9931	0.0039	0.0030	0.0244	0.8739	0.1017

<sup>a</sup> Standard uncertainties are  $u(T) = 0.1$  K,  $u(p) = 10$  kPa and  $u(w) = 0.0010$ .

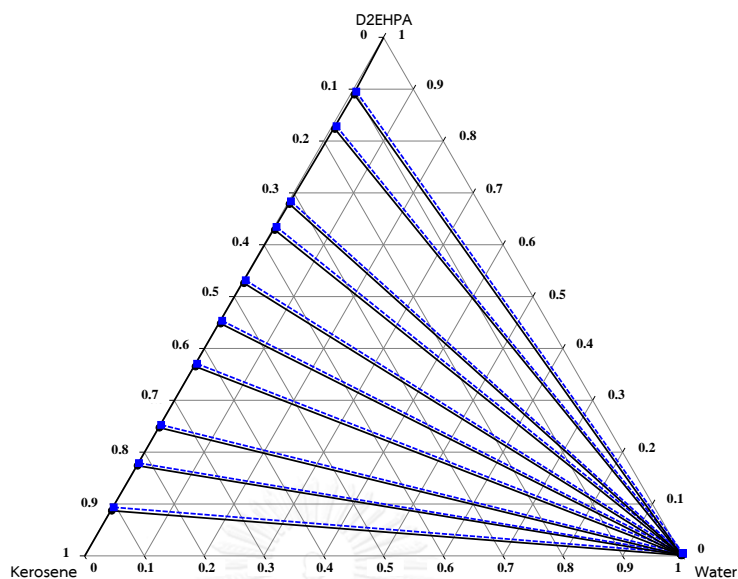


**Figure 5.2** LLE ternary diagram of water (1) + D2EHPA (2) + kerosene (3) at the temperature of 298.2 K along with atmospheric pressure; (—) solubility line for kerosene, (—●—) experimental tie-lines and (—■—) modeling NRTL results.

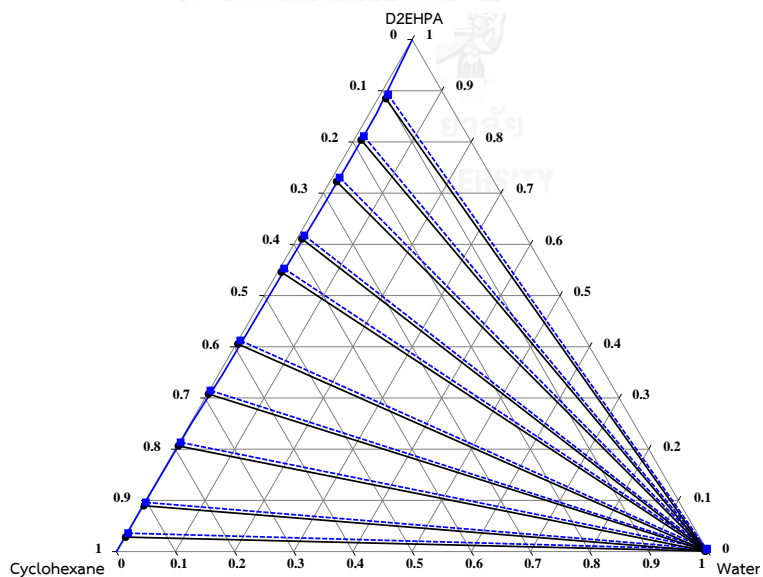


**Figure 5.3** LLE ternary diagram of water (1) + D2EHPA (2) + cyclohexane (3) at the temperature of 298.2 K along with atmospheric pressure; (—) solubility line for cyclohexane, (—●—) experimental tie-lines and (—■—) modeling NRTL results.

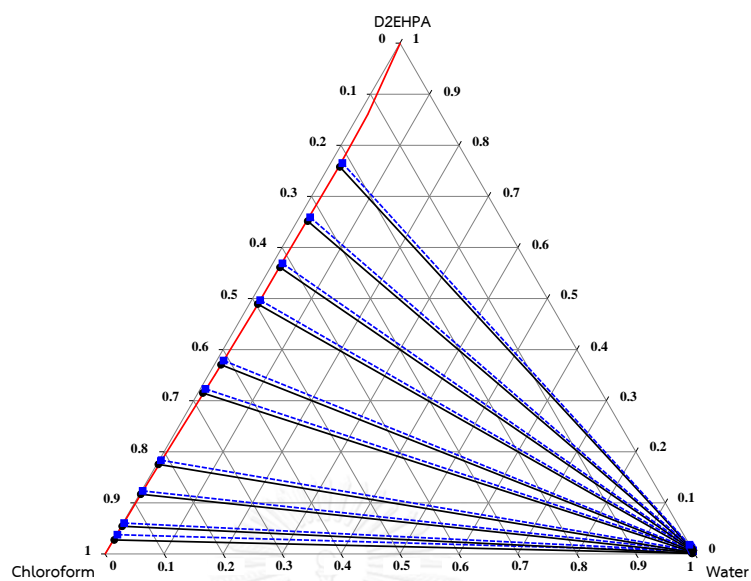


**Figure 5.4** LLE ternary diagram of water (1) + D2EHPA (2) + chloroform (3) at the temperature of 298.2 K along with atmospheric pressure; (—) solubility line for chloroform, (—●—) experimental tie-lines and (---■---) modeling NRTL results.

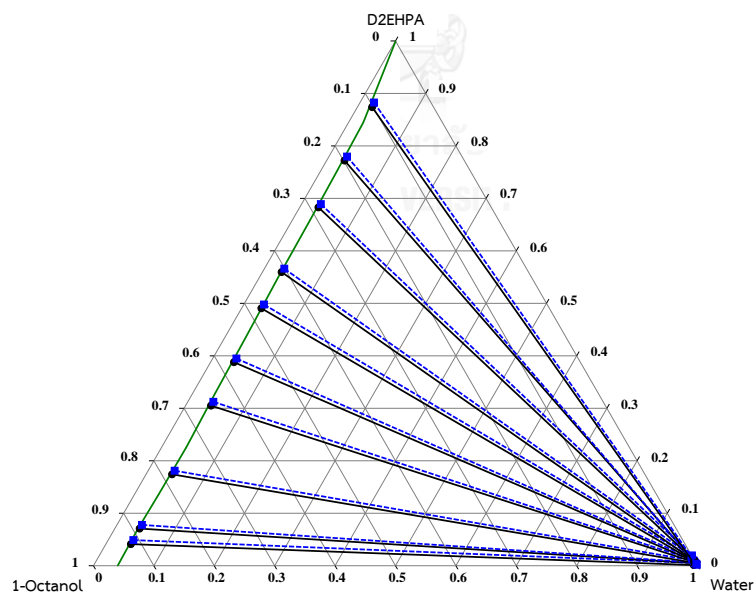


**Figure 5.5** LLE ternary diagram of water (1) + D2EHPA (2) + 1-octanol (3) at the temperature of 298.2 K along with atmospheric pressure; (—) solubility line for 1-octanol, (—●—) experimental tie-lines and (---■---) modeling NRTL results.

### 5.5.2 Extraction efficiency for different organic solvents

The extraction efficiency of silver ions for each organic solvent was expressed in the form of the percentage extraction ( $E$ ) as shown in Figure 5.6. The percentage extractions of silver ions with D2EHPA increased in the following order of organic solvents: kerosene < cyclohexane < chloroform < 1-octanol. Maximum extraction of silver ions at 94% was obtained for 1-octanol while the minimum extraction was 90% for kerosene. From the results, it can be observed that percentage extractions of silver ions increased when the dielectric constants of organic solvents increased. The increase of dielectric constants affected the extent of ion-pair interaction between the extractable complex and organic solvent [42]. It provided the additional interacting power that allowed more extractable complexes to stay in the organic phase [1]. Thus, this demonstrates the importance of solvent polarity on silver ion extraction.

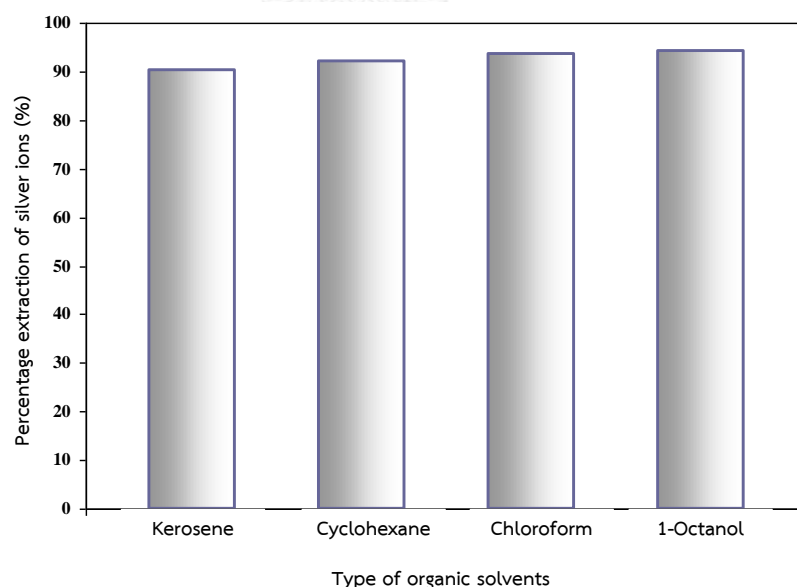


**Figure 5.6** Percentage extractions of silver ions by liquid-liquid extraction for different organic solvents: aqueous pH of 1, 0.01 mol/L of silver ions, 0.001 mol/L of D2EHPA and volume per phase of 0.045 L.

### 5.5.3 Extraction behaviors in different organic solvents

In order to study the extraction behaviors of silver ion and D2EHPA in the different organic solvents, the extractant concentrations, [D2EHPA], of 0.001-0.015 mol/L were investigated under a constant aqueous pH. In the case of all concentrations, the distribution ratios of silver-extractant complexes ( $K_{d,Ag^+}$ ), in the organic phase, were calculated based on Eq. (5.4) [43]. For each organic solvent,  $\log K_{d,Ag^+}$  was plotted versus  $\log [D2EHPA]$  as shown in Figure 5.7; the slopes of graphs were determined and reported in Table 5.6:

$$K_{d,Ag^+} = \frac{[Ag - D2EHPA \text{ complex}]_{org}}{[Ag^+]_{aq}} \quad (5.4)$$

where  $[Ag - D2EHPA \text{ complex}]_{org}$  is the concentration of silver-D2EHPA complexes in the organic phase (mol/L) and  $[Ag^+]_{aq}$  is the final concentration of silver ions in the aqueous phase (mol/L).

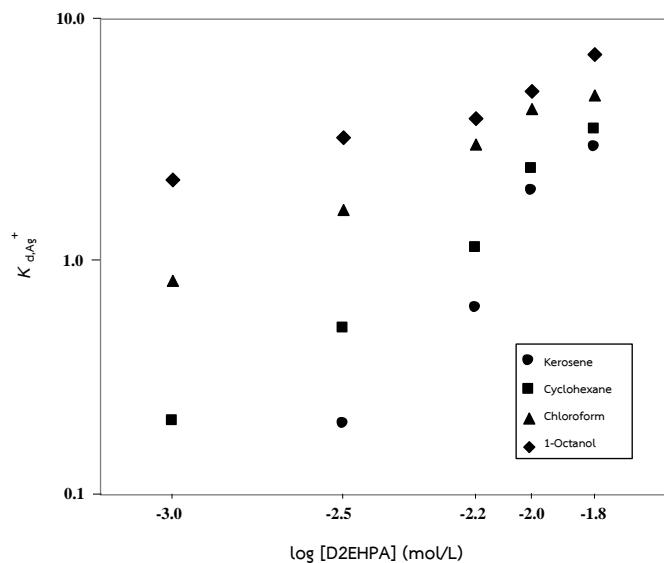


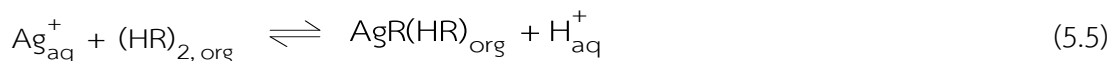
**Figure 5.7** Plot of  $K_{d,Ag^+}$  versus  $\log [D2EHPA]$ : aqueous pH of 1, 0.01 mol/L of silver ions and volume per phase of 0.045 L.

**Table 5.6** Slopes of log-log plot between  $K_{d,Ag^+}$  and D2EHPA concentration in various organic solvents at aqueous pH of 1.

Organic solvent	Slope
Kerosene	0.7462
Cyclohexane	0.8325
Chloroform	1.0502
1-Octanol	1.1787

In Table 5.6, the slopes of the graphs for any organic solvents had different values and varied from 0.75 to 1.18. Thus, it was clear that the stoichiometry of the D2EHPA molecule changed with the organic solvents. Change in the stoichiometry of the extractant molecule is based on the aqueous acidity and the concentration of the extractable complexes in the organic phase [12]. According to the stoichiometry in the range of 0.75 to 1.18, it indicated that the silver ion attached with the molecule of D2EHPA by the molar ratio of 1:0.75 to 1:1.18. This corresponded to the results of Stankovic et al. [44] who reported the molar ratio between silver ion and calixarene as the extractant by using dichloromethane as the organic solvent and

operating the aqueous pH of 1. From the results, the extraction behavior of silver ion with D2EHPA can be represented as follows:



where  $\text{Ag}_{\text{aq}}^{+}$  and  $\text{H}_{\text{aq}}^{+}$  are silver and hydrogen ions in the aqueous phase, and  $\text{HR}_{\text{org}}$  and  $\text{AgR}(\text{HR})_{\text{org}}$  are D2EHPA and silver-D2EHPA complex in the organic phase, respectively.

#### 5.5.4 Spectroscopic analysis for silver ion extraction

Analysis by FT-IR was also considered in this work in order to confirm the extraction behaviors of silver ions. The IR spectra of silver-D2EHPA complex in different organic solvents were compared with pure D2EHPA as shown in Figure 5.8. In this figure, the in-plane bending vibration of P-O-H in D2EHPA after attaching with silver ion shifted from  $1675 \text{ cm}^{-1}$  to  $1652 \text{ cm}^{-1}$ . This is similar to the work of Jin et al. [45] who reported the in-plane bending vibration of P-O-H in D2EHPA shifting from  $1693 \text{ cm}^{-1}$  to  $1631 \text{ cm}^{-1}$  in the case of ferric ion extraction. Results expressed the replacement of hydrogen ion in the P-O-H functional group by the silver ion. Thus, the silver ion in the aqueous phase was extracted by ion exchange with the hydrogen ion in the molecule of D2EHPA for staying in the organic phase.

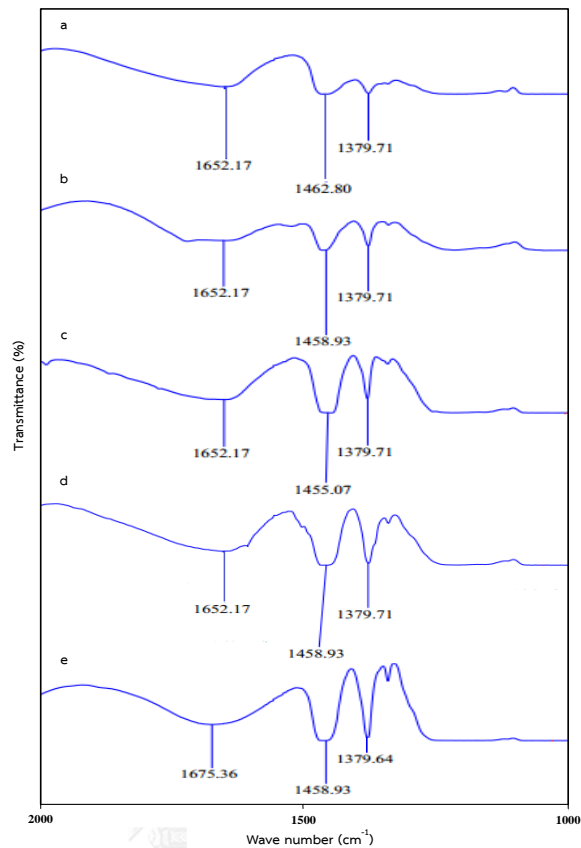


**Figure 5.8** IR spectra of silver-D2EHPA complex in the different organic solvents and pure D2EHPA: (a) 1-octanol, (b) chloroform, (c) cyclohexane, (d) kerosene and (e) pure D2EHPA.

### 5.5.5 Correlation of thermodynamic models

The activity coefficient model of NRTL was used to calculate the modeling data of tie-lines for correlation with the experimental results at  $T = 298.2$  K. The activity coefficient ( $\gamma_i$ ) for the component  $i$  in the aqueous and organic phases at equilibrium can be calculated based on the basic relationship as follows:

$$x_i^I \gamma_i^I = x_i^{II} \gamma_i^{II} \quad (5.6)$$

$$\sum x_i^I = \sum x_i^{II} = 1 \quad (5.7)$$

where  $x_i^I$ ,  $x_i^{II}$ ,  $\gamma_i^I$  and  $\gamma_i^{II}$  are the mole fractions and activity coefficients of component  $i$  in the aqueous (I) and organic (II) phases, respectively.

The NRTL activity coefficient ( $\gamma_i$ ) [46] is given by:

$$\ln \gamma_i = \frac{\sum_{j=1}^3 \tau_{ji} G_{ji} x_j}{\sum_{k=1}^3 G_{ki} x_k} + \sum_{j=1}^3 \frac{x_j G_{ij}}{\sum_{k=1}^3 G_{kj} x_k} \left( \tau_{ij} - \frac{\sum_{k=1}^3 x_k \tau_{kj} G_{kj}}{\sum_{k=1}^3 G_{kj} x_k} \right) \quad (5.8)$$

where  $x_i$  is the mole fraction of component  $i$ , the parameters  $\tau_{ij}$ ,  $\tau_{ji}$ ,  $\tau_{kj}$ ,  $G_{ij}$ ,  $G_{ji}$ ,  $G_{ki}$  and  $G_{kj}$  are the adjustable parameters for each binary pair in the model and  $i, j, k$  are the indices for all components.

These adjustable parameters can be determined as follows:

$$\tau_{ij} = a_{ij} + \frac{b_{ij}}{T} + e_{ij} \ln T \quad (5.9)$$

$$\alpha_{ij} = \alpha_{ji} = c_{ij} \quad (5.10)$$

$$G_{ij} = \exp(-\alpha_{ij} \tau_{ij}) \quad (5.11)$$

where  $a_{ij}$ ,  $b_{ij}$ ,  $c_{ij}$  and  $e_{ij}$  are the NRTL coefficients for the parameters of binary interactions and  $\alpha_{ij}$  and  $\alpha_{ji}$  are the non-randomness parameters.

The value of the non-randomness parameter ( $\alpha$ ) was obtained and its optimum value was found to be 0.2. The binary interaction parameters ( $b_{ij}$  and  $b_{ji}$ ) of the NRTL model for the investigated ternary systems were also obtained and are listed in Table 5.7. These parameter values were regressed by the minimum differences

between the modeling and experimental mole fractions for each component of both liquid phases.

**Table 5.7** Binary interaction parameters for water (1) + D2EHPA (2) + organic solvents (3) at the temperature of 298.2 K.

Ternary system	<i>i-j</i>	$(\alpha = 0.2)$	
		$b_{ij}$ (K)	$b_{ji}$ (K)
Water + D2EHPA + Kerosene	1-2	915.0332	209.0028
	1-3	912.0064	174.0033
	2-3	-674.6101	251.0074
Water + D2EHPA + Cyclohexane	1-2	0.9368	-982.2647
	1-3	862.1877	811.6291
	2-3	-1,067.3641	910.1002
Water + D2EHPA + Chloroform	1-2	126.3042	154.2167
	1-3	716.9221	-987.0658
	2-3	-723.1076	126.1891
Water + D2EHPA + 1-Octanol	1-2	118.2178	41.2188
	1-3	987.1183	827.9652
	2-3	-752.8439	173.0040

The correlations of experimental tie-line data and modeling results for all ternary systems are presented in Table 5.8 along with Figures 5.2 to 5.5. The validity of the correlations was evaluated by the root-mean square deviation (*rmsd*) as calculated by Eq. (5.12). Their valid results are also listed in Table 5.8. From this table, the modeling results of the ternary systems provided good correlation with the experimental results. The low *rmsd* values confirmed the ability of the NRTL model to predict the LLE data in this work:

$$rmsd = 100 \left( \frac{\sum_{k=1}^n \sum_{j=1}^2 \sum_{i=1}^3 (w_{ijk}^{expt.} - w_{ijk}^{cal.})}{6n} \right)^{1/2} \quad (5.12)$$

where  $n$  is the number of tie-lines,  $w^{expt.}$  and  $w^{cal.}$  are the mass fractions of experimental and modeling results, respectively. Subscript  $i$  is the component,  $j$  is the phase and  $k$  equals to 1, 2, ...,  $n$ .

**Table 5.8** Modeling results of tie-lines for water (1) + D2EHPA (2) + organic solvents (3) at the temperature of 298.2 K.

Aqueous phase				Organic phase				<i>rmsd</i> (%)
$w_{11}$		$w_{21}$		$w_{13}$		$w_{23}$		
Expt.	NRTL	Expt.	NRTL	Expt.	NRTL	Expt.	NRTL	
Water + D2EHPA + Kerosene								
0.9979	0.9980	0.0013	0.0053	0.0021	0.0020	0.0871	0.0937	0.36
0.9978	0.9980	0.0011	0.0039	0.0019	0.0017	0.1739	0.1789	
0.9981	0.9979	0.0009	0.0044	0.0017	0.0019	0.2473	0.2526	
0.9980	0.9981	0.0011	0.0054	0.0032	0.0031	0.3651	0.3705	
0.9978	0.9980	0.0009	0.0045	0.0038	0.0036	0.4480	0.4534	
0.9981	0.9980	0.0010	0.0046	0.0039	0.0040	0.5259	0.5315	
0.9980	0.9981	0.0011	0.0048	0.0041	0.0040	0.6285	0.6344	
0.9979	0.9981	0.0011	0.0041	0.0037	0.0035	0.6785	0.6837	
0.9981	0.9980	0.0010	0.0043	0.0072	0.0073	0.8233	0.8286	
0.9982	0.9981	0.0009	0.0050	0.0068	0.0069	0.8895	0.8954	
Water + D2EHPA + Cyclohexane								
0.9948	0.9944	0.0011	0.0046	0.0017	0.0021	0.0283	0.0360	0.47
0.9949	0.9946	0.0012	0.0053	0.0019	0.0021	0.0896	0.0961	
0.9948	0.9945	0.0013	0.0057	0.0019	0.0022	0.2063	0.2133	
0.9950	0.9951	0.0020	0.0048	0.0020	0.0019	0.3078	0.3146	
0.9947	0.9949	0.0017	0.0052	0.0030	0.0035	0.4054	0.4123	
0.9948	0.9946	0.0019	0.0051	0.0062	0.0074	0.5458	0.5528	
0.9949	0.9947	0.0021	0.0051	0.0085	0.0092	0.6107	0.6174	
0.9951	0.9948	0.0022	0.0055	0.0112	0.0124	0.7227	0.7304	
0.9948	0.9947	0.0023	0.0052	0.0121	0.0128	0.8039	0.8114	
0.9952	0.9957	0.0018	0.0042	0.0132	0.0134	0.8847	0.8924	
Water + D2EHPA + Chloroform								
0.9947	0.9945	0.0011	0.0053	0.0018	0.0020	0.0274	0.0337	0.51
0.9948	0.9940	0.0013	0.0059	0.0019	0.0021	0.0542	0.0604	
0.9950	0.9937	0.0021	0.0061	0.0020	0.0020	0.1169	0.1234	
0.9951	0.9931	0.0028	0.0066	0.0026	0.0029	0.1754	0.1835	
0.9949	0.9926	0.0034	0.0071	0.0082	0.0086	0.3151	0.3231	
0.9938	0.9918	0.0051	0.0081	0.0114	0.0116	0.3704	0.3786	
0.9935	0.9893	0.0059	0.0106	0.0142	0.0146	0.4893	0.4968	
0.9924	0.9875	0.0075	0.0124	0.0161	0.0163	0.5611	0.5689	
0.9906	0.9848	0.0092	0.0151	0.0178	0.0182	0.6516	0.6591	
0.9884	0.9819	0.0114	0.0180	0.0192	0.0197	0.7578	0.7653	
Water + D2EHPA + 1-Octanol								
0.9932	0.9927	0.0012	0.0052	0.0414	0.0416	0.0412	0.0489	0.55
0.9940	0.9927	0.0049	0.0062	0.0411	0.0414	0.0708	0.0778	
0.9935	0.9893	0.0053	0.0095	0.0431	0.0439	0.1742	0.1811	
0.9928	0.9862	0.0064	0.0113	0.0421	0.0423	0.3051	0.3124	
0.9919	0.9841	0.0078	0.0136	0.0387	0.0392	0.3879	0.3949	
0.9902	0.9825	0.0085	0.0158	0.0327	0.0334	0.4906	0.4978	
0.9900	0.9811	0.0093	0.0181	0.0317	0.0329	0.5596	0.5661	
0.9898	0.9809	0.0096	0.0197	0.0310	0.0319	0.6829	0.6891	
0.9945	0.9980	0.0051	0.0018	0.0296	0.0300	0.7721	0.7797	
0.9931	0.9960	0.0039	0.0039	0.0244	0.0231	0.8739	0.8827	

## 5.6 Conclusion

The organic solvents of kerosene, cyclohexane, chloroform and 1-octanol were selected in order to study their effect on silver ion extraction. The aspects of equilibrium data, kinetics of extraction behavior and thermodynamic model for each organic solvent were investigated at  $T = 298.2$  K and atmospheric pressure. The equilibrium solubility and tie-line data of the ternary systems (water + D2EHPA + organic solvents) exhibited type-2 LLE behavior. Their reliability was validated by the uncertainty propagation calculation. The organic solvent as resulted in the large two-phase region area in the triangular diagram is required for the extraction processes. Moreover, the tie-lines of all triangular diagrams expressed the low solubility of D2EHPA in water which is a good property of this extractant. The dielectric constants of the organic solvents provided the additional interacting power between the extractable complex and organic solvent that resulted in the increase in percentage extraction of silver ions. The maximum extraction of silver ions at 94% was obtained for 1-octanol. For the extraction behavior, the silver ion attached with D2EHPA by the molar ratio of 1:0.75 to 1:1.18 and its result is represented by the spectroscopic analysis. Thus, the stoichiometry of D2EHPA in the extraction reaction changed with the organic solvents. Finally, the modeling results of the NRTL model were in good correlation with the experimental LLE data as confirmed by the *rmsd* values which were less than 1%.

## 5.6 Nomenclature and units

$a, b, c, e$	NRTL coefficients for the binary interaction parameters
$\text{Ag}^+$	silver ions in the aqueous phase
$\text{AgR}$	extractable complexes in the organic phase
$E$	percentage extraction (%)
$G$	NRTL parameter in Eqs. (5.8) and (5.11)
GC	gas chromatography

$H^+$	hydrogen ions in the aqueous phase
HR	extractant in the organic phase
IR	infrared spectrometer
$K_{d,Ag}^+$	distribution ratio of extractable complexes in the organic phase
MW	molecular weight of chemicals (g/mol)
$n$	number of independent observations in Eqs. (5.2) and (5.3) or number of tie-lines in Eq. (5.12)
$p$	pressure (MPa)
$rmsd$	root-mean square deviation (%)
$T$	temperature (K)
$u(x_i)$	standard uncertainty
$w$	mass fraction
$x$	mole fraction
$X$	input quantity from the measurement in Eqs. (5.2) and (5.3)
Greek letters	
$\alpha$	non-randomness parameter
$\gamma$	activity coefficient
$\tau$	NRTL parameters in Eqs. (5.8 to 5.9) and (5.11)
Symbol	
[ ]	concentration of silver ions in the aqueous phase (mol/L)
$\Sigma$	sum of parameter
–	average value of parameter
Superscripts	
cal.	modeling results
expt.	experimental results

I	aqueous phase
II	organic phase

#### Subscripts

aq	aqueous phase
fin.	final concentration of silver ions in the aqueous phase
i, j, k	indices for all components
int.	initial concentration of silver ions in the aqueous phase
org	organic phase
1	water
2	D2EHPA
3	organic solvents

#### 5.8 Acknowledgements

The authors gratefully acknowledge the financial support by the Thailand Research Fund and Chulalongkorn University under the Royal Golden Jubilee Ph.D. program (Grant no. PHD/0272/2549) as well as the Ratchadaphiseksomphot Endowment Fund 2014 of Chulalongkorn University (CU-57-059-CC). Sincere thanks also go to Asst. Prof. Dr. Suvit Punnachaiya, Mrs. Khritsayaporn Thinnakorn, Ms. Paweena Ekkaphan and Mr. Wanchalerm Srirachat for their kind support.

#### 5.9 References

- [1] G. Yang, M.S. Jahan, L. Ahsan, Y. Ni, Influence of the diluent on the extraction of acetic acid from the prehydrolysis liquor of kraft based dissolving pulp production process by tertiary amine, *Separation and Purification Technology* 120 (2013) 341-345.

- [2] M.R. Chowdhury, S.K. Sanyal, Diluent effect on extraction of tellurium(IV) and selenium(IV) by tri-n butyl phosphate, *Hydrometallurgy* 34 (1994) 319-330.
- [3] A. Keshav, K.L. Wasewar, S. Chand, Recovery of propionic acid from an aqueous stream by reactive extraction: effect of diluents, *Desalination* 244 (2009) 12-23.
- [4] E. Löfström-Engdahl, E. Aneheim, C. Ekberg, M. Foreman, G. Skarnemark, Diluent Effects in Solvent Extraction: proceedings of the first ACSEPT international workshop, 2010, <http://www.acsept.org/AIWOproc/AIWO1-PR15-Lofstrom.pdf> (revised 2.4.10; accessed 20.7.14).
- [5] K. Wang, Z. Chang, Y. Ma, C. Lei, S. Jin, Y. Wu, I. Mahmood, C. Hua, H. Liu, Equilibrium study on reactive extraction of propionic acid with N1923 in different diluents, *Fluid Phase Equilibria* 278 (2009) 103-108.
- [6] A. Senol, Extraction equilibria of nicotinic acid using Alamine 336 and conventional solvents: effect of diluent, *Chemical Engineering Journal* 83 (2001) 155-163.
- [7] Z. Atik, M. Chaou, Solubilities and liquid-liquid equilibria of (water + ethanol +  $\alpha,\alpha,\alpha$ -trifluorotoluene) at temperatures  $T = (288.15, 298.15, \text{ and } 308.15)$  K and pressure  $p = 101.2$  kPa, *The Journal of Chemical Thermodynamics* 39 (2007) 583-587.
- [8] Y. Cui, J. Yang, G. Yang, G. Xia, Y. Nie, G. Sun, Effect of diluents on extraction behavior of rare earth elements with N,N,N',N'-tetrabutyl-3-oxy-glutaramide from hydrochloric acid, *Hydrometallurgy* 121-124 (2012) 16-21.
- [9] T. Wongsawa, M. Hronec, A.W. Lothongkum, U. Pancharoen, S. Phatanasri, Experiments and thermodynamic models for ternary (liquid-liquid) equilibrium systems of water + cyclopentanone + organic solvents at  $T = 298.2$  K, *Journal of Molecular Liquids* 196 (2014) 98-106.
- [10] M. Toikka, A. Samarov, M. Trofimova, A. Golikova, N. Tsvetov, A. Toikka, Solubility, liquid-liquid equilibrium and critical states for the quaternary system acetic acid-ethanol-ethyl acetate-water at 303.15 K and 313.15 K, *Fluid Phase Equilibria* 373 (2014) 72-79.
- [11] T. Wongsawa, M. Hronec, T. Soták, N. Leepipatpiboon, U. Pancharoen, S. Phatanasri, Ternary (liquid-liquid) equilibrium data of furfuryl alcohol with

- organic solvents at  $T = 298.2$  K: Experimental results and thermodynamic models, *Fluid Phase Equilibria* 365 (2014) 88-96.
- [12] S. Panja, P.K. Mohapatra, S.C. Tripathi, P.M. Gandhi, P. Janardan, Role of organic diluents on Am(III) extraction and transport behaviour using N,N,N',N'-tetraoctyl-3-oxapentanediamide as the extractant, *Journal of Membrane Science* 403-404 (2012) 71-77.
- [13] H. Ghanadzadeh, M. Ganji, S. Fallahi, Mathematical model of liquid-liquid equilibrium for a ternary system using the GMDH-type neural network and genetic algorithm, *Applied Mathematical Modelling* 36 (2012) 4096-4105.
- [14] A.G. Gilani, H.G. Gilani, S.L.S. Saadat, M. Janbaz, Ternary liquid-liquid equilibrium data for the (water + butyric acid + *n*-hexane or *n*-hexanol) systems at  $T = (298.2, 308.2, \text{ and } 318.2)$  K, *The Journal of Chemical Thermodynamics* 60 (2013) 63-70.
- [15] S.H. Shin, I.-C. Hwang, S.-J. Park, Liquid-liquid equilibria at 298.15 K for ternary mixtures of methyl *tert*-butyl ether + methanol (or ethanol) + imidazolium-based ionic liquids at atmospheric pressure, *Fluid Phase Equilibria* 342 (2013) 82-87.
- [16] H. Haghazarloo, M.N. Lotfollahi, J. Mahmoudi, A.H. Asl, Liquid-liquid equilibria for ternary systems of (ethylene glycol + toluene + heptane) at temperatures (303.15, 308.15, and 313.15) K and atmospheric pressure: experimental results and correlation with UNIQUAC and NRTL models, *The Journal of Chemical Thermodynamics* 60 (2013) 126-131.
- [17] U. Domanska, E.V. Lukoshko, M. Królikowski, Separation of thiophene from heptane with ionic liquids, *The Journal of Chemical Thermodynamics* 61 (2013) 126-131.
- [18] A.A. Amiri, A. Safavi, A.R. Hasaninejad, H. Shrghi, M. Shamsipur, Highly selective transport of silver ion through a supported liquid membrane using calix[4]pyrroles as suitable ion carriers, *Journal of Membrane Science* 325 (2008) 295-300.
- [19] S.W.P. Wijnhoven, W.J.G.M. Peijnenburg, C.A. Herberts, W.I. Hagens, A.G. Oomen, E.H.W. Heugens, B. Roszek, J. Bisschops, I. Gosens, D. van de Meent, S. Dekkers,

- W.H. de Jong, M. van Zijverden, A.J.A.M. Sips, R.E. Geertsma, Nano-silver-a review of available data and knowledge gaps in human and environmental risk assessment, *Nanotoxicology* 3(2) (2009) 109-138.
- [20] S. Altin, Y. Yildirim, A. Altin, Transport of silver ions through a flat-sheet supported liquid membrane, *Hydrometallurgy* 103 (2010) 144-149.
- [21] A. Gherrou, H. Kerdjoudj, R. Molinari, E. Drioli, Removal of silver and copper ions from acidic thiourea solutions with a supported liquid membrane containing D2EHPA as carrier, *Separation and Purification Technology* 28 (2002) 235-244.
- [22] N. Taoualit, D.E. Hadj-Boussaad, Metallic species ( $\text{Ag}^+$  and  $\text{Cu}^{2+}$  ions) transfer through a membrane-gel, *Desalination* 144 (2002) 273-277.
- [23] S.C. Lee, B.S. Ahn, W.K. Lee, Mathematical modeling of silver extraction by an emulsion liquid membrane process, *Journal of Membrane Science* 114 (1996) 171-185.
- [24] T.Zh. Sadyrbaeva, Liquid membrane system for extraction and electrodeposition of silver(I), *Journal of Electroanalytical Chemistry*, 648 (2010) 105-110.
- [25] Y.A. El-Nadi, Effect of diluents on the extraction of praseodymium and samarium by Cyanex 923 from acidic nitrate medium, *Journal of Rare Earths* 28(2) (2010) 215-220.
- [26] E. Bidari, M. Irannejad, M. Gharabaghi, Solvent extraction recovery and separation of cadmium and copper from sulphate solution, *Journal of Environmental Chemical Engineering* 1 (2013) 1269-1274.
- [27] V.S. Kislik, Chapter 11-final remarks on the competitive complexation/solvation theory of solvent extraction and its application, in: V.S. Kislik (Ed.), *Solvent Extraction: Classical and Novel Approaches*, 433-436, Elsevier B.V., 2012.
- [28] V.S. Kislik, Competitive complexation/solvation theory of solvent extraction, II solvent extraction of metals by acidic extractants, *Separation Science and Technology* 37(11) (2002) 2623-2657.
- [29] Shell Oil Company, Material safety data sheet of kerosene <<http://www.shell.com>> (revised 10.12.2010; accessed 27.10.2014).

- [30] Chevron Phillips Chemical Company, Material safety data sheet of cyclohexane <<http://www.cpchem.com>> (revised 23.09.2014; accessed 27.10.2014).
- [31] S.H. Yalkowsky, Y. He, Solubility data, in: S.H. Yalkowsky, Y. He (Eds.), Handbook of Aqueous Solubility Data, CRC Press, Florida, 2003, 1-1496.
- [32] Chemwatch, Material safety data sheet of nitric acid <<https://www.mso.anu.edu.au>> (revised 17.06.2005; accessed 27.10.2014).
- [33] Salt Lake Metals Company, Material safety data sheet of silver nitrate <<http://www.saltlakemetals.com/>> (revised 17.06.2005; accessed 27.10.2014).
- [34] JCGM, JCGM 100:2008; GUM 1995 with minor corrections, Evaluation of Measurement Data-Guide to the Expression of Uncertainty in Measurement, JCGM, 2008, pp. 1-120.
- [35] B.N. Taylor, C.E. Kuyatt, Guidelines for evaluating and expressing the uncertainty of NIST measurement results, in: NIST Technical Note 1297, National Institute of Standards and Technology (NIST), 1994, pp. 1-20.
- [36] S. Goldman, The determination and statistical mechanical interpretation of the solubility of water in benzene, carbon tetrachloride, and cyclohexane, Canadian Journal of Chemistry 52 (1974) 1668-1680.
- [37] R.M. Stephenson, Mutual solubilities: water-ketones, water-ethers, and water-gasoline-alcohols, Journal of Chemical and Engineering Data 37 (1992) 80-95.
- [38] R.M. Stephenson, J. Stuart, M. Tabak, Mutual solubility of water and aliphatic alcohols, Journal of Chemical and Engineering Data 29(3) (1984) 287-290.
- [39] H.G. Gilani, A.G. Gilani, M. Sangashekan, Tie-line data for the aqueous solutions of phenol with organic solvents at  $T = 298.2$  K, The Journal of Chemical Thermodynamics 58 (2013) 142-148.
- [40] K.C. Sole, Chapter 5: solvent extraction in the hydrometallurgical processing and purification of metals; process design and selected applications, in: M. Aguilar, J.L. Cortina (Eds.), Solvent Extraction and Liquid Membranes: Fundamentals and Applications in New Materials, 141-200, CRC Press: Florida, 2008.
- [41] V.S. Kislik, Chapter 2: carrier-facilitated coupled transport through liquid membranes; general theoretical considerations and influencing parameters, in:

- V.S. Kislak (Ed.), *Liquid Membranes: Principles and Applications in Chemical Separations and Wastewater Treatment*, 17-71, Elsevier: The Netherlands, 2010.
- [42] M. D. Jackson, W.R. Gilkerson, Ion-solvent interaction: effects of added polar compounds on the conductances of several alkali metal salts in 2-butanone at 25 °C, *Journal of the American Chemical Society* 101(2) (1979) 328-333.
- [43] K. Rezaei, H. Nedjate, Diluent effect on the distribution ratio and separation factor of Ni(II) in the liquid-liquid extraction from aqueous acidic solutions using dibutyldithiophosphoric acid, *Hydrometallurgy* 68 (2003) 11-21.
- [44] V. Stankovic, L. Outarra, F. Zonnevjlle, Ch. Comninellis, Solvent extraction of silver from nitric acid solutions by calix[4]arene amide derivatives, *Separation and Purification Technology* 61 (2008) 366-374.
- [45] Y. Jin, Y. Ma, Y. Weng, X. Jia, J. Li, Solvent extraction of Fe<sup>3+</sup> from the hydrochloric acid route phosphoric acid by D2EHPA in kerosene, *Journal of Industrial and Engineering Chemistry* 20 (2014) 3446-3452.
- [46] B. Mokhtarani, J. Musavi, M. Parvini, M. Mafi, A. Sharifi, M. Mirzaei, Ternary (liquid-liquid) equilibria of nitrate based ionic liquid + alkane + benzene at 298.15 K: experiments and correlation, *Fluid Phase Equilibria* 341 (2013) 35-41.

## Chapter VI

A reaction flux model for extraction of Cu(II) with LIX 84-I in HFSLM

Ura Pancharoen<sup>a</sup>, Thidarat Wongsawa<sup>a</sup>, Anchaleeporn Waritswat Lothongkum<sup>b</sup>

<sup>a</sup> *Department of Chemical Engineering, Faculty of Engineering, Chulalongkorn University, Phyathai Rd., Bangkok 10330, Thailand*

<sup>b</sup> *Department of Chemical Engineering, Faculty of Engineering, King Mongkut's Institute of Technology Ladkrabang, Chalongsong Rd., Bangkok 10520, Thailand*



จุฬาลงกรณ์มหาวิทยาลัย  
CHULALONGKORN UNIVERSITY

---

This article has been published in journal: Separation Science and Technology.

Page: 2183-2190. Volume: 46. Year: 2011.

---

## 6.1 Abstract

Hollow fiber supported liquid membrane (HFSLM) is a favorable method to extract both valuable compounds and heavy metal pollutants such as chromium, copper, and nickel at a very low concentration. In this work, the extraction of Cu(II) by LIX 84-I dissolved in kerosene was theoretically and experimentally investigated. A model to estimate the percentage of extraction of copper ions from synthetic water considering the effect of reaction flux in liquid membrane phase of the HFSLM was studied.  $\text{H}_2\text{SO}_4$  solution was used as the stripping solution. The facilitated transport mechanism of the chemical reaction at the feed-membrane interface was taken into account in the model equations. The percentage of copper ion extraction was plotted against its initial concentration in feed and also feed flow rate. Subsequently, the separation time and separation cycle were determined in accordance with the simulated values of copper ion concentration and the feed flow rate from the model. The modeled results were in good agreement with the experimental data at the average percentage of deviation about 2%.

**Keywords:** Copper ions; Extraction; Flux; Hollow fiber; Mass transfer; Modeling.

## 6.2 Introduction

Hollow fiber supported liquid membrane (HFSLM) draws considerable interest of many researchers due to its attractive advantages and several industrial applications such as the separation of dilute heavy metals from industrial wastewaters to meet the stringent environment-quality standards as well as a simple design in scaling up for industrial applications. This technique has specific characteristics of simultaneous extraction and recovery processes of low-concentration target species in one single stage, non equilibrium mass transfer, high selectivity, and low organic solvent used. Some other advantages of the hollow fiber supported liquid membrane over the traditional separation techniques include lower capital and operating costs, lower

energy consumption, and higher fluxes [1-4]. Using HFSLM in industrial, biomedical, and analytical fields have been reported in many articles [5-8].

In order to apply the hollow fiber supported liquid membrane to the industries, the reliable mathematical models are required since they help provide a guideline of mass transfer describing the transport mechanism of the target species through liquid membrane phase. Two general models considering the transport mechanism through liquid membrane phase are the diffusion and the facilitated transport mechanisms. The facilitated transport mechanism or carrier mediated transport relates to the reaction flux of chemical reaction between the target species and the selected single extractant or synergistic extractant to form target-extractant complexes [2, 9-11]. In principle, the metal ion transport through the liquid membrane phase occurs when the metal ions react with the selected extractant at the interface between feed or aqueous phase and organic liquid membrane phase, consequently target-extractant complexes diffuse through the liquid membrane phase. Different chemical interactions (reverse or irreversible) such as the formation of a new coordinate compound, dissociation or association, and aggregation are possibly observed [12, 13].

Since copper is used extensively in many manufacturing processes, for example, electroplating, electronic industry, hydrometallurgy, etc., therefore, copper ions, which are toxic and non-biodegradable, may contaminate wastewaters and cause the environmental problems and health effects if no appropriate treatment is taken [3, 14, 15]. In this work, a mathematical model describing the effect of reaction flux on facilitated transport mechanism of copper ions through the liquid membrane phase of the HFSLM system was developed. The model was verified with the experimental extraction results of copper ions in ppm level by LIX 84-I dissolved in kerosene. It is known that LIX-series compounds are the most selective extractants of high selectivity and widely used for copper ions [14, 16-26]. According to the model, the optimum conditions of the percentages of copper ion extraction as a function of its initial concentration in feed and the feed flow rate were used to determine the optimum separation time and cycle for the extraction of copper ions. Finally, the results were compared with previous works.

## 6.3 Theory

### 6.3.1 Transport mechanisms of copper ion extraction

The organic extractant or carrier is trapped in hydrophobic micro porous fibers of the hollow fiber module. Feed phase containing copper ions and the stripping solution are fed counter currently into tube and shell sides of hollow fibers, respectively. The transport mechanism of copper ion in the micro porous hollow fiber is presented schematically in Figure 6.1. The chemical reaction at the interface between the feed phase and the organic liquid membrane phase takes place when the extractant (HR) reacts with copper ion in the feed phase (Eq. (6.1)) [26-28]. The copper-extractant complex is formed and transported across the liquid membrane phase to the other side. No transport of copper ion passes this interface. At the interface between the liquid membrane phase and the stripping phase, the copper-extractant complex reacts with the stripping solution and release copper ion to the stripping phase.

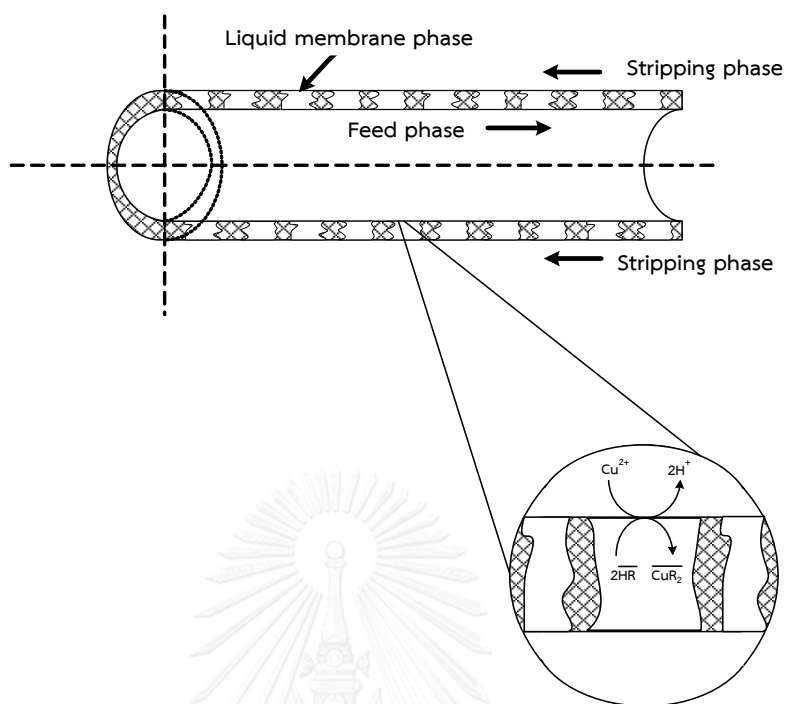


**Figure 6.1** Schematic transport mechanism of copper ion in the liquid membrane phase.



$\text{CuR}_{2,\text{org}}$  is the copper-extractant complex in the liquid membrane phase.

Equation (6.1) can be simplified as follows:



where A is copper ion, B is LIX 84-I, C is the complex species of copper ion and LIX 84-I, D is hydrogen ion and a, b, c, d are stoichiometric coefficients of A, B, C and D, respectively.

Thus, the reaction rate ( $r_A$ ) is

$$r_{-A} = k_f C_A^n(x,t) \quad (6.3)$$

$k_f$  is the reaction rate constant and  $n$  is the order of reaction.

The acilitated transport mechanism can be described by solute species partitioning (dissolving), ion complexation and diffusion [13]. The detailed steps are as follows:

Step 1: Metal ions in feed solution are transported to the interface between feed and liquid membrane phases, subsequently reacted with the extractant to form metal-extractant complexes.

Step 2: The metal-extractant complexes diffuse to the opposite side of liquid membrane phase by the concentration gradient.

Step 3: The metal-extractant complexes react with the stripping solution at the interface between liquid membrane and stripping phases to recover metal ions into the stripping phase.

Step 4: Metal ions are transferred into the stripping phase while the extractant moves back to the opposite side of the liquid membrane phase by the concentration gradient to react again with metal ions in feed phase.

### 6.3.2 Analysis of copper ion concentration in the feed phase

The transport of copper ions through a cylindrical hollow fiber is considered in the axial direction or bulk flow direction and radial direction. In order to develop the model, the following assumptions are made:

- The inside diameter of a hollow fiber are very small. Thus, the radial concentration profile of copper ions is constant.

- Due to very small inside diameter, it is presumed that the reaction occurs only in the axial direction of the hollow fibers. Mass flux of copper ions exists in the axial direction.
- Only the copper-extractant complexes occurring from the reaction, not copper ions, diffuse through the membrane phase.
- The extraction reaction is irreversible that means only the forward reaction of Eq. (6.1) is considered.

The conservation of mass for copper ion transport in the hollow fiber is considered as shown in Figure 6.2.

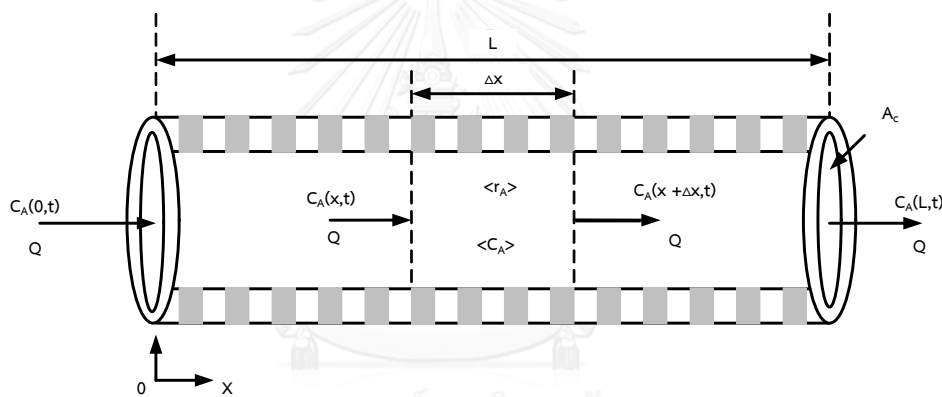


**Figure 6.2** Transport of copper ions in the hollow fiber.

At a small segment of  $\Delta x$ , the conservation of mass can be described below:

$$QC_{A(x,t)} - QC_{A(x+\Delta x,t)} - \langle r_A \rangle v_p = \frac{d\langle C_A \rangle}{dt} v_p \quad (6.4)$$

$\langle r_A \rangle$  and  $\langle C_A \rangle$  are the average values of the reaction rate and the concentration of copper ions, respectively and  $v_p$  is the pore volume of a hollow fiber and can determine as follows:

$$v_p = \frac{\varepsilon \Delta x}{2} (d_o - d_i) \quad (6.5)$$

where  $\varepsilon$  is the porosity of hollow fibers and  $d_i$  and  $d_o$  are the inside and outside diameters of a hollow fiber.

Dividing Eq. (6.4) by  $\Delta x A_c$  and taking a limit  $\Delta x \rightarrow 0$  obtains:

$$\frac{-Q \partial C_{A(x,t)}}{\partial x} - v r_{A(x,t)} = \frac{v \partial C_{A(x,t)}}{\partial t} \quad (6.6)$$

where 
$$v = \frac{\varepsilon}{2} (d_o - d_i)$$

### 6.3.2.1 At the initial condition ( $t = 0$ )

The conservation of mass in Eq. (6.6) is considered with regard to 3 cases of the reaction orders as follows:

Case 1:  $n = 0$

$$C_{A(L,0)} = C_{A(0,0)} - \frac{k_f v}{Q} L \quad (6.7)$$

Case 2:  $n = 1$

$$C_{A(L,0)} = e^{-\frac{k_f v}{Q} L} C_{A(0,0)} \quad (6.8)$$

Case 3:  $n \neq 0, 1$

$$C_{A(L,0)} = \left[ C_{A(0,0)}^{1-n} + \frac{(n-1)k_f v}{Q} L \right]^{\frac{1}{1-n}} \quad (6.9)$$

### 6.3.2.2 At time $t$ ( $t \neq 0$ )

The conservation of mass in Eq. (6.6) in the differential form is shown.

$$\frac{-Q \partial \bar{C}_A(x,t)}{\partial x} - v r_A(x,t) = \frac{v \partial \bar{C}_A(x,t)}{\partial t} \quad (6.10)$$

Where

$$\bar{C}_A(x,t) = C_A(x,t) - C_A(x,0)$$

$$r_A(x,t) = r_A(x,t) - r_A(x,0) = - \left( \frac{k_f n}{\lambda - \gamma x} \right) \bar{C}_A(x,t)$$

From Eq. (6.10) by taking Laplace transforms for linear operation and considering 3 cases of the reaction orders, we obtain:

Case 1:  $n = 0$

$$\bar{C}_A(L,t) = \bar{C}_A(0,t-\tau_0) \times u(t-\tau_0) - k_f \tau_0 \quad (6.11)$$

Case 2:  $n = 1$

$$\bar{C}_A(L,t) = e^{-\alpha} \bar{C}_A(0,t-v\tau_0) \times u(t-v\tau_0) \quad (6.12)$$

Case 3:  $n \neq 0, 1$

$$\bar{C}_A(L,t) = e^{-\beta} \bar{C}_A(0,t-v\tau_0) \times u(t-v\tau_0) \quad (6.13)$$

where

$$\tau_0 = \frac{L}{Q} \quad \alpha = vk_f \tau$$

$$\beta = \left( \frac{vk_f n}{Q\gamma} \right) \ln \left( \frac{\gamma L + \lambda}{\lambda} \right)$$

$$\gamma = \frac{(n-1)k_f V}{Q} \quad \lambda = C_{A(0,0)}^{1-n}$$

## 6.4 Experimental

### 6.4.1 Apparatus, feed and chemicals

A laboratory-scale hollow fiber module, Hoechst Liqui-Cel<sup>®</sup> Extra-flow 2.5 in × 8 in the membrane module was used for the experiments. The fibers were woven into fabric and wrapped around a central tube feeder to supply the shell side fluid. Detailed characteristics of the module are shown in Table 6.1.

**Table 6.1** Properties of the hollow fiber module.

Property	Description
Material	Polypropylene
Module diameter	0.63 dm
Module length	2.03 dm
Number of hollow fibers	35,000
Inside diameter of a hollow fiber	0.002 dm
Outside diameter of a hollow fiber	0.003 dm
Effective length of a hollow fiber	1.5 dm
Effective surface area of a hollow fiber	140 dm <sup>2</sup>
Area per unit volume	293 dm <sup>2</sup> /dm <sup>3</sup>
Pore size	3 × 10 <sup>-7</sup> dm
Porosity	25%
Tortuosity	2.6

The synthetic feed solution was prepared by dissolving  $\text{CuSO}_4 \cdot 5\text{H}_2\text{O}$ , analytical grade from Merck Ltd., in distilled water. The organic extractant, LIX 84-I ( $\text{C}_{17}\text{H}_{27}\text{NO}_2$ ), was supplied by Henkel Thai Ltd. The chemical structure of LIX84-I was shown in Figure 6.3. The extractant was diluted in kerosene, commercial grade from Thai Oil Public Co., Ltd., before feeding to the module. Sulfuric acid, analytical grade from Analar<sup>®</sup> BHD Ltd., was dissolved in distilled water and used as the stripping solution.

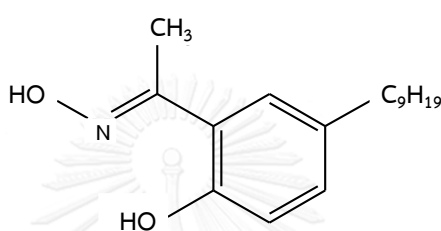
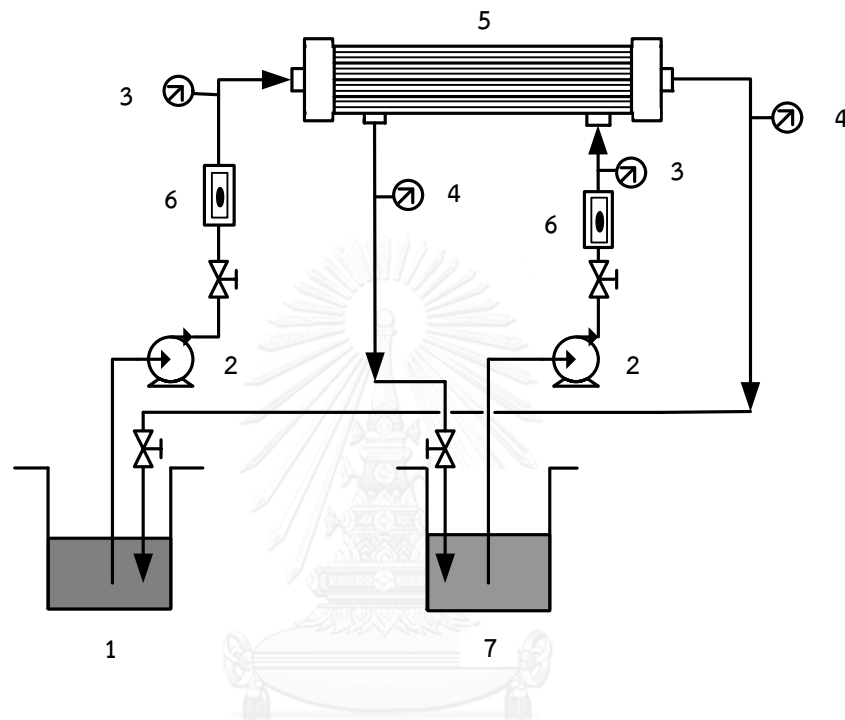


Figure 6.3 Chemical structure of LIX 84-I.

#### 6.4.2 Procedure

A single hollow fiber module operation for the extraction of copper ions was shown in Figure 6.4. Five liters of feed solution containing  $\text{Cu(II)}$  of 1-200 mg/L, and sulfuric acid solution 0.05-1.0 M were supplied counter-currently into the tube and shell sides of the module, respectively. The equal flow rates of the feed and stripping solutions of 70-250 mL/min were studied. The organic extractant (LIX 84-I) in kerosene of 500 mL with concentrations of 0.5-5% (v/v) was simultaneously pumped into the tube and shell sides of the hollow fibers for 40 min to ensure that the extractant was entirely embedded in the micro pores of the hollow fibers. It took about 20 min for each experimental condition. Finally, 15 mL of the outlet feed and stripping solutions were sampled and analyzed by the atomic absorption spectrometer (AAS: AA Spectromer Unicam 989 QZ, Unicam Ltd.) in case  $\text{Cu(II)}$  concentration was less than 10 mg/L, and by the atomic absorption/flame emission spectrometer (AA 670) in case  $\text{Cu(II)}$  concentration was higher than 10 mg/L.

The mathematical model was developed based on the aforementioned assumptions. The optimum separation time and cycle for the extraction were estimated. The model was verified with the experimental extraction results and other literature.



**Figure 6.4** Schematic counter-current flow diagram for a single-module operation in the HFSLM: 1) feed reservoir, 2) gear pumps, 3) inlet pressure gauges, 4) outlet pressure gauges, 5) hollow fiber module, 6) flow meters and 7) stripping reservoir.

## 6.5 Results and discussion

### 6.5.1 Validation of the model with the experimental results and other literature

The highest extraction of copper ions from the experiments was observed when using 3% (v/v) of LIX 84-I and sulfuric acid solution of 0.1 M. The integral concentrations of Cu(II) were plotted against time, as shown in Figure 6.5,

to determine the reaction order ( $n$ ) and the reaction rate constant ( $k_f$ ). The rate of diffusion and/or rates of chemical changes may control transport kinetics through liquid membrane depending on transport mechanisms.

From Figure 6.5, the reaction rate constants are  $0.393 \text{ min}^{-1}$  with respect to the first order ( $n = 1$ ) and  $0.708 \text{ L/mg}\cdot\text{min}$  with respect to the second order ( $n = 2$ ). The reaction rate constant obtained from the second order is, however, taken into consideration for further analysis since it is reported to provide a better curve fitting between the model and the experimental results, as shown by a better R-squared and less deviation in Table 6.2. Our results are more consistent with the second order. However, from previous publications [20, 29] it was reported that the reaction changed from first order to second order as the extraction proceeded. Yang et al. who studied the copper ion extraction via the HFSLM explained that the mass transfer was a first-order process at high copper concentration, but a second-order one at low copper concentration as a consequence of interfacial reaction [29]. In this work, the reaction order of copper extraction under the facilitated transport mechanism appears to agree with the phenomena observed by Yang et al.

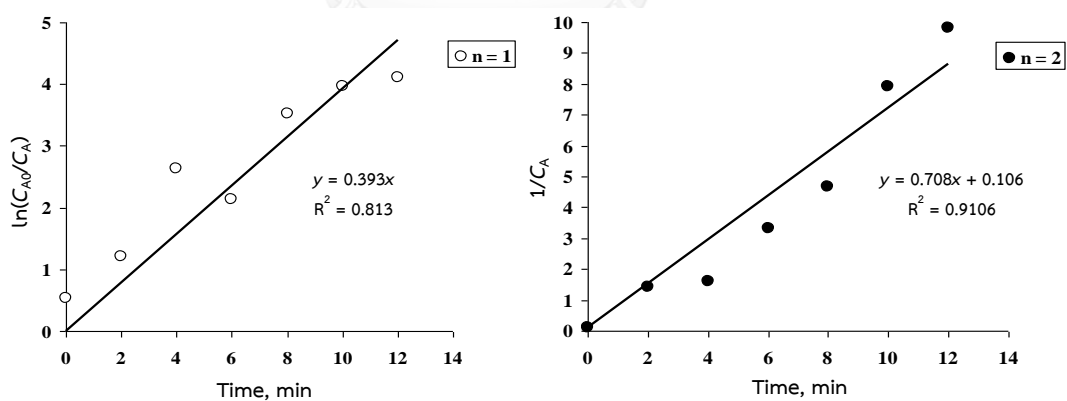


**Figure 6.5** The integral concentrations of Cu(II) and separation time.

**Table 6.2** Values of R-squared and percentage of deviation for 1 and 2 orders.

Reaction order ( <i>n</i> )	Reaction rate constant ( <i>k<sub>f</sub></i> )	R-squared	% Deviation
1	0.393 min <sup>-1</sup>	0.813	61.233
2	0.708 L/mg·min	0.911	1.453

The percentages of copper ion extraction from the experiments and the model were calculated by Eq. (6.14). The percentage of deviation was calculated by Eq. (6.15).

$$\% \text{extraction} = \frac{C_{f,\text{in}} - C_{f,\text{out}}}{C_{f,\text{in}}} \times 100 \quad (6.14)$$

$$\% \text{deviation} = \frac{\sum_{i=1}^j \left( \frac{C_{\text{Expt.}} - C_{\text{Theo.}}}{C_{\text{Expt.}}} \right)_i}{j} \times 100 \quad (6.15)$$

Figure 6.6 shows the percentages of copper ion extraction obtained from the experimental results and the model comparing to other works. The modeled results were in good agreement with the experimental data at the average percentage of deviation about 2%. These results imply that the transport of copper-extractant complexes in the liquid membrane phase depends on the reaction flux. The results were clearly seen that the highest percentage of copper extraction of 99% was attained at the initial concentration of 10 mg/L. Consequently, the percentage of extraction slowly decreased with the concentration due to a decrease in copper ion transport to the membrane interface. In this work, the amount of percentage of extraction from the model, based on the facilitated transport mechanism, was much higher than the experimental results by Ren et al. using 10% (v/v) of LIX 984-N [30], and Kittisupakorn et al. using 5% (v/v) of D2EHPA and the model based on diffusion transport mechanism [9].

This can be attributed to the efficiency of the selected extractant and the transport mechanism. Thus, it is obviously that the mathematical model based on the facilitated transport mechanism in our work can satisfactorily describe mass transfer of the target complex species through liquid membrane phase. Facilitated transport accelerates the transport, for example, trialkylphosphine sulfide increases the rate of phenol transport [31]. It is more drastic chemical changes of the solute species with the presence of a suitable extractant or synergistic extractant in liquid membrane phase to form new complexes (dissociated and undissociated forms) to diffuse through the membrane phase. Consequently, the efficiency and selectivity of transport across the liquid membrane may be markedly enhanced.

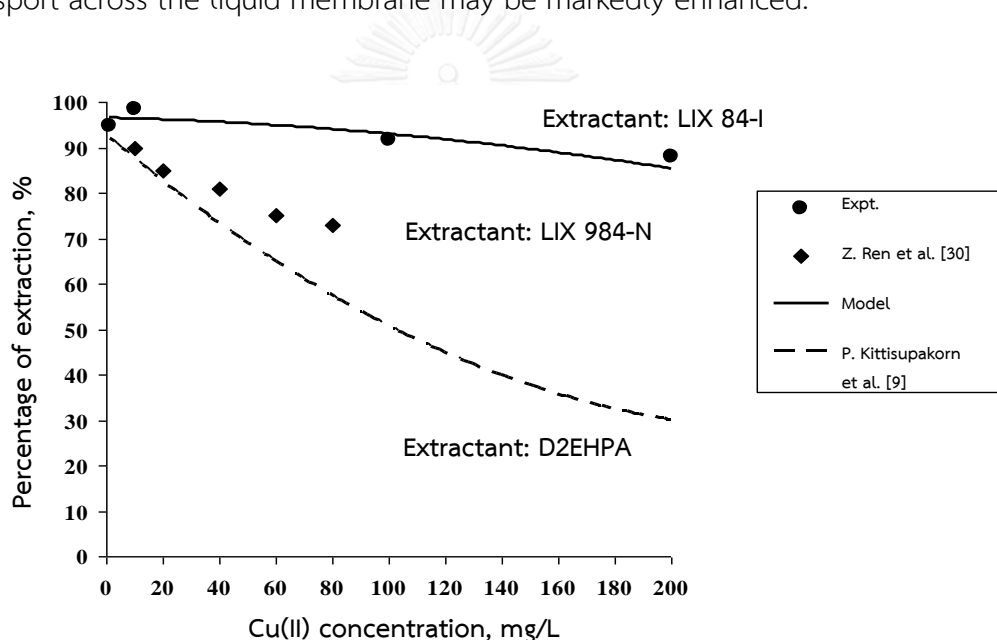


**Figure 6.6** Comparison of Cu(II) extraction by HFSLM with different extractants at different Cu(II) concentrations in feed solution.

Figure 6.7 shows the comparison results of Cu(II) extraction with feed flow rate. The percentages of extraction from the model were in good agreement with those from the experiments at the average percentage of deviation about 2%. The percentage of extraction increased up to the flow rate of 100 mL/min. The highest percentage of extraction of 99% was achieved. It is noted that the higher feed flow rate results in lower residence time or contact time [32].

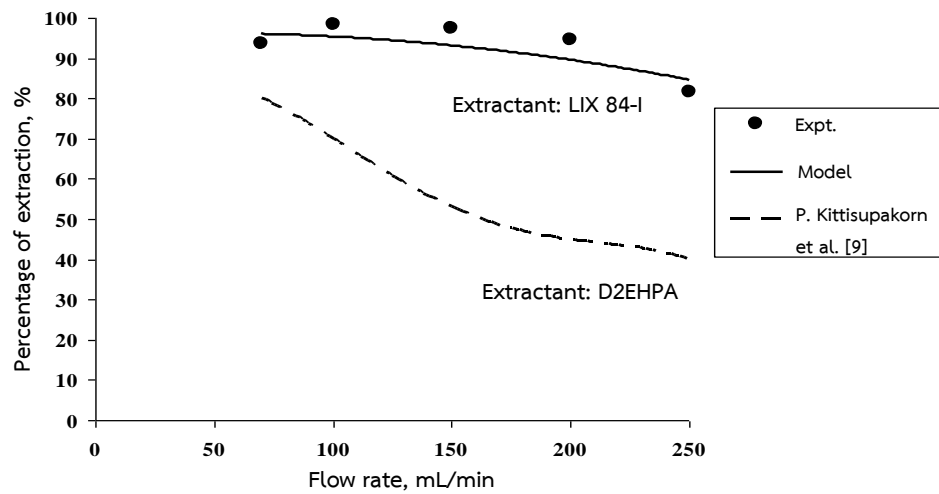


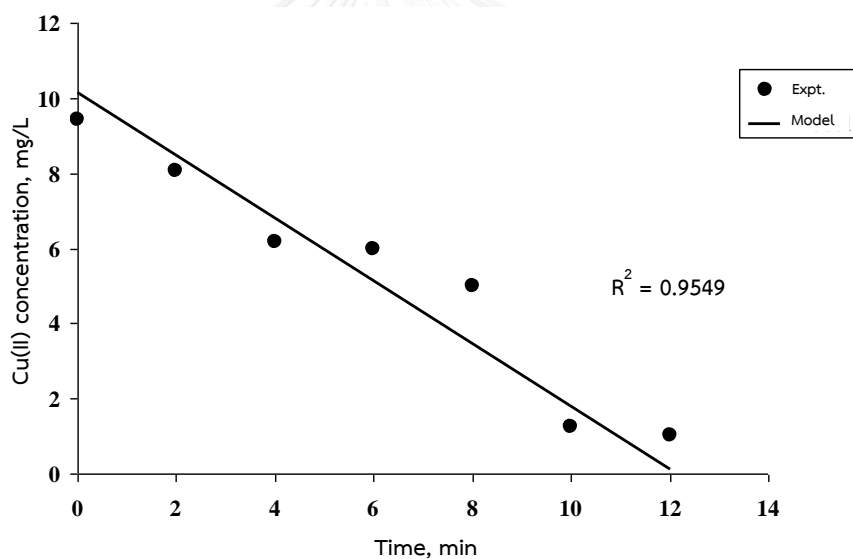
**Figure 6.7** Comparison of Cu(II) extraction by HFSLM with different extractants at different feed flow rates.

### 6.5.2 Estimation of separation time and separation cycle

The legislation concentration of copper ions in industrial wastewaters issued by the ministry of industry of Thailand must not exceed 2 mg/L. The optimum separation time and separation cycle to meet the permissible concentration were calculated from the model at the best condition, i.e., Cu(II) concentration in feed solution of 10 mg/L, the feed flow rate of 100 mL/min and the values in Table 6.3. From Figure 6.8 the estimated separation time was 10 min in 15 cycles. One cycle of feed flowing through the module was about 40 sec.

**Table 6.3** The relevant parameters used in the model.

Parameter	Value
$n$	2
$L$ (dm)	1.5
$\lambda$ (L/mg)	0.1
$k_f$ (L/mg·min)	0.708
$A_c$ (dm <sup>2</sup> )	$4.5 \times 10^{-6}$
$\beta$	$1.246 \times 10^{-2}$
$\tau_0$ (min)	$8.775 \times 10^{-4}$
$\gamma$ (dm <sup>2</sup> /mg)	$-3.186 \times 10^{-5}$

**Figure 6.8** The relationship between Cu(II) concentration and separation time.

## 6.6 Conclusion

The extraction of copper ions by HFSLM predicted by the reaction flux model based on the facilitated transport mechanism in this work fitted well with the experimental data. The average percentage of deviation was 2%. A number of different models have been developed to foretell the effect of mass transfer as a

function of operating parameters, membrane properties, and feed properties on the separation efficiency. However, due to the limitations of applications, or unclear phenomena around the membrane surface, no model so far is fully satisfactory and universally applicable. Even though, the models can help to understand and predict the operation as well as the separation performance. In case the separation of metal ions by HFSLM, as there are several parameters involved, e.g., metal ions vs. type of extractant and stripping solution, and transport mechanism, therefore this model probably has implications for other metals but it may need some modifications corresponding to such parameters.

In this work to attain the legislation Cu(II) concentration of 2 mg/L, the calculated separation time from the model was 10 min in 15 cycles. The percentage of extraction from this reaction flux model was much higher than the results from other works with different extractants and transport mechanisms. Types of the extractants and their concentrations play important roles on the separation of metal ions. For example, hard base extractant can extract both dissociated and undissociated forms in a basic or weak acidic condition but dissociated forms are high favored. While a neutral extractant normally reacts with undissociated forms, but in an acidic condition it can react with dissociated forms. Our recent work reported the synergistic extraction to enhance the simultaneous arsenic and mercury separation from co-produced water via HFSLM [33]. It is noteworthy to be aware that not only type of the extractant (single or synergistic), in this case LIX 84-I for Cu(II), but also the transport mechanism, e.g., facilitated transport mechanism (carrier-mediated transport), attribute to the extraction efficiency.

## 6.7 Nomenclature and units

$C$	concentration (mg/L)
$d_i$	inside diameter of a hollow fiber (dm)
$d_o$	outside diameter of a hollow fiber (dm)
$i$	number of hollow fibers

$j$	integer number
$k$	reaction rate constant or reaction rate coefficient (L/mg·min)
$L$	length of a hollow fiber (dm)
$n$	order of the reaction
$Q$	volumetric flow rate (mL/min)
$r$	rate of the reaction (mg/L·min)
$t$	time (min)
$v_p$	pore volume of a hollow fiber (mL)
$v$	parameter in the reaction flux model
$x$	direction of fiber axis (dm)

#### Greek letters

$\alpha$	constant in Eq. (6.12)
$\beta$	constant in Eq. (6.13)
$\gamma, \lambda$	parameters for $\beta$
$\epsilon$	porosity of hollow fibers
$\tau_0$	constant in Eqs. (6.11) to (6.13)

#### Symbol

$\langle \rangle$	average value
$\Delta$	difference between exit and entry values

#### Subscripts

f	feed solution
m	hollow fiber module
s	stripping solution
Expt.	experimental values

Theo. modeled values

## 6.8 Acknowledgements

The authors are highly grateful to the Royal Golden Jubilee Ph.D. Program (Grant No. PHD/0272/2549) which is supported by the Thailand Research Fund and Chulalongkorn University, Thai Oil Public Co., Ltd., and the Separation Laboratory, Department of Chemical Engineering, Chulalongkorn University, Bangkok, Thailand. Sincere appreciations also express to I. Kasemsestha, S. Chaturabul and T. Wannachod for their kind support.

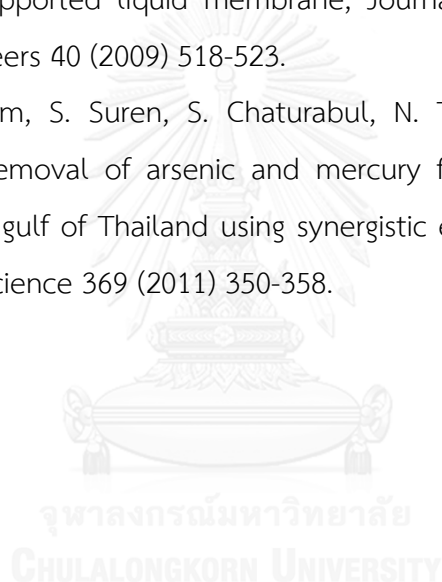
## 6.9 References

- [1] K. Soldenhoff, M. Shamieh, A. Manis, Liquid-liquid extraction of cobalt with hollow fiber contactor, *Journal of Membrane Science* 252 (2005) 183-194.
- [2] E. Bringas, M.F.S. Roman, J.A. Irabien, I. Ortiz, An overview of the mathematical modeling of liquid membrane separation processes in hollow fiber contactors, *Journal of Chemical Technology and Biotechnology* 84 (2009) 1583-1614.
- [3] W. Zhang, C. Cui, Z. Ren, Y. Dai, H. Meng, Simultaneous removal and recovery of copper(II) from acidic wastewater by hollow fiber renewal liquid membrane with LIX 984-N as carrier, *Chemical Engineering Journal* 157 (2010) 230-237.
- [4] P. Ramakul, E. Songkun, W. Pattaweekongka, M. Hronec, U. Pancharoen, Permeation study on the hollow-fiber supported liquid membrane for the extraction of Cobalt(II), *Korean Journal of Chemical Engineering* 23(1) (2006) 117-123.
- [5] U. Pancharoen, S. Somboonpanya, S. Chaturabul, A.W. Lothongkum, Selective removal of mercury as  $\text{HgCl}_4^{2-}$  from natural gas well produced water by TOA via HFSLM, *Journal of Alloys and Compounds* 489 (2010) 72-79.

- [6] A.W. Lothongkum, Y. Khemglad, N. Usomboon, U. Pancharoen, Selective recovery of nickel ions from wastewater of stainless steel industry via HFSLM, *Journal of Alloys and Compounds* 476 (2009) 940-949.
- [7] N. Parthasarathy, M. Pelletier, J. Buffle, Hollow fiber based supported liquid membrane: a novel analytical system for trace metal analysis, *Analytica Chimica Acta* 350 (1997) 183-195.
- [8] F.R. Valenzuela, C. Basualto, C. Tapia, J. Sapag, Application of hollow fiber supported liquid membrane technique to the selective recovery of a low content of copper from a Chilean mine water, *Journal of Membrane Science* 155 (1999) 163-168.
- [9] P. Kittisupakorn, W. Weerachaipichaskul, P. Thitiyasook, Modeling and simulation of copper-ion extraction with hollow fiber supported liquid membrane, *Journal of Industrial and Engineering Chemistry* 13 (2007) 903-910.
- [10] J.V. Sonawane, A.K. Pabby, A.M. Sastre, Au(I) extraction by LIX-79/*n*-heptane using the pseudo-emulsion-based hollow-fiber strip dispersion (PEHFSD) technique, *Journal of Membrane Science* 300 (2007) 147-155.
- [11] I. Ortiz, B. Galan, A. Irabien, Membrane mass transport coefficient for the recovery of Cr(VI) in hollow fiber extraction and back-extraction modules, *Journal of Membrane Science* 118 (1996) 213-221.
- [12] A.K. Pabby, S.S.H. Rizvi, A.M. Sastre, *Handbook of Membrane Separations*, Taylor & Francis Group: New York, 2009.
- [13] V.S. Kislik, *Liquid Membranes*, Elsevier, Amsterdam, The Netherlands, 2010.
- [14] S.H. Lin, R.S. Juang, Mass-transfer in hollow-fiber modules for extraction and back-extraction of copper(II) with LIX 64-N carriers, *Journal of Membrane Science* 188 (2001) 251-262.
- [15] Z. Ren, W. Zhang, Y. Lui, Y. Dai, C. Cui, New liquid membrane technology for simultaneous extraction and stripping of copper(II) from wastewater, *Chemical Engineering Science* 62 (2007) 6090-6101.
- [16] B. Sengupta, M.S. Bhakhar, R. Sengupta, Extraction of copper from ammoniacal solutions into emulsion liquid membranes using LIX 84-I, *Hydrometallurgy* 89 (2007) 311-318.

- [17] P.K. Parhi, K. Sarangi, Separation of copper, zinc, cobalt and nickel ions by supported liquid membrane technique using LIX 84-I, TOPS-99 and Cyanex 272, *Separation and Purification Technology* 59 (2008) 169-174.
- [18] R.W. Baker, M.E. Tuttle, D.J. Kelly, H.K. Lonsdale, Coupled transfer membranes, *Journal of Membrane Science* 2 (1977) 213-233.
- [19] T. Largman, S. Sifniades, Recovery of copper(II) from aqueous solution by means of supported liquid membranes, *Hydrometallurgy* 3 (1978) 153-162.
- [20] S.P. Carter, H. Freiser, Kinetics and mechanism of the extraction of copper with 2-hydroxy-5-nonylbenzophenone oxime, *Analytical Chemistry* 52 (1980) 511-514.
- [21] M. Harada, T. Miyake, Y. Kayahara, Kinetic mechanism of metal extraction with hydroxyoximes, *Journal of Chemical Engineering of Japan* 22 (1989) 168-177.
- [22] J.T. Patrick, R.D. Nobel, G.J. Hanna, Study of kinetics of copper extraction with (anti)-2-hydroxy-5-nonylbenzophenone oxime using a rotating diffusion cell, *Separation Science and Technology* 24 (1989) 199-211.
- [23] Z. Lazarova, L. Boyadzhiev, Kinetic aspect of copper(II) transport across liquid-membranes, *Journal of Membrane Science* 78 (1993) 239-245.
- [24] M.E. Campderros, A. Acosta, J. Marchese, Selective separation of copper with LIX 864 in a hollow fiber module, *Talanta* 47 (1998) 19-24.
- [25] S.Y.B. Hu, J.M. Wiencek, Emulsion-liquid-membrane extraction of copper using a hollow-fiber contactor, *AIChE Journal* 44 (1998) 570-581.
- [26] G.R.M. Breembroek, A. Straalen, G.J. Witkamp, G.M. Rosmalen, Extraction of cadmium and copper using hollow fiber supported liquid membranes, *Journal of Membrane Science* 146 (1998) 185-195.
- [27] F.R. Valenzuela, C. Basualto, C. Tapia, J. Sapag, C. Paratori, Recovery of copper from leaching residual solutions by means of a hollow-fiber membrane extractor, *Minerals Engineering* 9 (1996) 15-22.
- [28] F.R. Valenzuela, C. Basualto, J. Sapag, C. Tapia, Technical note membrane transport of copper with LIX-860 from acid leach waste solutions, *Minerals Engineering* 10 (12) (1997) 1421-1427.

- [29] C. Yang, E.L. Cussler, Reaction dependent extraction of copper and nickel using hollow fibers, *Journal of Membrane Science* 166 (2000) 229-238.
- [30] Z. Ren, W. Zhang, H. Meng, J. Liu, S. Wang, Extraction separation of Cu(II) and Co(II) from sulfuric solutions by hollow fiber renewal liquid membrane, *Journal of Membrane Science* 365 (2010) 260-268.
- [31] S. Schlosser, I. Rothova, H. Frianova, Hollow-fiber pertractor with bulk liquid membrane, *Journal of Membrane Science* 80 (1993) 99-106.
- [32] A.W. Lothongkum, P. Ramakul, W. Sasomsub, S. Laoharochanapan, U. Pancharoen, Enhancement of uranium ion flux by consecutive extraction via hollow fiber supported liquid membrane, *Journal of the Taiwan Institute of Chemical Engineers* 40 (2009) 518-523.
- [33] A.W. Lothongkum, S. Suren, S. Chaturabul, N. Thamphiphit, U. Pancharoen, Simultaneous removal of arsenic and mercury from natural-gas-co-produced water from the gulf of Thailand using synergistic extractant via HFSLM, *Journal of Membrane Science* 369 (2011) 350-358.



## Chapter VII

### High-efficiency HFSLM for silver-ion pertraction from pharmaceutical wastewater and mass-transport models

Thidarat Wongsawa<sup>a</sup>, Niti Sunsandee<sup>a</sup>, Ura Pancharoen<sup>a</sup>,  
Kasidit Nootong<sup>a</sup>, Anchaleeporn Waritswat Lothongkum<sup>b</sup>

<sup>a</sup> *Department of Chemical Engineering, Faculty of Engineering, Chulalongkorn University, Phyathai Rd., Bangkok 10330, Thailand*

<sup>b</sup> *Department of Chemical Engineering, Faculty of Engineering, King Mongkut's Institute of Technology Ladkrabang, Chalongkrung Rd., Bangkok 10520, Thailand*

จุฬาลงกรณ์มหาวิทยาลัย  
CHULALONGKORN UNIVERSITY

## 7.1 Abstract

Hollow fiber supported liquid membrane (HFSLM) is a favorable technique for the pertraction of metal ions, especially at a very low concentration. In this work, the pertraction of silver ions from pharmaceutical wastewater via HFSLM was investigated. Pharmaceutical wastewater containing 30 mg/L of silver ions and 120 mg/L of ferric ions was subjected to HFSLM as a feed solution. LIX 84-I dissolved in kerosene together with sodium thiosulphate solution were selected for use as the liquid membrane and stripping solutions, respectively. The influence of ferric ions on the pertraction of silver ions was studied firstly using wastewater with normal ferric ion concentration and secondly using wastewater with ferric ion precipitation by phosphoric acid solution. The highest pertraction of silver ions was achieved by using 0.1 M LIX 84-I and 0.5 M of sodium thiosulphate solution at pH 3.5 of feed and 2 of sodium thiosulphate solution. The flow rates of feed and sodium thiosulphate solutions were 0.2 dm<sup>3</sup>/min. Silver ions of 0.6 mg/L that remained in the wastewater was below the mandatory discharge limit. No effect of normal ferric ion concentration in the wastewater on silver ion pertraction was observed. Crucial parameters were defined to confirm the efficiency and reliability of the system. Finally, the controlling transport regime of silver ion pertraction in HFSLM was determined by the diffusion flux and reaction flux models.

**Keywords:** HFSLM; Silver ions; Pertraction; Pharmaceutical wastewater; Mass transport models.

## 7.2 Introduction

The contamination of silver in the environment is normally found in wastewater from the medical and photographic-imaging industry, electronics industry and the manufacturing of silverware and jewelry. Silver ions and free ions are toxic [1, 2]. A concentration of silver ions of only 1-5 mg/L can kill aqueous organisms, insects, trout and flounder. The accumulation of silver in plants and animals leads to

adverse effects on their growth but in humans it leads to convulsion and an argyria disease. This disease is an unusual illness marked by discoloration of skin, nails, mucous tissues and organs [3, 4]. Due to its toxicity, the pertraction of silver ions from wastewater is of paramount importance.

In compliance with the mandatory discharge limit of  $1.0 \text{ mg/dm}^3$  [5], common techniques have been used to extract silver ions from wastewater such as electrolysis, chemical precipitation, ion exchange and adsorption. Nevertheless, these methods are not insufficiently effective for the extraction of silver ions. Electrolysis requires a high current density, a long separation time and pH adjustment approaching 90% of extraction. In addition, its extraction efficiency is lower when it operates over extending time due to the precipitation of sulfide on the cathode. Chemical precipitation cannot achieve the mandatory discharge limit because of the difficult precipitation of silver compounds in the wastewater [6]. Ion exchange needs to regenerate the ion-exchange resin and consumes extra chemicals [7]. Nonselective adsorption using common adsorbents is a main drawback and is difficult and expensive to reuse [8].

To overcome these problems, liquid pertraction technologies have been accomplished in order to extract and recover metal ions from such diluted solutions. One promising technique of liquid pertraction technologies is the use of supported liquid membrane (SLM). This technique has a lot of advantages over the common techniques, such as low capital and processing costs, low energy consumption and easy operation [9, 10]. The SLM technique is a three-phase system in which the liquid membrane phase separates between the feed and stripping phases. Hollow fiber supported liquid membrane (HFSLM) is a system based on the SLM technique. HFSLM is found to be highly proficient in low-level metal extraction that can be shown by some examples of previous works as in Table 7.1. Other outstanding advantages of HFSLM are its high transport flux, very large interfacial area, no entrainment and flooding, simultaneous extraction and recovery steps in one single stage etc. [11-14]. However, the application of SLM technique, including HFSLM on a large scale is still limited due to its insufficient membrane stability [15]. Many factors, such as the characteristics of polymer support, the nature of extractants and organic

solvents as well as processing parameters, have an effect on the membrane stability of SLM [16].

**Table 7.1** Application of HFSLM to low-level metal extraction.

Initial ion concentration (mg/L)	Feed	Extractant	% Extraction
Cu(II) = 1-40 [17]	Synthetic water	D2EHPA	95
Cu(II) = 10 [18]	Synthetic water	LIX 84-I	99
Zr(IV) = 11 [19]	Synthetic water	0.5 M TNOA mixed with 0.5 M Aliquat 336	85
Hg(II) = 10 [20]	Synthetic water	<i>n</i> -Benzoyl- <i>n</i> / <i>n</i> / <i>-</i> diheptadecylthiourea	100
Cd(II) = (56.4-264.8)×10 <sup>-6</sup> [21]	Sea water	1-Octanol	89
Cr(VI) = 1 [22]	Synthetic water	Aliquat 336	90
Ni(II) = 8.1 [23]	Stainless steel- manufacturing wastewater	LIX 860-I	87
U(II) = 45 [24]	Monazite process solution	0.1 M Aliquat 336 mixed with 0.06 M TBP	99
Hg(II) = 1.3 [25]	Produced water	TOA	100
Hg(II) = 0.3 [26]	Produced water	Aliquat 336	97
As(V) = 4 [26]	Produced water	0.22 M Aliquat 336 mixed with 0.06 M Cyanex 471	94
Ta(V) = 10 [27]	Synthetic water	Aliquat 336	78
Pr(III) = 230 [11]	RE(NO <sub>3</sub> ) <sub>3</sub> solution	Cyanex 272	92
Cs(I) = 320 [28]	Nuclear wastewater	Calix[4]arene-bis-2,3- naphthocrown-6	100

RE is rare earth.

In general, the pertraction of metal ions by HFSLM depends on the type and concentration of a single extractant or types and concentration ratio of the synergistic extractants; type of organic solvent to dissolve the extractant; type and concentration of the stripping solution; concentration of metal ions in the feed solution; pH, flow rates and flow patterns of feed and stripping solutions. As a matter

of fact, the pertraction of metal ions across HFSLM involves diffusions - metal ions across the feed phase, complex species from the chemical reaction between metal ions and the extractant across the liquid membrane phase and metal ions across the stripping phase - as well as the chemical reactions at the feed-liquid membrane interface and at the liquid membrane-stripping interface. This indicates that the transport of metal ions is mainly controlled by either diffusion or chemical reaction.

It is of great importance to understand the transport of metal ions as it plays an important role on pertraction performance and separation time. An appropriate mathematical model can explain not only the transport but also can estimate the separation time. Mathematical models are classified into two categories depending on the transport regimes of metal ions. The diffusion flux model describes the diffusion transport regime where the rate of diffusion controls the transport of metal ions. The reaction flux model approaches the chemical reactions' kinetic transport regime where the rate of chemical reaction controls the transport of metal ions [16]. The overview of the mathematical models for metal ion pertraction by hollow fiber module based on diffusion flux and reaction flux models have been reported in previous works [18, 29-33].

This work investigated the effects of the above mentioned variables on the HFSLM system in order to determine the quantitative pertraction of silver ions from the pharmaceutical wastewater. The wastewater was supplied by the Government Pharmaceutical Organization of Thailand and contained 20-30 mg/L of silver ions and 100-120 mg/L of ferric ions that had pH of 5.5-6. To determine the optimum extractant and stripping solution for use in the HFSLM system, the types of extractants and stripping solutions were studied by liquid-liquid extraction. The extractants viz. Cyanex 923, D2EHPA and LIX 84-I as well as the stripping solutions viz. thiourea and sodium thiosulphate pentahydrate were selected due to their high pertraction of precious metals [1, 34-37]. Kerosene was also selected as the organic solvent due to its high performance in copper ion pertraction from the synthetic water via SLM as reported in the work of Ata [38]. The effects of all variables on the HFSLM system were studied, using only the optimum extractant and stripping solution. The quantitative pertraction of silver ions was determined and expressed in

terms of the extraction and pertraction efficiencies. In addition, the effect of ferric ions on silver ion pertraction was also studied. Other crucial parameters such as memory effect and repeatability were defined in order to confirm the efficiency and reliability of the HFSLM system. Corresponding to the diffusion transport regime as well as the chemical reactions' kinetic transport regime, the present work therefore formulated two relevant models - diffusion flux and reaction flux - in order to seek the controlling transport regime of silver ion pertraction in HFSLM.

### 7.3 Theory

#### 7.3.1 Pertraction of silver ions in the HFSLM system

The extractant that dissolves in the organic solvent is immobilized in the pores of the hydrophobic polymer fibers by capillary force. The feed solution containing silver ions together with the stripping solution are fed into the tube and shell sides of the hollow fibers. The transport of silver ions - from the feed phase across the liquid membrane phase into the stripping phase - occurs by extraction and recovery steps. These have chemical potential gradients as driving forces. Thus, the combination of extraction and recovery steps that are carried out simultaneously is called the pertraction process [39].

In order to determine the quantitative pertraction of silver ions via HFSLM, the extraction and pertraction efficiencies are proposed. The extraction efficiency ( $E$ ) is the parameter that indicates how much of the silver ions are extracted from the feed phase into the liquid membrane phase. The pertraction efficiency ( $P$ ) is the parameter that indicates how much of the silver ions are recovered in the stripping phase. Both parameters can be defined as follows [16]:

$$E = \frac{n_f - n_w}{n_f} \quad (7.1)$$

$$P = \frac{n_r}{n_f} \quad (7.2)$$

where  $n_f$ ,  $n_r$  are the amounts of silver ions in both feed and stripping phases, respectively and  $n_w$  is the amount of silver ions remaining in the wastewater after contact with the liquid membrane phase.

Furthermore, one parameter corresponding to the quantitative pertraction of silver ions is the memory effect ( $M$ ). This indicates how much of the complex species are captured in the liquid membrane phase after finishing the pertraction process. This parameter can be defined based on the extraction and pertraction efficiencies of silver ions as shown in Eq. (7.3) [40, 41]:

$$M = 1 - F - P \quad (7.3)$$

Where  $F = 1 - E$ .

### 7.3.2 Reliability of the HFSLM system

Repeatability is an acceptable parameter for showing the reliability of the HFSLM system. It refers to the variation of results which are obtained by the same experimental condition for each processing system. Thus, repeatability can be defined by Eq. (7.4) [42] as:

$$\text{Repeatability} = 2.83 \times \text{SD} \quad (7.4)$$

Since SD in Eq. (7.4) is the standard deviation and defines as:

$$SD = \frac{\langle Ag^+ \rangle \times RSD}{100}$$

Where  $\langle Ag^+ \rangle = \frac{\sum [Ag^+]}{p}$  and  $RSD = 0.67(2)^{(1-0.5 \log [Ag^+])}$  based on the work of Boyer et al. [43].

### 7.3.3 Facilitated coupled counter-transport of silver ions across the HFSLM

The pertraction of silver ions using LIX 84-I as extractant involved facilitated coupled counter-transport across HFSLM as shown in Figure 7.1 and is described by the following steps:

- Step 1: Silver ions in the feed phase are transported to the interface between the feed and liquid membrane phases. Then, it reacts with the extractant ( $\overline{HR}$ ) to form the silver-extractant complex ( $\overline{AgR}$ ) as shown in Eq. (7.5) and releases hydrogen ion into the feed phase.
- Step 2: The silver-extractant complex diffuses to the interface between the liquid membrane and stripping phases by its concentration gradient.
- Step 3: The silver-extractant complex reacts with the hydrogen ion and stripping solution ( $(S_2O_3)^{2-}$ ) as shown in Eq. (7.6) to recover silver ion into the stripping phase while the extractant transports back to the opposite side and reacts again with the silver ion in the feed phase. Thus, both silver and hydrogen ions are counter-transported across HFSLM.

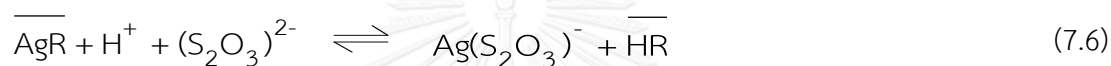
In short, when the diffusion steps in the facilitated transport are slower than the chemical reaction steps, the transport is described as the diffusion transport

regime. On the other hand, when the chemical reaction steps are slower, it is described as the chemical reactions' kinetic transport regime.

Based on the literature expressing the extraction reaction of LIX 84-I with metal ions [35, 44, 45], the extraction reaction of LIX 84-I with silver ion can be concluded as follows:



The recovery reaction of silver ion with the hydrogen ion and sodium thiosulphate solution was considered based on the work of Altin et al. [1] as follows:



The over bar denotes the species in the liquid membrane phase.

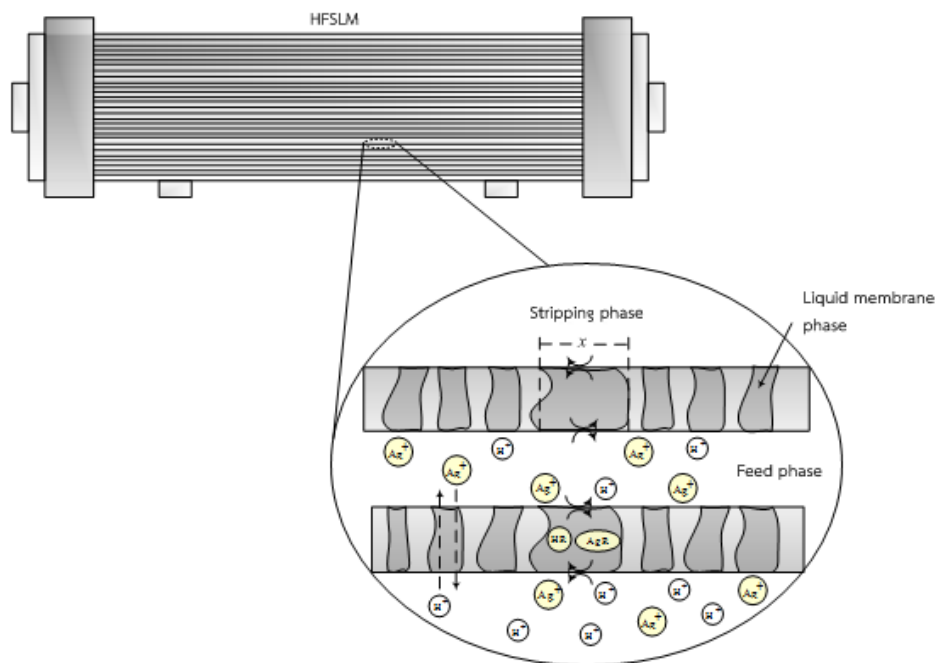


**Figure 7.1** Facilitated coupled counter-transport of silver ions across HFSLM.

The reaction rate of silver ion extraction can be described by Eq. (7.7):

$$r_{-\text{Ag}^+}(x,t) = k_r [\text{Ag}^+(x,t)]^n \quad (7.7)$$

where  $x$  is any distance along the axis of hollow fibers (dm,  $0 \leq x \leq L$ ),  $t$  is the separation time (min),  $k_r$  is the reaction rate constant,  $[\text{Ag}^+(x,t)]$  is the concentration of silver ions as a function of  $x$  and  $t$  (mg/L) and  $n$  is the reaction order.

Since the transport of silver ions from the feed phase to the liquid membrane phase corresponds to the reaction that takes place at the interface, it can be presumed that only the silver-extractant complexes, not silver ions, diffuse across the liquid membrane phase. Thus, the equilibrium constant ( $K_{\text{ex}}$ ) of silver ion extraction by LIX 84-I is determined using Eq. (7.5).

$$K_{\text{ex}} = \frac{[\text{AgR}][\text{H}^+]}{[\text{Ag}^+][\text{HR}]} \quad (7.8)$$

Diffusion flux model for silver ion concentration in feed solution

This section shows the analysis of the diffusion flux model in order to estimate the outlet concentration of silver ions in the feed solution after reacting with LIX 84-I. The flux of silver ions in the feed phase ( $J_f$ ) and the flux of silver-extractant complexes across the liquid membrane phase ( $J_m$ ) are considered as follows:

$$J_f R_f = [\text{Ag}^+]_f - [\text{AgR}]_{f_i} \quad (7.9)$$

$$J_m R_m = [\text{AgR}]_{f_i} - [\text{AgR}]_{r_i} \quad (7.10)$$

where  $R_f$  and  $R_m$  represent the mass transfer resistance in the feed and liquid membrane phases, respectively.  $R_f$  is equal to  $1/k_f$  (min/dm) where  $k_f$  is the mass transfer coefficient in the feed phase.  $[Ag^+]_f$  is the silver ion concentration in the feed phase.  $R_m$  is equal to  $1/k_m$  (min/dm) where  $k_m$  is the mass transfer coefficient of the silver-extractant complexes in the liquid membrane phase. The flux of the silver-extractant complexes correlates with the concentration of silver-extractant complexes at the feed-liquid membrane interface ( $[AgR]_{fi}$ ) and the liquid membrane-stripping interface ( $[AgR]_{si}$ ).

In Eq. (7.10),  $[AgR]_{si}$  can be neglected as regards the assumption of instantaneous reaction between the silver-extractant complexes and the stripping solution. This assumption specifies a rapid change in the silver-extractant complexes to the extractant at the interface between the liquid membrane and stripping phases.

Due to the instantaneous reaction of the silver ions and extractant to form the silver-extractant complexes, this reaction reaches equilibrium at the interface between the feed and liquid membrane phases. Thus,  $[AgR]_{fi}$  is related to the equilibrium constant in Eq. (7.8) and then substituted in Eq. (7.10) as follows:

$$[AgR]_{fi} = \frac{J_m R_m [H^+]}{K_{ex} [HR]} \quad (7.11)$$

From Eqs. (7.9) and (7.11), with the assumption of high driving forces in the liquid membrane phase, the diffusion of the silver-extractant complexes across the liquid membrane phase is fast. Thus, the flux of the silver-extractant complexes is based on the flux of silver ions in the feed phase. As a result, the equation of flux for silver ions can be written as:

$$J_f = \frac{K_{ex} [HR] [Ag^+]}{R_f K_{ex} [HR] + R_m [H^+]} \quad (7.12)$$

The extractant thereby reacts totally with the silver ions to form the silver-extractant complexes when they are at low concentration. Consequently, the concentration of the silver-extractant complexes is equal to the initial extractant concentration ( $\overline{[HR]}_0$ ) and determined by Eqs. (7.8) and (7.9) as follows:

$$\overline{[HR]} = \frac{\overline{[HR]}_0 [H^+]}{K_{ex} [Ag^+]_f} \quad (7.13)$$

Substituting Eq. (7.13) in Eq. (7.12), the flux of silver ions in the feed phase can be rewritten and set in the form as follows:

$$J_f = \frac{R_m [Ag^+]_f + R_f \overline{[HR]}_0 \pm \sqrt{\left( R_m [Ag^+]_f + R_f \overline{[HR]}_0 \right)^2 - 4R_f R_m \overline{[HR]}_0 [Ag^+]_f}}{2R_f R_m} \quad (7.14)$$

Considering Eq. (7.14), we have

$$\sqrt{\left( R_m [Ag^+]_f + R_f \overline{[HR]}_0 \right)^2 - 4R_f R_m \overline{[HR]}_0 [Ag^+]_f} \ll R_m [Ag^+]_f + R_f \overline{[HR]}_0$$

Thus, the term of  $\sqrt{\left( R_m [Ag^+]_f + R_f \overline{[HR]}_0 \right)^2 - 4R_f R_m \overline{[HR]}_0 [Ag^+]_f}$  is neglected and the flux of silver ions becomes

$$J_f = \frac{[Ag^+]_f}{2R_f} + \frac{\overline{[HR]}_0}{2R_m} \quad (7.15)$$

In determining the outlet concentration of silver ions in the feed solution at time  $t$ , the flux of silver ions is considered by the mass balance of silver ions in the feed phase following on the work of Lin and Juang [46] that accounted for a small

amount of copper ions which was extracted every time as the feed solution flowed through the hollow fiber module.

Combining and integrating Eq. (7.15) with the mass balance of silver ions at an initial condition and time  $t$ , the outlet concentration of silver ions in the feed solution,  $[Ag^+]_{f,out}$ , is obtained as follows:

At the initial condition ( $t = 0$ );

$$[Ag^+]_{f,out} = [Ag^+]_0 \quad (7.16)$$

$[Ag^+]_0$  is the initial concentration of silver ions in the feed solution (mg/L);

At time  $t$  ( $t > 0$ );

$$[Ag^+]_{f,out} = -\frac{R_f [HR]_0}{R_m} + \left( [Ag^+]_0 + \frac{R_f [HR]_0}{R_m} \right) \times \exp\left( \frac{-A}{2R_f R_m V_f} t \right) \quad (7.17)$$

To calculate Eq. (7.17), the mass transfer coefficients in the feed phase ( $k_f$ ) and liquid membrane phase ( $k_m$ ) were determined by the equations below.

In principle, the flow of feed solution through the tube side of the hollow fibers is laminar. Hence, the mass transfer coefficient in the feed phase can be determined based on the Sherwood-Graetz correlation as [47]:

$$Sh = mGz^b = \frac{k_f d_i}{D_f} \quad (7.18)$$

where  $Gz = \frac{d_i^2 v}{\nu D_f}$

where  $Sh$  and  $Gz$  are Sherwood number and Graetz number,  $d_i$  is the inside diameter of the hollow fiber,  $\mathcal{D}_f$  is the diffusion coefficient of silver ions in the feed phase as calculated by Eq. (7.19),  $v$  is the linear velocity of the feed solution and both  $m$  and  $b$  are constant values. For the mass diffusion with fast chemical reaction,  $m$  and  $b$  are equal to 1.62 and 0.33, respectively.

The diffusion coefficient of silver ions in the feed phase, which is the wastewater, can be calculated by the Wilke–Chang equation [48] as follows:

$$\mathcal{D}_f = \frac{7.4 \times 10^{-8} (\phi M_w)^{0.5} T}{\eta_w \nu_{Ag^+}^{0.6}} \quad (7.19)$$

where  $\phi$  is the association factor of water (equal to 2.6),  $M_w$  is the molecular weight of water,  $T$  is the temperature of the HFSLM system (equal to 303 K),  $\eta_w$  is the viscosity of water and  $\nu_{Ag^+}$  is the molar volume of silver ions at normal boiling point.

The individual mass transfer coefficient of silver-extractant complexes in the liquid membrane phase can be determined by Eq. (7.20) [27, 49, 50]:

$$k_m = \frac{\varepsilon D_m}{\tau r_i \ln(r_o / r_i)} \quad (7.20)$$

where  $\varepsilon$  and  $\tau$  are the porosity and tortuosity of the micro pores of the hollow fibers,  $r_i$  and  $r_o$  are the inside and outside radii of the hollow fiber and  $\mathcal{D}_m$  is the diffusion coefficient of silver-extractant complexes in the liquid membrane phase as calculated based on Eq. (7.19) that  $\phi$  is equal to 1 for non-associated solvent.

### 7.3.4 Reaction flux model for silver ion concentration in feed solution

The reaction flux model is considered based on the model of Pancharoen et al. [18] in order to estimate the outlet concentration of silver ions in the feed solution. The model is developed by the mass balance of silver ion transport through the hollow fibers as shown in Eq. (7.21):

$$\frac{-Q\partial[\text{Ag}^+(x,t)]}{\partial x} - vr_{-\text{Ag}^+}(x,t) = \frac{v\partial[\text{Ag}^+(x,t)]}{\partial t} \quad (7.21)$$

where  $Q$  is the volumetric flow rate of feed solution ( $\text{dm}^3/\text{min}$ ),  $[\text{Ag}^+(x,t)]$  is the concentration of silver ions in the distance along the axis of hollow fibers at time  $t$  and  $v$  is determined as follows:

$$v = \frac{\varepsilon}{2}(d_o - d_i)$$

where  $\varepsilon$  is the porosity of hollow fibers and  $d_i$  and  $d_o$  are the inside and outside diameters of a hollow fiber and  $0 \leq x \leq L$  which  $L$  is the length of the hollow fiber.

The mass balance in Eq. (7.21) is considered at the initial condition and time  $t$ . For the case of the reaction orders ( $n$ ) is equal to 1, then, the solution of the equation can be expressed as follows:

$$[\text{Ag}^+(x,0)] = e^{\frac{-k_r v}{Q} x} [\text{Ag}^+(0,0)] \quad (7.22-a)$$

$$[\text{Ag}^+(x,t)] = e^{-\alpha} [\text{Ag}^+(0,t - v\tau_0)] \times u(t - v\tau_0) \quad (7.22-b)$$

since  $[Ag^+(x,0)]$  is the concentration of silver ions in the distance along the axis of hollow fibers at initial time,  $[Ag^+(0,0)]$  is the concentration of silver ions in the initial distance at initial time,  $u(t - v\tau_0)$  is the shifting unit step function at lag time ( $\tau_0$ ), and

$$[Ag^+(x,t)] = [Ag^+(x,t)] - [Ag^+(x,0)] \quad (7.22-c)$$

where  $\tau_0 = \frac{x}{Q}$ ,  $\alpha = vk_r\tau_0$

## 7.4 Experimental

### 7.4.1 Pharmaceutical wastewater pretreatment

The feed solution was the wastewater from the pharmaceutical processing and was taken from the quantitative analysis of active-pharmaceutical ingredients like sodium chloride by silver nitrate solution. The feed solution contained 20-30 mg/L of silver ions and 100-120 mg/L of ferric ions. The initial pH of the feed solution was 6. Ferric ions were precipitated by phosphoric acid solution. Then,  $0.35 \text{ mg/dm}^3$  of ferric ions remained in the feed solution. The pH of feed solution was about 4.

### 7.4.2 Chemicals

Cyanex 923 ( $(CH_3(CH_2)_7)_3PO$ , MW = 348 g/mol), D2EHPA ( $C_{16}H_{35}O_4P$ , MW = 322.42 g/mol) and LIX 84-I ( $C_{17}H_{27}NO_2$ , MW = 277.40 g/mol) were used as extractants. The liquid membrane solution was prepared by dissolving the extractant in kerosene. Thiourea ( $CH_4N_2S$ , MW = 76.12 g/mol) and sodium thiosulphate pentahydrate ( $Na_2S_2O_3 \cdot 5H_2O$ , MW = 248.18 g/mol) dissolved in the distilled water was used as stripping solutions. Stock solution of 1,000 mg/L silver ions was used for the standard solution in the analytical process. In addition, both the pH of feed and stripping

solutions were adjusted by nitric acid solution. All chemicals were of analytical grade and were used without any further purification. The source and mass fraction purity of chemicals are listed in Table 7.2.

**Table 7.2** Sources and mass fraction purity of chemicals.

Chemical name	Source	Purity (%)
Cyanex 923	Henkel Thai Ltd.	93
D2EHPA	Cytec Industries Inc.	95
LIX 84-I	Dai-Hachi Chemical Industries Ltd.	100
Thiourea	BrightChem Sdn. Bhd.	99
Sodium thiosulphate pentahydrate	BrightChem Sdn. Bhd.	99.5
Stock solution of silver ions	Ajax Finechem Pty Ltd.	100
Nitric acid solution	BrightChem Sdn. Bhd.	65

### 7.4.3 Apparatus

A laboratory-scale hollow fiber module (Liqui-Cel<sup>®</sup> Extra-flow 2.5 in × 8 in) from Hoechst Celanese was used. The module consisted of micro-porous hydrophobic polypropylene fibers that were woven into fabric and wrapped around a central-tube feeder to supply the stripping solution in the shell side. The properties of the hollow fiber module are shown in Table 7.3. The concentration of silver ions in both feed and stripping solutions were analyzed by the atomic absorption spectrometer (AAS; model AA280FS, Varian, Walnut Creek CA). The pH of the solutions was measured by a BP3001 pH meter (Trans-Instruments, Singapore).

**Table 7.3** Properties of the hollow fiber module.

Property	Description
Material	Polypropylene
Module diameter	0.63 dm
Module length	2.03 dm
Number of hollow fibers	35,000
Inside diameter of a hollow fiber	0.002 dm
Outside diameter of a hollow fiber	0.003 dm
Effective length of a hollow fiber	1.5 dm
Effective surface area of a hollow fiber	140 dm <sup>2</sup>
Area per unit volume	293 dm <sup>2</sup> /dm <sup>3</sup>
Pore size	3 × 10 <sup>-7</sup> dm
Porosity	25%
Tortuosity	2.6

#### 7.4.4 Procedure

The separation time and the different types of solutions including extractants and stripping solutions were applied by liquid-liquid extraction in order to select their optimum condition for use in the HFSLM system. The single-module HFSLM operation is shown in Figure 7.2. The liquid membrane solution of 0.5 dm<sup>3</sup> was simultaneously pumped into the tube and shell sides of the module for 40 min to ensure that it was entirely impregnated in the micro pores of the hollow fibers [51]. The excess liquid membrane solution was rinsed lightly by distilled water. Subsequently, the feed and stripping solutions were fed into the tube and shell sides, respectively. The effects of variables on the pertraction of silver ions were investigated and the effect of ferric ions was also studied. The feed and stripping samples of each experimental condition were kept at 30 min. The concentration of silver ions was analyzed by an atomic absorption spectrometer. The quantitative pertraction of silver ions was determined by the extraction and pertraction efficiencies as shown in Eqs. (7.1) and (7.2). To confirm the efficiency and reliability,

the memory effect reproducibility and repeatability were defined by accurate equations.

In order to determine the controlling transport regime of silver ion pertraction across HFSLM, the mass transfer coefficients in the feed and liquid membrane phases, the reaction order and reaction rate constant were evaluated for use in the diffusion flux and reaction flux models. Results were validated by the experimental results as shown by the percent deviation in Eq. (7.23). Optimal separation time for the appropriate model was estimated.

$$\% \text{ Deviation} = \frac{\sum_{i=1}^j \left( \frac{[\text{Ag}^+]_{\text{Expt.}} - [\text{Ag}^+]_{\text{Theo.}}}{[\text{Ag}^+]_{\text{Expt.}}} \right)_i}{j} \times 100 \quad (7.23)$$

$[\text{Ag}^+]_{\text{Expt.}}$  and  $[\text{Ag}^+]_{\text{Theo.}}$  are the concentration of silver ions in the feed solution that were obtained from the experiments and models, respectively;  $i$  and  $j$  are integer numbers.

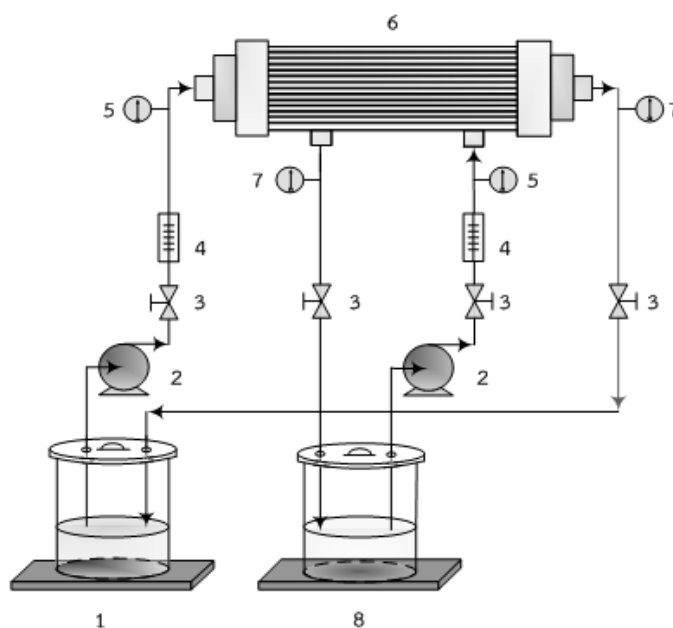


**Figure 7.2** Schematic diagram of a single hollow-fiber module with counter-current circulating flow patterns of feed and stripping solutions: 1) feed reservoir 2) gear pumps 3) gate valves 4) flow meters 5) inlet pressure gauges 6) hollow-fiber module 7) outlet pressure gauges and 8) stripping reservoir.

## 7.5 Results and discussion

### 7.5.1 Effects of extractant types for silver ion extraction

Three extractants including Cyanex 923, D2EHPA and LIX 84-I, which were dissolved in kerosene, were studied by liquid-liquid extraction in order to analyze their effects on silver ion extraction as shown in Figure 7.3. Each extractant of 0.1 M concentration was examined. Results indicated that LIX 84-I was the most suitable extractant. This resulted from the different chemical structures of each extractant for complexation with silver ions.

Based on the chemical reaction of silver ion extraction by LIX 84-I as shown in Eq. (7.5), the nitrogen atom in the molecule of LIX 84-I has a great affinity towards silver ion for bonding with hydrogen atom in its molecule [52]. Thus, LIX 84-I was selected as the extractant for future parameters.

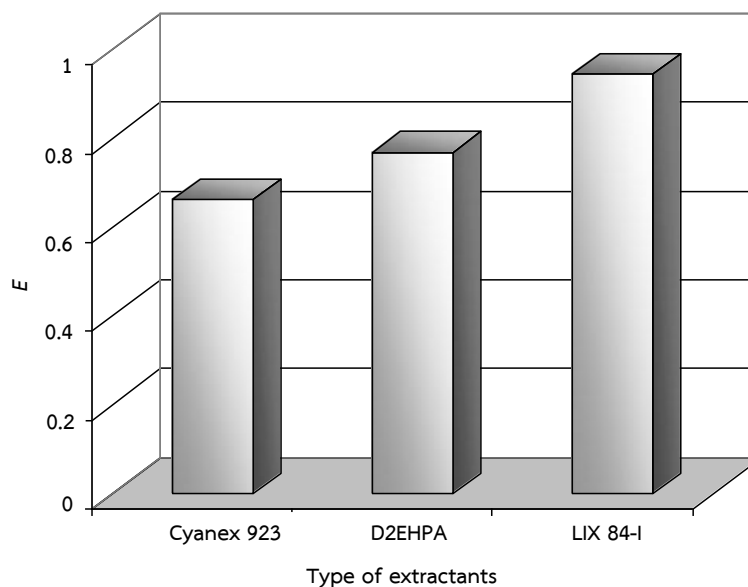


**Figure 7.3** Silver ion extraction ( $E$ ) by liquid-liquid extraction: Cyanex 923, D2EHPA and LIX 84-I dissolving in kerosene at the concentration of each 0.1 M.

### 7.5.2 Effects of stripping types for silver ion recovery

Thiourea ( $\text{CH}_4\text{N}_2\text{S}$ ) and sodium thiosulphate solutions ( $\text{Na}_2\text{S}_2\text{O}_3$ ) were also studied by liquid-liquid extraction in order to analyze their effects on silver ion recovery. The stripping solution of each 0.1 M was examined. Results as shown in Figure 7.4 indicated that sodium thiosulphate solution was the most suitable stripping solution. This corresponded to the results of Altin et al. [1] where sodium thiosulphate solution was used for silver ion recovery due to providing the rapid de-complexation of silver-extractant complex at the liquid membrane-stripping interface. On the other hand, the kinetics of silver ion with thiourea showed a black film which had a negative effect. This resulted in no efficiency for silver ion recovery. Thus, sodium thiosulphate solution was selected as the stripping solution for future parameters.

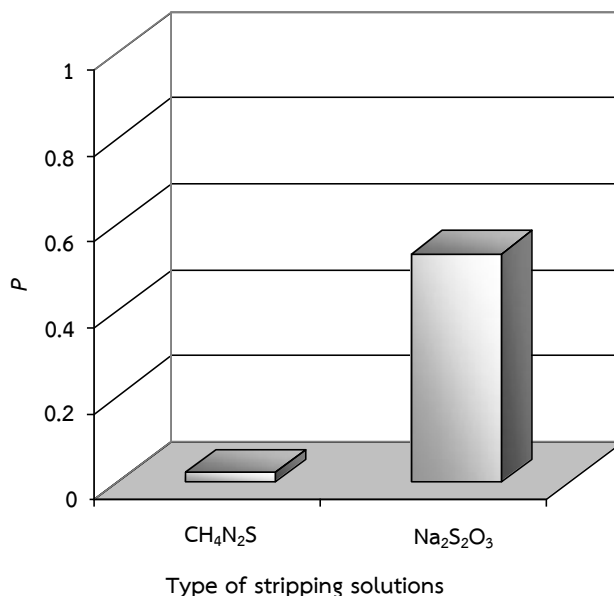


**Figure 7.4** Silver ion pertraction ( $P$ ) by liquid-liquid extraction:  $\text{CH}_4\text{N}_2\text{S}$  and  $\text{Na}_2\text{S}_2\text{O}_3$  solutions with each concentration 0.1 M.

### 7.5.3 Effect of pH feed solution

The pH of feed solution plays an important role in the reaction ability of hydrogen atom in the molecule of an acidic extractant because the acidity of feed solution has a direct effect on the acidity of the extractant. The acidity of an extractant can be expressed by the value  $\text{pK}_a$ . In addition, the acidity gradient between both feed and stripping solutions is required in order to enhance the driving force of hydrogen ions for counter-transport with silver ions across HFSLM. Accordingly, the pH of feed solution was studied as shown in Figure 7.5. The results indicated that the extraction efficiency ( $E$ ) and the pertraction efficiency ( $P$ ) increased when pH of feed solution was increased up to 3.5. However, both efficiencies remained constant when pH of feed solution was higher than 3.5 due to the equilibrium reaction of the extractant with the silver ions at the feed-liquid membrane interface.

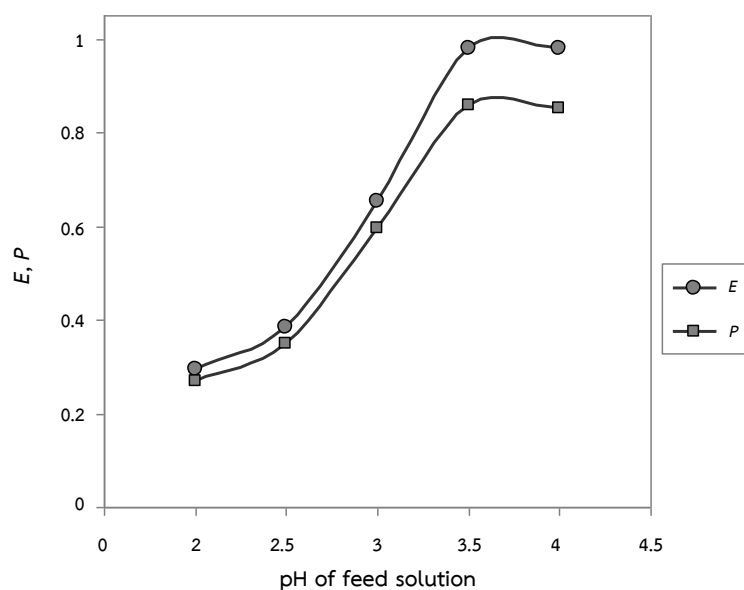


**Figure 7.5** Extraction ( $E$ ) and pertraction ( $P$ ) of silver ions by HFSLM in counter-current circulating flow patterns against pH of feed solution: pH sodium thiosulphate solution of 2; 0.1 M of LIX 84-I concentration; 0.5 M of sodium thiosulphate concentration; equal flow rates of feed and sodium thiosulphate solutions at  $0.2 \text{ dm}^3/\text{min}$ .

#### 7.5.4 Effect of pH stripping solution

The effect of pH stripping solution was studied as shown in Figure 7.6. The extraction ( $E$ ) and pertraction ( $P$ ) efficiencies were constant at pH of 1-2. Thereafter, the results decreased due to a decrease in the hydrogen driving force. In order to select the optimum pH of stripping solution, the pH value of 2 was chosen in order to prevent hard acid corrosion in the HFSLM system.

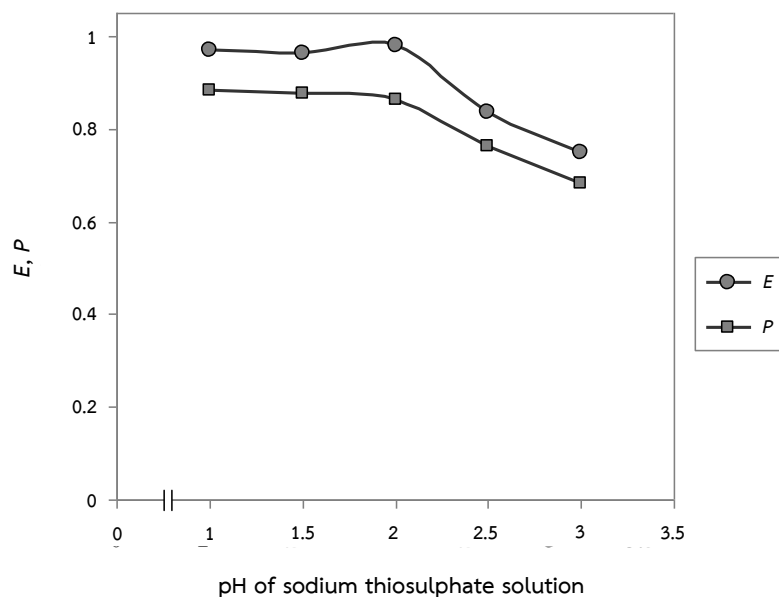


**Figure 7.6** Extraction ( $E$ ) and pertraction ( $P$ ) of silver ions by HFSLM in counter-current circulating flow patterns against pH of sodium thiosulphate solution: pH feed solution of 3.5; 0.1 M of LIX 84-I concentration; 0.5 M of sodium thiosulphate concentration; equal flow rates of feed and sodium thiosulphate solutions at  $0.2 \text{ dm}^3/\text{min}$ .

### 7.5.5 Effect of extractant concentration

In Figure 7.7, the effect of LIX 84-I on silver ion pertraction was studied by varying its concentration. The results indicated that the extraction ( $E$ ) and pertraction ( $P$ ) efficiencies increased when the concentration of LIX 84-I was increased up to 0.1 M. This resulted in an increase of reaction rate of silver ion extraction. However, both efficiencies slightly decreased when the concentration was higher than 0.1 M. This was due to an increase of extractant boundary at the interfaces and/or an increase of the viscosity of the liquid membrane phase.

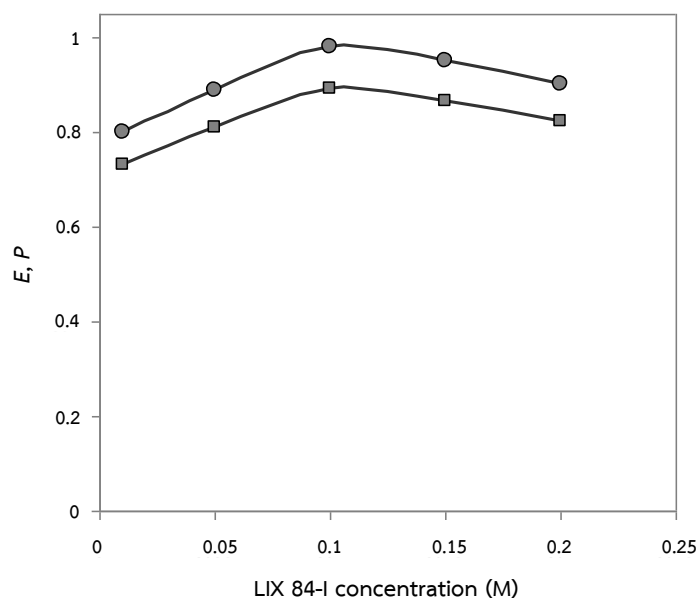


**Figure 7.7** Extraction ( $E$ ) and pertraction ( $P$ ) of silver ions by HFSLM in counter-current circulating flow patterns against the concentration of LIX 84-I: pH feed and pH sodium thiosulphate solutions of 3.5 and 2, respectively; 0.5 M of sodium thiosulphate concentration; equal flow rates of feed and sodium thiosulphate solutions at  $0.2 \text{ dm}^3/\text{min}$ .

### 7.5.6 Effect of stripping concentration

The effect of sodium thiosulphate concentration in the range of 0.1-2 M was studied as shown in Figure 7.8. The extraction ( $E$ ) and pertraction ( $P$ ) efficiencies increased when the concentration was increased to 0.5 M. Thereafter, results proved constant. This implied that maximum concentration of sodium thiosulphate solution for reaction with the silver-extractant complex was 0.5 M.

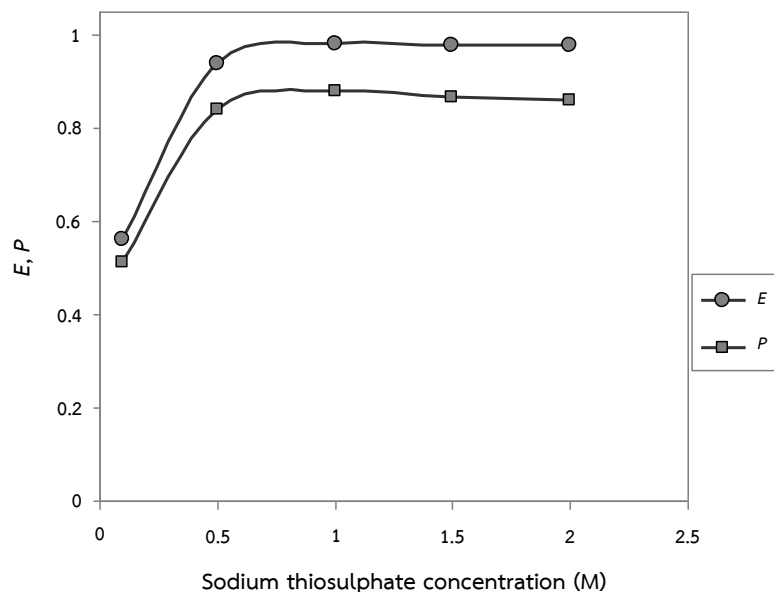


**Figure 7.8** Extraction ( $E$ ) and pertraction ( $P$ ) of silver ions by HFSLM in counter-current circulating flow patterns against the concentration of sodium thiosulphate solution: pH feed and pH sodium thiosulphate solutions of 3.5 and 2, respectively; 0.1 M of LIX 84-I concentration; equal flow rates of feed and sodium thiosulphate solutions at  $0.2 \text{ dm}^3/\text{min}$ .

### 7.5.7 Effects of flow rates of feed and stripping solutions

The effects of feed and stripping flow rates were studied in the range of  $0.2\text{--}1 \text{ dm}^3/\text{min}$  as shown in Figure 7.9. The extraction ( $E$ ) and pertraction ( $P$ ) efficiencies decreased rapidly when the flow rates were increased to  $1 \text{ dm}^3/\text{min}$ . The increase of flow rates yielded less resident time for reactions in the hollow fiber module. Where flow rates were lower than  $0.2 \text{ dm}^3/\text{min}$ , Altin et al. [1] reported that their effects yielded low extraction of silver ions in a flat-sheet supported liquid membrane.

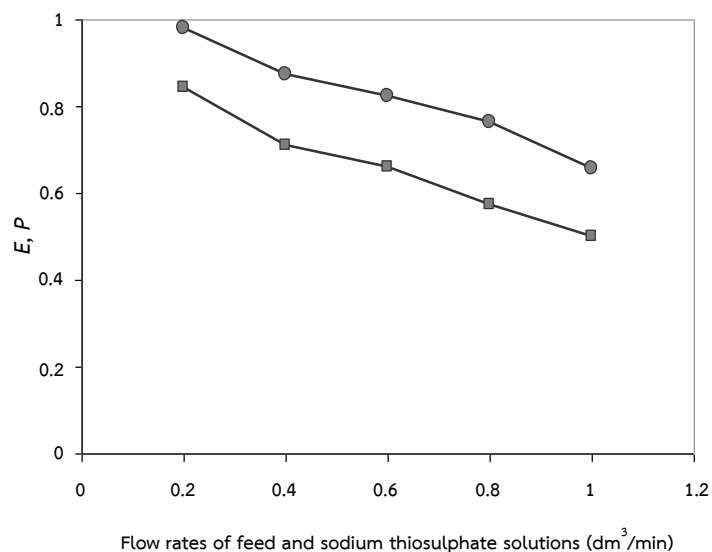


**Figure 7.9** Extraction ( $E$ ) and pertraction ( $P$ ) of silver ions by HFSLM in counter-current circulating flow patterns against the flow rates of feed and sodium thiosulphate solutions: pH feed and pH sodium thiosulphate solutions of 3.5 and 2, respectively; 0.1 M of LIX 84-I concentration; 0.5 M of sodium thiosulphate concentration.

### 7.5.8 Effects of flow directions between feed and stripping solutions

In Figure 7.10, the effect of co-current and counter-current flows between the feed and stripping solutions were studied. The results indicated that counter-current flow can achieve higher extraction and recovery rates of silver ions than the co-current flow. This was because of the higher stability of concentration gradients of silver and hydrogen ions between the feed and stripping phases. However, the co-current flow resulted in a reduction of silver ion transport. This was due to the decrease of concentration gradients of silver and hydrogen ions between both aqueous phases [53].

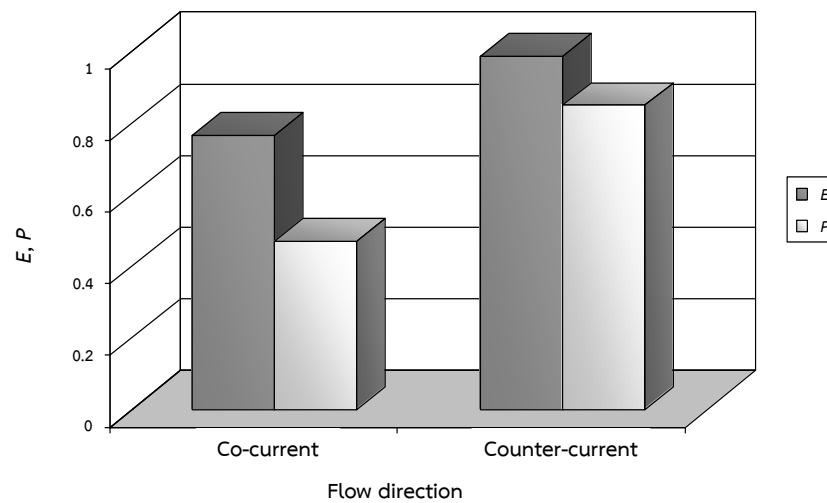


**Figure 7.10** Extraction ( $E$ ) and pertraction ( $P$ ) of silver ions by HFSLM in circulating flow patterns against the flow direction: pH feed and pH sodium thiosulphate solutions of 3.5 and 2, respectively; 0.1 M of LIX 84-I concentration; 0.5 M of sodium thiosulphate concentration; equal flow rates of feed and sodium thiosulphate solution at  $0.2 \text{ dm}^3/\text{min}$ .

### 7.5.9 Effects of flow patterns of feed and stripping solutions

The effect of three patterns of feed and stripping flows in the HFSLM system i.e. single-pass flows of feed and stripping solutions, circulating flows of feed and stripping solutions as well as single-pass flow of feed solution and circulating flow of stripping solution were studied as shown in Figure 7.11. The results indicated that the highest extraction ( $E$ ) and pertraction ( $P$ ) efficiencies were achieved by the circulating flows of both feed and stripping solutions. According to Alizadeh et al. [54], the pertraction of precious metals by solvent extraction was relatively the slow chemical reactions. This required long resident times. Thus, the circulating flows of feed and stripping solutions through HFSLM were appropriate.

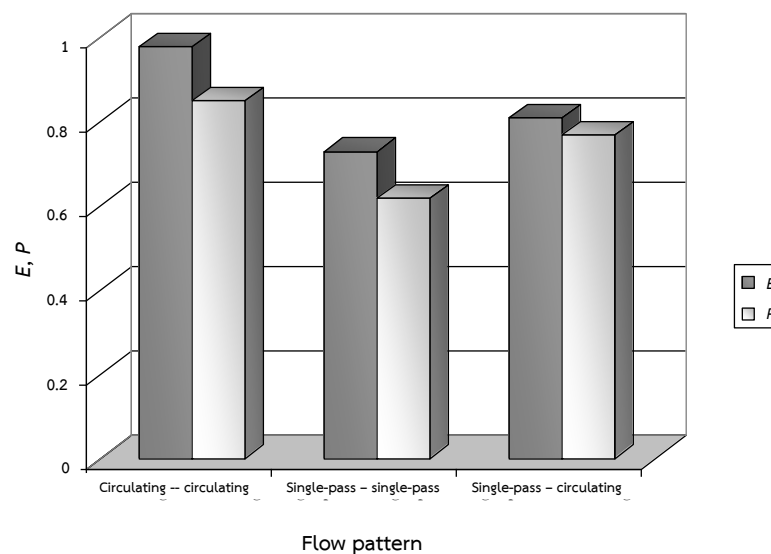


**Figure 7.11** Extraction ( $E$ ) and pertraction ( $P$ ) of silver ions by HFSLM in counter-current flow directions against the flow pattern: pH feed and pH sodium thiosulphate solutions of 3.5 and 2, respectively; 0.1 M of LIX 84-I concentration; 0.5 M of sodium thiosulphate concentration; equal flow rates of feed and sodium thiosulphate solutions at  $0.2 \text{ dm}^3/\text{min}$ .

#### 7.5.10 Effect of ferric ion presence on silver ion pertraction

The effect of ferric ions on the pertraction of silver ions was studied by using wastewater containing 100 mg/L of ferric ions. The results were compared with the case of ferric ion precipitation as shown in Figure 7.12. The extraction ( $E$ ) and pertraction ( $P$ ) efficiencies in the case of ferric ion presence were 0.96 and 0.82, respectively. In the case of ferric ion precipitation, both values were higher viz. 0.98 and 0.85. This resulted from the small disturbance of ferric ions whereby hydrogen ions were interchanged with both silver and ferric ions at pH of feed solution higher than 1.5 [55]. However, the extraction of silver ions by LIX 84-I was faster than the extraction of ferric ions because the silver ions wanted to share one electron with LIX 84-I to form eight electrons in its valence shell. For ferric ions, they wanted to share three electrons. This corresponded to the octet rule. Furthermore, the remaining amounts of silver ions in both cases were less than the mandatory

discharge limit. Thus, the presence of ferric ions in the wastewater had no effect on the silver ion pertraction.

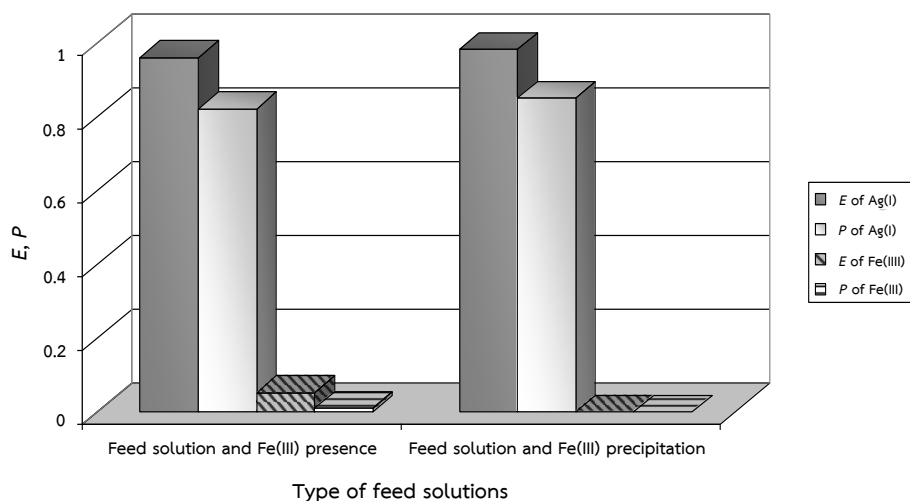


**Figure 7.12** Effect of ferric ions in wastewater on silver ion pertraction by HFSLM: pH of wastewater in ferric ion presence and ferric ion precipitation of 6 and 3.5; pH sodium thiosulphate solution of 2; 0.1 M of LIX 84-I concentration; 0.5 M of sodium thiosulphate concentration; equal flow rates of feed and sodium thiosulphate solutions at  $0.2 \text{ dm}^3/\text{min}$ .

### 7.5.11 Memory effect and repeatability

The memory effect was considered under optimum experimental conditions and determined by Eq. (7.3). The proposed value was 0.13. This indicated that a small amount of complex species remained in the liquid membrane phase. This may be due to the fact that the strong complexation between the metal ions and extractant resulted in the slow rate of de-complexation between the silver-extractant complex and stripping solution [16]. The repeatability of the HFSLM system was validated by repeating the experiments 3 times under optimum conditions. 3 analyses were carried out on the same sample of outlet feed solution. The repeatability value of 1.02% was calculated based on Eq. (7.4) where the RSD and SD values were 1.707

and 0.004, respectively. These results proved to be less than the standard precision of analytical quality assurance (AQA,  $\leq 5\%$ ) [42]. Thus, it can be concluded that HFSLM is an efficient and reliable system for the pertraction of silver ions.

#### 7.5.12 Controlling transport regime for silver ion pertraction across the HFSLM

Reaction flux and diffusion flux models were considered in order to determine the outlet concentration of silver ions. The reaction rate constant ( $k_r$ ) of  $0.164 \text{ min}^{-1}$ , as seen in the reaction flux model, was obtained from the first-order reaction. This provided the best curve fitting in with the experimental data. As regards the parameters used in the diffusion flux model, the mass transfer coefficients of silver ions in the feed phase ( $k_f$ ) and across the liquid membrane phase ( $k_m$ ) were determined by Eqs. (7.18) and (7.20), respectively. Their values were 0.063 and 2.179 dm/min. Other parameters are shown in Table 7.4. The results of the two above models were compared with the experimental results as shown in Figure 7.13. The reaction flux model was in good agreement with the experimental results showing 2% deviation. This result was better than the diffusion flux model which showed a deviation of 25%. This was attributed to the efficiency of the reaction flux model. It also indicated that the rate of chemical reactions were slower than the rate of diffusions. Thus, the transport of silver ions was controlled by the chemical reactions at the liquid membrane interfaces. In addition, these results confirmed the facilitated transport mechanism of silver ions. The unsatisfactory results of the diffusion flux model occurred because of the neglectful consideration of chemical reactions.

**Table 7.4** The relevant parameters used in the models.

Parameter	Value
$A$ ( $\text{dm}^2$ )	1.4
$[\text{Ag}^+ (0,0)]$ ( $\text{mg}/\text{dm}^3$ )	30
$k_f$ ( $\text{dm}/\text{min}$ )	0.063
$k_m$ ( $\text{dm}/\text{min}$ )	2.179
$k_r$ ( $\text{min}^{-1}$ )	0.164
$L$ ( $\text{dm}$ )	1.5
$n$	1
$Q$ ( $\text{dm}^3/\text{min}$ )	0.2
$R_f$ ( $\text{min}/\text{dm}$ )	15.873
$R_m$ ( $\text{min}/\text{dm}$ )	0.459
$V_f$ ( $\text{dm}^3$ )	0.5
$\tau_0$ ( $\text{min}$ )	1.185

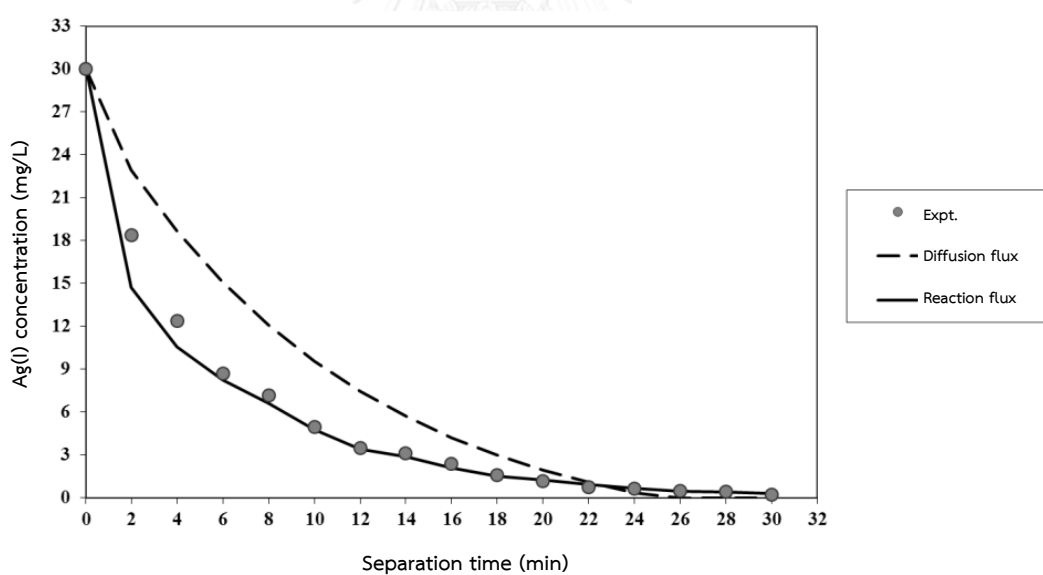


**Figure 7.13** Concentration of silver ions in HFSLM system with respect to diffusion flux and reaction flux models at different separation times: counter-current flow directions, pH feed and pH sodium thiosulphate solutions of 3.5 and 2, respectively; 0.1 M of LIX 84-I concentration; 0.5 M of sodium thiosulphate concentration; equal flow rates of feed and sodium thiosulphate solutions at  $0.2 \text{ dm}^3/\text{min}$ .

### 7.5.12 Optimization of separation time

Since the mandatory discharge limit of silver ions in industrial wastewaters must not exceed  $1.0 \text{ mg/dm}^3$ , an optimal separation time was necessary to meet the permissible concentration. From Figure 7.13, the estimated separation time of 26 min resulted in  $0.6 \text{ mg/L}$  of silver ion concentration which proved to be lower than the mandatory discharge limit.

## 7.6 Conclusion

HFSLM was an efficient and reliable system for the pertraction of silver ions from pharmaceutical wastewater at the low concentration level to meet the mandatory discharge limit. LIX 84-I was successful in extracting silver ions from the impurities of ferric ions. The highest extraction and pertraction efficiencies of 0.98 and 0.85 were achieved by pH values for both feed and stripping solutions of 3.5 and 2, respectively with units of concentration viz.  $0.1 \text{ M}$  LIX 84-I and  $0.5 \text{ M}$  sodium thiosulphate solution at equal flow rates of  $0.2 \text{ dm}^3/\text{min}$ . Again, the circulating flow patterns of feed and stripping solutions which were fed counter-currently in the hollow fiber module proved suitable. In conclusion, the transport of silver ions across HFSLM was mainly controlled by the rates of slow chemical reactions as shown by the average percent deviations of 2% (reaction flux model) and 25% (diffusion flux model). The separation time of 26 min resulted in a lower amount of silver ions being discharged than the mandatory limit.

## 7.7 Nomenclature and units

$A$	effective surface area of the hollow fibers ( $\text{dm}^2$ )
$b$	parameter in Eq. (7.18)
$d_i$	inside diameter of the hollow fiber

$d_o$	outside diameter of the hollow fiber
$E$	extraction efficiency
$F$	parameter in Eq. (7.3)
Gz	Graetz number
$i, j$	integer numbers
$J$	flux of silver ions ( $\text{mg}/\text{dm}^2 \cdot \text{min}$ )
$K_{ex}$	equilibrium constant ( $\text{dm}^3/\text{mg}$ )
$k_f$	mass transfer coefficient of silver ions in the feed phase ( $\text{dm}/\text{min}$ )
$k_m$	mass transfer coefficient of complex species across liquid membrane phase ( $\text{dm}/\text{min}$ )
$k_r$	reaction rate constant ( $\text{min}^{-1}$ )
$L$	length of a hollow fiber ( $\text{dm}$ )
$M$	memory effect
$M_w$	molecular weight of water ( $\text{mg}/\text{mol}$ )
$m$	parameter in Eq. (7.18)
$n$	reaction order of extraction reaction
$n_f$	silver ion amount in the feed phase ( $\text{mg}/\text{dm}^3$ )
$n_r$	silver ion amount in the stripping phase ( $\text{mg}/\text{dm}^3$ )
$n_w$	silver ion amount the wastewater after contact with the liquid membrane phase ( $\text{mg}/\text{dm}^3$ )
$P$	pertraction efficiency
$p$	number of repeated analysis
$Q$	volumetric flow rate of feed solution ( $\text{dm}^3/\text{min}$ )
$R$	mass transfer resistance ( $\text{min}/\text{dm}$ )
RSD	relative standard deviation
$r_{-\text{Ag}^+}$	reaction rate of silver ion extraction ( $\text{mg}/\text{dm}^3 \cdot \text{min}$ )
$r_i$	inside radius of the hollow fiber ( $\text{dm}$ )
$r_o$	outside radius of the hollow fiber ( $\text{dm}$ )
SD	standard deviation
Sh	Sherwood number

$T$	temperature of the HFSLM system (K)
$t$	separation time (min)
$v$	linear velocity of the feed solution (dm/min) or the parameter in reaction flux model
$x$	any distance along the axis of hollow fibers (dm)

#### *Greek letters*

$\alpha$	a constant in Eq. (7.22-b)
$\varepsilon$	porosity of the hollow fibers (%)
$\tau$	tortuosity of the micro pores of hollow fibers
$\tau_0$	a constant in Eq. (7.22-b)
$\eta_w$	viscosity of water (cP)

#### *Symbols*

$[\ ]$	concentration
$\langle \rangle$	average value
$-$	species in liquid membrane phase or difference of outlet concentrations of silver ions as considering at time $t$ and initial time in Eqs. (7.22-b) and (7.22-c).
$\varphi$	association factor of water
$\mathcal{D}$	diffusion coefficient of silver ions (dm <sup>2</sup> /min)
$v_{Ag^+}$	molar volume of silver ions at normal boiling point

#### *Subscripts*

$Ag^+$	silver ions
Expt.	experimental results
f	feed phase

f, in	inlet concentration of silver ions in the feed phase
f, out	outlet concentration of silver ions in the feed phase
fi	interface between feed and liquid membrane phases
m	liquid membrane phase
ri	interface between liquid membrane and stripping phases
Theo.	modeling results
w	water
0	initial concentration

## 7.8 Acknowledgements

The authors highly acknowledge financial supports by Thailand Research Fund and Chulalongkorn University under the Royal Golden Jubilee Ph.D. (Grant No. PHD/0272/2549). Sincere thanks also go to Asst. Prof. Dr. Prakorn Ramakul (Faculty of Engineering and Industrial Technology, Silpakorn University) and Asst. Prof. Dr. Natchanun Leepipatpiboon (Faculty of Science, Chulalongkorn University) as well as the Government Pharmaceutical Organization of Thailand and the Separation Laboratory, Department of Chemical Engineering, Chulalongkorn University, Bangkok, Thailand.

## 7.9 References

- [1] S. Altin, Y. Yildirim, A. Altin, Transport of silver ions through a flat-sheet supported liquid membrane, *Hydrometallurgy* 103 (2010) 144-149.
- [2] M.A. Chaudry, N. Bukhari, M. Mazhar, Coupled transport of Ag(I) ions through triethanolamine-cyclohexanone-based supported liquid membranes, *Journal of Membrane Science* 320 (2008) 93-100.
- [3] S.W.P. Wijnhoven, W.J.G.M. Peijnenburg, C.A. Herberts, W.I. Hagens, A.G. Oomen, E.H.W. Heugens, J. Bisschops, I. Gosens, D. van de Meent, S. Dekkers, W.H. de Jong, M. van Zijverden, A.J.A.M. Sips, R.E. Geertsma, Nano-silver-a review of

- available data and knowledge gaps in human and environment risk assessment, *Nanotoxicology* 3(2), (2009) 109-138.
- [4] Y.M. Sue, Y.Y. Lee, M.C. Wang, T.K. Lin, J.M. Sung, J.J. Huang, Generalized Argyria in two chronic hemodialysis patients, *American Journal of Kidney Diseases* 37(5) (2001) 1048-1051.
- [5] Announcement of the Industrial Estate Authority of Thailand, 1998. Effluent from Factory to Central Wastewater Treatment Plant Amata Nakorn and Amata City Industrial Estate: Last Revised: November 11, 1998. ([http://www.amatawater.com/upload/waterlawfile/26\\_Discharge%20from%2031-3-11.pdf](http://www.amatawater.com/upload/waterlawfile/26_Discharge%20from%2031-3-11.pdf); last accessed 5 January 2012).
- [6] N. Othman, H. Mat, M. Goto, Separation of silver from photographic wastes by emulsion liquid membrane system, *Journal of Membrane Science* 282 (2006) 171-177.
- [7] P.V. Vernekar, Y.D. Jagdale, A.W. Patwardhan, A.V. Patwardhan, S.A. Ansari, P.K. Mohapatra, V.K. Manchanda, Transport of cobalt(II) through a hollow fiber supported liquid membrane containing di-(2-ethylhexyl) phosphoric acid (D2EHPA) as the carrier, *Chemical Engineering Research and Design* 91 (2012) 141-157.
- [8] K.F. Lam, C.M. Fong, K.L. Yeung, G. McKay, Selective adsorption of gold from complex mixtures using mesoporous adsorbents, *Chemical Engineering Journal* 145 (2008) 185-195.
- [9] J. Lv, Q. Yang, J. Jiang, T.S. Chung, Exploration of heavy metal ions transmembrane flux enhancement across a supported liquid membrane by appropriate carrier selection, *Chemical Engineering Science* 62 (2007) 6032-6039.
- [10] Q. Yang, T.S. Chung, , Y. Xiao, K. Wang, The development of chemically modified P84 Co-polyimide membranes as supported liquid membrane matrix for Cu(II) removal with prolonged stability, *Chemical Engineering Science* 62 (2007) 1721-1729.
- [11] J. Markoš, *Mass Transfer in Chemical Engineering Processes*, InTech Open Access Publisher, Rijeka, Croatia, 2011,

- [12] A. Seidl, M. Bickford, K. Othmer, *Chemical Technology and the Environment*, John Wiley & Sons Inc, New Jersey, USA, 2007.
- [13] N.S. Rathore, J.V. Sonawane, A. Kumar, A.K. Venugopalan, R.K. Singh, D.D. Bajpai, J.P. Shukla, Hollow fiber supported liquid membrane: a novel technique for separation and recovery of plutonium from aqueous acidic wastes, *Journal of Membrane Science* 189 (2001) 119-128.
- [14] F. Valenzuela, C. Basualto, C. Tapia, J. Sapag, Application of hollow fiber supported liquid membranes technique to the selective recovery of a low content of copper from a Chilean mine water, *Journal of Membrane Science* 155 (1999) 163-168.
- [15] M. Szpakowska, O.B. Nagy, Stability of supported liquid membranes containing Acorga P-50 as carrier, *Journal of Membrane Science* 129 (1997) 251-261.
- [16] P. Dzygiel, P.P. Wieczorek, *Liquid Membranes: Principles and Applications in Chemical Separations and Wastewater Treatment*, first ed. Elsevier, The Netherlands, 2010.
- [17] C. Yang, E.L. Cussler, Reaction dependent extraction of copper and nickel using hollow fibers, *Journal of Membrane Science* 166 (2000) 229-238.
- [18] U. Pancharoen, T. Wongsawa, A.W. Lothongkum, A reaction flux model for extraction of Cu(II) with LIX 84-I in HFSLM, *Separation Science and Technology* 46 (2011) 2183-2190.
- [19] X.J. Yang, A.G. Fane, C. Pin, Separation of zirconium and hafnium using hollow fibers part I. supported liquid membranes, *Chemical Engineering Journal* 88 (2002) 37-44.
- [20] C. Fontàs, M. Hidalgo, V. Salvado, E. Antico, Selective recovery and preconcentration of mercury with a benzoylthiourea-solid supported liquid membrane system, *Analytica Chimica Acta* 547 (2005) 255-261.
- [21] J. Peng, R. Liu, J. Liu, B. He, X. Hu, G. Jiang, Ultrasensitive determination of cadmium in seawater by hollow fiber supported liquid membrane extraction coupled with graphite furnace atomic absorption spectrometry, *Spectrochimica Acta Part B* 62 (2007) 499-503.

- [22] R. Güell, E. Anticó, V. Salvadó, C. Fontàs, Efficient hollow fiber supported liquid membrane system for the removal and preconcentration of Cr(VI) at trace levels, *Separation and Purification Technology* 62 (2008) 389-393.
- [23] A.W. Lothongkum, Y. Khemglad, N. Usomboon, U. Pancharoen, Selective recovery of nickel ions from wastewater of stainless steel industry via HFSLM, *Journal of Alloys and Compounds* 476 (2009) 940-949.
- [24] A.W. Lothongkum, P. Ramakul, W. Sasomsub, S. Laoharochanapan, U. Pancharoen, Enhancement of uranium ion flux by consecutive extraction via hollow fiber supported liquid membrane, *Journal of the Taiwan Institute of Chemical Engineers* 40 (2009) 518-523.
- [25] U. Pancharoen, S. Somboonpanya, S. Chaturabul, A.W. Lothongkum, Selective removal of mercury as  $\text{HgCl}_4^{2-}$  from natural gas well produced water by TOA via HFSLM, *Journal of Alloys and Compounds* 489 (2010) 72-79.
- [26] A.W. Lothongkum, S. Suren, S. Chaturabul, N. Thamphiphit, U. Pancharoen, Simultaneous removal of arsenic and mercury from natural-gas-co-produced water from the Gulf of Thailand using synergistic extractant via HFSLM, *Journal of Membrane Science* 369 (2011) 350-358.
- [27] D. Buachuang, P. Ramakul, N. Leepipatpiboon, U. Pancharoen, Mass transfer modeling on the separation of tantalum and niobium from dilute hydrofluoric media through a hollow fiber supported liquid membrane, *Journal of Alloys and Compounds* 509 (2011) 9549-9557.
- [28] P. Kandwal, S.A. Ansari, P.K. Mohapatra, Transport of cesium using hollow fiber supported liquid membrane containing calix[4]arene-bis(2,3 naphtho)crown-6 as the carrier extractant: part II. recovery from simulated high level waste and mass transfer modeling, *Journal of Membrane Science* 384 (2011) 37-43.
- [29] M. Younas, S. Druon-Bocquet, J. Sanchez, Experimental and theoretical mass transfer transient analysis of copper extraction using hollow fiber membrane contactors, *Journal of Membrane Science* 382 (2011) 70-81.

- [30] P. Kittisupakorn, W. Weerachaipichaskul, P. Thitiyasook, Modeling and simulation of copper-ion extraction with hollow fiber supported liquid membrane, *Journal of Industrial and Engineering Chemistry* 13 (2007) 903-910.
- [31] P. Ramakul, W. Pattaweekongka, U. Pancharoen, Mass transfer modeling of membrane carrier system for extraction of Ce(IV) from sulfate media using hollow fiber supported liquid membrane, *Korean Journal of Chemical Engineering* 23(1) (2006) 85-92.
- [32] K. Soldenhoff, M. Shamieh, A. Manis, Liquid-liquid extraction of cobalt with hollow fiber contactor, *Journal of Membrane Science* 252 (2005) 183-194.
- [33] A. Kumar, R. Haddad, F.J. Alguacil, A.M. Sastre, Comparative performance of non-dispersive solvent extraction using a single module and the integrated membrane process with two hollow fiber contactors, *Journal of Membrane Science* 248 (2005) 1-14.
- [34] B. Tang, G. Yu, J. Fang, T. Shi, Recovery of high-purity silver directly from dilute effluents by an emulsion liquid membrane-crystallization process, *Journal of Hazardous Materials* 177 (2010) 377-383.
- [35] M.V. Rane, V. Venugopal, Study on the extraction of palladium(II) and platinum(IV) using LIX 84-I, *Hydrometallurgy* 84 (2006) 54-59.
- [36] J.Y. Lee, J.K. Rajesh, J.S. Kim, H.K. Park, H.S. Yoon, Liquid-liquid extraction/separation of platinum(IV) and rhodium(III) from acidic chloride solutions using tri-iso-octylamine, *Journal of Hazardous Materials* 168 (2009) 424-429.
- [37] F.J. Alguacil, A.G. Coedo, M.T. Dorado, I. Padilla, Phosphine oxide mediate transport: modeling of mass transfer in supported liquid membrane transport of gold(III) using Cyanex 923, *Chemical Engineering Science* 56 (2001) 3115-3122.
- [38] O.N. Ata, The selective transport of copper ion through supported liquid membrane, *Chemical and Biochemical Engineering Quarterly* 19(1) (2005) 25-30.
- [39] R.D. Noble, S.A. Stern, *Membrane Separations Technology: Principles and Applications*, Elsevier, London, 1995.

- [40] J. Doležal, C. Moreno, A. Hrdlička, M. Valiente, Selective transport of lanthanides through supported liquid membranes containing non-selective extractant, di-(2-ethylhexyl)phosphoric acid, as a carrier, *Journal of Membrane Science* 168 (2000) 175-181.
- [41] K. Kumrić, J. Dordević, G. Vladisavjević, T. Trtić-Petrović, Pertraction of Lu(III) in a hollow fiber contactor, CHISA: 20th International Congress on Chemical and Process Engineering, Prague, Czech Republic, 25th-29th August, 2012, p. 2.
- [42] I. Taverniers, M. de Loose, E. van Bockstaele, Trends in quality in the analytical laboratory: II analytical method validation and quality assurance, *Trends in Analytical Chemistry* 23(8) (2004) 535-552.
- [43] K.W. Boyer, W. Horwitz, R. Albert, Interlaboratory variability in trace element analysis, *Analytical Chemistry* 57 (1985) 454-459.
- [44] B. Sengupta, M.S. Bhakhar, R. Sengupta, Extraction of zinc and copper-zinc mixtures from ammoniacal solutions into emulsion liquid membranes using LIX 84-I, *Hydrometallurgy* 99 (2009) 25-32.
- [45] P.K. Parhi, K. Sarangi, Separation of copper, zinc, cobalt and nickel ions by supported liquid membrane technique using LIX 84-I, TOPS-99 and Cyanex 272, *Separation and Purification Technology* 59 (2008) 169-174.
- [46] S.H. Lin, R.S. Juang, Mass-transfer in hollow-fiber modules for extraction and back-extraction of copper(II) with LIX 64-N carriers, *Journal of Membrane Science* 188 (2001) 251-262.
- [47] N.M. Kocherginsky, Q. Yang, L. Seelam, Recent advances in supported liquid membrane technology, *Separation and Purification Technology* 53 (2007) 171-177.
- [48] C.R. Wilke, P. Chang, Correlation of diffusion coefficients in dilute solutions, *AIChE Journal* 1(2) (1955) 264-270.
- [49] R.S. Juang, H.L. Huang, Mechanistic analysis of solvent extraction of heavy metals in membrane contactors, *Journal of Membrane Science* 213 (2003) 125-135.

- [50] Q. Yang, N.M. Kocherginsky, Copper removal from ammoniacal wastewater through a hollow fiber supported liquid membrane system: modeling and experimental verification, *Journal of Membrane Science* 297 (2007) 121-129.
- [51] P. Ramakul, K. Nakararueng, U. Pancharoen, One-through selective separation of copper, chromium and zinc ions by hollow fiber supported liquid membrane, *Korean Journal of Chemical Engineering* 21(6) (2004) 1212-1217.
- [52] A.A. Amiri, A. Safavi, A.R. Hasaninejad, H. Shrghi, M. Shamsipur, Highly selective transport of silver ion through a supported liquid membrane using calix[4]pyrroles as suitable ion carriers, *Journal of Membrane Science* 325 (2008) 295-300.
- [53] S.S. Madaeni, M. Aminnejad, G. Zahedi, A mathematical method to study CO<sub>2</sub>-CH<sub>4</sub> separation in a hollow fiber module, *Indian Journal of Chemical Technology* 17 (2010) 274-281.
- [54] N. Alizadeh, S. Salimi, A. Jabbari, Transport study of palladium through a bulk liquid membrane using hexadecylpyridinium as carrier, *Separation and Purification Technology* 28 (2002) 173-180.
- [55] C.R. Merigold, LIX reagent solvent extraction plant operating manual for small and medium size leach-solvent extraction-electro wining copper recovery operations: Last Revised: August, 1996 (<http://www.performancechemicals.basf.com>; last accessed 22 May 2012).

## Chapter VIII

### Fluid-flow models operating on linear algebra for extraction and recovery of silver ions from pharmaceutical wastewater by HFSLM

Thidarat Wongsawa<sup>a</sup>, Natchanun Leepipatpiboon<sup>b</sup>, Nopphawat Thamphiphit<sup>a</sup>,  
Ura Pancharoen<sup>a</sup>, Anchaleeporn Waritswat Lothongkum<sup>c</sup>

<sup>a</sup> *Department of Chemical Engineering, Faculty of Engineering, Chulalongkorn University, Phyathai Rd., Bangkok 10330, Thailand*

<sup>b</sup> *Chromatography and Separation Research Unit, Department of Chemistry, Faculty of Science, Chulalongkorn University, Patumwan, Bangkok 10330, Thailand*

<sup>c</sup> *Department of Chemical Engineering, Faculty of Engineering, King Mongkut's Institute of Technology Ladkrabang, Chalongsong Rd., Bangkok 10520, Thailand*

---

This article has been published in journal: Chemical Engineering Journal.

Page: 361-373. Volume: 222. Year: 2013.

---

## 8.1 Abstract

The extraction and recovery of silver ions by hollow fiber supported liquid membrane (HFSLM) was examined. Pharmaceutical wastewater containing 30 mg/L of silver ions was used as the feed solution. LIX 84-I dissolved in kerosene, and sodium thiosulfate solution were used as the liquid membrane and stripping solution, respectively. The influences of several variables on the extraction and recovery of silver ions were investigated. Fluid-flow models for greater accuracy in describing the transport of silver ions from feed phase to stripping phase were developed. The models were calculated by linear algebra. The investigated parameters in the models were axial convections and axial diffusions on both sides, chemical reactions at the feed-liquid membrane and liquid membrane-stripping interfaces as well as the accumulation of silver ions in the system. The mass transfer coefficient in the liquid membrane ( $k_m$ ) was determined for use in the models. The final predicted concentrations of silver ions in feed and stripping phases were successfully in agreement with the experimental data. It indicates that the fluid-flow model can accurately estimate the transport of silver ions inside and outside the hollow fibers corresponding to the axial convections, axial diffusions, reactions at the feed-liquid membrane and liquid membrane-stripping interfaces. In accordance with this investigation, the HFSLM shows a practical implication for the use in pharmaceutical wastewater treatment.

**Keywords:** Fluid-flow; Linear algebra; Silver ions; Pharmaceutical wastewater; HFSLM.

## 8.2 Introduction

The presence of silver ions in the environment is of great concern because silver ions are toxic and non-biodegradable. Only 1-5 mg/L concentration of silver ions can kill aquatic microorganisms, insects, trout and flounder [1]. It is noted that the major

sources of silver ions in the environment are wastewaters from the manufacturing of electronics, silverware and jewelry as well as wastewaters from photographic-imaging industry, particularly from the medical processes [2, 3]. In Thailand, wastewaters from the pharmaceutical processes of the Government Pharmaceutical Organization of Thailand about 100 L per month are generated from the quantitative analysis of active pharmaceutical ingredients and are contaminated by 30 mg/L of silver ions. Thus, a challenging method to extract silver ions from this wastewater to comply with Thailand's mandatory discharge limit of  $\leq 1$  mg/L is essential [4].

Several methods have been used to separate silver ions, as shown in Table 8.1 [5-13]. The traditional methods such as chemical precipitation and electrodeposition are energy-inefficient at a concentration less than 100 mg/L. Ultrafiltration and membrane discs are solid membranes which are found to have lower mass-transfer fluxes than the supported liquid membrane [14]. In case of adsorption by common adsorbents [15] (e.g. silica gels, clays, ion-exchange resins, and activated carbons), although it is a simple method with low-energy consumption, it is rather difficult to recover target species and to regenerate the adsorbents. However, the adsorption by outstanding selective surface-modified adsorbents so-called MCM-41 (LUS-type) developed by Yeung et al. are excellent for selective adsorption of precious and heavy metals [16-19]. So far, powdered adsorbents are inconvenient to reuse and mostly their applications are not in continuous processes [78]. The concentration of the contaminated ions in the effluents after the treatment is higher than the standard water-quality regulation. In addition, traditional methods including adsorption are always ineffective at a very low concentration of the contaminated ions in ppm- or ppb-level [79].

**Table 8.1** Examples of the methods for the separation of silver ions.

Author	Method	Extractant	% Extraction	% Recovery	Reference
Pfrepper et al., 1989	Precipitation	N/A	99.8	N/A	[5]
El Bachiri et al., 1996	BLM	DC18C6	50	71	[6]
Aamrani et al., 1999	SLM	TCBA mixed with TCTH	88.9	90	[7]
Samsipur et al., 2002	Membrane disks	N/A	99.9	N/A	[8]
Chaudry et al., 2008	FSSLM	TEA	99	93	[9]
Çoruh et al., 2010	Adsorption	N/A	99	N/A	[10]
Tang et al., 2010	ELM	D2EHPA	99.9	99.2	[11]
Sadyrbaeva, 2010	BLM and Electrodeposi- tion	D2EHPA mixed with TOA	90	46	[12]
Desai et al., 2012	Complexation -Ultrafiltration	N/A	100	N/A	[13]
This work	HFSLM	LIX 84-I	98	85	

BLM: bulk liquid membrane, SLM: supported liquid membrane, FSSLM: flat-sheet supported liquid membrane, ELM: emulsion liquid membrane, HFSLM: hollow fiber supported liquid membrane.

A supported liquid membrane, particularly a hollow fiber supported liquid membrane (HFSLM) is a suitable method for simultaneous extraction and recovery of the target species at a dilute concentration in one single stage. It can be used as a secondary treatment to reduce a trace amount of the target species to meet the mandatory discharge limit [22-29]. Other attractive advantages of the HFSLM relate to high mass-transfer flux and selectivity, low extractant and high membrane surface area per volume [30, 31]. Although the HFSLM has several advantages for

dilute solutions, the major inherent drawbacks are membrane stability or fouling, and chemical and physical resistances of the hollow fibers in severe atmosphere [14]. Polypropylene hollow fibers can withstand the pH of the solutions no less than 1, at moderately high temperatures but it has less resistant to chemicals than polytetrafluoroethylene and is sensitive to chlorine [32]. To prevent and reduce membrane fouling, an overview of several approaches are mentioned herein [33], e.g., by feed pretreatment and treatment of the membrane surface. One concern issue in HFSLM operation is equal flow rates of feed and stripping solutions to prevent liquid membrane leakage. In a study of Uheida et al. [22], palladium ions at a concentration of  $10 \text{ mg/dm}^3$  in synthetic solution were extracted using nonylthiourea as the extractant, and sodium chloride solution as the stripping solution. Kumar et al. [34] extracted gold ions at a concentration of  $10 \text{ mg/L}$  using LIX 79 as the extractant and sodium hydroxide solution as the stripping solution. However, a few studies have been conducted on the extraction and recovery of silver ions by HFSLM.

By using the HFSLM method for industrial applications, reliable mathematical models are required to predict the mass transports and important parameters in the system. Mathematical models based on the extraction and recovery processes in hollow fiber modules can be achieved by considering the mass diffusion fluxes across the liquid membrane at a steady-state condition. Most researchers developed fluid-flow models relating to diffusion or reaction flux models to explain the phenomena only at feed-liquid membrane interface by the appropriate mass-conservation equations and the associated boundary conditions [35-39]. These models were considered based on the assumption of the steady-state condition at the interface by neglecting the mass diffusion in the axial direction. Zhang et al. [31] developed the model based on diffusion flux to predict the final concentration of Cu(II) in synthetic feed solution after the extraction. The predicted results fit with experimental data at the deviation less than 12%. Kandwal et al. [27] developed the acceptable model describing the transport of Cs(I) through HFSLM based on the facilitated diffusional transport mechanism by neglecting the chemical reaction. Nevertheless, the mass transport phenomena at liquid membrane-stripping interface

are also important for understanding the overall mass transport along the hollow fibers. In our work, the extraction and recovery of silver ions from pharmaceutical wastewater by HFSLM was examined. LIX 84-I was used as the extractant due to a greater transmembrane flux [40]. Sodium thiosulphate solution was used as the stripping solution due to its high recovery of silver ions [2]. The influences of several variables such as the pH of feed and stripping solutions, concentrations of the extractant and stripping solution, flow directions between feed and stripping solutions, as well as equal flow rates of feed and stripping solutions were investigated. A new perspective was approached by the fluid-flow models describing the transport phenomena of silver ions not only at the feed-liquid membrane interface but also in the liquid membrane and at liquid membrane-stripping interface. These models were executed by linear algebra in unsteady-state condition. The mass transfer coefficient of complex species across the liquid membrane ( $k_m$ ) was determined based on the equation of the overall permeability coefficient ( $P$ ) for use in the model. The MATLAB software was used to solve these models by Gaussian elimination method. The final calculated concentrations of silver ions in feed and stripping solutions were validated with the experimental data.

### 8.3 Theory

#### 8.3.1 Transport of silver ions across the liquid membrane phase

The extractant dissolved in organic solvent is trapped in the hydrophobic micropores of hollow fibers as the liquid membrane phase. The feed solution containing silver ions, and the stripping solution are generally fed counter-currently in the tube and shell sides of the hollow fibers, respectively. The transport of silver ions across liquid membrane phase is presented in Figure 8.1. Extraction at the feed-liquid membrane interface (subscript  $f_i$ ) takes place when the extractant ( $\overline{HR}$ ) reacts with silver ion in feed phase to form silver-extractant complex ( $\overline{AgR}$ ) and hydrogen ion

( $H^+$ ), as shown in Eq. (8.1). Subsequently, the silver-extractant complex diffuses across the liquid membrane phase to the liquid membrane-stripping interface (subscript  $_{si}$ ) due to the concentration gradient between the two interfaces. Then, the recovery reaction, Eq. (8.2), occurs and therefore silver ion is released into the stripping phase. Finally, silver and hydrogen ions are counter-transported across the liquid membrane phase.

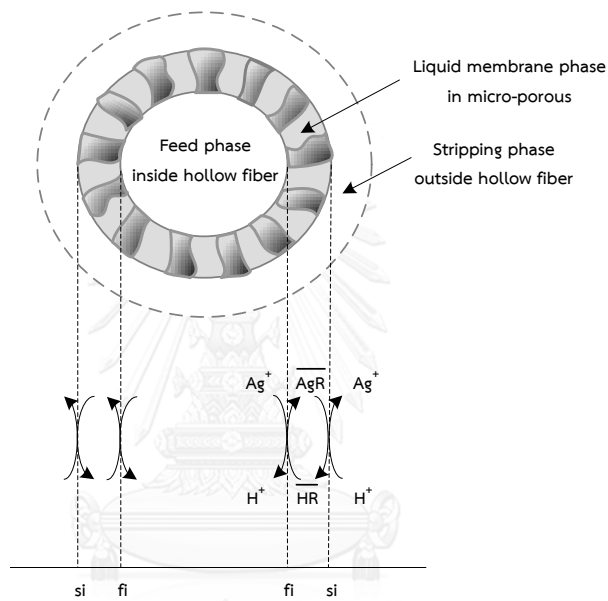


**Figure 8.1** Transport of silver ion in the HFSLM system.



The over bar denotes the species in the liquid membrane phase.

The rates of extraction ( $r_{-Ag^+}$ ) and recovery ( $r_{Ag^+}$ ) are described by Eqs. (8.3) and (8.4), respectively:

$$r_{-Ag^+}(x, t) = k_{\text{extraction}} C_{Ag^+,f}^m(x, t) = r_{-Ag^+}(C_{Ag^+,f}) \quad (8.3)$$

$$r_{Ag^+}(x, t) = k_{\text{stripping}} C_{Ag^+,s}^n(x, t) = r_{Ag^+}(C_{Ag^+,s}) \quad (8.4)$$

where  $x$  is the longitudinal axis of the hollow fiber,  $t$  is the extraction or recovery time,  $k_{\text{extraction}}$  and  $k_{\text{stripping}}$  are the reaction rate constants of extraction and recovery,  $C_{Ag^+,f}$  and  $C_{Ag^+,s}$  are the concentrations of silver ions in the feed and stripping phases as a function of longitudinal axis of the hollow fiber and time, and  $m$  and  $n$  are the reaction orders of the extraction and recovery, respectively.

### 8.3.2 Fluid-flow models of silver ion transport in feed and stripping phases

The laminar transport of silver ions in feed phase corresponds to the axial convection and diffusion. The extraction reaction is based on the facilitated coupled counter transport [41]. Additionally, the concentrations of silver ions along the hollow fibers vary depending on the longitudinal axis of the hollow fiber and the extraction time corresponding to the accumulation of silver ions in the feed phase [42]. The fluid-flow model in feed phase is made according to the following assumptions:

- The physical properties in the feed phase such as pressure, temperature and volume are constant;
- Based on the facilitated coupled counter-transport, the silver ions are transported across the feed-liquid membrane interface into the liquid membrane phase by the reaction flux;

- Since the inside diameter of hollow fibers is very small, the concentration of silver ions in the radial direction is constant. This means that the diffusion fluxes of silver ions in the feed phase exist only in the axial direction;
- Only silver-extractant complexes, not silver ions, are transported across the liquid membrane phase;
- The forward reaction is dominant.

In case the fluid-flow model of the stripping phase, the same concepts are approached:

- The physical properties in the stripping phase are constant;
- Only silver ions from the reaction flux at the liquid membrane-stripping interface are transported into the stripping phase;
- The diffusion fluxes of silver ions in the stripping phase exist only in the axial direction;
- The forward reaction is dominant.

The transports of silver ions through the small segments in the feed and stripping phases and the cross-sectional areas of the hollow fibers are shown in Figure 8.2.

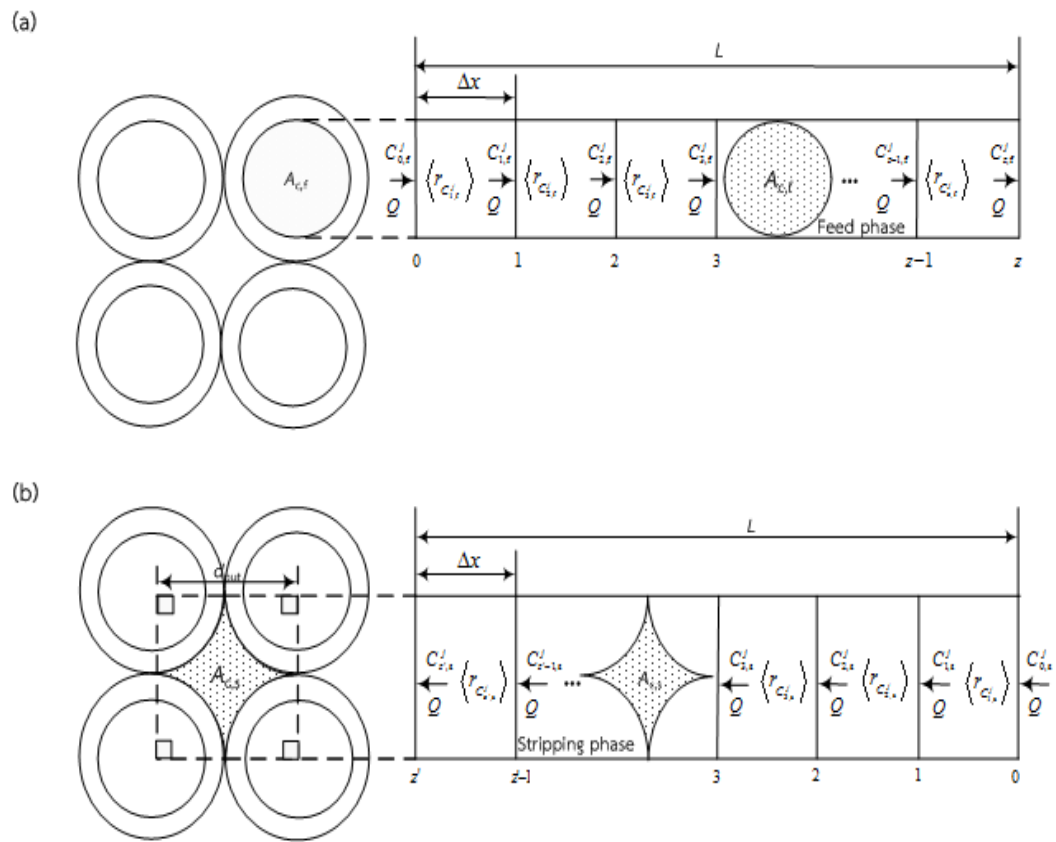


**Figure 8.2** Transport of silver ions through small segments (a) in feed phase (inside the hollow fibers) (b) in stripping phase (outside the hollow fibers).

For feed phase, the mass conservation of silver ions in each small segment ( $\Delta x$ ) is considered by Eqs. (8.5) and (8.6):

$$\left[ \begin{array}{c} \text{Rate of mass transport} \\ \text{into the system} \\ \text{by convection} \end{array} \right] - \left[ \begin{array}{c} \text{Rate of mass transport} \\ \text{out of the system} \\ \text{by convection} \end{array} \right] + \left[ \begin{array}{c} \text{Rate of mass transport} \\ \text{through the system} \\ \text{by diffusion} \end{array} \right] - \left[ \begin{array}{c} \text{Rate of mass} \\ \text{extracted by} \\ \text{extraction reaction} \end{array} \right] = \left[ \begin{array}{c} \text{Rate of mass} \\ \text{accumulation} \\ \text{within the system} \end{array} \right] \quad (8.5)$$

$$QC_{z-1,f}^j - QC_{z,f}^j + \frac{A_{c,f}D_f}{\Delta x} (C_{z,f}^j - C_{z-1,f}^j) - v \langle r_{c_{z,f}^j} \rangle = \frac{V}{\Delta t} (C_{z,f}^j - C_{z,f}^{j-1}) \quad (8.6)$$

where  $Q$  is the volumetric flow rate of feed solution,  $z$  is the number of small segments in feed phase,  $A_{c,f}$  is inside cross-sectional area of the hollow fibers,  $\mathcal{D}_f$  is the diffusion coefficient of silver ions in feed phase as calculated by the Wilke–Chang equation in Appendix A,  $j$  and  $j-1$  are the sequence of space times  $j$  and  $j-1$ ,  $C_z^j$  is the concentration of silver ions as a function of  $z$  and  $j$ ,  $\left\langle r_{C_z^j} \right\rangle$  is the average rate of the extraction as a function of silver ion concentration at segment  $z$  and sequence  $j$ ,  $\Delta t$  is the space time for the feed solution flowing inside the hollow fibers and  $v$  is determined as follows:

$$v = \frac{\varepsilon}{2}(d_o - d_i)$$

where  $\varepsilon$  is the porosity of hollow fibers and  $d_i$  and  $d_o$  are the inside and outside diameters of a hollow fiber and  $0 \leq x \leq L$  which  $L$  is the length of the hollow fiber.

Solving Eq. (8.6) by linear algebra and obtain Eq. (8.7)

$$[A][C] = [Y] \tag{8.7}$$

where  $[A]$  is the matrix of the constants in feed phase;  $[C]$  and  $[Y]$  are the matrices of silver ion concentrations in feed phase at the sequence of space times  $j$  and  $j-1$ .

These matrices are described detail in Appendix A.

At the stripping phase by a counter-current flow, the mass conservation of silver ions at the segment  $z'$  can be described in the respective equation:

$$QC_{z'-1,s}^j - QC_{z',s}^j + \frac{A_{c,s}D_s}{\Delta x} \left( C_{z',s}^j - C_{z'-1,s}^j \right) + v \left\langle r_{C_{z',s}^j} \right\rangle = \frac{v}{\Delta t} \left( C_{z',s}^j - C_{z',s}^{j-1} \right) \tag{8.8}$$

where  $z'$  is the number of small segments in the stripping phase,  $A_{c,s}$  is the outside cross-sectional area of the hollow fibers, and  $\mathcal{D}_s$  is the diffusion coefficient of silver

ions in the stripping phase which is equal to that in the feed phase of the same aqueous solution. Solving Eq. (8.8) by linear algebra and obtain Eq. (8.9)

$$[A'] [C'] = [Y'] \quad (8.9)$$

where  $[A']$  is the matrix of the constants in stripping phase;  $[C']$  and  $[Y']$  denote the matrices of silver ion concentrations in stripping phase at the sequence of space times  $j$  and  $j-1$ . These matrices are described detail in Appendix A.

### 8.3.3 Mass transfer coefficient of silver-extractant complexes across the liquid membrane phase

The mass transfer coefficient of silver-extractant complexes across the liquid membrane phase ( $k_m$ ) is determined based on the overall permeability coefficient ( $P$ ) of silver ion transport in a radial direction from feed phase to stripping phase.

The overall mass transfer coefficient of silver ions represents the mass-transfer resistances in feed phase, liquid membrane phase and stripping phase. The reciprocal of the overall mass transfer coefficient is [43]

$$\frac{1}{P} = \frac{1}{k_f} + \frac{r_{in}}{r_m} \frac{1}{P_m} + \frac{r_{in}}{r_{out}} \frac{1}{k_s} \quad (8.10)$$

where  $k_f$  and  $k_s$  are the mass transfer coefficients of silver ions in feed and stripping phases, respectively,  $r_m$  is the log-mean radius of a hollow fiber, and  $P_m$  is the permeability coefficient of silver-extractant complexes in liquid membrane phase.

The mass transfer resistance of silver ions in the stripping phase in Eq. (8.10) can be neglected due to the high mass transfer coefficient in this phase. Thus,

$$\frac{1}{P} = \frac{1}{k_f} + \frac{r_{in}}{r_{lm}} \frac{1}{P_m} \quad (8.11)$$

In this work, it is assumed that the mass transport across the liquid membrane phase is controlled by the extraction reaction at the feed-liquid membrane interface. Therefore, the overall mass transfer coefficient of silver ions can be determined by the permeability coefficient of silver ions in the feed phase as described by Danesi [44]:

$$-V_f \ln \left( \frac{C_{z,f}^j}{C_{0,f}^j} \right) = A_{eff} P \frac{\theta}{\theta + 1} t \quad (8.12)$$

and 
$$\theta = \frac{q}{PL\varepsilon\pi N r_{in}}$$
 (8.13)

where  $V_f$  is the volume of feed solution,  $A_{eff}$ ,  $L$  and  $\varepsilon$  represent the effective surface area, length and porosity of the hollow fibers. The plot of  $-V_f \ln(C_{z,f}^j / C_{0,f}^j)$  as a function of time  $t$  from Eq. (8.12) gives the slope of  $A_{eff} P(\theta / \theta + 1)$ . Subsequently,  $P$  is obtained from Eq. (8.13).

The permeability coefficient of complex species in liquid membrane phase in Eq. (8.11) is correlated by the relation between the distribution ratio of silver ions ( $D$ ) and the mass transfer coefficient of the silver-extractant complexes across the liquid membrane phase ( $k_m$ ) as shown in Eq. (8.14) [45].

$$P_m = Dk_m \quad (8.14)$$

Where 
$$D = \frac{[AgR]_m}{[Ag^+]_f}$$
 (8.15)

As it is not possible to measure the concentration of complex species in the liquid membrane phase, so the distribution ratio of silver ions can be derived by the relation with the extraction equilibrium constant of silver ions ( $K_{ex}$ ) based on Eq. (8.1) and obtain Eq. (8.16).

$$K_{ex} = \frac{\overline{[AgR]}_m [H^+]_f}{[Ag^+]_f \overline{[HR]}_m^2} \quad (8.16)$$

From Eq. (8.16), the distribution ratio of silver ions can be rewritten as follows:

$$D = K_{ex} \frac{\overline{[HR]}_m^2}{[H^+]_f} \quad (8.17)$$

Subsequently Eq. (8.17) into Eq. (8.14) for the permeability coefficient of complex species in liquid membrane phase in Eq. (8.11) then,

$$\frac{1}{P} = \frac{1}{k_f} + \frac{r_{in}}{r_{lm}} \frac{[H^+]_f}{K_{ex} k_m \overline{[HR]}_m^2} \quad (8.18)$$

According to the slope of the graph plotted between  $1/P$  and  $[H^+]_f / \overline{[HR]}_m^2$  from Eq. (8.18), the mass transfer coefficient of the complex species across the liquid membrane phase is attained.

## 8.4 Experimental

### 8.4.1 Chemicals

Pharmaceutical wastewater from a pharmaceutical plant of the Government Pharmaceutical Organization consisting of 30 mg/L silver ions and 120 mg/L ferric ions was used as the feed solution. To avoid the interference of ferric ions to the extraction of silver ions, ferric ions were precipitated by phosphoric acid solution to  $0.35 \text{ mg/dm}^3$ . The initial pH and other properties of this wastewater are listed in Table 8.2. Sodium thiosulfate pentahydrate ( $\text{Na}_2\text{S}_2\text{O}_3 \cdot 5\text{H}_2\text{O}$ ) (BrightChem Sdn. Bhd., Selangor, Malaysia) dissolved in distilled water was used as the stripping solution; its pH was about 6. Hydrophobic liquid membrane solution was prepared by embedding LIX 84-I (Henkel Thai Ltd., Bangkok) and kerosene in the micro-porous hollow fibers. LIX 84-I was selected in regards to the literature review, LIX series is favorable to the extraction of metal ions. The chemical structure of LIX 84-I is shown in Figure 8.3. Nitric acid solution (BrightChem) was used to adjust the pH of feed and stripping solutions. All chemicals used in this experiment were analytical grades. Aqueous solutions were prepared using Milli-Q<sup>®</sup> deionized water (Millipore<sup>®</sup>, USA).

**Table 8.2** Properties of pharmaceutical wastewater.

Property	Value
Ag(I) ( $\text{mg/dm}^3$ )	30
Fe(III) ( $\text{mg/dm}^3$ )	120
Temperature (K)	303.2
pH	6.0
Viscosity (Pa-s)	0.0010
Density (g/mL)	1.0015
TSS (mg/L)	730
BOD (mg/L)	1,740
COD (mg/L)	3,210
Conductivity ( $\mu\text{s/cm}$ )	2,750

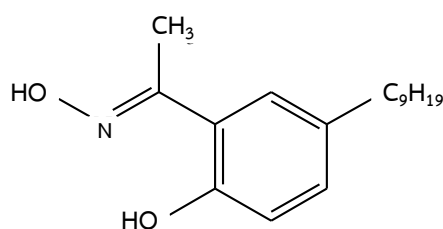


**Figure 8.3** Chemical structure of LIX 84-I.

#### 8.4.2 Apparatus

A laboratory-scale hollow fiber module (Liqui-Cel<sup>®</sup> Extra-flow 2.5 in × 8 in; Hoechst Celanese, Bridgewater NJ) was used. The key features of the hollow fiber module are as shown in Table 8.3. The hydrophobic polypropylene hollow fibers were woven into fabric and wrapped around a central tube of the module. The concentrations of silver ions in feed and stripping solutions were analyzed by the atomic absorption spectrometer (AAS) (model AA280FS; Varian, Walnut Creek CA), and the pH of the solutions were measured by a BP3001 pH meter (TransInstruments, Singapore).

**Table 8.3** Key features of the hollow fiber module.

Property	Description
Material	Polypropylene
Module diameter	0.63 dm
Module length	2.03 dm
Number of hollow fibers	35,000
Inside diameter of a hollow fiber	0.002 dm
Outside diameter of a hollow fiber	0.003 dm
Effective length of a hollow fiber	1.5 dm
Effective surface area of a hollow fiber	140 dm <sup>2</sup>
Area per unit volume	293 dm <sup>2</sup> /dm <sup>3</sup>
Pore size	3 × 10 <sup>-7</sup> dm
Porosity	25%
Tortuosity	2.6

### 8.4.3 Procedure

A single hollow fiber module, shown in Figure 8.4, was set up. The amount of the liquid membrane (LIX 84-I dissolved in kerosene) about  $0.5 \text{ dm}^3$  was simultaneously pumped into shell and tube of the hollow fibers for 40 min to ensure that the liquid membrane solution was entirely embedded in the micro-pores of the hollow fibers. Wastewater as the feed solution, and the stripping solution ( $0.5 \text{ dm}^3$  each) were, respectively, supplied in the counter-current circulating mode to tube and shell sides of the hollow fibers. The pH of feed solution was adjusted to acidic solution. The parameters, i.e., pH of feed solution (2.0-4.0) and pH of stripping solution (1.0-3.0), concentrations of the extractant (0.01-0.20 M) and stripping solution (0.1-2.0 M) as well as the equal flow rates of feed and stripping solutions ( $0.2$ - $1.0 \text{ dm}^3/\text{min}$ ) were investigated. One separation cycle was 30 min. The final feed and stripping solutions were collected to analyze the amount of silver ions by AAS. The percentages of extraction and recovery were calculated by Eqs. (8.19) and (8.20). The stability of the HFSLM system was investigated by a continuous operation for 4 hours. In practice, for applicability to a large scale separation, the estimation of the important parameters such as separation time by a reliable model is absolutely unavoidable. In this work, the fluid-flow models considering the reaction fluxes in feed and stripping phases were approached. To verify the model, the model results were certified with the experimental results of the related parameters at each optimum condition. The samples were collected and analyzed every 2 min. The average percentage of deviation was calculated by Eq. (8.21).

$$\% \text{ Extraction} = \frac{C_{0,f}^j - C_{z,f}^j}{C_{0,f}^j} \times 100 \quad (8.19)$$

$$\% \text{ Stripping} = \frac{C_{z,s}^j}{C_{0,f}^j} \times 100 \quad (8.20)$$

$$\% \text{ Deviation} = \frac{\sum_{i=1}^i \left( \frac{C_{\text{Expt.}}^j - C_{\text{Theo.}}^j}{C_{\text{Expt.}}^j} \right)_i}{i} \times 100 \quad (8.21)$$

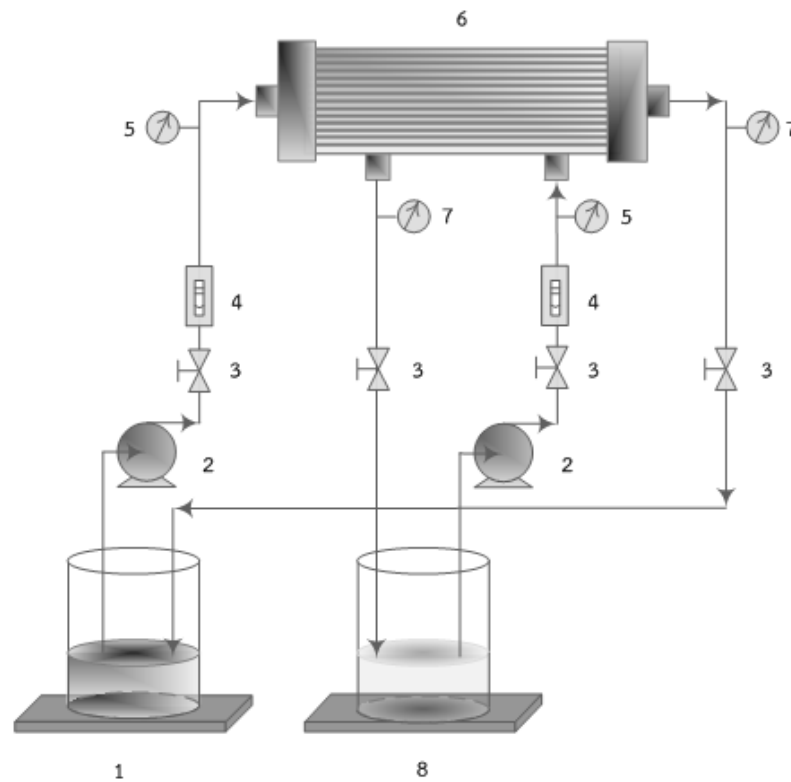


**Figure 8.4** Schematic diagram of a single hollow fiber module with counter-current circulating flow patterns of feed and stripping solutions: (1) feed reservoir, (2) gear pumps, (3) gate valves, (4) flow meters, (5) inlet pressure gauges, (6) hollow fiber module, (7) outlet pressure gauges, and (8) stripping reservoir.

## 8.5 Results and discussion

### 8.5.1 Experimental operation conditions for HFSLM stability

The properties of the pharmaceutical wastewater used in this work are shown in Table 8.2. It consists of 30 mg/L of silver ions and 120 mg/L of ferric ions. According to our previous work [46] with wastewater from stainless steel-cold rolled plate process by using LIX series (LIX 860-I), we found that at a pH of wastewater 4 and 0.8 M, LIX 860-I is the most selective extractant to retrieve Ni(II) compared to Fe(II) and Cr(III), respectively. No chromium ions were found in the stripping solution. For a double-module operation, the percentage of recovery of nickel ions was 87%. However, to avoid the interference from other ions in the pharmaceutical wastewater to the extraction and recovery of silver ions, the pharmaceutical wastewater was pretreated by precipitation method before the experiments. Ferric ions were precipitated by phosphoric acid solution and therefore a trace amount of ferric ions of 0.35 mg/L was observed in the feed solution.

### 8.5.2 Influences of pH of feed and stripping solutions

It is known that LIX series has good performance for the extraction of metal cations from the acidic and dilute aqueous solutions. Thus, the pH of the wastewater was adjusted from pH of 6 to be acidic (2.0-4.0) for a good driving force of hydrogen ions. In Figure 8.5(a), the percentages of extraction and recovery increased rapidly with the pH of the feed solution to 3.5 because of an increase in driving force. It is likely to be constant when pH is greater than 4.0 due to the equilibrium reaction at the feed-liquid membrane interface. In Figure 8.5(b), the percentages were rather constant at pH of 1.0-2.0 and decreased at a pH higher than 2.0 due to less driving force. To select the optimum pH of feed and stripping solutions, we do not take account of the stripping solution of pH lower than 2.0 in order to prevent a strong acid atmosphere to polypropylene hollow fibers and its module. Thus, we consider

the optimum pH of feed solution of 3.5 for highly extracted silver ions, and 2 for the stripping solution.

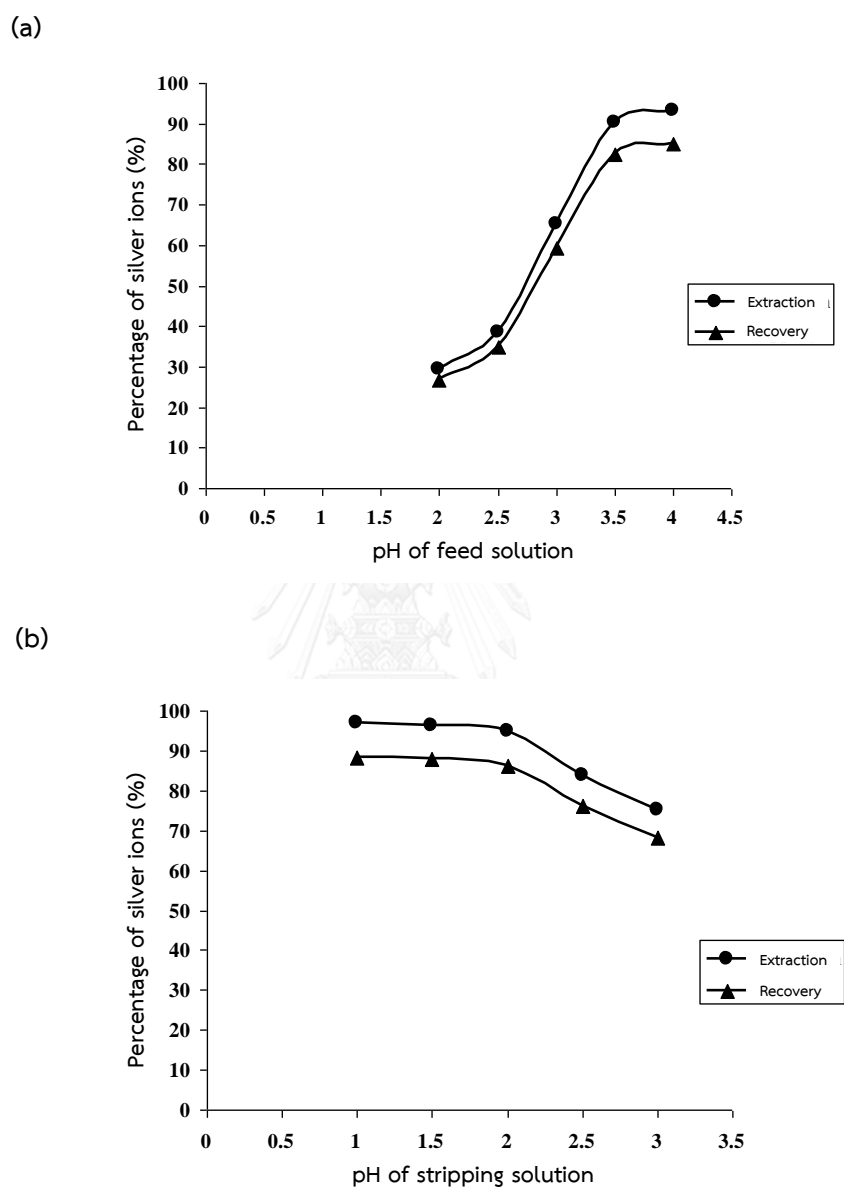


**Figure 8.5** Extraction and recovery of silver ions via the HFSLM by counter-current flow against (a) pH of feed solution and (b) pH of stripping solution ( 0.1 M LIX 84-I, 0.5 M  $\text{Na}_2\text{S}_2\text{O}_3$ , and equal flow rates of feed and stripping solutions at  $0.2 \text{ dm}^3/\text{min}$ ).

### 8.5.3 Influence of extractant concentration

The influence of the concentration of LIX 84-I was demonstrated in Figure 8.6. Generally, the reaction rate increases with the concentration of the extractant. From Figure 8.6, the percentages of extraction and recovery increased with the concentration of the extractant up to 0.1 M. Nevertheless, the extraction and recovery of silver ions decreased at the concentration higher than 0.1 M due to an increase in liquid membrane viscosity that obstructed mass transfer in the liquid membrane phase corresponding to our previous works [14, 26]. Thus, the optimum concentration of the extractant is 0.1 M.

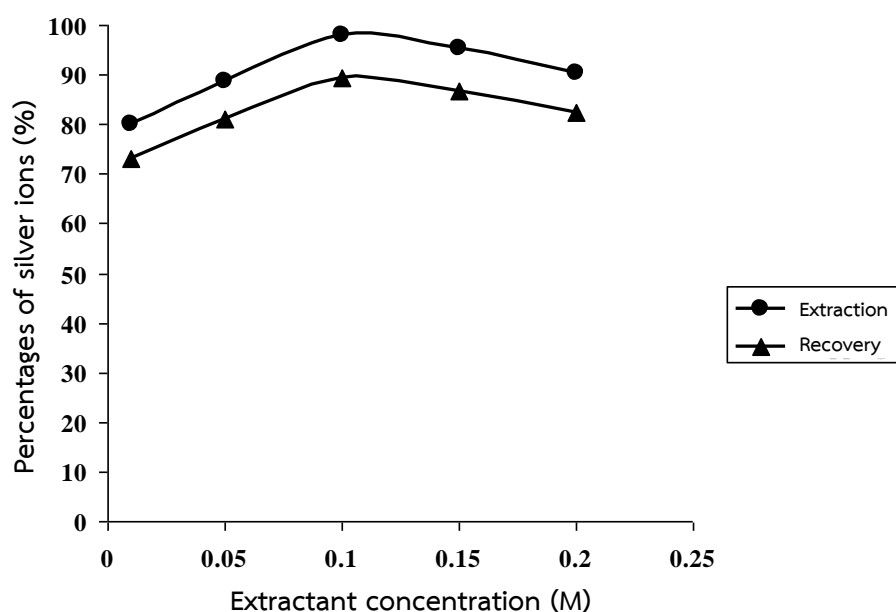


**Figure 8.6** Extraction and recovery of silver ions via the HFSLM by counter-current flow against concentration of the extractant (pH of feed and stripping solutions at 3.5 and 2, 0.5 M  $\text{Na}_2\text{S}_2\text{O}_3$ , and equal flow rates of feed and stripping solutions at  $0.2 \text{ dm}^3/\text{min}$ ).

### 8.5.4 Influence of stripping concentration

In the case of the concentration of stripping solution in Figure 8.7, the percentages of extraction and recovery increased up to 0.5 M then remained constant from the concentration higher than 0.5 M (excess stripping solution). It indicated that the amount of silver ions in the stripping solution was limited up on the amount of complex species that reacted with the stripping solution at the liquid membrane-stripping interface. Thus, the optimum stripping solution concentration is 0.5 M.

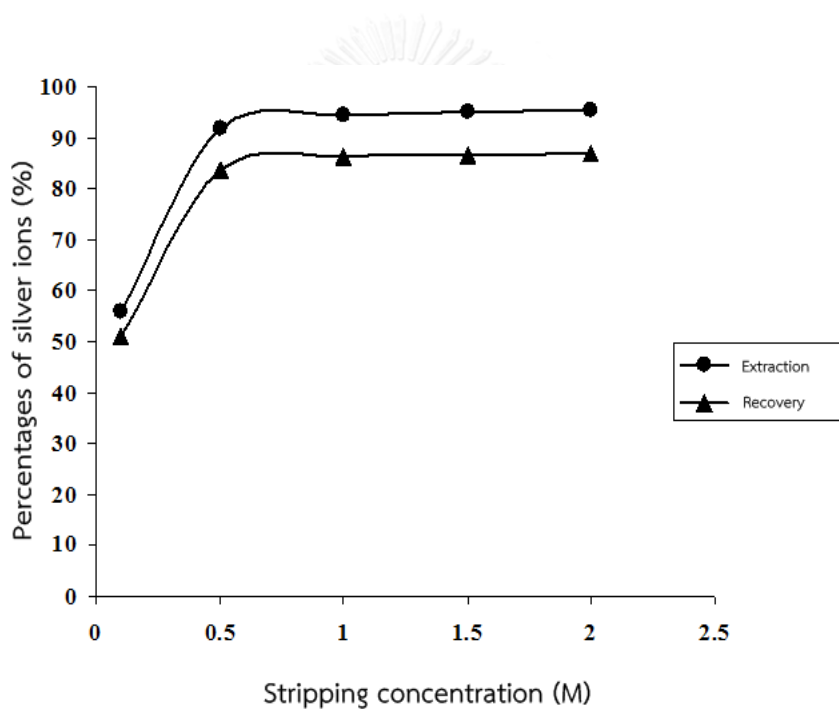


**Figure 8.7** Extraction and recovery of silver ions via the HFSLM by counter-current flow against concentration of the stripping solution (pH of feed and stripping solutions at 3.5 and 2, 0.1 M LIX 84-I, and equal flow rates of feed and stripping solutions at  $0.2 \text{ dm}^3/\text{min}$ ).

### 8.5.5 Influences of flow rates of feed and stripping solutions

Equal flow rates of feed and stripping solutions were studied, as shown in Figure 8.8. The percentages of extraction and recovery decreased rapidly from the flow rates of  $0.2 \text{ dm}^3/\text{min}$  ( $200 \text{ mL}/\text{min}$ ). The maximum extraction and recovery at  $0.2 \text{ dm}^3/\text{min}$  were 98 and 85%. From our experience in some cases the maximum extraction and recovery were attained at  $0.1 \text{ dm}^3/\text{min}$ . Altin et al. [2] studied the extraction of silver ions by a flat-sheet supported liquid membrane using the flow rates of  $0.05 \text{ dm}^3/\text{min}$  (lower than we used in this study) and yielded the maximum extraction and recovery at this flow rate. This is because the silver-extractant complexes formed slowly in the feed-liquid membrane interface and released at the liquid membrane-stripping interface rapidly. As per these observations, it is worth to note that not only types of the extractants and the pH in feed solution but also flow rates of feed and stripping solutions relate to a greater or lesser ion complexation in the HFSLM system. The chemical structure of LIX 84-I consists of acetophenone oxime which contains nitrogen coordination sites that generates a great affinity towards silver ions [47].

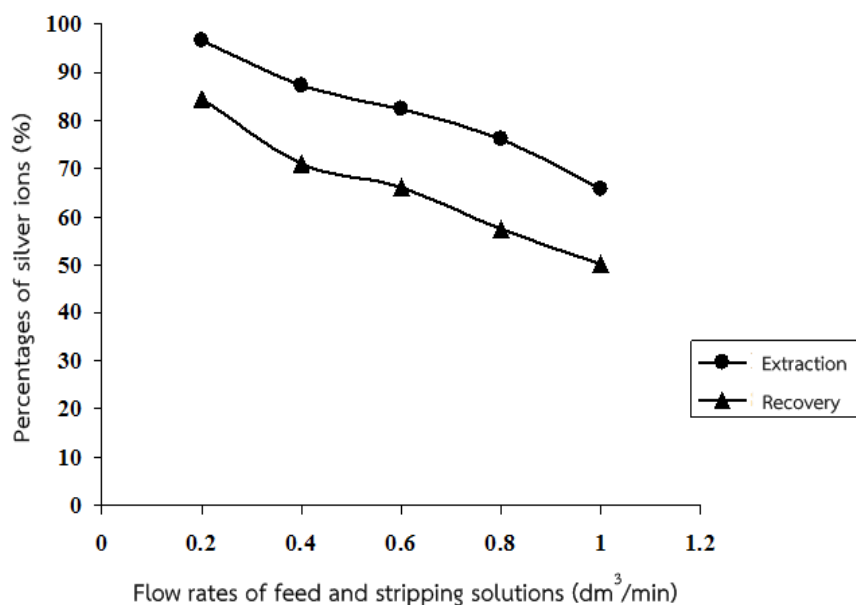


**Figure 8.8** Extraction and recovery of silver ions via the HFSLM by counter-current flow against flow rates of feed and stripping solutions (pH of feed and stripping solutions at 3.5 and 2, 0.1 M of LIX 84-I, and 0.5 M Na<sub>2</sub>S<sub>2</sub>O<sub>3</sub>).

### 8.5.6 Mass transfer parameters in the HFSLM

#### 8.5.6.1 Extraction equilibrium constant and distribution ratio

The extraction equilibrium constant and the distribution ratio of silver ion extraction were estimated under the optimum conditions from the experiment. A high extraction equilibrium constant about 95.29 dm<sup>3</sup>/mg was obtained from the slope of the graph between  $[Ag^+]_f [HR]_m^2$  and  $[AgR]_m [H^+]_f$  in Figure 8.9. The distribution ratio of silver ions was calculated by Eq. (8.18) and found to be 3.24. It is confirmed that the forward reaction of Eq. (8.1) controlled the extraction reaction of silver ions.

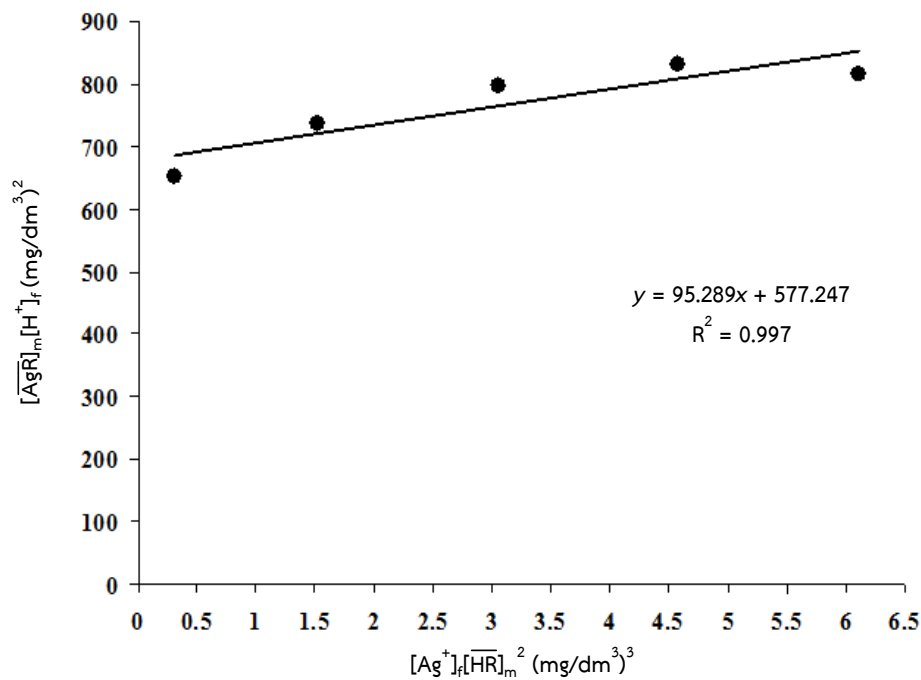


**Figure 8.9** Plot of  $[AgR]_m [H^+]_f$  against  $[Ag^+]_f [HR]_m^2$  for the extraction equilibrium constant of silver ion extraction via the HFSLM at the optimum conditions (pH of feed and stripping solutions at 3.5 and 2, 0.1 M LIX 84-I, 0.5 M  $Na_2S_2O_3$ , and equal flow rates of feed and stripping solutions at  $0.2 \text{ dm}^3/\text{min}$ ).

#### 8.5.6.2 Permeability coefficient

In case of the permeability coefficient of silver ions in the feed phase, it was estimated from the slope of the graph between  $-V_f \ln(C_{z,f}^j / C_{0,f}^j)$  and  $t$  in Eq. (8.12), as shown in Figure 8.10. A low permeability coefficient of  $5.71 \times 10^{-2} \text{ dm/min}$  was obtained suggesting that the radial diffusion flux is not significant on the radial transport of silver ions in the feed phase.

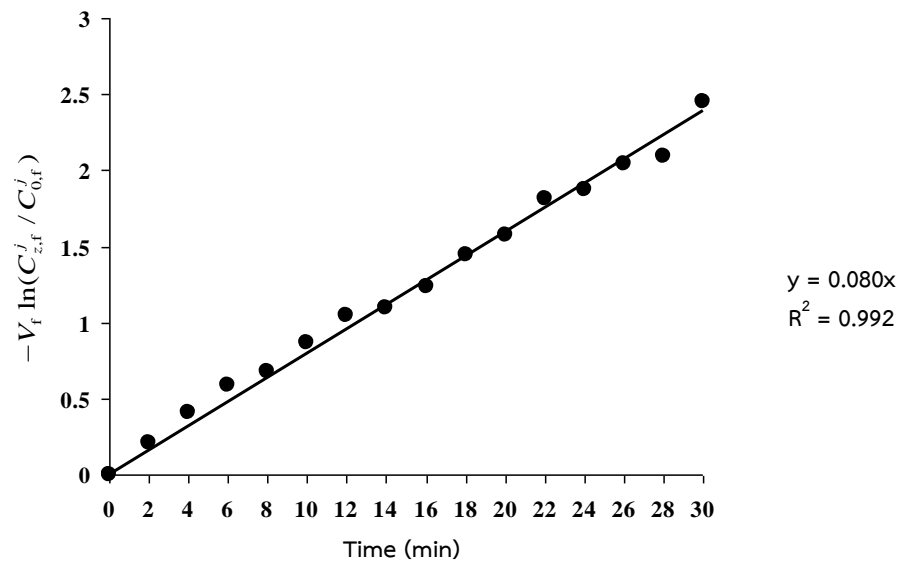


**Figure 8.10** Plot of  $-V_f \ln(C_{z,f}^j / C_{0,f}^j)$  against  $t$  for the permeability coefficient of silver ions in the feed phase at the optimum conditions (pH of feed and stripping solutions at 3.5 and 2, 0.1 M LIX 84-I, 0.5 M  $\text{Na}_2\text{S}_2\text{O}_3$ , and equal flow rates of feed and stripping solutions at  $0.2 \text{ dm}^3/\text{min}$ ).

### 8.5.6.3 Mass transfer coefficients of the complex species

The mass transfer coefficients of silver ions in feed solution ( $k_f$ ) and in liquid membrane ( $k_m$ ) depend on the extractant concentration and the pH in feed solution, and were determined from the intercept and slope of  $[\text{H}^+]_f / [\text{HR}]_m^2$  plotting against  $1/P$  in Eq. (8.18), as shown in Figure 8.11. Consequently, the mass transfer coefficients in feed solution and in liquid membrane were found to be 0.06 and 2.18 dm/min, respectively. High mass transfer coefficient in liquid membrane designated the rapid diffusion of complex species across the liquid membrane phase and therefore led to a positive effect on silver ion recovery of 85%.

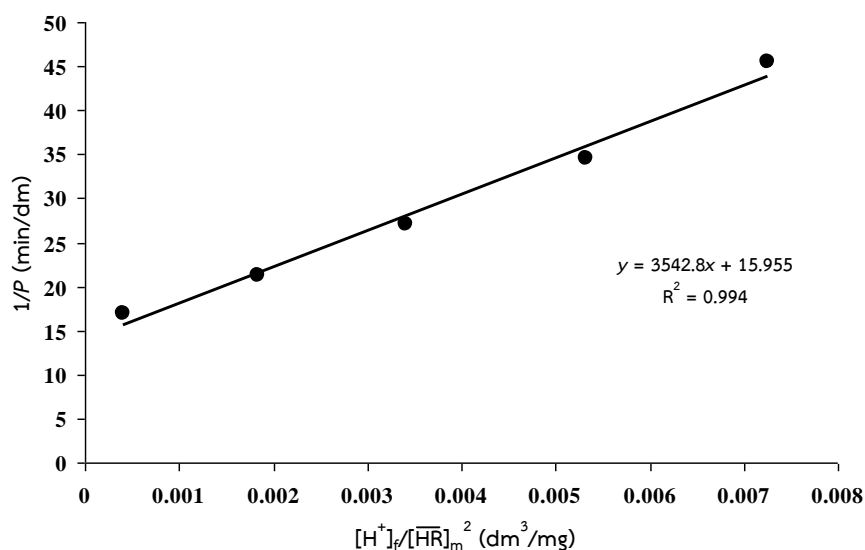


**Figure 8.11** Plot of  $1/P$  against  $[H^+]_f / [HR]_m^2$  for mass transfer coefficient of silver ions in feed solution and in liquid membrane at the optimum experimental conditions (pH of feed and stripping solutions at 3.5 and 2, 0.5 M  $\text{Na}_2\text{S}_2\text{O}_3$ , and equal flow rates of feed and stripping solutions at  $0.2 \text{ dm}^3/\text{min}$ ).

## 8.5.7 Analysis of fluid-flow models in feed and stripping phases

### 8.5.7.1 Parameters in the models

As shown in Table 8.4, the highest  $R^2$  denoted the first order reactions. The reaction rate constants of the extraction ( $k_{\text{extraction}}$ ) and recovery ( $k_{\text{stripping}}$ ) were determined from the slopes of the integral concentration of silver ions plotting against time and found to be  $0.164 \text{ min}^{-1}$  and  $0.094 \text{ min}^{-1}$ , respectively. Other relevant parameters for the models are listed in Table 8.5.

**Table 8.4** Reaction orders and reaction-rate constants of extraction and recovery of silver ions.

$m, n$	Plot		$k_{\text{extraction}}$	$R^2$	$k_{\text{stripping}}$	$R^2$
	Feed phase	Stripping phase				
0	$C_z^j$ and $t$	$C_0^j$ and $t$	0.562 mg/dm <sup>3</sup> ·min	0.798	1.094 mg/dm <sup>3</sup> ·min	0.985
1	$\ln(C_0^j / C_z^j)$ and $t$	$\ln(C_z^j / C_0^j)$ and $t$	0.164 min <sup>-1</sup>	0.984	0.094 min <sup>-1</sup>	0.992
2	$1 / C_z^j$ and $t$	$1 / C_0^j$ and $t$	0.040 L/mg·min	0.802	0.009 L/mg·min	0.922

**Table 8.5** Relevant parameters used in the fluid-flow models.

Parameter	Value
$a$ (-)	0.32
$A_{c,f}$ (dm <sup>2</sup> )	0.16
$A_{c,s}$ (dm <sup>2</sup> )	0.07
$b$ (-)	$1.50 \times 10^{-5}$
$c$ (-)	0
$C_0^0$ (mg/dm <sup>3</sup> )	30
$d$ (-)	$1.82 \times 10^{-4}$
$\mathcal{D}_f$ (dm <sup>2</sup> /min)	$4.65 \times 10^{-5}$
$\mathcal{D}_m$ (dm <sup>2</sup> /min)	$6 \times 10^{-7}$
$\mathcal{D}_s$ (dm <sup>2</sup> /min)	$4.65 \times 10^{-5}$
$e$ (-)	$5.97 \times 10^{-7}$
$f$ (-)	0
$k_m$ (dm/min)	2.18
$L$ (dm)	1.5
$Q$ (dm <sup>3</sup> /min)	0.2
$\Delta t$ (min)	0.5
$\Delta x$ (dm)	$1.15 \times 10^{-4}$
$z$	13,000
$z'$	13,000

### 8.5.7.2 Stability of HFSLM operation and validation of the fluid-flow models

In order to investigate the stability of the HFSLM operation, a series of experiments at each optimum condition were carried in a single hollow fiber module for 4 hours. The pharmaceutical wastewater flowed counter-currently through the tube side of the hollow fiber module while the stripping solution flowed through the shell side. Equal flow rates of feed and stripping phases were controlled to maintain a positive pressure on the tube side with respect to the shell side of the module to prevent the leak between the two sides. From Figure 8.12, the extraction and recovery reaction reached the equilibrium in 30 min and maintained a consistently high stability as long as the operating time. The extraction and recovery results showed that our proposed fluid-flow models have high accuracy as the calculated values were in line with the experimental results at the deviation of about 2%. We can state that the transport of silver ions in the feed and stripping phases corresponded to the axial convections, the axial diffusions and the chemical reactions of silver ions at the interfaces as in our assumptions. It is in accordance with the explanation of mass transport convection and diffusion of fluid stream by Geankoplis [48].

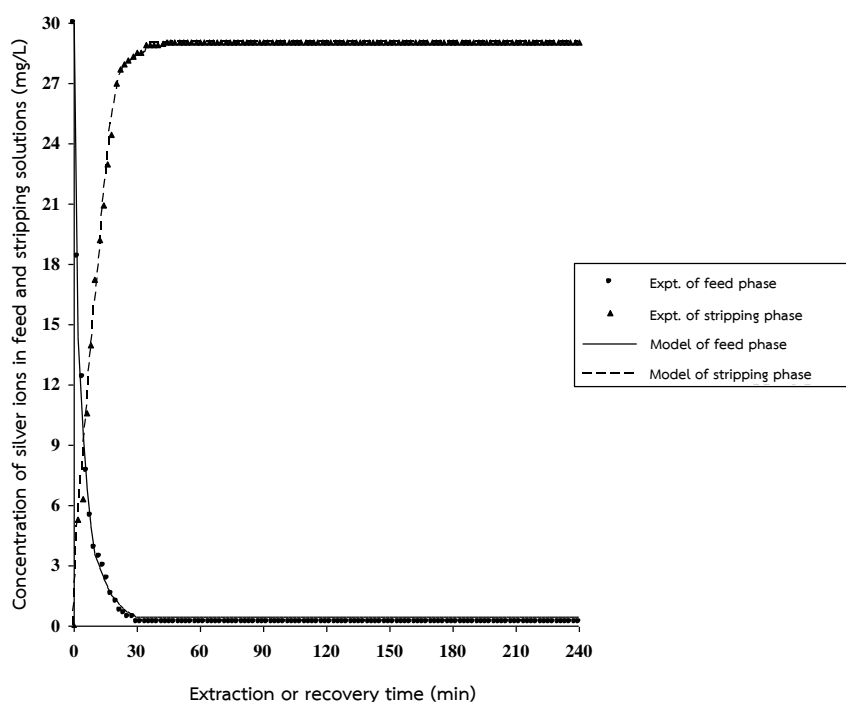


**Figure 8.12** Stability of HFSLM for extraction and recovery of silver ions and the validation of fluid-flow models at the optimum conditions (pH of feed and stripping solutions at 3.5 and 2, 0.1 M LIX 84-I, 0.5 M  $\text{Na}_2\text{S}_2\text{O}_3$ , and equal flow rates of feed and stripping solutions at  $0.2 \text{ dm}^3/\text{min}$ ).

### 8.5.7.3 Silver ion extraction: experimental and model results by fluid-flow model and other models and adaptability of fluid-flow model

Again, Figure 8.13 illustrates the excellent agreement of our experimental and model results by fluid-flow model. Since most of the models applied either the diffusion flux model or reaction flux model to explain the phenomena of metal transport at feed-liquid membrane interface, thus the results in Figure 8.13 were plotted in feed phase only. By comparing the extraction results of silver ions with the values predicted by the fluid-flow model which considered axial convection, the reaction fluxes in feed and stripping phases, axial diffusion and accumulation of silver ions in feed phase and from the experiments, and the values predicted by

the reaction flux model from our previous work with the extraction of copper ions [49], we can see that the plot of silver extraction in this work predicted by the proposed fluid-flow model had the similar trend with that predicted by the reaction flux model. Nevertheless, the fluid-flow model is more accurate. It is likely that by integration of the axial diffusion into the model make the model more precise. On the contrary, the plot of silver extraction applied to the mass transfer model, which was derived by Lin et al. [50] and considered only the diffusion flux, did not correspond to the plot of silver extraction predicted by the fluid-flow model. Moreover, we considered the applicability of the fluid-flow model to the extraction of copper ions by the HFSLM, it can be seen that the plots of copper extraction predicted by the reaction flux model [49] and this fluid-flow model, as well as the plot of silver extraction applied to the reaction flux model were in good agreement. These findings identifies that the extraction of metal ions such as silver and copper significantly depends upon axial convection, the reaction fluxes in feed and stripping phases, axial diffusion and the accumulation of metal ions in the feed phase. The transport in the radial direction is controlled by the extraction reaction at the feed-liquid membrane interface corresponding to the research by Alizadeh et al. [51] with slow extraction reaction of precious metal in the solvent extraction system. The transport of metal ions in the radial direction is, in principle, controlled by the slower radial diffusion rate or the reaction at the interface [41]. However, the controlling rate and the mechanisms of extraction of metal ions are in accordance with types and properties of extractants, organic solvents or diluents, stripping solutions, and operating temperature [52].

In addition to copper ions, another observation on the adaptability of the fluid-flow model to tantalum ions [53] was illustrated. The average percent deviation of the plot of tantalum extraction which was applied to the fluid-flow model was about 2%.

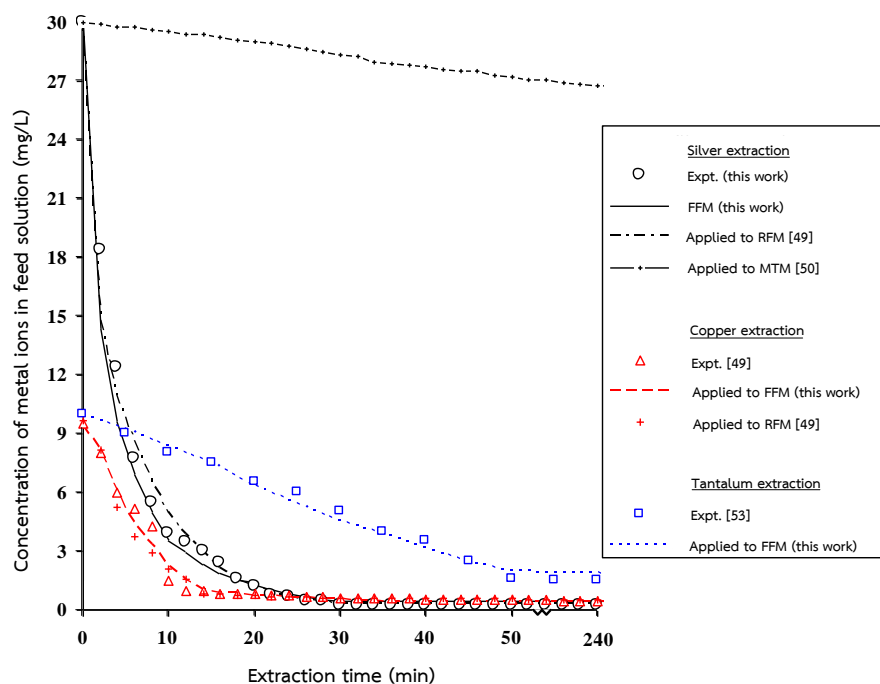


**Figure 8.13** Experimental and model results by fluid flow model compared with other models and adaptability of fluid-flow model (FFM = fluid-flow model; RFM = reaction flux model; MTM = mass transfer model).

## 8.6 Conclusion

LIX 84-I can successfully extract silver ions at a very low concentration from pharmaceutical wastewater by the HFSLM. High stability in extraction and recovery as high as 98% and 85% is observed. The optimum conditions for the extraction and recovery by a counter-current flow of feed and stripping solutions are pH of feed and stripping solutions at 3.5 and 2, respectively, 0.1 M LIX 84-I, 0.5 M  $\text{Na}_2\text{S}_2\text{O}_3$ , and equal flow rates of feed and stripping solutions at  $0.2 \text{ dm}^3/\text{min}$ .

Corresponding to the fluid-flow models which attributes to axial convections, the reaction fluxes in feed and stripping phases, axial diffusions and the accumulation of silver ions, we can conclude that the transport of silver ions along the hollow fibers is the reaction regime at the feed-liquid membrane and liquid membrane-stripping interfaces. The transport of silver ions from feed phase across

liquid membrane phase is facilitated coupled counter-transport. The accumulation of silver ions exhibits the unsteady of the HFSLM system. The model is validated and can be applied to other metal ions, e.g., copper ions and tantalum ions.

## 8.7 Appendix A

### Mathematics and assumptions for fluid-flow models of silver ion transport through HFSLM

Based on Eq. (8.5), mass conservation equations of silver ions in segments 1, 2, 3,..., z for feed phase are as follows:

$$QC_{0,f}^j - QC_{1,f}^j + \frac{A_{c,f}\mathcal{D}_f}{\Delta x} (C_{1,f}^j - C_{0,f}^j) - v \left\langle r_{C_{1,f}^j} \right\rangle = \frac{v}{\Delta t} (C_{1,f}^j - C_{1,f}^{j-1}) \quad (\text{A-8.1})$$

$$QC_{1,f}^j - QC_{2,f}^j + \frac{A_{c,f}\mathcal{D}_f}{\Delta x} (C_{2,f}^j - C_{1,f}^j) - v \left\langle r_{C_{2,f}^j} \right\rangle = \frac{v}{\Delta t} (C_{2,f}^j - C_{2,f}^{j-1}) \quad (\text{A-8.2})$$

$$QC_{2,f}^j - QC_{3,f}^j + \frac{A_{c,f}\mathcal{D}_f}{\Delta x} (C_{3,f}^j - C_{2,f}^j) - v \left\langle r_{C_{3,f}^j} \right\rangle = \frac{v}{\Delta t} (C_{3,f}^j - C_{3,f}^{j-1}) \quad (\text{A-8.3})$$

$$QC_{z-1,f}^j - QC_{z,f}^j + \frac{A_{c,f}\mathcal{D}_f}{\Delta x} (C_{z,f}^j - C_{z-1,f}^j) - v \left\langle r_{C_{z,f}^j} \right\rangle = \frac{v}{\Delta t} (C_{z,f}^j - C_{z,f}^{j-1}) \quad (\text{A-8.4})$$

The diffusion coefficients of silver ions in feed phase ( $\mathcal{D}_f$ ) in Eqs. (A-8.1)-(A-8.4) are calculated by the Wilke-Chang equation [54], as shown in Eq. (A-8.5):

$$\mathcal{D}_f = \frac{7.4 \times 10^{-8} (\phi M_w)^{0.5} T}{\eta_w V_{Ag^+}^{0.6}} \quad (\text{A-8.5})$$

where  $\phi$  is the association factor of water ( $\phi = 2.6$ ),  $M_w$  is the molecular weight of water,  $T$  is the temperature of feed phase in Kelvin,  $\eta_w$  is the viscosity of water, and  $v_{Ag^+}$  is the molar volume of silver ions at normal boiling point.

By linearization the rate of extraction in Eqs. (A-8.1)-(A-8.4) using Taylor series for any reaction order ( $m$ ), the rate of extraction becomes:

$$r_{C_{z,f}^j} = \alpha C_{z,f}^j + \beta \quad (\text{A-8.6})$$

where  $\alpha = -mk_{\text{extraction}} \left( C_{0,f}^j \right)^{m-1}$ ,  $\beta = (m-1)k_{\text{extraction}} \left( C_{0,f}^j \right)^m$

$C_{0,f}^j$  is the concentration of silver ions in feed phase at  $z = 0$ , and represents an individual value of each sequence of the space time  $j$ .

Dividing the mass conservation equations (Eqs. (A-8.1)-(A-8.4)) by the volumetric flow rate of feed phase ( $Q$ ) and deriving in matrix, therefore

$$[A][C] = [Y] \quad (\text{A-8.7})$$

where

$$[A] = \begin{bmatrix} -(1-a+b+d) & 0 & 0 & \dots & 0 & 0 \\ (1-a) & -(1-a+b+d) & 0 & \dots & 0 & 0 \\ 0 & 1-a & -(1-a+b+d) & \dots & 0 & 0 \\ \cdot & & & & & \cdot \\ \cdot & & & \dots & & \cdot \\ \cdot & & & & & \cdot \\ 0 & & & \dots & (1-a) & -(1-a+b+d) \end{bmatrix}_{z \times z}$$

$$[C] = \begin{bmatrix} C_{1,f}^j \\ C_{2,f}^j \\ C_{3,f}^j \\ \cdot \\ \cdot \\ \cdot \\ C_{z,f}^j \end{bmatrix}_{z \times 1}, \quad [Y] = \begin{bmatrix} c - (1-a)C_{0,f}^j - dC_{1,f}^{j-1} \\ c - dC_{2,f}^{j-1} \\ c - dC_{3,f}^{j-1} \\ \cdot \\ \cdot \\ \cdot \\ c - dC_{z,f}^{j-1} \end{bmatrix}_{z \times 1}$$

where  $a = \frac{A_{c,f} \mathcal{D}_f}{Q \Delta x}$ ,  $b = \frac{v \alpha}{Q}$ ,  $c = \frac{v \beta}{Q}$ ,  $d = \frac{v}{Q \Delta t}$

In case of the stripping phase, the mass conservation equations of silver ions are considered in the opposite direction of those in the feed phase due to a counter-current flow. The mass conservation equations in each small segment are expressed as follows:

$$QC_{0,s}^j - QC_{1,s}^j + \frac{A_{c,s} \mathcal{D}_s}{\Delta x} (C_{1,s}^j - C_{0,s}^j) + v \left\langle r_{C_{1,s}^j} \right\rangle = \frac{v}{\Delta t} (C_{1,s}^j - C_{1,s}^{j-1}) \quad (\text{A-8.8})$$

$$QC_{1,s}^j - QC_{2,s}^j + \frac{A_{c,s} \mathcal{D}_s}{\Delta x} (C_{2,s}^j - C_{1,s}^j) + v \left\langle r_{C_{2,s}^j} \right\rangle = \frac{v}{\Delta t} (C_{2,s}^j - C_{2,s}^{j-1}) \quad (\text{A-8.9})$$

$$QC_{2,s}^j - QC_{3,s}^j + \frac{A_{c,s} \mathcal{D}_s}{\Delta x} (C_{3,s}^j - C_{2,s}^j) + v \left\langle r_{C_{3,s}^j} \right\rangle = \frac{v}{\Delta t} (C_{3,s}^j - C_{3,s}^{j-1}) \quad (\text{A-8.10})$$

$$QC_{z'-1,s}^j - QC_{z',s}^j + \frac{A_{c,s} \mathcal{D}_s}{\Delta x} (C_{z',s}^j - C_{z'-1,s}^j) + v \left\langle r_{C_{z',s}^j} \right\rangle = \frac{v}{\Delta t} (C_{z',s}^j - C_{z',s}^{j-1}) \quad (\text{A-8.11})$$

The outside cross-sectional area of the hollow fibers ( $A_{c,s}$ ), as shown in Figure 8.2(b), is calculated by Eq. (A-8.12).

$$A_{c,s} = N \left( d_o^2 - \frac{\pi d_o^2}{4} \right) \quad (\text{A-8.12})$$

where  $N$  is the number of hollow fibers, and  $d_o$  is outside diameter of a hollow fiber.

To linearize the rate of recovery ( $r_{C_{z',s}^j}$ ) in Eqs. ((A-8.8)-(A-8.11)), the Taylor series is applied:

$$r_{C_{z',s}^j} = \gamma C_{z',s}^j + \lambda \quad (\text{A-8.13})$$

$$\text{where} \quad \gamma = nk_{\text{stripping}} (C_{0,s}^j)^{n-1}, \quad \lambda = (1-n)k_{\text{stripping}} (C_{0,s}^j)^n$$

$C_{0,s}^j$  is the concentration of silver ions in stripping phase at  $z' = 0$ , and represents an individual value for each sequence of space time  $j$ .

The mass conservation equations of silver ions Eqs. ((A-8.8)-(A-8.11)) are divided by the volumetric flow rate of stripping phase ( $Q$ ), and deriving in matrix, as shown below:

$$[A'] [C'] = [Y'] \quad (\text{A-8.14})$$

where

$$[A'] = \begin{bmatrix} -(1-e-f+d) & 0 & 0 & \dots & 0 & 0 \\ (1-e) & -(1-e-f+d) & 0 & \dots & 0 & 0 \\ 0 & 1-e & -(1-e-f+d) & \dots & 0 & 0 \\ \cdot & & & & & \cdot \\ \cdot & & & \dots & & \cdot \\ \cdot & & & & & \cdot \\ 0 & & & \dots & (1-e) & -(1-e-f+d) \end{bmatrix}_{z' \times z'}$$

$$[C'] = \begin{bmatrix} C_{1,s}^j \\ C_{2,s}^j \\ C_{3,s}^j \\ \cdot \\ \cdot \\ \cdot \\ C_{z',s}^j \end{bmatrix}_{z' \times 1}, \quad [Y'] = \begin{bmatrix} -g - (1-a)C_{0,s}^j - dC_{1,s}^{j-1} \\ -g - dC_{2,s}^{j-1} \\ -g - dC_{3,s}^{j-1} \\ \cdot \\ \cdot \\ -g - dC_{z',s}^{j-1} \end{bmatrix}_{z' \times 1}$$

$$\text{when } e = \frac{A_{c,s} D_s}{Q \Delta t}, \quad f = \frac{v \gamma}{Q}, \quad g = \frac{v \lambda}{Q}$$

The concentration of silver ions in the stripping phase depends on the concentration of complex species at the liquid membrane-stripping interface which is estimated from the diffusion flux by Eq. (A-8.15).

$$J_m = k_m \left( C_{z,fi}^j - C_{z',si}^j \right) \quad (\text{A-8.15})$$

where  $J_m$  is the diffusion flux of complex species across liquid membrane phase,  $k_m$  is the mass transfer coefficient of complex species across the liquid membrane phase,  $C_{z,fi}^j$  is the concentration of complex species at segment  $z$  of the feed-liquid membrane interface, and  $C_{z',si}^j$  is the concentration of complex species at segment  $z'$  of the liquid membrane-stripping interface.

$C_{z,fi}^j$  is calculated based on the concentration difference of silver ions in feed phase between segment  $z - 1$  and segment  $z$ , as follows:

$$C_{z,fi}^j = C_{z-1,f}^j - C_{z,f}^j \quad (\text{A-8.16})$$

By substituting Eq. (A-8.16) into Eq. (A-8.15), the diffusion flux of complex species across liquid membrane phase becomes:

$$J_m = k_m \left( C_{z-1,f}^j - C_{z,f}^j - C_{z',si}^j \right) \quad (\text{A-8.17})$$

With respect to the assumption of high driving force (concentration gradient) in liquid membrane phase, the diffusion of complex species across the liquid membrane phase ( $J_m$ ) is relatively fast. Thus, the mass flux in this phase depends on the reaction flux across the feed-liquid membrane interface ( $J_r$ ), which can be defined as follows:

$$J_r = k_{\text{extraction}} C_{z,f}^j - k_{\text{extraction}} C_{z,fi}^j = k_{\text{extraction}} C_{z,f}^j - k_{\text{extraction}} (C_{z-1,f}^j - C_{z,f}^j) \quad (\text{A-8.18})$$

Substituting the reaction flux in Eq. (A-8.18) into Eq. (A-8.17), the concentration of complex species at segment  $z'$  of the liquid membrane-stripping interface can be determined by Eq. (A-8.19):

$$C_{z',si}^j = \frac{(k_m + k_{\text{extraction}})C_{z-1,f}^j - (k_m + 2k_{\text{extraction}})C_{z,f}^j}{k_m} \quad (\text{A-8.19})$$

### 8.8 Nomenclature and units

$a$	parameter in Eqs. (A-8.7) and (A-8.14)
$A_{\text{eff}}$	effective surface area of the hollow fibers ( $\text{dm}^2$ )
$A_{c,f}$	inside cross-sectional area of the hollow fibers ( $\text{dm}^2$ )
$A_{c,s}$	outside cross-sectional area of the hollow fibers ( $\text{dm}^2$ )
$\text{AgR}$	complex species of silver ions and extractant in liquid membrane phase
$b$	parameter in Eq. (A-8.7)
$c$	parameter in Eq. (A-8.7)
$C$	concentration of silver ions ( $\text{mg/L}$ )
$C_0^j$	concentration of silver ions at $z = 0$ representing an individual value of each sequence of the space time $j$ ( $\text{mg/L}$ )
$C_z^j$	concentration of silver ions at segment $z$ representing an individual value of each sequence of the space time ( $\text{mg/L}$ )
$d$	parameter in Eqs. (A-8.7) and (A-8.14)
$d_i$	inside diameter of a hollow fiber ( $\text{dm}$ )
$d_o$	outside diameter of a hollow fiber ( $\text{dm}$ )
$D$	distribution ratio of silver ion extraction
$\mathcal{D}_f$	diffusion coefficient of silver ions in feed phase ( $\text{dm}^2/\text{min}$ )
$\mathcal{D}_s$	diffusion coefficient of silver ions in stripping phase ( $\text{dm}^2/\text{min}$ )
$e$	parameter in Eq. (A-8.14)

$f$	parameter in Eq. (A-8.14)
$H^+$	hydrogen ion
$\overline{HR}$	extractant in liquid membrane phase
$i$	integer number
$j$	sequence of space time for feed and stripping solutions flowing inside and outside the hollow fibers
$J_m$	diffusion flux of complex species across liquid membrane phase ( $\text{mg}/\text{dm}^2 \cdot \text{min}$ )
$J_r$	reaction flux of silver ions at feed–liquid membrane interface ( $\text{mg}/\text{dm}^2 \cdot \text{min}$ )
$k_f$	mass transfer coefficient of silver ions in feed phase ( $\text{dm}/\text{min}$ )
$k_{\text{extraction}}$	reaction rate constant of the extraction of silver ions ( $\text{min}^{-1}$ )
$k_m$	mass transfer coefficient of complex species across liquid membrane phase ( $\text{dm}/\text{min}$ )
$k_s$	mass transfer coefficient of silver ions in stripping phase ( $\text{dm}/\text{min}$ )
$k_{\text{stripping}}$	reaction rate constant of the recovery of silver ions ( $\text{min}^{-1}$ )
$K_{\text{ex}}$	equilibrium constant of silver ion extraction ( $\text{dm}^3/\text{mg}$ )
$L$	length of a hollow fiber ( $\text{dm}$ )
$m$	reaction order of the extraction of silver ions
$M_w$	molecular weight of water ( $\text{mg}/\text{mol}$ )
$n$	reaction order of the recovery of silver ions
$N$	number of hollow fibers
$P$	overall mass transfer coefficient of silver ion transport in the HFSLM system ( $\text{dm}/\text{min}$ )
$P_m$	permeability coefficient of complex species in liquid membrane phase ( $\text{dm}/\text{min}$ )
$Q$	volumetric flow rate ( $\text{dm}^3/\text{min}$ ) of feed and stripping phases
$r_{-\text{Ag}^+}$	rate of silver ion extraction ( $\text{mg}/\text{dm}^3 \cdot \text{min}$ )
$r_{\text{Ag}^+}$	rate of silver ion recovery ( $\text{mg}/\text{dm}^3 \cdot \text{min}$ )

$r_{C_z}^j$	average rate of silver ion extraction as a function of silver ion concentration at segment $z$ and sequence of space time $j$
$r_{in}$	inside radius of a hollow fiber (dm)
$r_{lm}$	log-mean radius of a hollow fiber (dm)
$r_{out}$	outside radius of a hollow fiber (dm)
$t$	extraction or recovery time (min)
$T$	temperature of feed phase (K)
$v$	molar volume of silver ions at normal boiling point ( $\text{dm}^3/\text{mol}$ ) or parameter in fluid-flow model
$V_f$	volume of feed solution ( $\text{dm}^3$ )
$x$	longitudinal axis of the hollow fibers (dm)
$z$	number of small segments in feed phase
$z'$	number of small segments in stripping phase

#### Greek letters

$\alpha$	parameter a constant in Eq. (A-8.6)
$\beta$	parameter a constant in Eq. (A-8.6)
$\gamma$	parameter a constant in Eq. (A-8.13)
$\varepsilon$	porosity of hollow fibers (%)
$\eta_w$	viscosity of water (cP)
$\theta$	parameter in Eqs. (8.12) and (8.13)
$\lambda$	parameter a constant in Eq. (A-8.13)
$\tau$	tortuosity of hollow fibers

#### Symbols

$\langle \rangle$	average value of the reaction rate
$\Delta$	small segment of longitudinal axis of the hollow fibers
$\phi$	association factor of water

[ ]	concentration (mg/L)
[A]	matrix of the constants in feed phase
[A']	matrix of the constants in stripping phase
[C]	matrix of silver ion concentrations in feed phase at sequence of space times j
[C']	matrix of silver ion concentrations in stripping phase at sequence of space times j
[Y]	matrix of silver ion concentrations in feed phase at sequence of space times j - 1
[Y']	matrix of silver ion concentrations in stripping phase at sequence of space times j-1

### *Subscripts*

Ag <sup>+</sup>	silver ion
Expt.	experimental results
f	feed phase
fi	feed-liquid membrane interface
m	liquid membrane phase
s	stripping phase
si	liquid membrane-stripping interface
Theo.	modeling results
w	water

## **8.9 Acknowledgements**

The authors gratefully acknowledge financial support by the Thailand Research Fund and Chulalongkorn University under the Royal Golden Jubilee Ph.D. program (Grant No. PHD/0272/2549). Sincere thanks also go to the Government Pharmaceutical Organization of Thailand, the Separation Laboratory, Department of

Chemical Engineering, Chulalongkorn University, Bangkok, Thailand, Asst. Prof. Dr.Prakorn Ramakul, Faculty of Engineering and Industrial Technology, Silpakorn University, and Mr. Siwapat Tochan for their kind support.

### 8.10 References

- [1] S.W.P. Wijnhoven, W.J.G.M. Peijnenburg, C.A. Herberts, W.I. Hagens, A.G. Oomen, E.H.W. Heugens, B. Roszek, J. Bisschops, I. Gosens, D. van de Meent, S. Dekkers, W.H. de Jong, M. van Zijverden, A.J.A.M. Sips, R.E. Geertsma, Nano-silver-a review of available data and knowledge gaps in human and environmental risk assessment, *Nanotoxicology* 3(2) (2009) 109-138.
- [2] S. Altin, Y. Yildirim, A. Altin, Transport of silver ions through a flat-sheet supported liquid membrane, *Hydrometallurgy* 103 (2010) 144-149.
- [3] N. Othman, H. Mat, M. Goto, Separation of silver from photographic wastes by emulsion liquid membrane system, *Journal of Membrane Science* 282 (2006) 171-177.
- [4] Announcement of the Industrial Estate Authority of Thailand, 1998. Effluent from Factory to Central Wastewater Treatment Plant Amata Nakorn and Amata City Industrial Estate: Last Revised: November 11, 1998. ([http://www.amatawater.com/upload/waterlawfile/26\\_Discharge%20from%2031-3-11.pdf](http://www.amatawater.com/upload/waterlawfile/26_Discharge%20from%2031-3-11.pdf); last accessed 5 January 2012).
- [5] G. Pfrepper, R. Pfrepper, M. Knothe, Recovery of palladium and silver from process solution by precipitation with thiocyanates and iron cyanides, *Hydrometallurgy* 21 (1989) 377-383.
- [6] A. El Bachiri, A. Hagège, M. Burgard, Recovery of silver nitrate by transport across a liquid membrane containing dicyclohexano 18 crown 6 as a carrier, *Journal of Membrane Science* 121 (1996) 159-168.
- [7] F.Z. El Aamrani, A. Kumar, L. Beyer, A. Florido, A.M. Sastre, Mechanistic study of active transport of silver(I) using sulfur containing novel carriers across a liquid membrane, *Journal of Membrane Science* 152 (1999) 263-275.

- [8] M. Samsipur, M. Javanbakht, Z. Ghasemi, M.R. Ganjali, V. Lippolis, A. Garau, Separation, preconcentration and determination of trace amounts of silver ion in aqueous samples using octadecyl silica membrane disks modified with some recently synthesized mixed aza-thioether crowns containing 1,10-phenanthroline sub-unit and atomic absorption spectrometry, *Separation and Purification Technology* 28 (2002) 141-147.
- [9] M.A. Chaudry, N. Bukhari, M. Mazhar, Coupled transport of Ag(I) ions through triethanolamine-cyclohexanone-based supported liquid membranes, *Journal of Membrane Science* 320 (2008) 93-100.
- [10] S. Çoruh, G. Şenel, O.N. Ergun, A comparison of the properties of natural clinoptilolites and their ion-exchange capacities for silver removal, *Journal of Hazardous Materials* 180 (2010) 486-492.
- [11] B. Tang, G. Yu, J. Fang, T. Shi, Recovery of high-purity silver directly from dilute effluents by an emulsion liquid membrane-crystallization process, *Journal of Hazardous Materials* 177 (2010) 377-383.
- [12] T. Zh. Sadyrbaeva, Liquid membrane system for extraction and electrodeposition of silver(I), *Journal of Electroanalytical Chemistry* 648 (2010) 105-110.
- [13] K.R. Desai, Z.V.P. Murthy, Removal of silver from aqueous solutions by complexation-ultrafiltration using anionic polyacrylamide, *Chemical Engineering Journal* 185-186 (2012) 187-192.
- [14] U. Pancharoen, S. Somboonpanya, S. Chaturabul, A.W. Lothongkum, Selective removal of mercury as  $\text{HgCl}_4^{2-}$  from natural gas well produced water by TOA via HFSLM, *Journal of Alloys and Compounds* 489 (2010) 72-79.
- [15] K.F. Lam, H. Kassab, M. Pera-Titus, K.L. Yeung, B. Albela, L. Bonneviot, MCM-41 "LUS": alumina tubular membranes for metal separation in aqueous solution, *Journal of Physical Chemistry C* 115 (2011) 176-187.
- [16] X.Q. Chen, K.F. Lam, K.L. Yeung, Selective removal of chromium from different aqueous systems using magnetic MCM-41 nanosorbents, *Chemical Engineering Journal* 172 (2011) 728-734.

- [17] X.Q. Chen, K.F. Lam, Q. Zhang, B. Pan, M. Arruebo, K.L. Yeung, Synthesis of highly selective magnetic mesoporous adsorbent, *Journal of Physical Chemistry C* 113 (2009) 9804-9813.
- [18] K.F. Lam, C.M. Fong, K.L. Yeung, G. McKay, Selective adsorption of gold from complex mixtures using mesoporous adsorbents, *Chemical Engineering Journal* 145 (2008) 185-195.
- [19] K.F. Lam, X.Q. Chen, C.M. Fong, K.L. Yeung, Selective mesoporous adsorbents for  $\text{Ag}^+/\text{Cu}^{2+}$  separation, *Chemical Communications* 17 (2008) 2034-2036.
- [20] K.F. Lam, K.L. Yeung, G. McKay, Selective mesoporous adsorbents for  $\text{Cr}_2\text{O}_7^{2-}$  and  $\text{Cu}^{2+}$  separation, *Microporous and Mesoporous Materials* 100 (2007) 191-201.
- [21] B.S. Inbaraj, J.S. Wang, J.F. Lu, F.Y. Siao, B.H. Chen, Adsorption of toxic mercury(II) by an extracellular biopolymer poly( $\gamma$ -glutamic acid), *Bioresource Technology* 100 (2009) 200-207.
- [22] A. Uheida, Y. Zhang, M. Muhammed, Transport of palladium(II) through hollow fiber supported liquid membrane facilitated by nonylthiourea, *Journal of Membrane Science* 241 (2004) 289-295.
- [23] D. Huang, K. Huang, S. Chen, S. Liu, J. Yu, Rapid reaction-diffusion model for the enantioseparation of phenylalanine across hollow fiber supported liquid membrane, *Separation Science and Technology* 43 (2008) 259-272.
- [24] U. Pancharoen, W. Poonkum, A.W. Lothongkum, Treatment of arsenic ions from produced water through hollow fiber supported liquid membrane, *Journal of Alloys and Compounds* 482 (2009) 328-334.
- [25] Z. Weidong, C. Chunhua, H. Zisu, Transport study of Cu(II) through hollow fiber supported liquid membrane, *Chinese Journal of Chemical Engineering* 18(1) (2010) 48-54.
- [26] A.W. Lothongkum, S. Suren, S. Chaturabul, N. Thamphiphit, U. Pancharoen, Simultaneous removal of arsenic and mercury from natural-gas-co-produced water from the Gulf of Thailand using synergistic extractant via HFSLM, *Journal of Membrane Science* 369 (2011) 350-358.

- [27] P. Kandwal, S. Dixit, S. Mukhopadhyay, P.K. Mohapatra, Mass transport modeling of Cs(I) through hollow fiber supported liquid membrane containing calix-[4]-bis(2,3-naphtho)-crown-6 as the mobile carrier, *Chemical Engineering Journal* 174 (2011) 110-116.
- [28] N. Sunsandee, N. Leepipatpiboon, P. Ramakul, U. Pancharoen, The selective separation of (S)-amlodipine via a hollow fiber supported liquid membrane: modeling and experimental verification, *Chemical Engineering Journal* 180 (2012) 299-308.
- [29] S. Suren, T. Wongsawa, U. Pancharoen, T. Prapasawat, A.W. Lothongkum, Uphill transport and mathematical model of Pb(II) from dilute synthetic lead-containing solutions across hollow fiber supported liquid membrane, *Chemical Engineering Journal* 191 (2012) 503-511.
- [30] Y. Liu, B. Shi, Hollow fiber supported liquid membrane for extraction of ethylbenzene and nitrobenzene from aqueous solution: a Hansen solubility parameter approach, *Separation and Purification Technology* 65 (2009) 233-242.
- [31] W. Zhang, C. Cui, Z.i Ren, Y. Dai, H. Meng, Simultaneous removal and recovery of copper(II) from acidic wastewater by hollow fiber renewal liquid membrane with LIX984N as carrier, *Chemical Engineering Journal* 157 (2010) 230-237.
- [32] Water Environment Federation, Membrane equipment and system overview, *Membrane Systems for Wastewater Treatment*, McGraw-Hill, New York, 2006, p. 27.
- [33] R. Field, Fundamentals of fouling, in: K.-V. Peonemann and S.P. Nunes (Eds.), *Membranes for Water Treatment*, Wiley-VCH, Weinheim, 2010, p. 15.
- [34] A. Kumar, A.M. Sastre, Hollow fiber supported liquid membrane for the separation/concentration of gold(I) from aqueous cyanide media: modeling and mass transfer evaluation, *Industrial & Engineering Chemistry Research* 39 (2000) 146-154.
- [35] E. Bringas, M.F. San Román, J.A. Irabien, I. Ortiz, An overview of the mathematical modelling of liquid membrane separation processes in hollow

- fiber contactors, *Journal of Chemical Technology and Biotechnology* 84 (2009) 1583-1614.
- [36] Z. Wang, Y. Cui, W. Wu, S. Ji, J. Yao, H. Zhang, X. Zhao, The convective model of flux prediction in a hollow-fiber module for a steady-state cross-flow microfiltration system, *Desalination* 238 (2009) 192-209.
- [37] D. Trébouet, M. Burgard, J.M. Loureiro, Guideline for the application of a stationary model in the prediction of the overall mass transfer coefficient in a hollow fiber membrane contactor, *Separation and Purification Technology* 50 (2006) 97-106.
- [38] E. Nagy, P. Hadik, Analysis of mass transfer in hollow-fiber membranes, *Desalination* 145 (2002) 147-152.
- [39] A.I. Alonso, C.C. Pantelides, Modelling and simulation of integrated membrane processes for recovery of Cr(VI) with Aliquat 336, *Journal of Membrane Science* 110 (1996) 151-167.
- [40] B. Sengupta, M.S. Bhakhar, R. Sengupta, Extraction of zinc and copper-zinc mixtures from ammoniacal solutions into emulsion liquid membranes using LIX 84-I, *Hydrometallurgy* 99 (2009) 25-32.
- [41] V.S. Kislik, Carrier-facilitated coupled transport through liquid membranes: general theoretical considerations and influencing parameters, in: V.S. Kislik (Ed.), *Liquid Membranes: Principles and Applications in Chemical Separations and Wastewater Treatment*, first ed., Elsevier, The Netherlands, 2010, pp. 17-18.
- [42] O.N. Ata, Mathematical modelling of unsteady-state transport of metal ions through supported liquid membrane, *Hydrometallurgy* 87 (2007) 148-156.
- [43] A. Kumar, R. Haddad, G. Benzal, R. Ninou, A.M. Sastre, Use of modified membrane carrier system for recovery of gold cyanide from alkaline cyanide media using hollow fiber supported liquid membranes: feasibility studies and mass transfer modeling, *Journal of Membrane Science* 174 (2000) 17-30.
- [44] P.R. Danesi, A simplified model for the coupled transport of metal ions through hollow-fiber supported liquid membranes, *Journal of Membrane Science* 20 (1984) 231-248.

- [45] N.S. Rathore, J.V. Sonawane, A. Kumar, A.K. Venugopalan, R.K. Singh, D.D. Bajpai, J.P. Shukla, Hollow fiber supported liquid membrane: a novel technique for separation and recovery of plutonium from aqueous acidic wastes, *Journal of Membrane Science* 189 (2001) 119-128.
- [46] A.W. Lothongkum, Y. Khemglad, N. Usomboon, U. Pancharoen, Selective recovery of nickel ions from wastewater of stainless steel industry via HFSLM, *Journal of Alloys and Compounds* 476 (2009) 940-949.
- [47] A.A. Amiri, A. Safavi, A.R. Hasaninejad, H. Shrghi, M. Shamsipur, Highly selective transport of silver ion through a supported liquid membrane using calix[4]pyrroles as suitable ion carriers, *Journal of Membrane Science* 325 (2008) 295-300.
- [48] C.J. Geankoplis, Molecular mass transport phenomena in fluids, in: C.J. Geankoplis (Ed.), *Mass Transport Phenomena*, Holt, Rinehart and Winston, Inc., U.S., 1972, p. 35.
- [49] U. Pancharoen, T. Wongsawa, A.W. Lothongkum, A reaction flux model for extraction of Cu(II) with LIX 84-I in HFSLM, *Separation Science and Technology* 46 (2011) 2183-2190.
- [50] S.H. Lin, R.S. Juang, Mass-transfer in hollow-fiber modules for extraction and back-extraction of copper(II) with LIX 64N carriers, *Journal of Membrane Science* 188 (2001) 251-262.
- [51] N. Alizadeh, S. Salimi, A. Jabbari, Transport study of palladium through a bulk liquid membrane using hexadecylpyridinium as carrier, *Separation and Purification Technology* 28 (2002) 173-180.
- [52] A.W. Lothongkum, U. Pancharoen, T. Prapasawat, Roles of facilitated transport through HFSLM in engineering applications, in: J. Markoš (Ed.), *Mass Transfer in Chemical Engineering Processes*, InTech Open Access Publisher, Rijeka, Croatia, 2011, p. 199.
- [53] D. Buachuang, P. Ramakul, N. Leepipatpiboon, U. Pancharoen, Mass transfer modeling on the separation of tantalum and niobium from dilute hydrofluoric media through a hollow fiber supported liquid membrane, *Journal of Alloys and Compounds* 509 (2011) 9549-9557.

- [54] C.R. Wilke, P. Chang, Correlation of diffusion coefficients in dilute solutions, *AIChE Journal* 1(2) (1955) 264-270.



## Chapter IX

### Conclusion and recommendations

#### 9.1 Conclusion

This research has been instrumental in achieving a high rate of success in the extraction and recovery of silver ions from pharmaceutical wastewater via HFSLM. Percentages of extraction and recovery reached 98% and 85% respectively, under the following conditions: feed and stripping pH of 3.5 and 2, 0.1 mol/L LIX 84-I, 0.5 mol/L sodium thiosulfate solution, feed and stripping flow rates of 200 mL/min, separation time of 26 min and operating by counter-circulating mode. The final concentration of silver ions in the feed solution was lower than the mandatory discharge limit.

A study on the solubility of organic diluents (MIBK, ethyl acetate, furfural or *n*-butanol) with organic compounds (furfuryl alcohol, cyclopentanone or cyclopentanol) and water was investigated to select a suitable organic diluent for use in the extraction processes. Tie-lines were also studied to confirm the extraction capability of the organic diluents.

A further study on solubility was also undertaken highlighting the extraction of silver ions using D2EHPA as extractant. Organic diluents such as kerosene, cyclohexane, chloroform and 1-octanol having different dielectric constants were used to carry out this study. Solubility increased with the polarity of organic diluents. However, the increase in polarity led to an increase in solubility between the organic diluent and water. In extraction processes, the solubility of organic diluents in water can cause the loss of the organic phase into the aqueous phase. The influence of organic diluents on silver ion extraction was investigated by liquid-liquid extraction. The polarity of organic diluents resulted in a slight increase in extraction efficiency.

From both studies, kerosene was found to be the most suitable organic diluent for use in the extraction of silver ions.

The mathematical model involving convection, reaction and accumulation of copper ions in the HFSLM was noted for its high reliability (deviation of 2%) to predict the concentration of copper ions in the feed phase. Separation time of 10 min and 15 separation cycles were determined by the modeling results. This model was also applied for silver ion extraction. The results were compared with another model that considered only diffusion. The lower deviation of the first model demonstrated its validity to describe the transport of silver ions that involved convection, reaction and accumulation in the HFSLM. In addition, a comparison of the results of both models indicated the influence of reaction on the transport of silver ions through the liquid membrane phase.

The mathematical model was further developed to include diffusion of silver ions using a matrix formation. Concentration of silver ions in the feed phase was determined by varying the time interval. Higher reliability (deviation of 1.78%) of the developed model changed the status of silver ion transport to involve convection, diffusion, reaction and accumulation in the HFSLM. Thereafter, the model was applied for silver ion recovery and other metal ion extractions i.e. copper and tantalum ions. The model still provided high reliability for these studies as confirmed by the deviation of 2%.

The highlights of this dissertation can be summarized as follows:

1. HFSLM is highly efficient on the extraction and recovery of metal ions at low concentration. Thus, it is a most suitable method for treatment of industrial wastewater containing metal ions at ppm level.
2. The study on solubility is easily carried out in order to select a suitable organic diluent for use in the separation processes.

3. The mathematical models involving convection, diffusion, reaction and accumulation of metal ions in the HFSLM proved to have high reliability in the prediction of their extraction and recovery as well as their transport mechanisms. The modeling results were able to determine the suitable separation time and separation cycles. In addition, they are able to use as a case study for other metal ion extractions and recoveries.
4. The recycling of silver ions in the stripping solution can be precipitated by operating the pH of stripping solution at a value greater than 7.

## 9.2 Problems and constraints

1. In the solubility experiments, turbidity of samples was observed by eyesight but this can cause an error in measurement. Thus, repeat experiments must be operated more than three times and the results should be validated with other accurate data.
2. In the HFSLM, liquid membrane used was recycled three times.
3. pH of feed and stripping solutions must be lower than 1 to prevent the corrosion of acid in the HFSLM.
4. For a mathematical model, the value of metal ion concentration at the segment of  $z = z' = 0$  is determined by the different principles as based on the flow patterns in the HFSLM. In the case of the circulating flow pattern, the average value of metal ion concentration in the feed or stripping reservoir is used. However, for the single-pass flow pattern the initial concentration of metal ions is referred in the model.

## 9.3 Recommendations for future research

1. Pre-treatment of wastewater must be operated to prevent fouling in the HFSLM.
2. Other wastewater sources of silver ions such as silverware, jewelry, photography and electronics should be applied to the HFSLM.

3. Study on the stability of the HFSLM should be undertaken for scaling up.
4. A mathematical model should be applied for other metal ion extractions and recoveries.



## REFERENCES

1. Announcement of the Industrial Estate Authority of Thailand, Effluent from Factory to Central Wastewater Treatment Plant Amata Nakorn and Amata City Industrial Estate, [http://www.amatawater.com/upload/waterlawfile/26 Discharge%20from%2031-3-11.pdf](http://www.amatawater.com/upload/waterlawfile/26%20Discharge%20from%2031-3-11.pdf). (revised 11.11.98; accessed 05.01.12).
2. S.W.P. Wijnhoven, W.J.G.M. Peijnenburg, C.A. Herberts, W.I. Hagens, A.G. Oomen, E.H.W. Heugens, B. Roszek, J. Bisschops, I. Gosens, D. van de Meent, S. Dekkers, W.H. de Jong, M. van Zijverden, A.J.A.M. Sips, R.E. Geertsma, Nano-silver - a review of available data and knowledge gaps in human and environmental risk assessment, *Nanotoxicology* 3(2) (2009) 109-138.
3. Y.-M. Sue, J.Y.-Y. Lee, M.-C. Wang, T.-K. Lin, J.-M. Sung, J.-J. Huang, Generalized argyria in two chronic hemodialysis patients, *American Journal of Kidney Diseases* 37(5) (2001) 1048-1051.
4. J. Albrechtsen, Toxicology Brief, managing common poisonings in companion animals: the toxicity of iron, an essential element, *Veterinary Medicine* (2006) 82-90.
5. B. Tang, G. Yu, J. Fang, T. Shi, Recovery of high-purity silver directly from dilute effluents by an emulsion liquid membrane-crystallization process, *Journal of Hazardous Materials* 177 (2010) 377-383.
6. R. Güell, E. Antico, V. Salvadó, C. Fontàs, Efficient hollow fiber supported liquid membrane system for the removal and preconcentration of Cr(VI) at trace levels, *Separation and Purification Technology* 62 (2008) 389-393.
7. A. Uheida, Y. Zhang, M. Muhammed, Transport of palladium(II) through hollow fiber supported liquid membrane facilitated by nonylthiourea, *Journal of Membrane Science* 241 (2004) 289-295.
8. X.J. Yang, A.G. Fane, C. Pin, Separation of zirconium and hafnium using hollow fibers: part I supported liquid membranes, *Chemical Engineering Journal* 88 (2002) 37-44.

9. N.S. Rathore, J.V. Sonawane, A. Kumar, A.K. Venugopalan, R.K. Singh, D.D. Bajpai, J.P. Shukla, Hollow fiber supported liquid membrane: a novel technique for separation and recovery of plutonium from aqueous acidic wastes, *Journal of Membrane Science* 189 (2001) 119-128.
10. Y. Liu, B. Shi, Hollow fiber supported liquid membrane for extraction of ethylbenzene and nitrobenzene from aqueous solution: a Hansen solubility parameter approach, *Separation and Purification Technology* 65 (2009) 233-242.
11. N. Othman, M. Goto, H. Mat, Solvent extraction of metals from liquid photographic waste using acidic extractants, *Jurnal Teknologi* 42(F) (2005) 25-34.
12. S. Suren, T. Wongsawa, U. Pancharoen, T. Prapasawat, A.W. Lothongkum, Uphill transport and mathematical model of Pb(II) from dilute synthetic lead-containing solutions across hollow fiber supported liquid membrane, *Chemical Engineering Journal* 191 (2012) 503-511.
13. G. Yang, M.S. Jahan, L. Ahsan, Y. Ni, Influence of the diluent on the extraction of acetic acid from the prehydrolysis liquor of kraft based dissolving pulp production process by tertiary amine, *Separation and Purification Technology* 120 (2013) 341-345.
14. N.M. Kocherginsky, Q. Yang, L. Seelam, Recent advances in supported liquid membrane technology, *Separation and Purification Technology* 53 (2007) 171-177.
15. E. Bringas, M.F. San Roman, J.A. Irabien, I. Ortiz, An overview of the mathematical modeling of liquid membrane separation processes in hollow fiber contactors, *Journal of Chemical Technology and Biotechnology* 84 (2009) 1583-1614.
16. S. Suren, "The application of hollow fiber supported liquid membrane to separate lead, mercury and arsenic ions from synthetic water and mathematical model for prediction", Doctoral Dissertation, Chulalongkorn University, July 2013.

17. P.W. Atkins, J.S.E. Holker, A.K. Holliday, Chapter 1: Properties of ligands and chelate rings, in: P.W. Atkins, J.S.E. Holker, A.K. Holliday (Eds.), *Principles and Applications of Metal Chelation*, 9-29, Oxford: Oxford University Press, 1977.
18. Cognis: *Mining Chemicals Technology*, MCT Redbook: *Solvent Extraction Reagents and Applications*, 1-73, Cognis Group, 2007.
19. R.-S. Juang, H.-L. Huang, Modeling of nondispersive extraction of binary Zn(II) and Cu(II) with D2EHPA in hollow fiber devices, *Journal of Membrane Science* 208 (2002) 31-38.
20. B. Sengupta, M.S. Bhakhar, R. Sengupta, Extraction of zinc and copper-zinc mixtures from ammoniacal solutions into emulsion liquid membranes using LIX 84-I, *Hydrometallurgy* 99 (2009) 25-32.
21. A. Grzeszczyk, M. Regel-Rosocka, Extraction of zinc(II), iron(II) and iron(III) from chloride media with dibutyl butylphosphonate, *Hydrometallurgy* 86 (2007) 72-79.
22. V.S. Kislík, Chapter 5: examples of application of solvent extraction techniques in chemical, radiochemical, biochemical, pharmaceutical, analytical separations, and wastewater treatment, in: V.S. Kislík (Ed.), *Solvent Extraction: Classical and Novel Approaches*, 185-313, The Netherlands: Elsevier, 2012.
23. P.K. Parhi, K.-H. Park, H.-I. Kim, J.-T. Park, Recovery of molybdenum from the sea nodule leach liquor by solvent extraction using Alamine 304-I, *Hydrometallurgy* 105 (2011) 195-200.
24. V.S. Kislík, Chapter 2: Carrier-facilitated coupled transport through liquid membranes: general theoretical considerations and influencing parameters, in: V.S. Kislík (Ed.), *Liquid Membranes: Principles and Applications in Chemical Separations and Wastewater Treatment*, 17-71, The Netherlands: Elsevier, 2010.
25. A. Gherrou, H. Kerdjoudj, R. Molinari, E. Drioli, Removal of silver and copper ions from acidic thiourea solutions with a supported liquid membrane containing D2EHPA as carrier, *Separation and Purification Technology* 28 (2002) 235-244.

26. S.C. Lee, B.S. Ahn, W.K. Lee, Mathematical modeling of silver extraction by an emulsion liquid membrane process, *Journal of Membrane Science* 114 (1996) 171-185.
27. T.Zh. Sadyrbaeva, Liquid membrane system for extraction and electrodeposition of silver(I), *Journal of Electroanalytical Chemistry* 648 (2010) 105-110.
28. S. Altin, Y. Yildirim, A. Altin, Transport of silver ions through a flat-sheet supported liquid membrane, *Hydrometallurgy* 103 (2010) 144-149.
29. A. El Bachiri, A. Hagege, M. Burgard, Recovery of silver nitrate by transport across a liquid membrane containing dicyclohexano18crown6 as a carrier, *Journal of Membrane Science* 121 (1996) 159-168.
30. A. Gherrou, H. Kerdjoudj, Specific membrane transport of silver and copper as  $\text{Ag}(\text{CN})_3^{2-}$  and  $\text{CuCN}_4^{3-}$  ions through a supported liquid membrane using  $\text{K}^+$ -crown ether as a carrier, *Desalination* 151 (2002) 87-94.
31. M. Shamsipur, M.H. Mashhadizadeh, Highly efficient and selective membrane transport of silver(I) using hexathia-18-crown-6 as a specific ion carrier, *Separation and Purification Technology* 20 (2000) 147-153.
32. M.S. Alam, K. Inoue, K. Yoshizuka, Y. Dong, P. Zhang, Solvent extraction of silver from chloride media with some commercial sulfur-containing extractants, *Hydrometallurgy* 44 (1997) 245-254.
33. N. Othman, H. Mat, M. Goto, Separation of silver from photographic wastes by emulsion liquid membrane system, *Journal of Membrane Science* 282 (2006) 171-177.
34. M.R. Chowdhury, S.K. Sanyal, Diluent effect on extraction of tellurium(IV) and selenium(IV) by tri-n butyl phosphate, *Hydrometallurgy* 34 (1994) 319-330.
35. T.H. Lowry, K.S. Richardson, Chapter 2: some fundamentals of physic organic chemistry, in: T.H. Lowry, K.S. Richardson (Eds.), *Mechanism and Theory in Organic Chemistry*, 57-123, New York: Harper and Row, Publishers, Inc., 1976.
36. E. Buncl, R.A. Stairs, H. Wilson, The solvent as medium, in: E. Buncl, R.A. Stairs, H. Wilson (Eds.), *The role of the solvent in chemical reactions*, 159, New York: Oxford University Press, Inc., 2003.

37. K. Wang, Z. Chang, Y. Ma, C. Lei, S. Jin, Y. Wu, I. Mahmood, C. Hua, H. Liu, Equilibrium study on reactive extraction of propionic acid with N1923 in different diluents, *Fluid Phase Equilibria* 278 (2009) 103-108.
38. A.P. de los Ríos, F.J. Hernandez-Fernandez, F. Tomás-Alonso, J.M. Palacios, G. Villora, Stability studies of supported liquid membranes based on ionic liquids: effect of surrounding phase nature, *Desalination* 245 (2009) 776-782.
39. Y.A. El-Nadi, Effect of diluents on the extraction of praseodymium and samarium by Cyanex923 from acidic nitrate medium, *Journal of Rare Earths* 28(2) (2010) 215-219.
40. S. Shailesh, P.N. Pathak, P.K. Mohapatra, V.K. Manchanda, Role of diluents in uranium transport across a supported liquid membrane using di(2-ethylhexyl)isobutyramide as the carrier, *Desalination* 232 (2008) 281-290.
41. N. Taoualit, D.E. Hadj-Boussaad, Metallic species ( $\text{Ag}^+$  and  $\text{Cu}^{2+}$  ions) transfer through a membrane-gel, *Desalination* 144 (2002) 273-277.
42. K. Ohto, H. Yamaga, E. Murakami, K. Inoue, Specific extraction behavior of amide derivative of calix[4]arene for silver(I) and gold(III) ions from highly acidic chloride media, *Talanta* 44 (1997) 1123-1130.
43. S.H. Yalkowsky, Y. He, Solubility data, in: S.H. Yalkowsky, Y. He (Eds.), *Handbook of Aqueous Solubility Data*, 1-1496, Florida: CRC Press, 2003.
44. Acros Organics, Material safety data sheet: chloroform, <https://www.fishersci.ca/viewmsds.do?catNo=AC406470050> (revised 22.12.14; accessed 22.12.14).
45. P. Dzygiel, P.P. Wiczorek, Chapter 3: Supported liquid membranes and their modifications: definition, classification, theory, stability, application and perspectives, in: V.S. Kislík (Ed.), *Liquid Membranes: Principles and Applications in Chemical Separations and Wastewater Treatment*, 72-140, The Netherlands: Elsevier, 2010.
46. M. Cox, Chapter 1: Liquid-liquid extraction and liquid membranes in the perspective of the twenty-first century, in: M. Aguilar, J.L. Cortina (Eds.), *Solvent Extraction and Liquid Membranes: Fundamentals and Applications in New Materials*, 1-19, U.S.: Taylor and Francis Group, 2008.

47. L. Pei, L. Wang, G. Yu, Study on a novel flat renewal supported liquid membrane with D2EHPA and hydrogen nitrate for neodymium extraction, *Journal of Rare Earths* 30(1) (2012) 63-68.
48. Y.T. Mohamed, A.H. Ibrahim, Extraction of copper from waste solution using liquid emulsion membrane, *Journal of Environmental Protection* 3 (2012) 129-134.
49. L. Pei, L. Wang, W. Guo, N. Zhao, Stripping dispersion hollow fiber liquid membrane containing PC-88A as carrier and HCl for transport behavior of trivalent dysprosium, *Journal of Membrane Science* 378 (2011) 520-530.
50. M.W. Ashraf, M.A. Iqbal, Removal of cadmium(II) from aqueous waste effluents by using supported liquid membrane technology, *Scientific Journal of Environmental Sciences* 1(3) (2012) 30-39.
51. F. de M. Fábrega, M.B. Mansur, Liquid-liquid extraction of mercury(II) from hydrochloric acid solutions by Aliquat 336, *Hydrometallurgy* 87 (2007) 83-90.
52. A.A. Amiri, A. Safavi, A.R. Hasaninejad, H. Shrghi, M. Shamsipur, Highly selective transport of silver ion through a supported liquid membrane using calix[4]pyrroles as suitable ion carriers, *Journal of Membrane Science* 325 (2008) 295-300.
53. M. Shamsipur, S.Y. Kazemi, Highly efficient and selective membrane transport of silver(I) using dibenzodiaza-15-crown-4 as a selective ion carriers, *Journal of the Chinese Chemical Society* 54 (2007) 963-968.
54. L. Pei, L. Wang, G. Yu, Separation of Eu(III) with supported dispersion liquid membrane system containing D2EHPA as carrier and HNO<sub>3</sub> solution as stripping solution, *Journal of Rare Earths* 29 (2011) 7-14.
55. K.K. Bhatluri, M.S. Manna, P. Saha, A.K. Ghoshal, Supported liquid membrane-based simultaneous separation of cadmium and lead from wastewater, *Journal of Membrane Science* 459 (2014) 256-263.
56. V.S. Kislik, Chapter 7: competitive complexation/solvation theory of solvent extraction: general mechanisms and kinetics, in: V.S. Kislik (Ed.), *Solvent Extraction: Classical and Novel Approaches*, 334-354, The Netherlands: Elsevier, 2012.

57. C.S. Kedari, S.S. Pandit, P.M. Gandhi, Separation by competitive transport of uranium(VI) and thorium(IV) nitrates across supported renewable liquid membrane containing trioctylphosphine oxide as metal carrier, *Journal of Membrane Science* 430 (2013) 188-195.
58. B. Swain, J. Jeong, J.-C. Lee, G.-H. Lee, Extraction of Co(II) by supported liquid membrane and solvent extraction using Cyanex 272 as an extractant: a comparison study, *Journal of Membrane Science* 288 (2007) 139-148.
59. Z. Huidong, C. Jingjing, W. Biyu, Z. Suying, Recovery of copper ions from wastewater by hollow fiber supported emulsion liquid membrane, *Chinese Journal of Chemical Engineering* 21(8) (2013) 827-834.
60. J.V. Sonawane, A.K. Pabby, A.M. Sastre, Au(I) extraction by LIX-79/n-heptane using the pseudo-emulsion-based hollow-fiber strip dispersion (PEHFSD) technique, *Journal of Membrane Science* 300 (2007) 147-155.
61. P.C. Rout, K. Sarangi, Separation of vanadium using both hollow fiber membrane and solvent extraction technique - a comparative study, *Separation and Purification Technology* 122 (2014) 270-277.
62. N. Alizadeh, S. Salimi, A. Jabbari, Transport study of palladium through a bulk liquid membrane using hexadecylpyridinium as carrier, *Separation and Purification Technology* 28 (2002) 173-180.
63. A. Kumar, R. Haddad, F.J. Alguacil, A.M. Sastre, Comparative performance of non-dispersive solvent extraction using a single module and the integrated membrane process with two hollow fiber contactors, *Journal of Membrane Science* 248 (2005) 1-14.
64. J. Marchese, M. Campderros, Mass transfer of cadmium ions in a hollow-fiber module by pertraction, *Desalination* 164 (2004) 141-149.
65. P. Ramakul, W. Pattaweekongka, U. Pancharoen, Mass transfer modeling of membrane carrier system for extraction of Ce(IV) from sulfate media using hollow fiber supported liquid membrane, *Korean Journal of Chemical Engineering* 23(1) (2006) 85-92.

66. Z. Weidong, C. Chunhua, H. Zisu, Transport study of  $\text{Cu(II)}$  through hollow fiber supported liquid membrane, *Chinese Journal of Chemical Engineering* 18(1) (2010) 48-54.
67. S.H. Lin, R.S. Juang, Mass-transfer in hollow-fiber modules for extraction and back-extraction of copper(II) with LIX 64-N carriers, *Journal of Membrane Science* 188 (2001) 251-262.
68. P. Kandwal, S. Dixit, S. Mukhopadhyay, P.K. Mohapatra, Mass transport modeling of  $\text{Cs(I)}$  through hollow fiber supported liquid membrane containing calix-[4]-bis(2,3-naphtho)-crown-6 as the mobile carrier, *Chemical Engineering Journal* 174 (2011) 110-116.
69. Q. Yang, N.M. Kocherginsky, Copper removal from ammoniacal wastewater through a hollow fiber supported liquid membrane system: modeling and experimental verification, *Journal of Membrane Science* 297 (2007) 121-129.
70. S. Chaturabul, K. Wongkaew, U. Pancharoen, Selective transport of palladium through a hollow fiber supported liquid membrane and prediction model based on reaction flux, *Separation Science and Technology* 48 (2012) 93-104.
71. T. Wongsawa, M. Hronec, T. Sotak, N. Leepipatpiboon, U. Pancharoen, S. Phatanasri, Ternary (liquid-liquid) equilibrium data of furfuryl alcohol with organic solvents at  $T = 298.2$  K: experimental results and thermodynamic models, *Fluid Phase Equilibria* 365 (2014) 88-96.
72. T. Wongsawa, M. Hronec, A.W. Lothongkum, U. Pancharoen, S. Phatanasri, Experiments and thermodynamic models for ternary (liquid-liquid) equilibrium systems of water + cyclopentanone + organic solvents at  $T = 298.2$  K, *Journal of Molecular Liquids* 196 (2014) 98-106.
73. T. Wongsawa, M. Hronec, U. Pancharoen, S. Phatanasri, Solubility and tie-line data for ternary aqueous mixtures of cyclopentanol with organic solvents at  $T = 298.2$  K: experiments and NRTL model, *Fluid Phase Equilibria* 379 (2014) 10-18.
74. T. Wongsawa, N. Sunsandee, A.W. Lothongkum, U. Pancharoen, S. Phatanasri, The role of organic diluents in the aspects of equilibrium, kinetics and

- thermodynamic model for silver ion extraction using an extractant D2EHPA, *Fluid Phase Equilibria* 388 (2015) 22-30.
75. U. Pancharoen, T. Wongsawa, A.W. Lothongkum, A reaction flux model for extraction of Cu(II) with LIX 84-I in HFSLM, *Separation Science and Technology* 46 (2011) 2183-2190.
76. T. Wongsawa, N. Sunsandee, A.W. Lothongkum, U. Pancharoen, High-efficiency HFSLM for silver-ion pertraction from pharmaceutical wastewater and mass-transport models, *Chemical Engineering Research and Design* 92 (2014) 2681-2693.
77. T. Wongsawa, N. Leepipatpiboon, N. Thamphiphit, U. Pancharoen, A.W. Lothongkum, Fluid-flow models operating on linear algebra for extraction and stripping of silver ions from pharmaceutical wastewater by HFSLM, *Chemical Engineering Journal* 222 (2013) 361-373.



## VITA

Ms. Thidarat Wongsawa was born in Ubon Ratchathani on March 15, 1986. She received her Bachelor's Degree in Chemical Engineering from Ubon Ratchathani University in 2007. She continued her graduate study in Doctoral degree at Separation Technology Laboratory, Department of Chemical Engineering, Faculty of Engineering, Chulalongkorn University since 2008 and received scholarship from the Thailand Research Fund and Chulalongkorn University under the Royal Golden Jubilee Ph.D. Program (Grant No. PHD/0272/2549). Moreover, she spent one year to do the research at Department of Organic Technology, Faculty of Chemical and Food Technology, Slovak University of Technology in Bratislava, Slovak.

